Extinguish the fire!

New insights into the pathogenicity mechanisms of *Botrytis* fire blight in *Lilium*

Michele Carlo Malvestiti

Propositions

1) The phylogenetic section *Sinomartagon* contains *Lilium* species that harbor genetic traits which confer enhanced *Botrytis* fire blight resistance.

(this thesis)

2) *Botrytis elliptica* possess effector proteins that contribute to virulence in lily during the biotrophic phase of the plant-fungus interaction.

(this thesis)

3) Transparency, humbleness and trust in your teammates are essential requirements for team works.

4) Science is at the same time limited and unlimited in its own phenomenological essence.

5) The best way to limit the anthropogenic impact on the atmospheric circulation is to promote anabolic activity in natural ecosystems.

6) The future of globalization requires a zero km-based economy.

Propositions belonging to this thesis, entitled:

'Extinguish the fire! New insights into the pathogenicity mechanisms of *Botrytis* fire blight in *Lilium*'

Michele C. Malvestiti

Wageningen 19th June 2023

Extinguish the fire!

New insights into the pathogenicity mechanisms of *Botrytis* fire blight in *Lilium*

Michele Carlo Malvestiti

Thesis committee

Promotor
Dr Jan A. L. van Kan
Associate Professor, Laboratory of Phytopathology
Wageningen University & Research

Co-promotors
Prof. Dr Richard G. H. Immink
Special Professor, Flowering and Reproduction of Ornamentals
Wageningen University & Research

Dr Paul Arens
Researcher, Plant Breeding
Wageningen University & Research

Other members
Dr Peter Solomon, Australian National University, Canberra, Australia
Prof. Dr Armin Djamei, Universität Bonn, Germany
Prof. Dr Dolf Weijers, Wageningen University & Research
Dr Emmanouil Domazakis, Enza Zaden Research and Development B.V., Enkhuizen

This research was conducted under the auspices of the Graduate School Experimental Plant Sciences

Extinguish the fire!

New insights into the pathogenicity mechanisms of *Botrytis* fire blight in *Lilium*

Michele Carlo Malvestiti

Thesis

submitted in fulfilment of the requirements for the degree of doctor
at Wageningen University
by the authority of the Rector Magnificus,
Prof. Dr. A.P.J. Mol,
in the presence of the
Thesis Committee appointed by the Academic Board
to be defended in public
on Monday 19 June 2023
at 1:30 p.m. in the Omnia Auditorium.

Michele Carlo Malvestiti

Extinguish the fire! New insight into the pathogenicity mechanisms of *Botrytis* fire blight in *Lilium*, 176 pages.

PhD thesis, Wageningen University, Wageningen, the Netherlands (2023)
With references, with summary in English

Printed by ProefschriftMaken B. V.

ISBN: 978-94-6447-677-4

DOI: https://doi.org/10.18174/629570

The research described in this thesis was financially supported by the Dutch Organization for Scientific Research (NWO).

Financial support from Wageningen University and from NWO for printing this thesis is gratefully acknowledged.

TABLE OF CONTENTS

Chapter 1
General introduction

LIFESTYLE OF PHYTOPATHOGENIC NECROTROPHIC ASCOMYCOTA

No matter whether they settle in natural habitats or in agricultural systems, plants live in environments which teem with infectious fungi, among which many belong to the phylum Ascomycota. These fungi have evolved different lifestyles to acquire nutrients from their host plants. Some of them require living plant tissue to obtain nutrients for growth and they are classified as biotrophic fungi (biotrophs). These Ascomycota are able to colonize the plant by suppressing the host immune responses when growing in the invaded tissue. Biotrophs have evolved specialized feeding structures to exploit carbon and nitrogen sources and therefore it is essential for them to keep their host cells alive. Differently from biotrophs, other phytopathogenic Ascomycota can acquire nutrients for growth and reproduce exclusively from dead plant tissue. Successful infection is achieved upon active killing of host cells and therefore, Ascomycota with such lifestyle are classified as necrotrophic fungi (necrotrophs). In the final decades of the 20th century, necrotrophs were thought to colonize their hosts in a rather brutal manner. It was considered that they first kill plant cells through the activity of phytotoxins and cell wall degrading enzymes (CWDEs), and subsequently grow saprophytically on dead host tissue. In the past two decades, however, evidence has accumulated that the interaction between necrotrophs and their host plants is more subtle and sophisticated than previously assumed. Necrotrophs have evolved strategies to exploit the plant immune system for their own benefit. They can co-opt dominant Host Susceptibility Genes (HSGs) to trigger Programmed Cell Death (PCD) in the host plant thereby achieving disease and plant susceptibility in an inverse gene-for-gene manner (Hammond-Kosack and Rudd, 2008; Tan et al., 2010; Oliver and Solomon 2010; Friesen and Faris 2012 and 2020; Thanthrige et al., 2020). Necrotrophs can drive the plant cell towards apoptosis-like PCD (Dickman et al., 2017; Kabbage et al., 2017), which differs from autophagy-like PCD that is observed as a resistance response during plant-biotroph interactions and is referred to as hypersensitive response (HR) (Minina et al., 2014). Autophagy- and apoptosis-like PCD are regulated by different genes and these two types of PCD can be distinguished by cellular and biochemical hallmarks. Nevertheless, detailed descriptions of the hallmarks that distinguish autophagy- from apoptosis-like PCD are beyond the scope of this chapter. For readers interested in learning more comprehensively about the different types of PCD, several reviews are recommended (Minina et al., 2014; Dickman et al., 2017; Kabbage et al., 2017; Balint-Kurti, 2019; Thanthrige et al., 2020). In plant-necrotroph interactions, apoptosis-like PCD is induced by the activity of fungal secreted compounds which are defined here as necrotrophic effectors (NEs). Effector recognition may occur in the apoplast as a consequence of effector binding to the extracellular domain of an RLP/RLK type receptor protein.

Alternatively, the effector may first be internalized via endocytosis into the plant cell and subsequently trigger PCD induction by direct or indirect recognition via a cytoplasmic NB-LRR-type receptor which causes the activation of an adjacent intracellular immune receptor responsible for PCD induction (**Figure 1**).

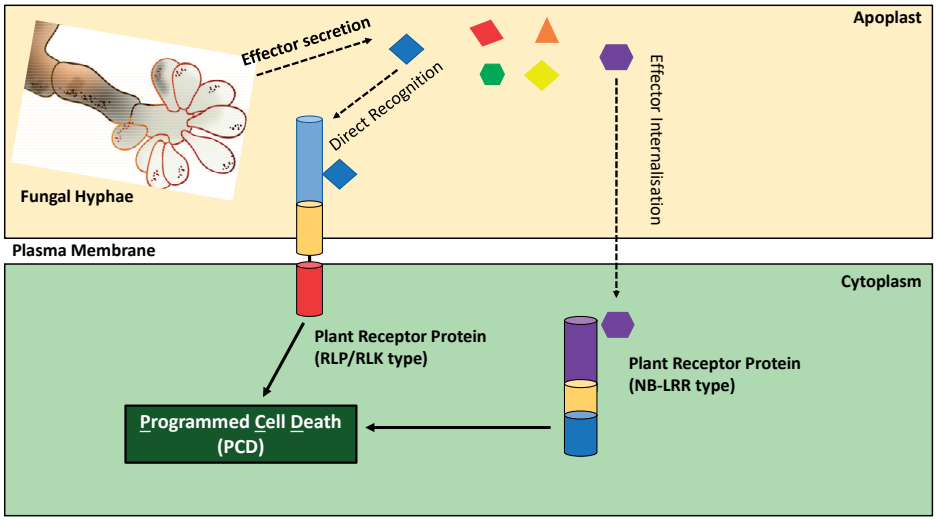

Figure 1. Schematic illustration of delivery of necrotrophic effectors (indicated by coloured shapes) into the apoplast and recognition by plant receptors leading to PCD induction and disease susceptibility in plant-necrotroph interactions. RLP = Receptor-Like Protein; RLK = Receptor-Like Kinase; NB-LRR = Nucleotide binding-leucin rich repeats.

NEs comprise proteinaceous compounds and phytotoxic secondary metabolites. In older literature they have often been referred to as Host Selective Toxins (HSTs) (Yoder, 1980; Markham and Hille 2001; Wolpert et al., 2002; Friesen et al., 2008; Oliver and Solomon 2010) since they were detected only in certain fungal species or even isolates, and confer pathogenicity only to a single host plant species or a specific genotype within a species. Moreover, many of these PCD-inducing compounds were of non-proteinaceous nature. Nevertheless, to avoid confusion in this thesis, all compounds involved in PCD induction and required for pathogenicity in plant-necrotroph interactions fall under the definition of NEs, no matter whether they are ribosomal synthetized proteins or secondary metabolites, and regardless whether they might be fungal isolate-specific or operate in a host-specific context. PCD induction by means of NEs is a key-step in disease development and successful plant colonization (Tan et al., 2010; Stergiopoulos et al., 2013; Kabbage et al., 2017; Veloso and van Kan, 2018) (**Figure 1**). The cell death response occurring upon NE recognition often relies on perception and signaling mechanisms analogous to the recognition of biotrophic effectors, but in this case, these lead to disease susceptibility

instead of disease resistance (Lorang et al., 2007; Tan et al., 2010; Friesen and Faris 2012 and 2020). Depending on the number of NEs and the corresponding targets present in the plant, the level of host susceptibility as well as the virulence of the fungal isolate can vary in a quantitative manner. The more functional NEs are produced by a given fungal isolate, and the more corresponding functional NE targets are present in a given plant genotype, the more aggressive is the fungus and the more susceptible is the host (**Figure 2**). The best example to illustrate such a scenario results from studies on the necrotrophic fungus *Parastagonospora nodorum*, causal agent of Septoria Nodorum Blotch (SNB) in wheat (*Triticum* spp., Poaceae). Secreted NEs are determinants for pathogenicity in this pathosystem. Upon perception by the host cell, NEs trigger PCD induction, thereby allowing disease development. The severity of infection depends in a quantitative manner on the number and identity of pathogen NEs and corresponding HSGs present in the wheat genotype (Oliver et al., 2012; Phan et al., 2016; Ruud et al., 2017; Haugrud et al., 2019). In total, nine proteinaceous NEs and nine HSGs have been genetically characterized in this pathosystem which are listed in Table 1.

Table 1. Necrotrophic Effector (NE)-Host Susceptibility Gene (HSG) interactions in P. nodorum-wheat pathosystem. WAK = Wall-Associated Kinase. PK-MSD = Protein Kinase-Major Sperm Protein. PR = Pathogenesis-Related Proteins. PC = Plastocyanin.

***P. nodorum* NE**	**Wheat HSG**	**NE isoforms**	**NE target**	**Orthologous NE genes in other fungi**	**Study**
SnToxA	*Tsn-1*	14	TaNHL10 ToxABP1 PC PR-1-5	*Phaeosphaeria avenaria f. sp. tritici* 1 *Pyrenophora tritici-repentis* *Cochliobolus heterostrophus*	Dagvadorj et al., 2022
SnTox1	*Snn1*	18	Snn1 WAK receptor	*Phaeosphaeria avenaria f. sp. tritici* 1	Shi et al., 2016
SnTox2	*Snn2*	?	?	?	Zhang et al., 2009
SnTox3	*Snn3-B1* and *Snn3-D1*	11	Snn3-D1 PK-MSD	*Phaeosphaeria avenaria f. sp. tritici 1*	Outram et al., 2021
SnTox4	*Snn4*	?	?	?	Abeysekara et al., 2012
SnTox5	*Snn5*	20	?	?	Kariyawasam et al., 2022
SnTox6	*Snn6*	?	?	?	Gao et al., 2015
SnTox7	*Snn7*	?	?	?	Shi et al., 2015
SnTox267	*Snn2*; *Snn6* and *Snn7*	32	?	?	Richards et al., 2022

Some of the nine described NEs appear to be unequally distributed among the *P. nodorum* isolates worldwide. A population study performed in 2013 (McDonald et al., 2013) showed that functional SnToxA, SnTox1 and SnTox3 alleles were present only in certain isolates and that they displayed substantial diversity at the amino acid sequence level. In fact, a total of 18, 11 and 14 protein isoforms were reported for SnTox1, SnTox3 and SnToxA, respectively (McDonald et al., 2013). For SNB, selection of wheat genotypes displaying NE insensitivity was fruitful for the development of wheat lines displaying increased resistance to SNB (Oliver and Solomon, 2010; Oliver et al., 2014; Downie et al., 2018 and 2021; Shackley et al., 2020). To achieve this goal a so-called effector assisted breeding strategy was implemented (Vleeshouwers and Oliver, 2014). This strategy consists in the utilization of purified NE proteins to screen plant germplasm and select the genotypes displaying insensitivity to the NE protein for further breeding. If the plant is insensitive to the NE, it can be predicted that the plant will display increased disease resistance since the fungus will not be able to exploit these particular molecular weapons to trigger PCD induction. A quantitative contribution of NEs to fungal virulence and plant susceptibility may also be hypothesized for other necrotrophic Ascomycota such as fungi of the genus *Botrytis* (Sclerotiniaceae) which exploit the capacity of their NEs to induce PCD and achieve infection (Veloso and van Kan 2018).

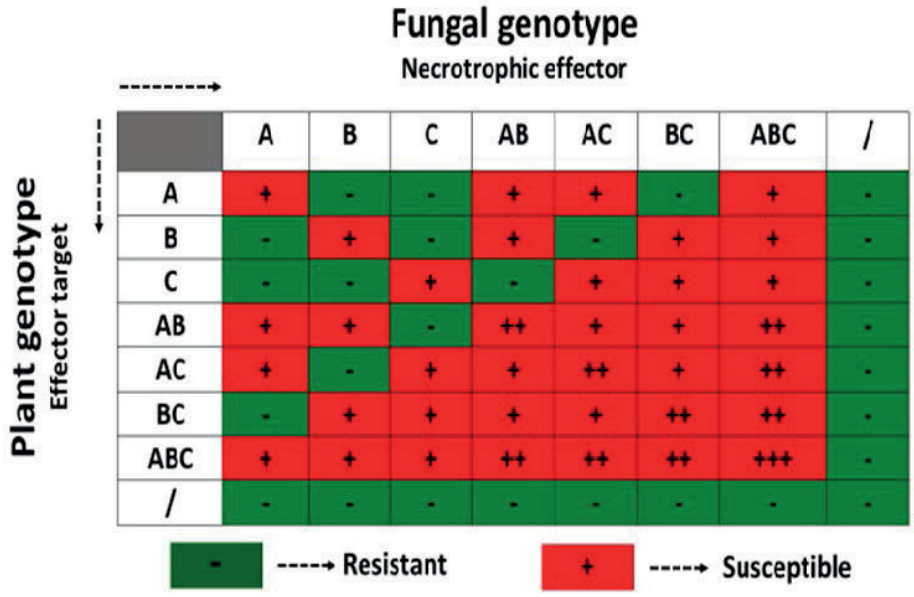

Figure 2. Schematic representation of an inverse gene-for-gene interaction between fungal NEs and plant NE targets, which governs the (quantitative) disease susceptibility in plant-necrotroph interactions. The existence of three effector-target pairs is hypothetical and purely meant for conceptual clarification.

Effectoromics: from *in silico* prediction to plant germplasm screening

In the field of plant pathology, the term "effectoromics" was proposed to describe a high-throughput, functional genomics approach that utilizes pathogen effectors for testing plant germplasm to identify host resistance and susceptibility genes and it currently represents a widespread methodology in modern breeding (Vleeshouwers and Oliver 2014; Todd et al., 2022). Effector candidates are usually selected based on the following criteria: presence of a signal peptide for secretion; amino acid sequence length below 300 amino acids; cysteine richness (>4 cysteine residues); absence of transmembrane and specific enzyme domains; limited taxonomic distribution and sequence homology to other organisms (Saunders et al., 2012; Raffaele and Kamoun, 2012; Lo Presti et al., 2015; Carreón-Anguiano et al., 2020). The selected effector candidates can be prioritized according to an increased transcript level during plant infection. Thanks to the development of new -omics approaches and bioinformatic tools, the number of identified and functionally characterized effectors in plant pathogenic fungi has increased from 96 in 2018 to more than 300 in 2022 (Todd et al., 2022; Carreón-Anguiano et al., 2021; Jones et al., 2021). A turning-point for effector prediction coincided with the development of machine-learning methods that predict effectors according to amino acid sequence characteristics shared among experimentally validated effectors. At the moment, EffectorP represents the most commonly used machine learning algorithm for the prediction of fungal effectors (Sperschneider et al., 2021). Additional bioinformatic tools for effector characterization include SignalP for detection of the secretion signal peptide (Teufel et al., 2022), LOCALIZER (Sperschneider et al., 2017) for predicting the subcellular localization of the effector and DeepTMHMM (Krogh et al., 2001) for the prediction of transmembrane domains. Alternative computational search engines for effector prediction are represented by EffHunter (Carreón-Anguiano et al., 2020) and Predector (Jones et al., 2021) which integrate multiple software tools and methods to combine diverse features that are relevant to fungal effectors (such as protein size, localization, and cysteine content), and enable ranking of effector candidates. Finally, AlphaFold allows to study the 3D structure of the protein and thus to identify effector candidates based on structural similarities with other known effectors even if they are unrelated in their protein sequence (Jumper, 2021; Rocafort et al., 2022; Varadi et al., 2022).

Depending on the lifestyle of the pathogen, the cell death response observed in effector-sensitive plant genotypes would correlate to plant resistance or susceptibility to the pathogen which produces that effector. In early stage of infection, hemi-biotrophic pathogens secrete effectors to avoid recognition by the plant immune system and effector perception events that trigger PCD will result in plant resistance. By contrast, necrotrophs utilize effector proteins to induce cell death and promote virulence, and effector recognition correlates therefore to plant susceptibility. Parallel to the progresses achieved for *in silico* effector prediction, several experimental strategies have been developed for

high throughput functional validation of the candidate effectors that are predicted. For example, Agrobacterium-mediated Transient Transformation (ATTA) and agroinfection are two transient expression systems for functional analysis of candidate effector genes *in planta* (Domazakis et al., 2017; Du and Vleeshouwers 2017; Du et al., 2014). Both methods are based on transient expression of pathogen genes in the plant. For ATTA, the broad host range bacterial pathogen *Agrobacterium tumefaciens* mediates the transfer of T-DNA from a plasmid, which carries the *in vitro* cloned candidate effector gene, into the nucleus of the plant cell. Upon infiltration of *Agrobacterium* suspensions into leaf tissue, plant cells will be transiently transformed and express the transgene(s) contained in the T-DNA in the infiltrated zone only (van der Hoorn et al., 2000). On the other hand, agroinfection relies on a systemic infection with a plant virus that serves as an expression cassette for the effector gene of interest. For agroinfection, RNA viruses represent ideal vectors for transient gene expression because of their high proliferation rate and dispersal through the inoculated plant tissue. Among the plant RNA viruses, Potato Virus X (PVX) is the most widely used vector for effector validation (Kanneganti et al., 2007; Oh et al., 2009). Constant high transgene expression can be achieved by constructing binary vectors for *A. tumefaciens* harboring the PVX genome under the control of a strong, constitutive Cauliflower mosaic virus 35S promoter. Once *A. tumefaciens* has transferred the T-DNA into plant cells, the PVX genome contained in the plasmid is transcribed, translated into proteins and begins to produce viral particles. Systemic spread of viral particles in the infected tissue causes homogeneous expression of the effector embedded in the viral genome.

Both in ATTA and agroinfection, recognition of the effector by the plant cell results in necrotic symptoms because of the PCD response that is induced. Both systems have been successfully implemented for the functional validation of pathogen effectors in Oomycota (Vleeshouwers et al., 2008 and 2009; Oh et al., 2009; Bailey et al., 2011), Ascomycota (Hunziker et al., 2021), and Basidiomycota (Lorrain et al., 2019) and for the identification of genotypes harboring resistance genes in potato (*Solanum tuberosum*, Solanaceae) (Rietman et al., 2012; Lin et al., 2022), tomato (*Solanum lycopersicum*, Solanaceae) (Mesarich et al., 2018), lettuce (*Lactuca sativa*, Asteraceae) (Stassen et al., 2013) and banana (*Musa acuminata*, Musaceae) (Noar and Daub, 2016; Nejat et al., 2017).

Besides by transient expression of effector candidates in a host plant, effectoromic studies can be conducted with purified effector proteins (Vleeshouwers and Oliver 2014). In this approach, the candidate effector gene is first cloned in an expression vector for heterologous protein production, thereby allowing not only functional validation but also to study the protein structure and its biological function. The yeast *Pichia pastoris* is often chosen as expression system for effector proteins because it possesses the eukaryotic post-translational modification machinery of the endoplasmic reticulum (ER) and Golgi apparatus

which is required for proper protein folding and extracellular secretion (Kombrink, 2012). On the other hand, excessive *N*- and *O*-linked glycosylation of the protein of interest can in some cases occur in *P. pastoris* fermentative culture. N-linked glycosylation begins in the ER with the transfer of an oligosaccharide core unit to the asparagine residue in the recognition sequence Asn-X-Ser/Thr. By contrast, *O*-linked glycosylation occurs when mannose residues are attached to the hydroxyl group of the amino acids Ser and Thr. Both *N*- and *O*-linked glycosylation may impact the protein activity, thereby causing a different response in the infiltrated plant tissue (Juturu and Wu, 2018; Radoman et al., 2021). Alternative methods have been developed to express candidate effectors in *Escherichia coli* as in case of the cysteine-rich effectors AvrP, AvrP123 and AvrP4 from the biotrophic fungus *Melampsora lini* and the NE proteins SnToxA, SnTox1 and SnTox3 from *P. nodorum* (Zhang et al., 2017). Despite *E. coli* represents a widely used protein production system because of its relatively low cost, rapid application, high yield and well-characterized genomics, large-scale production of disulfide bond-containing proteins in *E. coli* is challenging because the cytoplasmic redox potential of *E. coli* does not facilitate intracellular disulfide bond formation and thus, disulfide bond-containing proteins are often incorrectly folded after translation (Lobstein et al., 2012). To tackle this problem several strategies can be implemented, such as forcing the secretion of proteins into the periplasm and the use of commercially available *E. coli* strains that have been engineered to enhance intracellular disulfide bond formation (Berkmen, 2014). After protein expression and purification, the effector can be applied to the plant via infiltration. The *P. nodorum* effectors SnToxA, SnTox1 and SnTox3 were produced in *E. coli* and used to screen the wheat germplasm in Australia and to eliminate wheat genotypes that were highly susceptible to SNB, because these genotypes showed sensitivity to the fungal effectors due to the presence of the matching HSGs *Tsn1*, *Snn1* and *Snn3* respectively (Friesen et al., 2007; Liu et al., 2012; Shi et al., 2016). Analogously the purified *B. squamosa* effector protein BsNEP1 was produced and purified from *Pichia* cultures and used for screening germplasm in onion (Steentjes et al., 2022).

Botrytis species and their NEs repertoire

The genus *Botrytis* comprises around 40 species. The most notorious and best studied is *Botrytis cinerea*, a generalist necrotrophic fungus, causal agent of the grey mold disease in more than 1400 plant species (Hyde et al., 2014; Fillinger and Elad, 2016; Garfinkel et al., 2017). Most *Botrytis* species, however, are host-specific since they are pathogenic on a single host or on few taxonomically related host species. For example, the lily fire blight pathogen *B. elliptica* and its sister species *B. squamosa*, causal agent of onion leaf blight, are specific pathogens of *Lilium* spp. (Liliaceae) and *Allium cepa* (Amaryllidaceae), respectively (Steentjes et al., 2022). Moreover, several *Botrytis* species have found their ecological niche in a specific plant organ, such as *B. aclada*, *B. byssoidea* and their hybrid *B. allii*, which are all causal agents of neck rot in onion bulbs (Nielsen and Yohalem, 2001;

Chilvers and du Toit, 2006). Phylogenetically, *Botrytis* spp. are divided in two distinct clades. Clade I contains *Botrytis* species which infect exclusively dicots and includes the generalists *B. cinerea* and *B. pseudocinerea*. By contrast, Clade II contains only host-specific *Botrytis* species, whereby the majority of them is pathogenic on a specific bulbiferous monocot plant taxon (Staats et al., 2007; Valero-Jimenéz et al., 2020). *Botrytis* fungi initiate their disease cycle when wind and rain-dispersed conidia land on the host surface. Under moist conditions the conidia germinate, form a germ tube that develops into an unicellular appressorium or into a multicellular structure described as infection cushion to facilitate host tissue penetration (Deising et al., 2000; Choquer et al., 2021). The initial infection stage of *Botrytis* is characterized by a short biotrophic phase which is crucial for the outcome of the interaction between *Botrytis* and its host. For successful disease progression, the fungus must suppress the induction of autophagy-like PCD and drive the host cell towards an apoptosis-like PCD (Kabbage et al., 2017; Veloso and van Kan, 2018; Bi et al., 2022). Autophagy suppression gives the fungus time to feed within the host tissue and to accumulate sufficient biomass for the transition into the necrotrophic phase. At this point, compounds secreted by the fungus induce the apoptosis-like PCD and mark the formation of necrotic lesions (Veloso and van Kan 2018). Vigorous outgrowth of the necrotic lesions causes rapid maceration of plant tissue, on which the fungus eventually sporulates to produce inoculum for the next infection. A common feature of (probably) all *Botrytis* species is their capacity to secrete of a wide array of proteinaceous NEs during host colonization (van Baarlen et al., 2004; van Kan, 2006; Steentjes et al., 2022; Leisen et al., 2022). Traditionally CWDEs are not considered NEs, given the assumption that CWDEs are exclusively involved in hydrolysis of plant cell wall polysaccharides. However, several CWDEs were shown to be capable of PCD induction upon protein recognition in the apoplast by plant receptor proteins and the PCD-inducing capacity did not require the hydrolytic activity of the enzyme. For example *B. cinerea* PGs induce PCD upon protein infiltration in *Arabidopsis* lines harboring the leucine-rich repeat receptor-like protein (LRR-RLP) RBPG1 (Zhang et al., 2014). Analogously, the xylanases BcXyl1 and BcXyn11 and the xyloglucanase BcXyg1 induced PCD in *Nicotiana benthamiana* and *Solanum lycopersicum* (Solanaceae) independently from their enzymatic activity and the signal transmission leading to PCD required the receptor like kinase complex BAK1-SOBIR1 (Noda et al., 2010; Zhu et al., 2017; Yang et al., 2018a; van der Burgh et al., 2019). In addition, infiltration of the glycoprotein BcGs1 caused a necrotic response and ROS (Reactive Oxygen Species) accumulation in tomato and tobacco leaves (Zhang et al., 2015) and the transglycolase BcCrh1 induces PCD and defense responses in *Arabidopsis* upon translocation into the plant cytoplasm (Bi et al., 2021). Besides CWDEs with cell death-inducing activity, *B. cinerea* also secretes NEs that lack an enzymatic domain. For example the necrosis- and ethylene-inducing peptide 1 (Nep1)-like proteins (NLPs) Nep1 and Nep2 are NEs which have been studied also in *B. elliptica* and *B. squamosa* (Staats et al., 2007; Schouten et al., 2008; Arenas et al., 2010; Steentjes et al., 2022). NLPs are currently the only proteinaceous NEs

which possess membranolytic activity in plant cells of both dicot and monocot species (Steentjes et al., 2022). NLPs can interact with the plant plasma membranes because of their affinity to glycosylinositol phosphorylceramide (GIPCs), plant-specific sphingolipids present in both dicots and monocots (Lenarčič et al., 2017; Steentjes et al., 2022). Recently, the membranolytic activity of NLPs has been elucidated as a multistep process that causes pore formation in the plasma membrane (Pirc et al., 2022). After secretion into the apoplast NLPs target the GIPC-rich plant cell membrane. The low ionic strength in the apoplast enables an electrostatically driven initial interaction of NLPs with anionic GIPCs. NLPs then associate into clusters and cause the formation of membrane openings leading to leakage of the cell content. It has been proposed that clusters of NLP molecules interact with multiple GIPCs, which may cause disruption of GIPC homeostasis, leading to reassembling of membrane layers and pore formation (Pirc et al., 2022). In addition to their membranolytic activity, NLPs can be perceived in *Arabidopsis* by the RLP AtRLP23 through the binding of an NLP-derived 20 amino acid epitope, nlp20. After binding to nlp20, RLP23 forms a complex with the RLKs SOBIR1 and BAK1 causing the activation of immune responses and PCD induction (Böhm et al., 2014; Albert et al., 2015). Finally, the cerato-platanin protein BcSpl1, the hypersensitive response inducing protein BcHip1 and the glycoprotein BcIEB1 were capable of inducing PCD upon protein infiltration or transient expression in leaf tissue (Frías et al., 2011; Frías et al., 2016; Jeblick et al., 2023). Next to proteinaceous NEs, *Botrytis cinerea* also secretes secondary metabolites that contribute to PCD induction: the metabolites botrydial and botcinic acid cause chlorosis and cell collapse when applied onto leaf and fruit tissue of different hosts (Cutler et al., 1996; Colmenares et al., 2002). These compounds are synthetized by biosynthetic gene clusters that are present in the genomes of several, but not all, *Botrytis* species (Valero-Jiménez et al., 2020).

Importance of lily and fire blight disease

Either as bulb, potted plant or cut flower, lily (*Lilium* spp., Liliaceae) is the second most important flower bulb in the Netherlands, with a production area of 5300 hectares (Andersen 2021; CBS, 2020). Lily sales at Dutch auctions yield a return of more than 150 Million € per year (Royal Flora Holland, 2021). Lily breeding mainly focussed on ornamental traits, such as shape, colour and vase life (Marasek-Ciolakowska et al., 2018). Unfortunately, resistance breeding has been rather neglected in the past, and chemical protection is still the most adopted strategy to combat various diseases and pests which affect the lily production. In total, more than 600 tons of active compounds are applied yearly on the 5300 hectares of Dutch farmland dedicated to lily (CBS, 2020). Issues derived from fungicide utilisation are not only restricted to their production and application costs and the derived pollution of soil-water ecosystems. The most serious implication is the development of fungicide resistance mechanisms in human pathogenic fungi which survive in plant waste. Of special concern is the situation for *Aspergillus fumigatus*, causal agent

of human chronic pulmonary aspergillosis (RIVM, 2017). Evidence is accumulating that clinical cases of fungicide resistance in *Aspergillus fumigatus* are likely related to the use of fungicides in the flower bulb industry, leading to selection of resistant isolates during composting of plant waste (Hortipoint, 2017). As part of the Farm to Fork Strategy of the European Green Deal, the European Commission has demanded an overall reduction of chemical use by 20% by 2030 (European Commission, 2020). This illustrates the need for alternative solutions to the application of chemical compounds in order to protect plants from diseases and pests. In lily, fire blight represents the most destructive disease and is caused by the necrotrophic Ascomycota *Botrytis elliptica* and *B. cinerea* (Doss et al., 1998; Fang Hsieh et al., 2001; Furukawa et al., 2005; Chastagner and Garfinkel, 2020). While the generalist *B. cinerea* can usually colonize already damaged plant tissue and is mostly found on cut lilies in the post-harvest stage, the specialist *B. elliptica* inflicts serious economic losses since it is able to cause disease on undamaged, vigorous plants (Hou and Chen, 2003; Staats et al., 2007; Chastagner and Garfinkel, 2020). Lily breeders and growers are well aware of the fact that the lily germplasm displays differences in susceptibility to *B. elliptica* (Doss et al., 1986; Beers et al., 2005; Gao et al., 2018; Jang et al., 2018). However, these differences are not easy to be quantified because of the phylogenetic complexity of the genus *Lilium* (Li et al., 2022; Pelkonen and Pirttilä, 2012) and the huge number of commercial genotypes which have been developed in the past decades (van Tuyl and Arens, 2011). In addition, large genetic variation is found among *B. elliptica* isolates which indicates that sexual reproduction is frequently used by this fungus to increase genetic diversity in the fungal population (Staats et al., 2007) and to facilitate adaptation to hosts and environment (Van den Ende and Pennock-Vos, 1997; Huang et al., 2001; Terhem et al., 2015). Given the complex situation, the selection of *Botrytis* resistant lily genotypes still mostly relies on field observations and cultivation practices. To allow a more accurate selection of resistant lilies, it is essential to investigate at molecular level which pathogenicity factors are involved in the *B. elliptica*-lily interaction. Earlier studies showed that pathogenicity of *B. elliptica* in lily relies on the activity of secreted proteins, capable of causing apoptosis-like PCD upon contact with lily cells (van Baarlen et al., 2004). In such a scenario, it can be hypothesized that disease development by *B. elliptica* in lily is determined by the presence or absence of active alleles of NE genes in the fungus and by the presence or absence of functional NE targets in the plant. As shown for the *P. nodorum*-wheat pathosystem, NEs can be implemented to select for plant genotypes which display higher disease resistance since they are insensitive to the NE used by the fungus to induce PCD (Vleeshouwers and Oliver, 2014, Downie et al., 2018; Ruud et al., 2018). Therefore, the overall objective of this research is to gain insights into the repertoire of *B. elliptica* NEs which are important for virulence in lily. This will provide the lily breeders with information to implement NEs as biological tools to identify lily genotypes which display insensitivity to NEs and thereby select for lilies with (predicted) increased resistance to *B. elliptica*.

Outline of the thesis

Research on *Botrytis* fire blight in lily has a long history but only few studies investigated the molecular aspects at the basis of this pathosystem. New approaches are needed to obtain a deeper fundamental understanding of the molecular mechanisms required for pathogenicity of *B. elliptica* in lily and to identify NEs to allow a more efficient selection of lily genotypes displaying increased fire blight resistance. In this thesis, several aspects of the *B. elliptica*-lily interaction were investigated at genetic, biochemical, molecular and cellular level.

Chapter 2 describes the variation of *B. elliptica* susceptibility in a panel of lily genotypes and the variation in fungal virulence among a set of *B. elliptica* isolates. It was observed that virulence of *B. elliptica* correlates in a quantitative manner with the production of cell death inducing compounds and that disease susceptibility in lily correlates in a quantitative manner with sensitivity to the cell death inducing compounds. This chapter illustrates the complexity of the pathosystem given the large genetic variation both in the lily and in the fungus. At the same time, these findings set the milestone to pursue the search for NEs as tools to select more efficiently lily genotypes with increased fire blight resistance.

In **Chapter 3** the secretome of *B. elliptica* was analyzed. A list of candidate NE genes was generated by combining genomic, transcriptomic and proteomic data. From the list, one NE candidate was selected for heterologous expression to test its cell death inducing capacity when infiltrated in lilies and tobacco as purified protein. The differences in response between lily genotypes upon protein infiltration make this NE an interesting tool for effector-assisted selection in lily.

Chapter 4 is dedicated to the molecular study of an effector protein with homology to Chorismate Mutases, which may be capable of inducing cell death by targeting the chloroplast. The enzymatic activity as well as the subcellular localization of the protein were assessed with different methods. The contribution of the effector to fungal virulence was tested by generating deletion mutants and comparing symptom development upon lily inoculation with the mutants and the recipient *B. elliptica* isolate.

In **Chapter 5** we assessed the role of the phytotoxic secondary metabolite botrydial as a virulence factor in the *B. elliptica*-lily pathosystem. First, cell death inducing activity of botrydial in lily was tested by applying pure botrydial onto different tissues. Then, the contribution of botrydial to fungal virulence was assessed by generating mutants which were deficient in botrydial biosynthesis and by comparing symptom development upon lily inoculation with the mutants and the recipient *B. elliptica* isolate.

Chapter 6 discusses the advantages and the perspective of the implementation of the effector-assisted screening to set up breeding programs for the development of *Botrytis*-resistant genotypes. In addition, it highlights the interesting perspectives of studying Ribosomally Synthesized and Post-translationally Modified Peptides (RiPPs), a class of small secreted fungal compounds which is gaining increasing attention from many researchers for their versatile functions in the biology of fungi, including their role as phytotoxic bioactive peptides.

Chapter 2

Fire blight susceptibility in *Lilium* correlates to sensitivity to *Botrytis elliptica* secreted cell death inducing compounds.

Michele C. Malvestiti[1], Richard G. H. Immink[2,3], Paul Arens[4], Thomas Quiroz Monnens[1], and Jan A. L. van Kan[1]

[1] Laboratory of Phytopathology, Wageningen University & Research, Wageningen, Netherlands,
[2] Department of Bioscience, Wageningen University & Research, Wageningen, Netherlands,
[3] Laboratory of Molecular Biology, Wageningen University & Research, Wageningen, Netherlands,
[4] Department of Plant Breeding, Wageningen University & Research, Wageningen, Netherlands.

ABSTRACT

Fire blight represents a widespread disease in *Lilium* and is caused by the necrotrophic Ascomycota *Botrytis elliptica*. There are >100 *Lilium* species that fall into distinct phylogenetic groups and these have been used to generate the contemporary commercial genotypes. It is known among lily breeders and growers that different groups of lilies differ in susceptibility to fire blight, but the genetic basis and mechanisms of susceptibility to fire blight are unresolved. The aim of this study was to quantify differences in fire blight susceptibility between plant genotypes and differences in virulence between fungal isolates. To this end we inoculated, in four biological replicates over two years, a set of 12 *B. elliptica* isolates on a panel of 18 lily genotypes representing seven *Lilium* hybrid groups. A wide spectrum of variation in symptom severity was observed in different isolate-genotype combinations. There was a good correlation between the lesion diameters on leaves and flowers of the *Lilium* genotypes, although the flowers generally showed faster expanding lesions. It was earlier postulated that *B. elliptica* pathogenicity on lily is conferred by secreted proteins that induce programmed cell death in lily cells. Two aggressive and one mild *B. elliptica* isolates were selected and culture filtrate (CF) samples were collected to compare the cell death inducing capacity of their secreted compounds in lily. After leaf infiltration of the CFs, variation was observed in cell death responses between the diverse lilies. The severity of cell death responses upon infiltration of the fungal CF observed among the diverse *Lilium* hybrid groups correlated well to their fire blight susceptibility. These results support the hypothesis that susceptibility to fire blight in lily is mediated by their sensitivity to *B. elliptica* secreted proteins in a quantitative manner. Cell death-inducing proteins may provide an attractive tool to predict fire blight susceptibility in lily breeding programs.

INTRODUCTION

Since the dawn of time, lily (*Lilium* spp., Liliaceae, L.) represents one of the most prestigious ornamental flowering plants in the Occidental culture as it was considered the symbol of divine purity. Either as bulb, potted plant or cut flower, lily is one of the main flower bulb crops sold worldwide (Kamenetsky, 2014). The genus *Lilium* consists of approximately 120 described species (Angiosperm Phylogeny Group (APG), 2020). Based on their geographical distribution and morphological traits (De Jong, 1974), ribosomal DNA sequences (Nishikawa et al., 1999; Nishikawa, 2007; Li et al., 2022) and the chloroplast genome (Du et al., 2017; Kim et al., 2019; Li et al., 2022), the genus *Lilium* is phylogenetically divided into seven taxonomic sections (Pelkonen and Pirttilä, 2012; Angiosperm Phylogeny Group, 2022). The assortment of commercial lily genotypes includes thousands of hybrids that were generated via intrasectional crosses between different *Lilium* species and these have been divided into four hybrid groups: Asiatic (A), Longiflorum (L), Trumpet (T), and Oriental (O). To combine ornamental traits and obtain more vigorous plants, a variety of intersectional hybrids were subsequently generated using artificial pollination, embryo rescue and polyploidization techniques (van Tuyl et al., 1991; Lim et al., 2008; van Tuyl and Arens, 2011), resulting in the interspecific hybrid groups LA (Longiflorum-Asiatic), LO (Longiflorum-Oriental), OA (Oriental-Asiatic) and OT (Oriental-Trumpet). Despite its flourishing breeding and cultivation history, the lily industry is threatened by pests and diseases. Breeding efforts have thus far predominantly focused on ornamental traits and to lesser extent on the resistance to pests and pathogens. Given the current challenges more focus on disease resistance is needed. Among several pests and diseases the most destructive is fire blight, a fungal disease caused by the filamentous Ascomycota *Botrytis elliptica* and *Botrytis cinerea* (Doss et al., 1986; Fang Hsieh et al., 2001; Furukawa et al., 2005; Chastagner et al., 2017). Both fungi initially cause small brownish necrotic lesions on leaves and flowers. Outgrowth of necrotic lesions leads to rapid death of the entire plant. While the generalist *B. cinerea* was reported to occur only on damaged plant tissue and especially on cut lilies, the specialist *B. elliptica* inflicts serious economic losses since it is able to cause disease on undamaged, healthy plants (Hou and Chen, 2003; Staats et al., 2007; Chastagner and Garfinkel, 2020). The fungus can infect both leaves and flowers. Leaf infection can be devastating (hence the name “lily fire blight”), however this is usually controlled by intensive chemical control. Flower infection is a postharvest problem and is therefore economically more damaging, as it affects the quality at the retailer or leads to dissatisfied consumers. Both *B. cinerea* and *B. elliptica* belong to the genus *Botrytis* (Sclerotiniaceae) which includes around 40 species (Valero-Jiménez et al., 2019). According to their necrotrophic lifestyle, *Botrytis* species kill the host cells to gain nutrients from the dead plant tissue for growth and reproduction (van Kan, 2006). The fungus is able to trigger the host plant cells to commit suicide via Programmed Cell Death (PCD) (van Kan, 2006; Veloso and van Kan, 2018). In the lily–*B. elliptica* interaction, PCD induction is medi-

ated by secreted proteins, and the generalist *B. cinerea* and the tulip specialist *B. tulipae* acquired the ability to cause necrotic lesions when inoculated on lily leaves, previously infiltrated with *B. elliptica* secreted proteins (van Baarlen et al., 2004). There are anecdotic reports among lily growers and breeders that certain lily genotypes are less susceptible to *B. elliptica* than others. Published studies by Doss et al. (1986) reported a large variation in disease incidence (25–98%) and lesion size among 35 genotypes, of which the hybrid type was in most cases undescribed. A more recent study by Jang et al. (2018) also reported large variation in susceptibility among genotypes from four hybrid types and seven Korean genotypes from distinct indigenous species, with Asiatic hybrid genotypes generally falling in the highly resistant group, and the Korean genotypes generally falling in the susceptible group. A study by Gao et al. (2018), however, classified Oriental-Trumpet and Oriental hybrid genotypes as resistant, while Asiatic and Trumpet hybrids were classified as susceptible. Crosses between resistant and susceptible genotypes provided evidence for very complex inheritance of susceptibility to *B. elliptica* in hybrid progenies, with hybrid offspring displaying a large spectrum of susceptibility (Beers et al., 2005; Hu et al., 2017). These previous studies, however, show several limitations that hamper obtaining a clear overview of the variation in susceptibility in lily and the variation in virulence in the *B. elliptica* population. Several studies included a single fungal isolate (Beers et al., 2005; Hu et al., 2017; Gao et al., 2018; Jang et al., 2018) and distinct inoculation methods. Sometimes agar plugs were used as inoculum (Hu et al., 2017; Gao et al., 2018), while in another case, leaf tips were inoculated with fungal conidia (Beers et al., 2005). Some studies were performed with genotypes of undescribed hybrid groups (Doss et al., 1986; Balode, 2009; Daughtrey and Bridgen, 2013) or performed in the field under unknown disease pressure and uncontrolled conditions (Balode, 2009; Daughtrey and Bridgen, 2013). Only a single study (Daughtrey and Bridgen, 2013) comprised repetitions over multiple years, and the method for disease scoring differed between all studies. Furthermore the variation in susceptibility of lily flowers was not addressed in any of the above mentioned studies. We aimed to analyze and quantify the disease development under controlled conditions in a panel of commercial lily genotypes from seven hybrid groups upon inoculation with a collection of *B. elliptica* isolates. Disease assays were principally performed on leaves, and a subset of genotypes was also inoculated on flowers. We selected three fungal isolates that differed in virulence and evaluated the capacity of their Culture Filtrates (CFs) to cause cell death in leaves of different lily genotypes. These experiments enabled us to investigate a correlation between the susceptibility of lily genotypes to fire blight and their sensitivity to cell death induction in response to fungal secreted compounds.

MATERIALS AND METHODS

Plant material and growth conditions

Eighteen *Lilium* genotypes (Table 1) were used in this study representing the hybrid groups Asiatic (A), Longiflorum (L), Oriental (O) or intersectional hybrid groups Longiflorum-Asiatic (LA), Longiflorum-Oriental (LO), Oriental-Asiatic (OA), Oriental-Trumpet (OT), respectively. Material was provided by breeding companies as fresh bulbs and stored in potting soil at -1 °C in darkness until planting. For commercial reasons, the names of genotypes have been anonymized. Lilies used in the disease assays in early spring (April-May 2019 and 2020) were planted as bulbs in the second week of February 2019 and 2020, whereas lily bulbs used in the disease assays in late spring (May-June 2019 and 2020) were planted in the third week of March 2019 and 2020. For repetitions of the assay, each of the 18 lily genotypes was planted in batches of 10 bulbs in plastic crates containing potting soil and grown in a greenhouse under natural day/night light regime at a minimum night temperature between 12 and 15°C and a maximum day temperature between 24 and 26°C. Temporal differences in shoot emergence from soil, vegetative growth and transition into flowering were observed. Disease assays in the early spring were conducted with mature leaves (as defined by Bar and Ori, 2014) of 6-7 weeks old plants in their vegetative stage, whereas disease assays in the late spring were conducted with mature leaves of 4-5 weeks old plants in their vegetative stage. Disease assays on flowers were conducted in June 2020. Lilies used for disease assays on flowers were planted as bulbs in the second week of May 2020 and grown in a greenhouse under natural day/night light regime. Depending on the genotype, flower buds started to develop after 4-6 weeks. Lilies carrying flower buds at initiation of bud color were harvested as cut flowers and transported to the laboratory to be inoculated. Fungal inoculations on lily flowers were conducted within 2 days after bud opening. From the same lilies used for inoculation on flowers, leaves were detached to be inoculated with fungal conidia.

Table 1. Lily genotypes used in this study.

Lily hybrid group	Genotype		
Asiatic (A)	A 1 [1, 2, 3]	A 2 [1, 3]	A 3 [1, 2]
Longiflorum (L)	L 1 [1]	L 2 [1, 2, 3]	L 3 [1, 2 , 3]
Oriental (O)	O 1 [1, 2, 3]	O 2 [1, 3]	O 3 [1, 2]
Longiflorum x Asiatic	LA 1 [1, 2, 3]	LA 2 [1, 3]	LA 3 [1, 2]
Longiflorum x Oriental	LO 1 [1, 2]	LO 2 [1, 2, 3]	
Oriental x Asiatic (OA)	OA 1 [1, 3]		
Oriental x Trumpet (OT)	OT 1 [1, 3]	OT 2 [1, 2]	OT 3 [1, 2, 3]

[1] Lily genotypes used for disease assays in leaves.
[2] Lily genotypes used for disease assays in flowers and leaves.
[3] Lily genotypes used for leaf infiltration with culture filtrate samples.

Fungal material and growth conditions

Botrytis elliptica isolates used in this research (Table 2) were stored as conidia suspensions in 20% glycerol at -80°C. To obtain conidia for inoculation, fungi were grown on Malt Extract Agar (50 g/L, Oxoid) at 20°C and sporulation was induced by illumination with UV-A lamps. After harvesting, the conidia were collected and washed in demineralized water, counted with the Bürker-Türk counting chamber, adjusted to a concentration of $1x10^6$ conidia/mL and stored until use in darkness at 4 °C. Disease assays with *B. cinerea* were conducted similarly using isolate B05.10 (van Kan et al., 2017).

Table 2. *Botrytis* isolates used in this study.

Fungal isolate	Year of isolation	Sampling location
B. elliptica 9174 [1]	1991	Lisse (Netherland)
B. elliptica 9401 [1, 2, 3]	1994	Lisse (Netherland)
B. elliptica 9605 [1]	1996	Lisse (Netherland)
B. elliptica 9610 [1]	1996	Bergentheim (Netherland)
B. elliptica 9612 [1]	1996	Anerveen (Netherland)
B. elliptica 9714 [1]	1997	Elsloo (Netherland)
B. elliptica 9732 [1, 2, 3]	1997	Lisse (Netherland)
B. elliptica 0006 [1, 2, 3]	2000	Rutten (Netherland)
B. elliptica 254-2 [1]	unknown	unknown
B. elliptica 254-8 [1]	unknown	unknown
B. elliptica 254-11 [1]	unknown	unknown
B. elliptica 748 [1]	unknown	unknown
B. cinerea B05.10 [2]	1995	Münster (Germany)

[1] fungal isolates used for disease assays in leaves.

[2] fungal isolates used for disease assays in flowers and leaves.

[3] fungal isolates used for production of CF samples.

Disease assays in lily leaves

Four rounds of disease assays were conducted in 2019 and 2020, both in the early (April–May) and late spring (May–June) season. In each round of assays all 18 lily genotypes were tested with 12 *B. elliptica* isolates. Nine lily genotypes were tested in two consecutive weeks, each week with six *B. elliptica* isolates, for a total of 4 weeks per round. Each disease assay was carried out as follows. From each genotype, 30 mature leaves (as defined by Bar and Ori, 2014) were detached from 10 plants and transported in clean plastic bags to the laboratory for inoculation. Per genotype, three random detached leaves were placed in plastic boxes on plastic grids placed on a layer of wet filter paper, with a total of three lily genotypes per box. The leaves were inoculated with each *B. elliptica* isolate at a concentration of $1x10^5$ conidia/mL in Potato Dextrose Broth (12 g/L, PDB, Oxoid). Leaves were abaxially inoculated with four 2 µL droplets of conidial suspension on well separated spots avoiding leaf edges and leaf veins. In total, 12 inoculations were performed per

genotype and per isolate in each round of disease assay. Mock inoculation was carried out in separate boxes on three detached leaves with 2 µL droplets of PDB. Plastic boxes were closed with a transparent plastic lid and sealed with tape to maintain high humidity. After 4 days of incubation at constant temperature (19-21 °C) and under regular day/night light regime, inoculated leaves were photographed and lesion diameters measured with a caliper. Given the ellipsoidal shape of necrotic spots, the lesion diameter was measured as a conjugate diameter. Specifically, we measured the length of the chord that connects the middle of the top-left quadrant with the middle of the bottom-right quadrant of the ellipse.

Disease assays in lily flowers

To compare the susceptibility to *B. elliptica* in flowers and leaves and to test the pathogenicity of *B. cinerea* in lily, combined disease assays on flower and leaf tissues were conducted in June 2020. In these experiments, leaves and flowers of 12 lily genotypes were used, representing all but one of the hybrid groups (Table 1). Conidia of three *B. elliptica* isolates that showed variation in aggressiveness in leaf assays (Table 2) and of *B. cinerea* isolate B05.10 were inoculated on flowers and leaves with 2 µL droplets of conidial suspension at a concentration of $5x10^4$ conidia/mL PDB (6 g/L). Disease assays on flowers were carried out with two just opened flowers that were harvested from the inflorescence of lilies and fixed into wet oasis foams, which were placed into plastic boxes containing tap water. Of the six tepals of each flower, five were inoculated with one droplet of conidial suspension and one was marked with paper tape and mock inoculated. Simultaneously to the flowers, three leaves per genotype were inoculated with the same fungal isolates. After 3 days of incubation at constant temperature (19-21 °C) and under regular day/night light regime, the inoculated plant material was photographed and lesion diameters were measured.

Production of *B. elliptica* culture filtrate and leaf infiltration

Botrytis elliptica CF were obtained by growing each isolate (*B. elliptica* isolates 9401, 0006, and 9732) in a 250 mL flask containing 50 mL of liquid medium with 3 g/L Gamborg B5 salts (Duchefa,Haarlem, Netherlands), 10 mM KPO_4 pH = 6 (LabChem, Tiel, Netherlands), 1% sucrose (Duchefa) and 30% lily leaf extract in demineralized water. The leaf extract was obtained by grinding with a blender 30 g of fresh harvested leaf material of genotypes A 3, L 2 and OT 3 (10 g each) in 250 mL demineralized water. The homogenate was centrifuged (3500 rpm, 20 min) and the supernatant was concentrated by freeze drying. The obtained concentrate was filter-sterilized (0.45 µm pore size, Millipore, Amsterdam, Netherlands) and added to the liquid medium. The liquid culture was started at a spore concentration of $1x10^5$ conidia/50 mL medium. Flasks were closed with a cotton plug and fungal cultures were grown in a shaking incubator for 7 days (20°C, 150 rpm). When the liquid cultures were harvested, the pH of the CF was adjusted to 6 with 1 M KOH, and the CF was passed

through a layer of Miracloth (Calbiochem, San Diego, CA, United States), filter-sterilized (0.45 µm pore size) and ice-chilled. A mock liquid medium was prepared and processed in the same way without fungal conidia added. For leaf infiltration with the CF samples and mock solution, three detached leaves were used of non-flowering plants from 12 different lily genotypes, representing all seven lily hybrid groups (Table 1). The leaves were placed in moist plastic boxes and 0,1 mL CF sample from each fungal culture was abaxially infiltrated in four different spots per leaf with the aid of a 1 mL sterile plastic syringe. After 3 days incubation at 19-21°C under ambient day length, leaves were photographed and the response evaluated.

Statistical analysis

The statistical analysis was performed using R (Version 4.0.2). Lesion diameters measured in disease assays on lily leaves and flowers were plotted on a box-plot diagram using ggplot2 (Version 3.2.2). To determine the contributions of plant and pathogen genotype, and the seasonal effect on observed variation, the following linear mixed model was used:

$$ls = be + group + be{:}group + season + season{:}group + season{:}be + year_R$$

whereby: *ls*, lesion diameter measured; *be*, *B. elliptica* isolate; *group*, lily hybrid group; *season*, late or early spring; *year*, 2019 or 2020, as random variable. As the data were not balanced, a REML model was built using lmer() from the lme4 package (Version 1.1-22; Bates et al., 2015). The year was added to the model as a random effect to correct for year effect. To quantify the impact of the year on the variation observed, a variance component analysis was performed with lme4. Estimated marginal means (EMMs) of lesion diameters per fungal isolate, per hybrid group, were obtained using emmeans (Version 1.5.0). Differences in EMMs were calculated using the pairwise comparison function of emmeans, and p-values for differences in EMMS were adjusted by Tukey's method. Pairwise differences for the average lesion diameters within isolate, for each hybrid group were plotted on a dot plot using ggplot().

Lesion diameters measured in lily flowers and in leaves of cut lilies were analyzed with the following linear model.

$$ls = be + group + group{:}be$$

whereby: *ls*, lesion diameter measured; *be*, *Botrytis* isolate; *group*, lily hybrid group. This simpler, linear model was chosen because the flower infection assays were performed only in one season (early summer 2020). EMMs were obtained using emmeans(). Differences in EMMs were calculated and plotted similarly to the EMMs for lesion diameter on leaves.

RESULTS

To assess the susceptibility of lily genotypes to *B. elliptica* and the virulence of *B. elliptica* isolates in a quantitative manner, we inoculated 12 fungal isolates (**Table 2**) on leaves of 18 lily genotypes (**Table 1**) representing three intrasectional (Asiatic, Longiflorum and Oriental) and four intersectional hybrid groups (LA, LO, OA, OT). Lesion development was quantified over the course of 3–4 days post inoculation (dpi). The experiments were conducted in four replicates over 2 years and each experiment contained 12 inoculation spots per genotype-isolate combination.

Disease assays in leaves distinguish sections and interspecific hybrids

Upon inoculation with conidial suspensions, disease symptoms initially appeared as small necrotic spots of brownish, collapsed abaxial epidermal tissue which were surrounded by a water soaked translucent area (Supplementary Figures S1 and S2). In the most susceptible genotypes the lesions became visible from 2 dpi onward (Supplementary Figure S2). In the following days, the necrotic areas expanded, a larger portion of the abaxial leaf epidermis collapsed and the mesophyll tissue started to shrink inwards until the necrotic tissue could be observed also on the adaxial side of the leaf. With disease progression, the typical fire blight ellipsoidal necrotic lesions developed and especially for the most virulent isolates, growth of fungal mycelium was observed on the dead leaf tissue. Moreover, a dark discoloration was observed in the leaf vasculature and leaf yellowing was observed at a distance from the necrotic lesion. Mock inoculated leaves remained symptomless for the entire incubation period (Supplementary Figure S2). At 4 dpi, symptoms were quantified by measuring the lesion diameter. Despite the variation in lesion diameters among the specific genotype-isolate combinations, a general trend was noticed. Upon inoculation with all *B. elliptica* isolates, lily genotypes belonging to the groups A, LA, and OA developed larger lesions when compared to genotypes belonging to the groups L, O, LO, and OT (**Figures 1** and **2**). As illustrated in Supplementary Figure S3, experiments in late spring (May–June 2019 and 2020) developed slightly larger lesions as compared to the experiments conducted in early spring (April–May 2019 and 2020). The largest variation in lesion diameter was observed among the groups A, LA, OA, and OT where lesion diameters ranged from 0 to 30 mm in the A genotypes and from 0 to 20 mm in the LA, OA and OT groups (**Figure 1**). By contrast, lily genotypes belonging to the groups L, O, and LO showed lesion diameters that ranged from 0 to 12 mm (**Figure 1**). This trend was consistently observed in both years and seasons (Supplementary Figure S3).

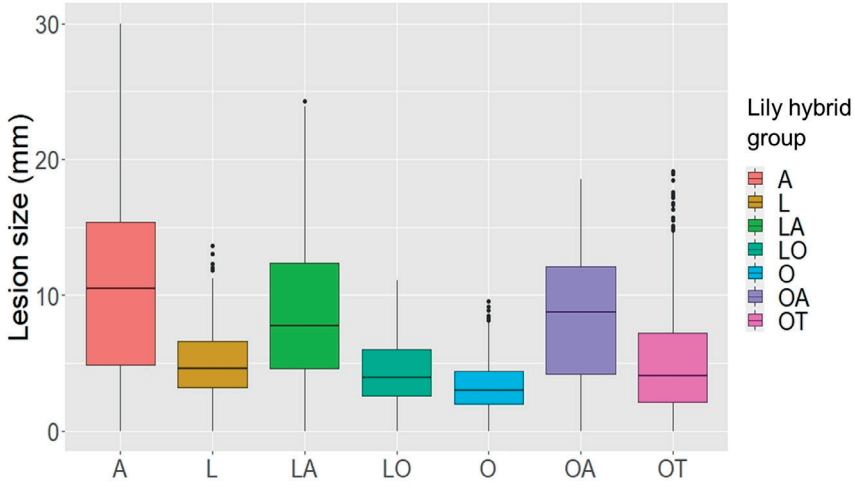

Figure 1. Lesion diameters at 4 dpi upon inoculation of 12 different *B. elliptica* isolates on leaves of seven different lily hybrid groups. Each box represents all compiled lesion diameters (in mm) for a given lily hybrid group in all four repetitions of the disease assays.

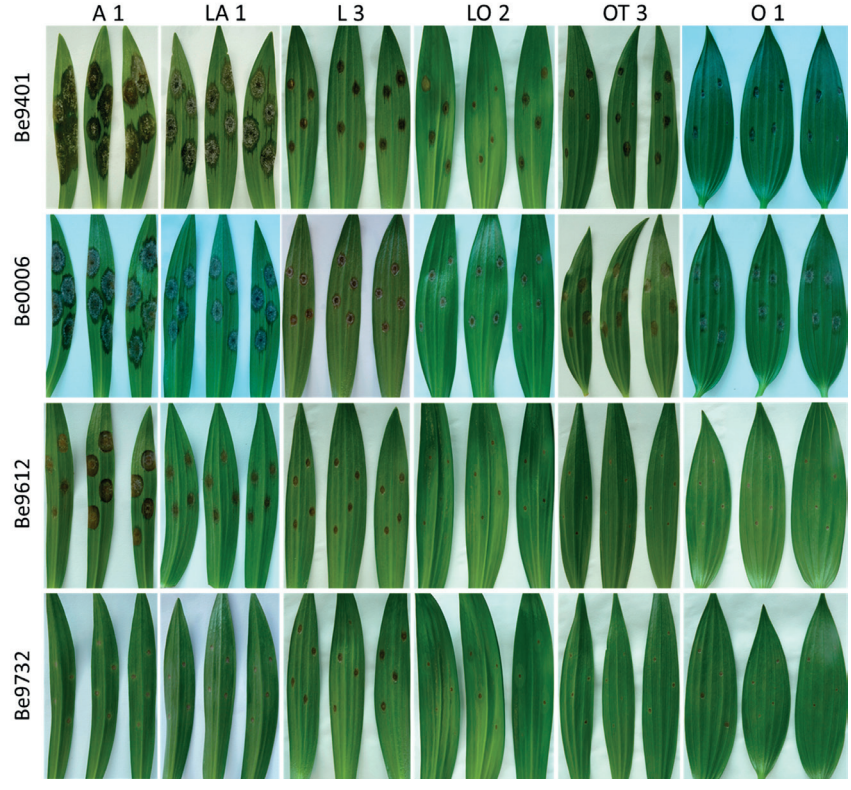

Figure 2. Necrotic lesions at 4 dpi upon inoculation with four distinct *B. elliptica* isolates (specified in left margin) on leaves of six lily genotypes (specified at the top). For each repetition of the disease assay, three representative leaves are shown.

Variation between lily genotypes within sections and interspecific hybrids

Differences in lesion diameters were not only detected between the different lily hybrid groups but also between individual genotypes within the same hybrid group (**Figure 3**). The most evident differences were observed when comparing lily genotypes of the groups A (**Figure 3A**), LA (**Figure 3B**), and OT (**Figure 3C**). In genotypes A 1 and A 2 the lesion diameters ranged from 15 to 25 mm, whereas in genotype A 3 only the more aggressive fungal isolates caused lesions larger than 10 mm (**Figure 3A**). In the genotypes LA 1 and LA 2 lesion diameters ranged from 15 to 20 mm upon inoculation with the more aggressive isolates whereas in genotype LA 3 the lesion diameters ranged from 10 to 15 mm (**Figure 3B**). In genotype OT 1 lesion diameters ranged from 12 to 18 mm whereas in genotypes OT 2 and OT 3 lesion diameters ranged from 4 to 12 mm (**Figure 3C**).

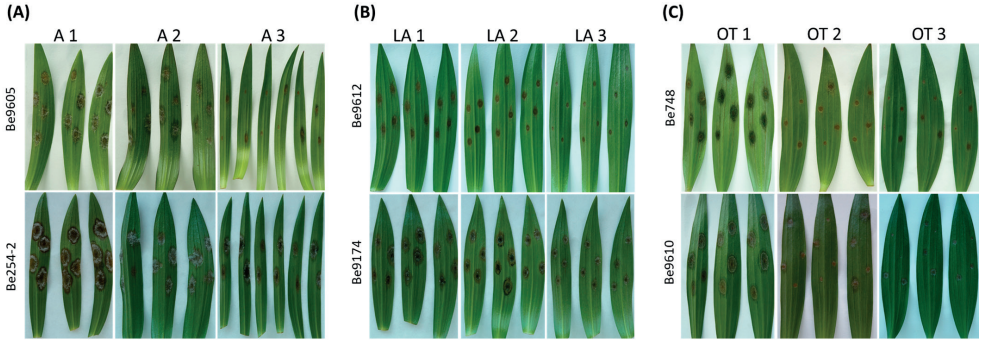

Figure 3. Necrotic lesions at 4 dpi on leaves of three different lily genotypes belonging to the hybrid group Asiatic inoculated with *Be*9605 and *Be*254-2 (**A**), hybrid group LA inoculated with *Be*9612 and *Be*9174 (**B**), and hybrid group OT inoculated with *Be*748 and *Be*9610 (**C**).

Variation in virulence between fungal isolates

The variation in lesion diameter and symptom development was also related to differences in virulence of the tested *B. elliptica* isolates (**Figures 2**, **4**). All 12 *B. elliptica* isolates were able to cause disease symptoms on leaves of all lily genotypes. Inoculation with *B. elliptica* isolates 9401 and 0006 resulted in lesions ranging from 10 to 30 mm on leaves of susceptible hybrid groups A, LA, and OA, and ranging from 8 to 20 mm on OT genotypes. These two isolates were classified as aggressive. By contrast, inoculation with *B. elliptica* isolates 9612, 9714, and 9732 resulted in lesions ranging from 3 to 12 mm in the susceptible hybrid groups A and LA, and even smaller lesions on less susceptible lily groups (**Figure 4**), classifying these three isolates as mild pathogens. The lesions diameters of the other seven isolates classified these as intermediate aggressive. All isolates, including the aggressive ones, developed lesions < 10 mm when inoculated on leaves of the groups O and LO and lesions < 15 mm on leaves of groups L and OT (**Figure 4**) confirming the relatively resistant nature of these lily hybrid groups.

Statistical analysis of the variation in lesion diameter in the disease assays on lily leaves

The linear mixed model of lesion diameter on leaves shows that diversity in both the fungal isolates and in the lily hybrid group, as well as the interaction between fungal isolate and lily group were the main contributors to the variation in lesion diameter (Table 3). The model shows that also the season and the interaction terms which included the season had a significant contribution on the variation in lesion diameter, while the year contributed to the variance only to a minimal extent (Table 3). Figure 5 and Supplementary Figure S4 show the differences in EMMs calculated for each lily hybrid group in the early and late spring, respectively (see also Supplementary Figure S2). Each colored dot represents the estimated difference of the lesion diameter in one particular *B. elliptica* isolate-lily hybrid group interaction in comparison to the lesion diameter for the same *B. elliptica* isolate during the interaction with a different lily hybrid group. Three main patterns can be recognized:

(1) For all isolates in both seasons, dots representing the groups A (red), LA (green), and OA (violet) show a positive value in differences of EMMs. This indicates that in general, all isolates caused bigger lesions when inoculated on genotypes of these groups in comparison to genotypes of the groups L, O, LO, and OT. On the other hand, dots representing the groups O (light blue), LO (blue-green), and OT (pink) show negative values in differences of EMMs indicating that in general all isolates caused smaller lesions when inoculated on genotypes of these lily hybrids in comparison to genotypes of the groups A, LA, and OA. Finally, EMMs calculated for the interaction of each *B. elliptica* isolate with genotypes of group L (brown dots) cluster around the base line and in most of the cases they remain within the confidence intervals.

(2) For the more aggressive isolates (*B. elliptica* 0006 and 9401), larger differences in EMMs are observed when comparing the interaction of these isolates with the different hybrid groups. This indicates that the plant genotype significantly influenced the outcome of the isolate - plant interaction.

(3) The differences in EMMs for the isolates *B. elliptica* 9612, 9714, and 732 showed little variation, both within lily groups and between groups.

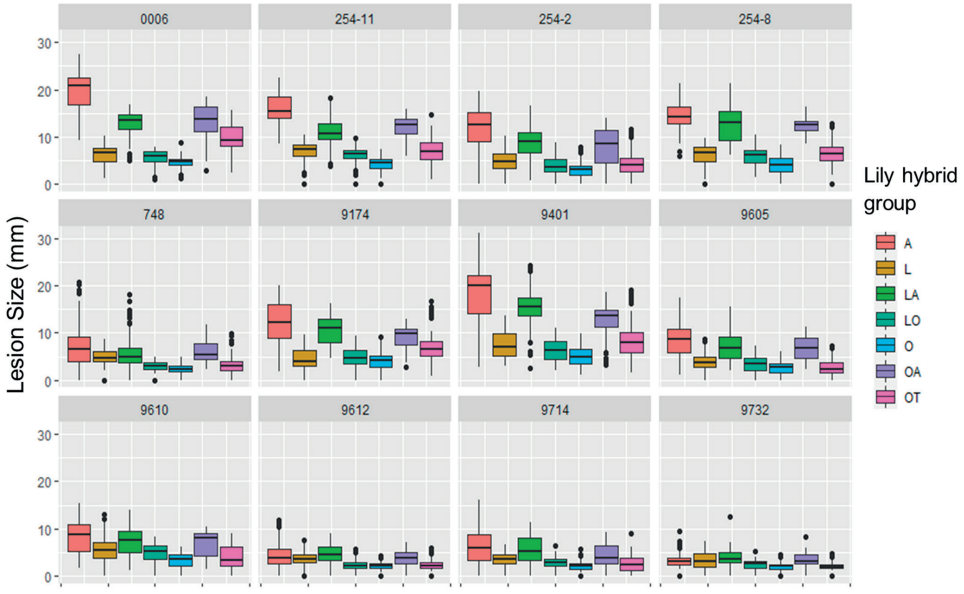

Figure 4. Lesion diameters at 4 dpi upon inoculation of 12 different *B. elliptica* isolates on leaves of 18 different lily genotypes. Lesion diameters measured in mm are plotted for each single isolate in 12 separate panels. Each of the colored boxes represents all lesion diameters measured for a given lily hybrid group in all four repetitions of the disease assays.

Table 3.

	Sum Sq	Mean Sq	NumDF	DenDF	F value	Pr(>F)
be	59305	5391.4	11	10272	960.3156	< 2.2e-16 ***
group	74220	12370.1	6	10272	2203.3600	< 2.2e-16 ***
season	7107	7106.6	1	10272	1265.8363	< 2.2e-16 ***
be:group	26653	403.8	66	10272	71.9296	< 2.2e-16 ***
group:season	247	41.2	6	10272	7.3365	7.62e-08 ***
be:season	1348	122.6	11	10272	21.8344	< 2.2e-16 ***
Random effects:						
Groups	**Name** (Intercept)	**Variance**	**Std.Dev.**			
Year		0.38747	0.62247			
Residual		5.61418	2.36943			
Number of obs: 10377, group; years, 2						

ANOVA results of the interaction in leaves between 18 lily genotypes and 12 *B. elliptica* isolates measured as lesion diameter. Type III Analysis of Variance with Satterthwaite's method. P-value ≤ 0.05.

Terms are as follows: be = the 12 *B. elliptica* isolates tested; group = the seven lily hybrid groups tested; season = early or late spring time period where the disease assays were conducted.

In addition, interactions of these factors were tested (:). The degrees of freedom and p-values are shown. The experiment tests the random effect of four independent replicate experiments.

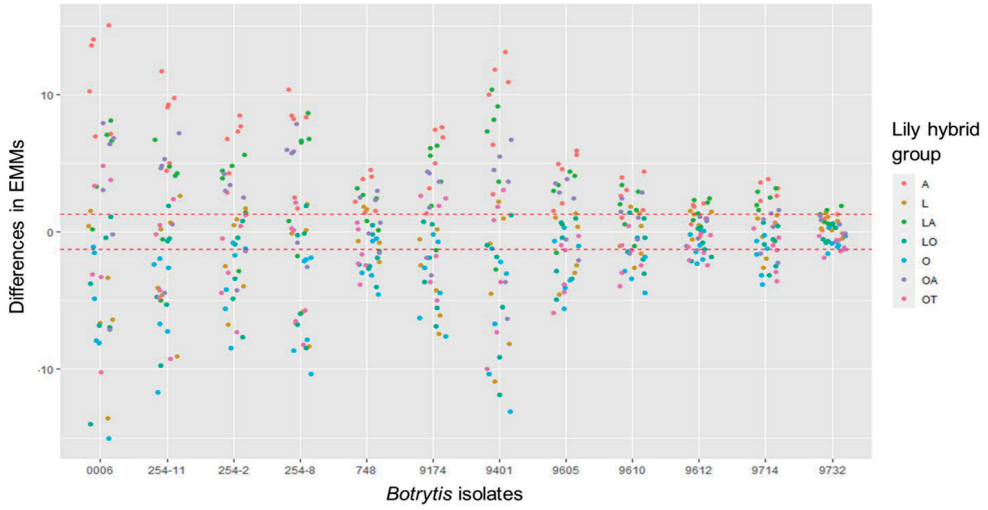

Figure 5. Dot plot showing differences in EMMs of lesion diameters on lily leaves in early spring for a given *B. elliptica* isolate, calculated using lily hybrid group as predicted factor. Red dotted line indicates the average p-value cut off for estimated differences which are significantly different from 0 ($p > 0.05$). P-values were adjusted using Tukey's comparison for a family of 84 estimates.

Disease assays in lily flowers

The most appreciated organ in lily is the flower and fire blight is known to affect also the reproductive organs, especially at the cut flower stage (Munafo and Gianfagna, 2011). We examined the susceptibility of flowers among representatives of the seven lily hybrid groups. A pilot experiment revealed that the conidial density for flower inoculation needed to be reduced to prevent excessively rapid lesion outgrowth. The optimal density for discriminative infection assays on flowers was $5x10^4$/mL conidia, while for leaves we used a density of 10^5/mL. For logistic reasons, the experiment could not be conducted with all 18 lily genotypes and 12 isolates. A panel of 12 lily genotypes (**Table 1**) was inoculated with three *B. elliptica* isolates (two aggressive isolates and one mild isolate; **Table 2**) and also one *B. cinerea* isolate and disease progression was monitored over time. *B. cinerea* was included because it was reported to cause necrotic lesions on lily flowers in the postharvest stage. Because cutting of the inflorescence caused natural perigone abscission upon prolonged incubation, even in mock-treated samples and symptoms on lily flowers developed faster than on leaves and the size of necrotic lesions on tepals was therefore measured at 3 dpi (**Table 4**). All three *B. elliptica* isolates and *B. cinerea* were able to cause disease symptoms on lily flowers. As depicted in **Figures 6**, **7**, flowers of lily genotypes belonging to the groups A and LA showed the most severe symptoms, irrespective of the isolate used. By contrast, lily genotypes of the groups O, LO, and OT showed smaller lesions upon inoculation with all four fungi (**Figure 6**, fifth and sixth column from the left). Inoculated flowers of L developed lesions with diameters that were in-between

those observed on the groups A, O, LA, LO, and OT. Differences in lesion diameters were also observed among the fungal isolates when tested on flowers. *B. elliptica* isolates 9401 and 0006 caused larger lesions on flowers of all lily genotypes tested, as compared to *B. elliptica* 9732 and *B. cinerea* (Figure 7 and Table 4). To compare *Botrytis* susceptibility of flowers and leaves as consistently as possible, we inoculated at the same spore density ($5x10^4$/mL) conidia of the same three *B. elliptica* isolates and *B. cinerea* on leaves which were detached from the same lilies used to perform the flower assays. Overall, it was observed that at 3 dpi, inoculated leaves of lilies belonging to the groups A, L, LA, and LO developed smaller lesions in leaves in comparison to flowers (Table 4). The trends in relative susceptibility between the hybrid groups and trends in differences in virulence among the isolates (Supplementary Figures S5 and S6) were consistent with trends observed in the leaf inoculations on the entire set of lily genotypes with all fungal isolates (**Figures 1**, **2**, **4**). We calculated the ratios of lesion diameters on flowers and leaves from the same plants at 3 dpi and observed that for genotypes from the groups A, L, and LA, those ratios exceeded 1.5 for all three *B. elliptica* isolates, indicating that flowers were substantially more susceptible than leaves. For genotypes belonging to the hybrid group OT, the ratios were <0.5, indicating that leaves were more susceptible than flowers. For genotypes belonging to the hybrid groups O and LO, the ratios differed depending on the genotype-isolate combination (Table 4). Inoculation with *B. cinerea* conidia resulted in development of lesions of highly variable sizes on flowers of all hybrid groups, except OT (no lesions). By contrast, *B. cinerea* caused only small necrotic lesions on leaves of genotypes belonging to the groups A and LA, but rarely caused any lesions on genotypes of the other groups (Table 4 and Supplementary Figure S6). The statistical analysis of the data for flower and leaf inoculations of cut lilies showed that the genetic diversity of fungal and plant genotype, and the interaction between fungal isolate–plant genotype significantly contributed to the variation observed in lesion diameter (Supplementary Tables 1 and 2). When the differences in EMMs were calculated for the lesion diameters observed on flowers and on leaves of cut lilies (Supplementary Figures S7 and S8), it was found that for all *Botrytis* isolates tested, dots representing the hybrid groups A (red dots) and LA (green dots) show a significant positive difference in EMMs. On the other hand, dots representing the groups O (light blue dots), LO (blue-green dots), and OT (pink dots) show negative differences in EMMs. The differences in EMMs calculated for the interaction of each *B. elliptica* isolate with L show a reduced spread and in several cases they remain within the confidence intervals. Moreover, it can be noticed that the differences in EMMs were larger when the interactions of the most aggressive *B. elliptica* isolates 0006 and 9401 with a given lily genotype were compared, while smaller differences in EMMs were observed for the milder isolates *B. elliptica* 9732 and *B. cinerea*.

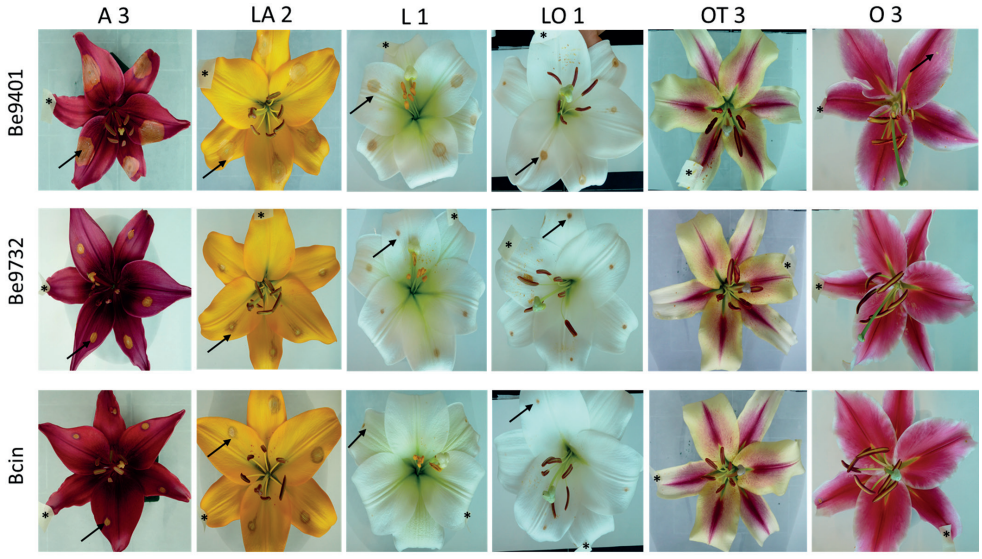

Figure 6. Necrotic lesions at 3 dpi upon inoculation of *B. elliptica* isolates 9401, 9732 and one *B. cinerea* isolate on flowers of lily genotype A 3, LA 2, L 1, LO 1, OT 3, and O 3. For each genotype, one representative flower is shown that was inoculated on five different tepals. Black arrows indicate necrotic lesions observed on the tepals. Mock inoculation was labeled with a piece of paper tape on the tepal and is marked with a black asterisk (*).

Table 4. Ratios between average lesion diameters (given in mm) on lily flowers and leaves inoculated with three different *B. elliptica* isolates and one *B. cinerea* isolate at 3 dpi. Ratio < 0.5, flower less susceptible than leaf (yellow); 0.5 < ratio < 2, flower equally susceptible as leaf (green); ratio > 2, flower more susceptible than leaf (red). F = flower; L= leaf.

	***B. elliptica* 9401**			***B. elliptica* 0006**			***B. elliptica* 9732**			***B. cinerea* B05.10**		
	F	L	Ratio F/L	F	L	Ratio F/L	F	L	Ratio F/L	F	L	Ratio F/L
A 1	22	10	2.2	27	12	2.3	7.5	3.8	2.0	14	2.4	5.8
A 3	19	9.1	2.1	20	9.5	2.2	7	3.0	2.3	3.8	2.7	1.4
LA 1	17	3.9	4.2	16	5.4	3.0	8.6	1.9	4.5	7.3	1.8	4.2
LA 3	25	5.8	4.2	20	6.2	3.2	7.4	3.0	2.5	8.7	2.5	3.5
L 2	11	3.0	3.6	11	2.8	3.9	1.9	0.3	6.0	3.4	0.1	34
L 3	10	2.5	4.1	8.0	2.7	2.9	3.0	1.2	2.6	1.4	0	-
LO 1	5.3	3.2	1.7	11	2.9	3.8	3.4	0.4	7.9	2.4	0	-
LO 2	1.9	3.4	0.6	7.2	4.3	1.7	1.9	1.8	1.0	4.2	0.6	6.7
OT 2	1.5	3.4	0.4	0	3.5	0	0	1.3	0	0	0	-
OT 3	0.4	2.5	0.1	0.2	3.4	0.1	0.4	1.7	0.3	0	0	-
O 1	1.0	0.8	1.2	2.7	2.6	1.0	0.4	0.1	3.1	2.4	0.2	12
O 3	3.0	1.5	2.0	4.2	2.0	2.2	0.1	0	-	2.8	0	-

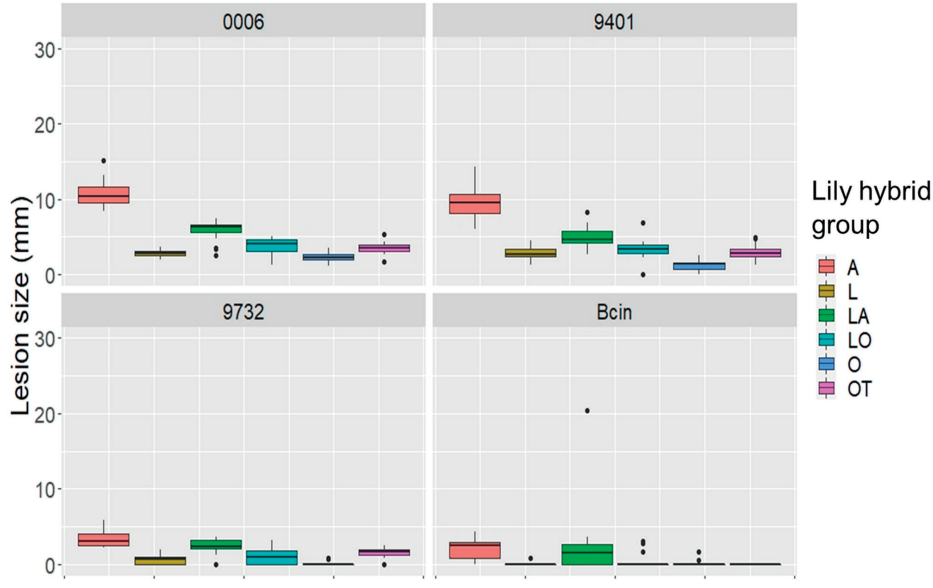

Figure 7. Lesion diameters at 3 dpi upon inoculation of *B. elliptica* isolates 9401, 9732, and 0006 and one *B. cinerea* isolate on flowers of 12 lily genotypes. Lesion diameters measured in mm of each single fungus are plotted separately in the four panels. Each of the colored boxes represents all lesion diameters measured for a given lily hybrid group.

Leaf infiltration assays with CF samples

Crude CF samples were collected from the same three *B. elliptica* isolates that were used in flower and leaf inoculations to test whether disease susceptibility and virulence correlate to effector sensitivity (of the lily genotype) and effector production (by the fungal isolate). CF samples were infiltrated in leaves of 12 lily genotypes (Table 1). At 3 days post infiltration, the leaf responses were observed (**Figure 8** and Supplementary Figure S2). Lily genotypes displayed cell death responses of the infiltrated leaf area to different extents. A severe cell death response (tissue collapse, drying and slight browning) was observed for genotypes from the groups A, L, LA (**Figure 8**) and OA (Supplementary Figure S2) when infiltrated with CF samples from the aggressive *B. elliptica* 9401 and 0006. By contrast, a mild response (translucence, discoloration and softening of infiltrated tissue) was observed for genotypes representing the groups O, LO and OT when infiltrated with CF samples from these same isolates. The infiltration of genotype L 3 with the CF from *B. elliptica* 9401 resulted in symptoms very distinct from other combinations, typified by a dark discoloration, yet with a transparent appearance indicative of severe tissue degradation (**Figure 8**). The response of genotype L 3 to CF samples from *B. elliptica* 0006 and 9732 was similar to that of many other genotypes tested. Moreover, CF from *B. elliptica* 9401 did not cause similarly dark, macerated tissues in other lily genotypes. There were no visible responses in any lily genotype to infiltration with the CF sample obtained from *B. elliptica* 9732 (**Figure 8**, third row). Leaf infiltration with culture medium in which no fungi were grown did not induce any visible symptoms (Supplementary Figure S2).

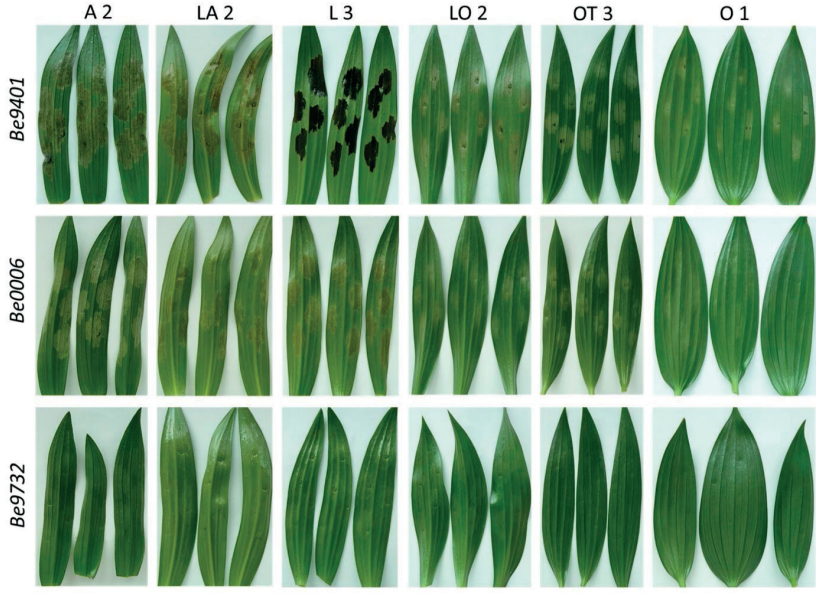

Figure 8. Cell death symptoms at 3dpi caused by infiltration of CF samples obtained from liquid cultures of three *B. elliptica* isolates (specified in left margin) on leaves of six lily genotypes (specified at the top).

DISCUSSION

Variation in fire blight susceptibility in *Lilium*

Our data unveil significant phenotypic variation in fire blight susceptibility within the phylogenetically complex genus *Lilium*. Genotypes belonging to the hybrid groups A, LA, and OA showed significantly more severe symptoms than genotypes of hybrid groups L, O, LO, and OT upon inoculation with all *B. elliptica* isolates tested (Figures 1, 2, 4, 5). This trend was consistently observed in all repetitions of the disease assays, both in leaves and flowers. These observations are in line with other studies, however our research provides more comprehensive data, as it included 18 lily genotypes, representing seven of the eight existing hybrid groups, as well as a set of 12 *B. elliptica* isolates collected over multiple years. Asiatic (A) hybrids are obtained from lily species which belong to the taxonomic section *Sinomartagon* that is closely related to *L. longiflorum* (L). On the other hand, Trumpet (T) hybrids are generated from species which are closely related to species of the section *Archelirion* from which Oriental (O) hybrids derive (Nishikawa et al., 1999; Arzate-Fernández et al., 2005; Shahin et al., 2014; Kim et al., 2019; Li et al., 2022). Intersectional hybrids LA, OA and OT were developed after chromosome doubling in the F1 progeny and backcrossing to A or O hybrids, respectively, in order to obtain a more vigorous, triploid genotype (van Tuyl and Arens, 2011). Breeding efforts have thus far predominantly focused on ornamental traits and to lesser extent on disease resistance. Genetic loci associated with resistance to *Fusarium oxysporum* f. sp. *lilii* and lily mottle virus were mapped via QTL analysis (Arens et al., 2014). However, traits and loci related to *Botrytis* susceptibility remain unknown. This may be due to the fact that resistance to necrotrophic pathogens is often inherited as a recessive and quantitative trait (Wolpert and Lorang, 2016; Kariyawasam et al., 2016; Liu et al., 2017; Koladia et al., 2017; Faris et al., 2020) and may have not been considered during the breeding selection. Although the A, LA, and OA genotypes tested were in general the more susceptible groups, there was substantial variation in lesion diameters and symptom severity between individual genotypes within these groups (**Figure 3A** and **B**). *Lilium* species of the section *Sinomartagon* (from which the Asiatic hybrids derive) are characterized by large genetic diversity because of their polyphyletic origin (Huang et al., 2018; Kim and Kim, 2018; Kim et al., 2019; Li et al., 2022). Our results suggest that traits for reduced fire blight susceptibility (i.e., quantitative resistance) may be present in the germplasm of the Asiatic hybrids. Depending on the genotype(s) of the parents and of the line to which the F1 hybrid was backcrossed, traits conferring recessive resistance to fire blight may have been retained to different extents in the genomes of the new hybrid genotypes. It remains important to investigate a wider assortment of Asiatic hybrids for fire blight susceptibility. On the other hand, different genotypes of the hybrid group Longiflorum, showed little variation in lesion diameter upon inoculation with all *B. elliptica* isolates (**Figures 1** and **Figure 4**). The genetic diversity of Longiflorum hybrid genotypes is narrower as compared to other

sections, because either a single or very few species have been involved in the generation of these hybrid genotypes (van Tuyl, 1985).

Flower pathology in *Botrytis-Lilium* interaction

Botrytis species are sometimes considered opportunistic pathogens which exploit wounded and senescing plant tissues to promote host infection. This assumption is supported by our results in the disease assays on flowers. Inoculated lily tepals developed larger necrotic lesions when compared to leaves of the same plant. Fungi of the genus *Botrytis* require PCD induction to infect plant tissue (van Kan, 2006; Veloso and van Kan, 2018) and during natural senescence of flower tissue, tepal cells begin to die before flower wilting becomes visible (van Doorn et al., 2003; van Doorn and Woltering, 2008; Rogers, 2013; Shibuya et al., 2016). In several monocot taxa (*Alstroemeria*, *Hemerocallis*, *Iris*, and *Lilium*) flower senescence shows typical hallmarks of PCD such as closure of plasmodesmata, starvation of tepal cells due to ATP depletion, formation of small vesicles, vacuolar swelling and tonoplast rupture. The progression of the PCD process involves the action of caspases and other intracellular proteases (Battelli et al., 2011), causing loss of cell integrity and breakdown of the cytoplasmic content including plastids and mitochondria, as well as the release of hydrolytic enzymes that degrade cell wall polysaccharides (van Doorn and Woltering, 2008; Rogers, 2013; Shibuya et al., 2016). Chromatin condensation and DNA fragmentation are considered as hallmark diagnostic features for PCD (van Baarlen et al., 2004; Yamada et al., 2006). Even though the PCD regulatory mechanisms at subcellular and molecular level are not fully understood, the micro-environment that is created during flower senescence (water-, sugar-, and amino acid-rich apoplast) represents an attractive growth substrate for necrotrophic pathogens. Therefore, the autonomous initiation and progression of PCD in cut flowers may benefit both *B. elliptica* and *B. cinerea* in their infection process and thereby cause larger lesions in lily flowers than in leaves. The disease symptoms on lily flowers upon inoculation with *B. cinerea*, which is not specific to lily (van Baarlen et al., 2004), were comparable to those caused by the mild *B. elliptica* isolate 9732. These observations suggest that these two fungi lack virulence factors that specifically promote infection in lily, however, they may benefit from the endogenous flower senescence process. The relative ranking of flower susceptibility of lily hybrid types to fire blight showed a similar pattern to that in leaves. A and LA genotypes showed significantly larger lesions on flowers when compared to O, OT, and LO, with L genotypes showing intermediate lesion diameters. The ratio of lesion diameters in flowers versus leaves of the same plants (**Table 4**) showed a pattern that yet remains to be understood. Flowers of genotypes from the groups A, L, and LA were more susceptible than their leaves. By contrast, the leaves of genotypes from the OT group were more susceptible than their flowers, while genotypes from the groups O and LO showed a mixture of ratios, depending on the genotype-isolate combination. Whether *B.*

elliptica uses different effectors for the infection of lily flowers and leaves will be subject of further studies.

Fire blight susceptibility and fungal virulence correlate to effector sensitivity and effector production

Botrytis elliptica secreted proteins can induce PCD when infiltrated in lily leaves (van Baarlen et al., 2004). We hypothesize that disease development in the *B. elliptica*-lily interaction is determined in a quantitative manner by the production by *B. elliptica* isolates of effector proteins that can induce PCD in the host, as well as by the sensitivity of lily genotypes to these effectors. CF samples from liquid cultures of *B. elliptica* were capable of causing cell death in lily leaves to different extents. Genotypes belonging to the hybrid groups A, L, LA, and OA showed a more severe necrotic response upon CF infiltration, as compared to genotypes belonging to the groups O, LO, and OT (**Figure 7** and Supplementary Figure S2F). These observations support the hypothesis that lily genotypes that developed the most severe disease symptoms in leaves and flowers were the same genotypes that showed a more pronounced necrotic response upon CF infiltration. Conversely, CF samples that caused the strongest necrotic response were obtained from *B. elliptica* isolates that caused the largest lesions on lily leaves and flowers in the disease assays, while CF from a less aggressive isolate caused little visible symptoms in any lily genotype. The response observed in Longiflorum leaves upon infiltration with the CF sample from *B. elliptica* 9401 was an outlier, despite the similar disease symptoms that this fungus caused upon inoculation. These leaves showed a much more severe response than all other infiltrated lily leaves. The infiltrated leaf segment had a dark brown color and yet appeared transparent, as if the tissue architecture was completely destroyed and the cell content dissolved. The dark pigmentation may derive from the combined activity of fungal and plant (poly)phenol oxidases which caused the oxidation of phenolic compounds released from dying lily cells during PCD (Schouten et al., 2002; Boeckx et al., 2015). At the same time, the leaf tissue collapse likely resulted from the action of fungal cell wall degrading enzymes in the CF sample, which cause maceration leading to loss of cell integrity and tissue architecture (van Kan, 2006). It is also important to consider that, differently from the situation in the disease assays, where necrotic lesions expand gradually over time upon fungal colonization, leaf infiltration with CF samples leads to the immediate and homogeneous exposure of all leaf cells to the PCD inducing compounds. Thereby, the activity of such compounds might become more effective and cause a stronger and faster response in the infiltrated leaf tissue. The physiological processes underlying the distinct response of the Longiflorum genotype could be unraveled by comparing the protein composition of CF samples from *B. elliptica* isolate 9401 with those of *B. elliptica* isolates 0006 and 9732, the latter two causing a milder response in Longiflorum leaves (**Figure 8**, second row). The broad spectrum of susceptibility (in the lily genotypes) and virulence (in the fungal isolates) suggests that there might be multiple effectors, each of them contributing

quantitatively to PCD induction. In the *Parastagonospora nodorum*-wheat interaction, nine distinct cell death inducing effectors have been reported, each requiring a specific plant susceptibility gene (Friesen et al., 2008; Friesen and Faris, 2010; Zhang et al., 2011; Friesen et al., 2012; Gao et al., 2015; Shi et al., 2015). Three of these susceptibility genes, *Snn1* (Shi et al., 2016), *Tsn1* (Faris et al., 2010) and *Snn3* (Zhang et al., 2021), have been cloned from wheat and appeared to encode proteins from distinct plant receptor genes families that also contain many resistance genes. Recent work (Downie et al., 2018) has identified several additional QTLs in wheat germplasm that might also be involved in effector recognition to mediate susceptibility. We hypothesize that the lily-*B. elliptica* interaction relies on similar effector-receptor interactions. At this point it is unknown how many effector proteins and their cognate receptors are at play in this plant-fungus interaction. The difference in susceptibility of the lily genotypes may be related to variation in the numbers and types of functional receptor proteins. In view of the huge genome size of lily, and the hybrid (diploid or triploid) nature of most genotypes, unraveling the molecular nature of such receptor genes will require a major effort. The *B. elliptica* effector proteins may be useful tools for mapping sensitivity genes and identify molecular markers for breeding purposes. The difference in virulence between fungal isolates may be related to the repertoire of active PCD-inducing effector proteins that they secrete. Whether the most virulent isolates produce a different spectrum of effector proteins or possess more active allelic variants, or they produce larger quantities of effector proteins, remains to be analyzed once such effector genes are identified. Our next step will be to use mass spectrometry and identify proteins in the crude CFs that were generated in this study. The annotated genomes of two *B. elliptica* isolates (Valero- Jiménez et al., 2019, 2020) are instrumental in the identification of effector genes.

Perspectives for lily breeding

We propose that the sensitivity of lily genotypes to *B. elliptica* effector proteins that induce PCD is predictive of the susceptibility of that individual plant to a fungal isolate that produces such effector(s). Given the logistic and experimental challenges of performing disease assays with living pathogens in a commercial breeding setting, PCD inducing proteins might provide an attractive alternative as prediction tool for fire blight susceptibility. Testing breeding material by a simple infiltration (of pure proteins or mixtures) and monitoring cell death responses presents a fast, low-tech solution to identify the most sensitive genotypes and eliminate them from the breeding program in early stages. This offers opportunities to pursue a breeding program only with a subset of breeding lines that will display increased fire blight resistance. Such an “effectoromics” approach has multiple advantages that will be discussed in more details in **Chapter 6**. Furthermore, the good correlation that was observed between leaf and flower susceptibility is an encouraging incentive to presume that leaf infiltration of effector proteins is also predictive for fire blight susceptibility in flower. After a cross it usually takes two years before new offspring

lilies will be able to flower and testing leaves as a proxy for flower susceptibility gains precious time and saves greenhouse space and labor enabling to extend breeding efforts. In other pathosystems, purified effectors have been implemented as tools to screen plant germplasm to predict disease resistance traits (Wolpert et al., 2002; Faris et al., 2010; Tan et al., 2012) and make recommendations to breeders. The development of a similar procedure to identify and eliminate the fire blight susceptible genotypes in a lily breeding population will support breeders in their efforts to develop new genotypes that may thrive with lower input of fungicide applications.

SUPPLEMENTARY MATERIAL

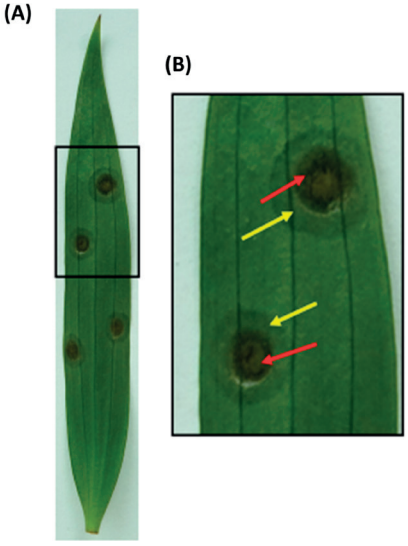

Supplementary Figure S1. (**A**) Fire blight symptoms observed upon conidia inoculation of *B. elliptica* isolates 9605 on leaf of lily genotype OT1 at 3dpi. (**B**) Zoom in of two representative necrotic lesions highlighted in the black quadrant in (**A**). Yellow arrows indicate area of leaf tissue showing translucence, softening and water soaking. Red arrows indicate necrotic collapsed leaf tissue.

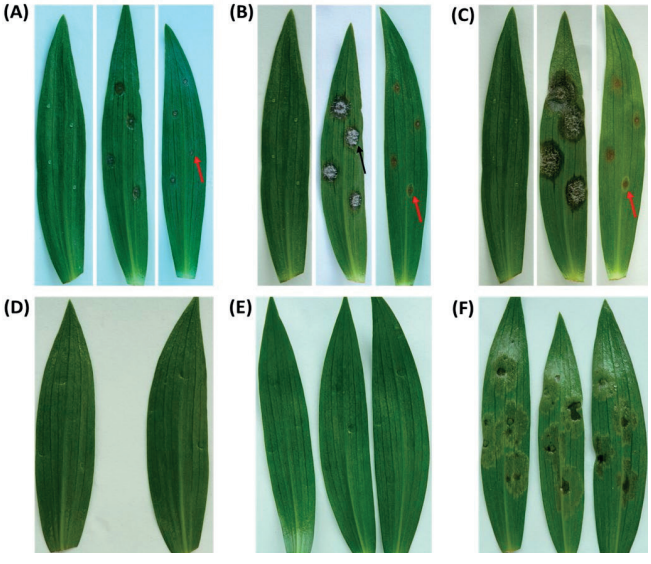

Supplementary Figure S2. Symptoms observed upon mock (left) and conidia inoculation of *B. elliptica* isolates 9401 and 9732 at 2 (**A**), 3 (**B**) and 4 dpi (**C**) on leaves of lily genotype OA. Red arrows indicate translucence and maceration around the necrotic spot. Black arrows indicate dark brown colouration in the leaf vasculature. Cell death response observed at 3 days post infiltration of mock liquid medium (**D**), *B. elliptica* isolates 9732 CF sample (**E**) and *B. elliptica* isolates 9401 CF sample (**F**) in leaves of lily genotype OA.

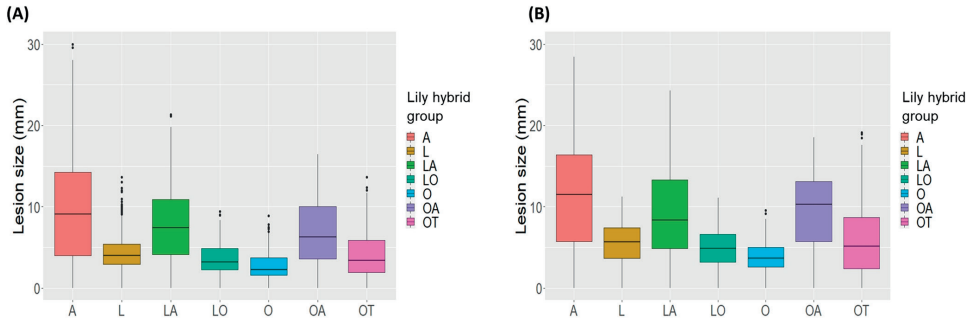

Supplementary Figure S3. Lesion diameters at 4 dpi upon inoculation of 12 different *B. elliptica* isolates on leaves of 18 different lily genotypes in early spring 2019 and 2020 (**A**) and in late spring 2019 and 2020 (**B**). Each box represents all compiled lesion diameters measured in mm for a given lily hybrid group in the two seasonal repetitions of the disease assays.

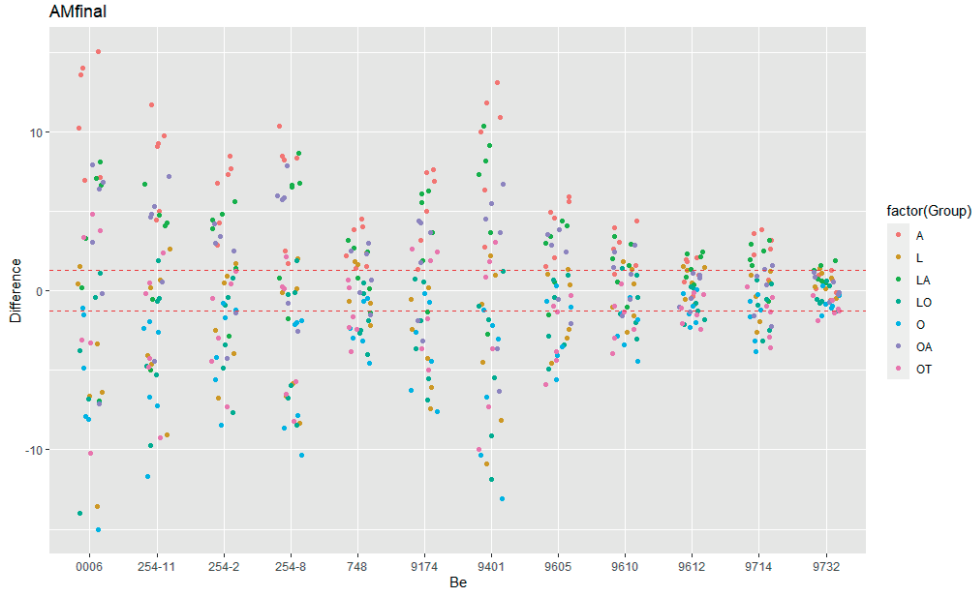

Supplementary Figure S4. Dot plot showing differences in EMMs of lesion diameters on lily leaves in late spring for a given *B. elliptica* isolate, calculated using lily hybrid group as predicted factor. Red dotted line indicates the average p-value cut off for estimated differences which are significantly different from 0 ($p>0.05$). P-values were adjusted using Tukey's comparison for a family of 84 estimates.

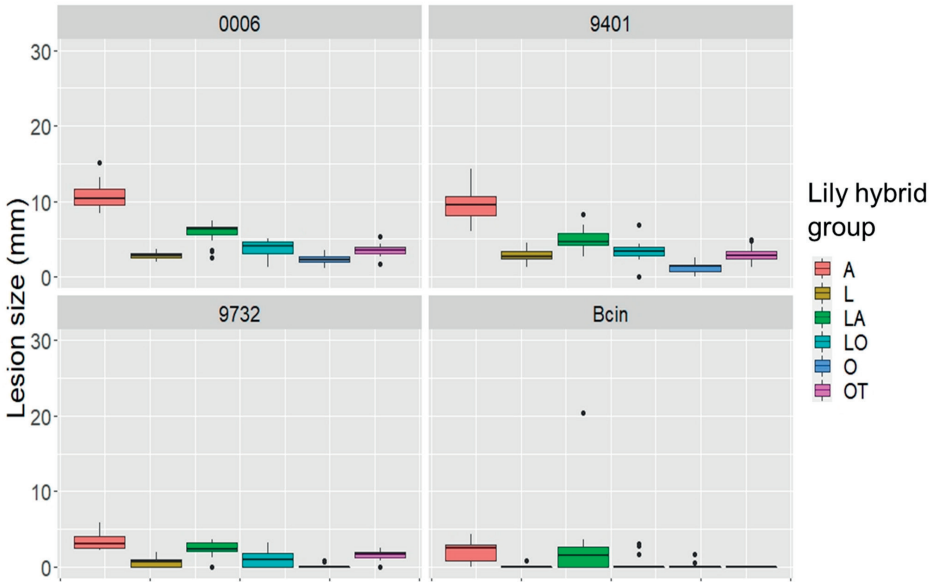

Supplementary Figure S5. Lesion diameters at 3 dpi upon inoculation of *B. elliptica* isolates 9401, 9732 and 0006 and *B. cinerea* isolate B05.10 on detached leaves of 12 cut lily genotypes. Lesion diameters measured in mm of each single fungus are plotted separately in the four panels. Each of the coloured boxes represents all lesion diameters measured for a given lily hybrid group.

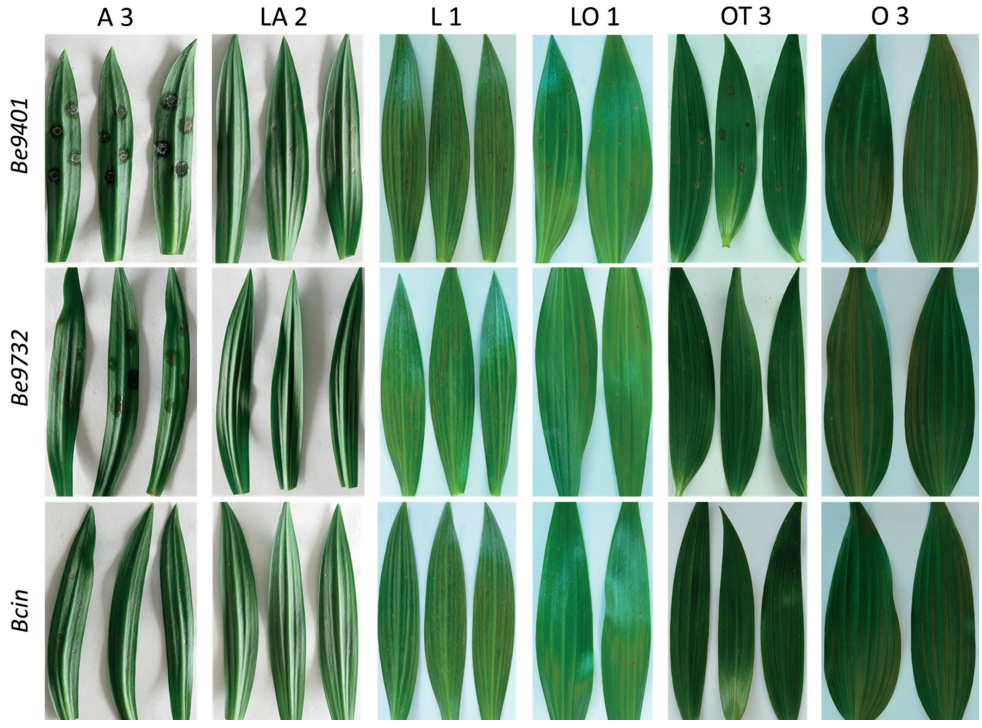

Supplementary Figure S6. Necrotic lesions developing at 3 dpi upon inoculation of *B. elliptica* isolates 9401, 9732 and *B. cinerea* isolate B05.10 on leaves of cut lily genotypes A3, LA2, L1, LO1, OT3 and O3 from which also the flowers were tested. For each genotype, 12 inoculations were performed on two or three leaves detached from fresh harvested lilies.

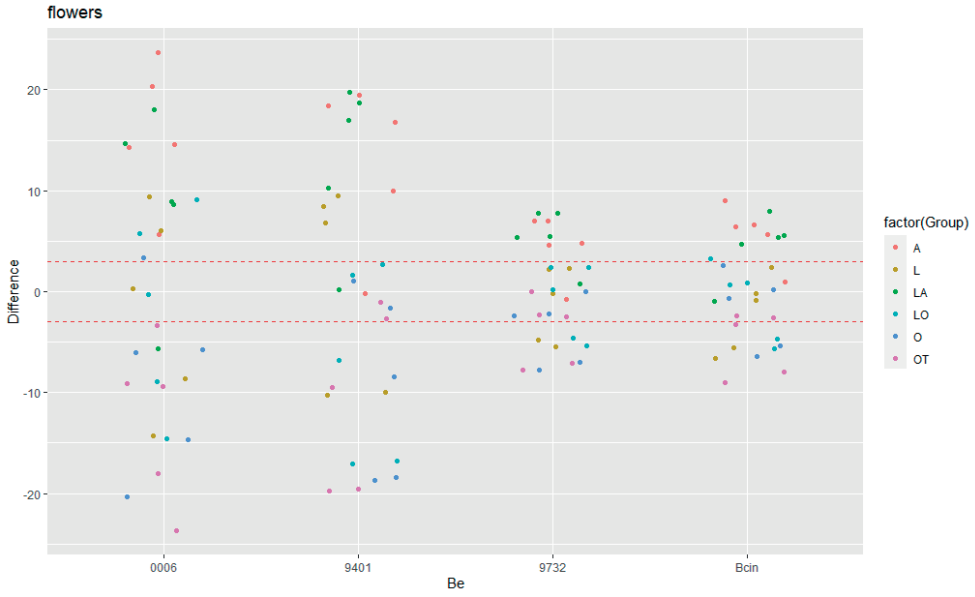

Supplementary Figure S7. Dot plot showing differences in EMMs of lesion diameters on lily flowers for a given *Botrytis* isolate calculated using lily hybrid group as predicted factor. Red dotted line indicates the average p-value cut off for estimated differences which are significantly different from 0 (p>0.05). P-values were adjusted using Tukey's comparison for a family of 24 estimated.

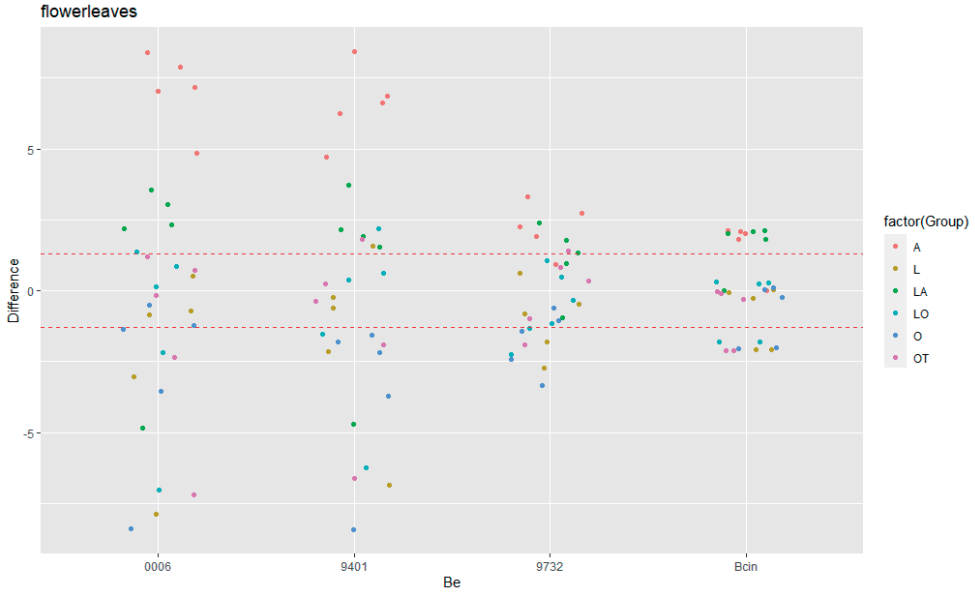

Supplementary Figure S8. Dot plot showing differences in EMMs of lesion diameters measured on leaves of lilies for a given *Botrytis* isolate calculated using lily hybrid group as predicted factor. Red dotted line indicates the average p-value cut off for estimated differences which are significantly different from 0 (p>0.05). P-values were adjusted using Tukey's comparison for a family of 24 estimated.

Supplementary Table 1.

	Df	Sum Sq	Mean Sq	F value	Pr (>F)
be	3	4926.5	1642.18	251.722	< 2e-16 ***
group	5	14858.4	2971.67	455.514	< 2e-16 ***
be:group	15	3610	240.7	36.895	< 2e-16 ***
Residual	456	2975	6.5		

ANOVA results of the interaction in flowers between 12 *Lilium* genotypes and three *B. elliptica* and one *B. cinerea* isolates measured as lesion diameter.
Analysis of Variance with Satterthwaite's method. P-value ≤ 0.05. The experiment tests the random effect of one experiment. Terms are as follow: be = the three *B. elliptica* and one *B. cinerea* isolates tested; group = the six lily hybrid groups tested. In addition, interactions of these factors were tested (:). The degrees of freedom and p-value are shown.

Supplementary Table 2.

	Df	Sum Sq	Mean Sq	F value	Pr (>F)
be	3	1637.2	545.7	331.74	< 2e-16 ***
group	5	1981.2	396.2	240.87	< 2e-16 ***
be:group	15	540.7	36	21.91	< 2e-16 ***
Residual	552	908.1	1.6		

ANOVA results of the interaction in leaves of cut lilies between 12 *Lilium* genotypes and three *B. elliptica* and one *B. cinerea* isolates measured as lesion diameter.
Analysis of Variance with Satterthwaite's method. P-value ≤ 0.05. The experiment tests the random effect of one experiment. Terms are as follow: be = the three *B. elliptica* and one *B. cinerea* isolates tested; group = the six lily hybrid groups tested. In addition, interactions of these factors were tested (:). The degrees of freedom and p-value are shown.

Chapter 3

Analysis of plant cell death inducing proteins of the necrotrophic fungal pathogens *Botrytis elliptica* and *Botrytis squamosa*

Michele C. Malvestiti[1], Maikel B.F. Steentjes[1], Sjef Boeren[2], Henriek G. Beenen[1], Jan A. L. van Kan[1] and Xiaoqian Shi-Kunne[1]

[1]*Wageningen University, Laboratory of Phytopathology, Wageningen, Netherlands,*
[2]*Wageningen University, Laboratory of Biochemistry, Wageningen, Netherlands*

ABSTRACT

Botrytis fungi are necrotrophic phytopathogenic Ascomycetes that kill the host cell to establish disease and colonize the plant. Cell death is achieved by mean of secreted necrotrophic effector proteins. In this study we aim to identify necrotrophic effectors in the sister species *Botrytis elliptica* and *Botrytis squamosa*, host specific in lily and onion, respectively. Despite their occurrence on different hosts, genomic and transcriptomic data suggested that both species share many orthologous genes encoding predicted effectors, some of which were highly expressed during infection in their respective hosts. To study the cell death inducing capacity of secreted proteins each species was grown in liquid culture and all secreted proteins were collected in culture filtrate samples. Infiltration of lily, onion and tobacco leaves with the culture filtrate samples caused a necrotic response. Mass spectrometry analysis revealed the presence of effector candidates as well as peptidases and plant cell wall hydrolases in both culture filtrates. Since the filtrate derived from *Botrytis elliptica* caused the most severe response in all tested plants and contained the highest number of effector candidates, this was further fractionated via ion exchange chromatography. Lily infiltration with the different protein fractions showed differences in necrotic response and an incremental necrotizing effect was observed when fractions were combined and simultaneously infiltrated. Mass spectrometry analysis of protein fractions identified one particularly abundant protein in the most active fractions. The corresponding gene was subsequently cloned and transformed into a yeast for heterologous expression. The purified protein was tested in different lily genotypes and it indeed caused a necrotic response. Differences in sensitivity for the effector protein were observed among the tested lilies. These findings indicate that necrotrophic effector proteins can be used to screen lily germplasm to identify genotypes that are insensitive to the protein and therefore likely to display increased resistance to *B. elliptica*.

INTRODUCTION

In the battle for survival, plant pathogenic fungi have evolved different strategies to colonize their hosts. While biotrophic fungi obtain nutrients from living host cells via specialized feeding structures, necrotrophs kill the cells of their host to acquire nutrients. For a long time, fungi with a necrotrophic lifestyle have been considered to invade their hosts in a rather unsophisticated manner. Using lytic and degradative enzymes, the fungus first kills and subsequently grows into host cells and eventually colonizes host tissue. In the past decades however, evidence has been accumulating that the interaction between necrotrophs and their hosts is more subtle and sophisticated than previously assumed. Necrotrophs actively induce plant cell death by co-opting the programmed cell death (PCD) machinery of the host using specialized necrotrophic effector (NE) proteins, to a certain extent similar to biotrophs (Dickman et al., 2001; van Kan, 2006). The induction of plant cell death using NEs is vital for the success of infection (Tan et al., 2010; Stergiopoulos et al., 2013; Veloso and van Kan, 2018). For some NEs the corresponding plant receptor proteins required for effector recognition and triggering of the cell death response have been identified (Schürch et al., 2004; Abeysekara et al., 2009; Gao et al., 2015; Shi et al., 2016). The cell death response to effectors of necrotrophs is based on similar mechanisms as the recognition of effectors from biotrophic pathogens, but leads to disease susceptibility instead of disease resistance as is the case for biotrophs (Lorang et al., 2007; Tan et al., 2010). The role of NEs in plant-pathogen interactions is best studied in Septoria Nodorum Blotch in wheat (*Triticum aestivum*, Poaceae), caused by the Ascomycota *Parastagonospora nodorum*. The first identified NE from *P. nodorum* was SnTox1, a small secreted protein that induced necrosis upon infiltration in wheat genotypes carrying the sensitivity gene *Snn1* (Liu et al., 2004). SnTox1 knockout mutants lost virulence on *Snn1*-carrying wheat lines, and introduction of the *SnTox1* gene into an avirulent *P. nodorum* isolate conferred pathogenicity on a wheat genotype harboring *Snn1* (Liu et al., 2012). By genetic analysis, more *P. nodorum* NEs and corresponding wheat sensitivity genes were identified such as SnToxA-*Tsn1*, SnTox4-*Snn4*, and SnTox6-*Snn6* (Abeysekara et al., 2009; Faris et al., 2010; Tan et al., 2012; Gao et al., 2015). To date, nine necrotrophic effectors and corresponding host sensitivity loci have been identified in the *P. nodorum*-wheat pathosystem (**Chapter 1**; Duba et al., 2018; Cowger et al., 2020). The severity of infection depends in a quantitative manner on the number and identity of pathogen effectors and corresponding wheat sensitivity genes (Oliver et al., 2012; Phan et al., 2016; Ruud et al., 2017; Haugrud et al., 2019). The broad host range model necrotroph *Botrytis cinerea* is also known to secrete proteins that induce cell death upon recognition by the host. *B. cinerea* endopolygalacturonases (PGs) induce cell death upon infiltration in *Arabidopsis thaliana*, but only in lines harboring leucine-rich repeat (LRR) receptor-like protein RBPG1 (Zhang et al., 2014). Other proteinaceous virulence factors that function as cell death inducers in *B. cinerea* are BcXyn11a, BcXyl1 and BcXYG1, hemicellulases that

cause necrosis in plant tissue independent from their catalytic activity (Noda et al., 2010; Zhu et al., 2017; Yang et al., 2018). In addition to the cell wall degrading enzymes with cell death-inducing capacity, often considered as PAMPs or catalytic necrosis-inducing proteins (NIPs), *B. cinerea* also secretes cell death-inducing NEs that lack a known enzymatic domain. Amongst others BcNep1, BcNep2, BcSpl1 and BcIEB1 have been heterologously produced and induced cell death upon infiltration in plant leaf tissue (Arenas et al., 2010; Frías et al., 2011; Frías et al., 2016).

The genus *Botrytis* comprises 40 described species of which a few, including *B. cinerea*, are generalist plant pathogens with very broad host ranges (Hyde et al., 2014; Garfinkel et al., 2017). Most *Botrytis* species, however, are considered host-specific since they are pathogenic on a single host or a few taxonomically related hosts. An inventory of polyphagy indices of *Botrytis* species (Mercier et al., 2019) indicated that *B. elliptica* (commonly considered to be a pathogen specifically to lily and known as "lily fire blight") was reported to infect as many as 21 host species from 10 distinct genera, and has a polyphagy index of 7.1. By contrast, its close relatives *B. deweyae*, *B. sinoalli* and *B. squamosa*, that cluster with *B. elliptica* in a subclade of the phylogenetic tree of the genus *Botrytis* (Valero-Jimenéz et al., 2020), have polyphagy indices below 1.5 (Mercier et al., 2019). This study focussed on *B. elliptica* and *B. squamosa*, two closely related sister species that are reported to cause disease in lily and onion, respectively. For both species, induction of PCD is a key step in the infection process and it is achieved by means of secreted proteins (**Chapter 2**; Van Baarlen et al., 2004; Steentjes et al., 2022). We aimed to analyze whether orthologous secreted proteins shared between these two closely related species possess cell death inducing capacity in their respective host and non-host plants. To achieve this goal, the genomes of *B. elliptica* and *B. squamosa* that were previously published by Valero et al. (2020) were improved by sequencing with Nanopore read technology and assembled to a higher quality than previously available, as described in Malvestiti et al. (2022). This Chapter will focus on the proteomic analyses that were performed to identify necrotrophic effectors in these two sister species and to assess their cell death inducing capacity *in planta.* After verifying the host specificity, the cell death inducing capacity of the culture filtrates (CFs) of *B. elliptica* and *B. squamosa* was compared. Then, the protein composition of the CFs and the expression of the corresponding genes during host infection were analyzed. Finally, one effector candidate was selected for heterologous expression and its cell death inducing capacity was tested via infiltration as single protein.

MATERIALS AND METHODS

Plant material and growth conditions

Lily genotypes used in this study (*Lilium* "Asiatic" A, "Longiflorum-Asiatic" LA, "Longiflorum" L, and "Oriental-Trumpet" OT) were planted as bulbs and grown as described in **Chapter 2**. *Nicotiana benthamiana* plants were grown in potting soil in a climate chamber with 16 h light at 24°C and 8 h darkness at 22°C and 75% relative humidity. Both disease and infiltration assays were carried out on leaves that were still attached to the plant. Onion plants (*Allium cepa* genotype Ceresco F1) were grown from seeds in potting soil in a climate chamber with 12 h light, 70% relative humidity, 18°C day temperature and 16°C night temperature. Fully grown leaves of 8 to 10 weeks-old onion plants were used for inoculation and infiltration assays. Disease assays were conducted on cut onion leaves, whereas for infiltration assays the leaves remained attached to the plant.

Fungal material and growth conditions

Botrytis elliptica isolate 9401 (**Chapter 2**), *Botrytis squamosa* isolate MUCL31421 (Steentjes et al., 2021) and *Botrytis cinerea* isolate B05.10 (Van Kan et al., 2017) used in this research were stored as conidia suspensions in 20% glycerol at -80°C. *B. elliptica* and *B. cinerea* were grown on Malt Extract Agar (50 g/L, Oxoid), whereas *B. squamosa* was grown on autoclaved onion leaves on top of water agar (Oxoid). Sporulation was induced by illumination with UV-A lamps. After harvesting, the conidia were collected and stored as described in **Chapter 2**.

Disease assays

Freshly harvested conidia of *B. squamosa*, *B. elliptica* and *B. cinerea* were inoculated on the different plants as described in **Chapter 2**. For onion, three detached leaves were first gently wiped with clean tissue paper to remove the epicuticular layer and then inoculated each with four 2 µL droplets per fungus. Two *N. benthamiana* plants were kept in the pot and placed in boxes containing water. Three leaves per plant were adaxially inoculated with each fungus by applying four droplets on distinct sectors of the leaves, avoiding leaf veins and edges. Each plant-fungus combination was inoculated in a separate box and incubated as described in **Chapter 2**. After four days of incubation, inoculated leaves were photographed and lesions were measured with a caliper. Lesion diameters were plotted using ggplot2 in R (Version 4.0.2).

Production of culture filtrate, ammonium sulfate precipitation and leaf infiltration

B. elliptica and *B. squamosa* Culture Filtrate (CF) samples were obtained by growing each fungus in a 250 mL flask containing 50 mL of liquid medium with 3 g/L Gamborg B5 salts (Duchefa, Haarlem, Netherlands), 10 mM KPO4 pH = 6, 0.1% D-Glucose and 5mL of lily or onion leaf extract in demi water, respectively. The leaf extract of both onion and lily was obtained as described in **Chapter 2**. The liquid culture was inoculated with a spore concentration of $1x10^5$ conidia/50 mL medium and grown in darkness in a shaker incubator (140 rpm, 20°C). After 5 days of growth, the CF was passed through a layer of Miracloth (Calbiochem, San Diego, CA, USA), filter-sterilized (0.45 µm pore size, Millipore, Amsterdam, Netherlands) and kept on ice. A mock liquid medium was prepared without fungal conidia. Of the ca 45 mL harvested CF samples, 2 mL were stored at 0°C for one night. To the remaining volume $(NH_4)_2SO_4$ (Millipore, Amsterdam, Netherlands) was gradually added and mixed on a rolling bench at 4°C until the CFs were saturated with salt. Samples were centrifuged 30 min at 4°C (4000 rpm). After centrifugation a solid pellet of precipitated compounds was collected. The pellet was redissolved in 10 mM KPO_4 pH = 6 and transferred to a prewetted dialysis membrane (Spectra/Por3 Dialysis Membrane 3.5 kD MWCO, Repligen), and dialyzed overnight at 4°C in 5 L 10 mM KPO_4 pH = 6. The dialyzed samples were collected and stored at 0°C until infiltration. The same plant genotypes used in the disease assays were tested for the infiltration assays. For lily, ca 100 µL of each sample (crude CFs, dialyzed pellets and mock liquid media) was infiltrated with a 1 mL syringe in two spots of two different detached leaves on their abaxial side. The leaves were placed in moist plastic boxes and incubated at 20°C under ambient light. The same volume of sample was infiltrated in two spots on two onion and *N. benthamiana* leaves that remained attached to the plant. After 3 days incubation all leaves were photographed and the response was evaluated using red light imaging (Landeo-Villanueva et al., 2021).

Ion Exchange Chromatography

Purification of protein fractions from *B. elliptica* CF was performed by ion exchange chromatography (IEX) using Streamline SP XL (cation exchanger, pH = 4.5) and Streamline Q (anion exchanger, pH = 8.5) (GE Healthcare, Uppsala, Sweden). 40 mL of CF sample was incubated over night with 3 mL of pre-equilibrated resin at 4°C on the horizontal rotor to allow proteins to bind to the resin. Next, the resin-CF homogenates were loaded onto a glass Econo-column (Bio-Rad) and washed with 5 mL 10 mM MES pH = 4.5, and 10 mM Tris-HCl pH = 8.5 respectively. Protein elution was carried oud stepwise with 5 mL 10 mM MES pH = 4.5, and 10 mM Tris-HCl pH = 8.5 containing KCl at different concentration as listed in Table 1. For all fractions the pH was adjusted to 6-7 before leaf infiltration. Fractions were infiltrated alone or in combination (1:1, v/v) on detached lily leaves, and the response was evaluated after 3 days incubation as described above.

Table 1. Protein fractions generated in this study

Fraction number	Salt concentration	Resin
1	65 mM KCl	Streamline SP XL
2	130 mM KCl	Streamline SP XL
3	65 mM KCl	Streamline Q
4	130 mM KCl	Streamline Q

Proteomic analysis

B. elliptica and *B. squamosa* proteins that were analyzed with mass spectrometry (MS) derived from CF samples collected from the fungal liquid cultures and IEX purified fractions. Proteins were prepared for MS as follows. Proteins present in 1 mL crude CF sample or in the IEX fractions were precipitated with 20% TCA . The precipitated pellets were boiled for 10 min in 20 µL Laemmli buffer (4% SDS; 20% glycerol; 125 mM Tris-HCl, pH = 6.8), loaded on precast stain-free protein gel (4–20% Mini-PROTEAN TGX Stain-Free, Biorad) and run for 15 minutes at 70 V. After running the gel was stained 30 min with Coomassie Brillant Blue (CBB 50%; 40% EtOH; 10% AcOH; 0.1% R250), washed two times with de-staining solution (AcOH/EtOH/MQ-H2O 10:30:60 v/v/v) and store in 50% MeOH at 4°C. Stained protein bands were cut with a scalpel in ca 1 mm^2 pieces and transferred to a clean 0.5 mL protein low binding tube. Then, cysteine disulfide bridges were reduced by adding 100 µL 10 mM dithiothreitol (DTT, 1.5 mg/mL) in 50 mM ammonium bicarbonate (ABC) pH=8 and by one hour shaking at 45°C. After cooling down to 20°C, DDT was replaced by 100 µL 15 mM acrylamide (1.1 mg/mL) in 50 mM Tris (pH = 8) for protein alkylation and the samples were shake incubated 30 min at 20°C. Subsequently the acrylamide was washed out two times with 50 mM ABC pH = 8 and the samples were frozen to facilitate trypsin digestion. Trypsin digestion took place by adding to the samples 100 µL trypsin solution (5 ng/µL trypsin in 50mM ABC pH = 8) and after overnight incubation on the shaking plate at 20°C. Two pieces of C18 Empore disk (3M Empore C18 Extraction Disks, Fisher) were tapped into a clean 200 µL pipet tip and washed with 200 µL MeOH. A 50% slurry of LichoprepC18 column matrix (LiChrosorb RP-8 HPLC Column, Merk) in MeOH was prepared and 4 µL of the 50% slurry were added into the MeOH containing 200 µL pipet tip. The 200 µL MeOH were pressed out with a 10 mL plastic syringe and fresh 100 µL MeOH were added. The column material was equilibrated once with 100 µL 1mL/L formic acid in water and the tryptic peptides were dissolved in 100 µL formic acid. The sample was added to the microcolumn and the gel pieces were washed once extra with 100 µL formic acid and add to the microcolumn. The microcolumn was transferred to a protein low binding 0.5 mL tube (Thermofisher) and 50 µL of 50% acetonitrile in formic acid were added to the microcolumn. Tryptic peptides bound to the column matrix were eluted with a syringe into a 0.5 mL protein low binding tube. The samples were then dried in a vacuum concentrator (Eppendorf Vacufuge) at 45 °C for 30 min until the volume decreased to 15 µL, and store at -20 °C. The samples were subjected to LC–MS/MS according to the parameters described

in (Xiong et al., 2020). For protein identification and quantification, each run with all MS/MS spectra obtained was analyzed with Maxquant 2.0.3.0 with the Andromeda search engine. *B. elliptica* and *B. squamosa* annotated genomes were used for protein mapping (Valero-Jiménez et al., 2020). A maximum of two missed cleavages and a mass deviation of 20 ppm for the fragment MS/MS peaks were allowed. The false discovery rate (FDR) was set to 1% on both peptide and protein level. The length of peptides was set to at least seven amino acids. Protein identification required minimally two distinct peptides of which at least one unique and at least one unmodified. Intensity based absolute quantification (iBAQ) algorithm was calculated as the sum of all peptide intensities divided by the number of theoretically observable tryptic peptides.

RNA extraction and gene expression analysis

For *B. elliptica*, RNAs used to create RNAseq library and to analyze gene expression profiles were isolated from 5 days old mycelial tissue of *B. elliptica* isolate 9401 grown on MAE plates and from lily leaf tissue of genotype "Asiatic" inoculated with conidia suspension. Infected tissue was collected at 16, 24 and 40 hours post inoculation (hpi), with three replicate samples per timepoint. RNA extraction was carried out from 100 mg freeze-dried, grinded material using the RNA extraction protocol of Maxwell® RSC Plant RNA Kit (Product AS 1500, Promega). For *B. squamosa* RNAs were extracted as described in Valero-Jiménez et al., (2020). RNAs of both *Botrytis* species were sequenced at Beijing Genomic Institute (BGI), Shenzhen, China. Mapping and quantifying gene transcripts from sequenced RNA-seq reads of both *B. elliptica* and *B. squamosa* were performed using Kallisto (Bray et al., 2016). The +1 log10 TPM value was calculated for plotting the expression heatmap.

BeE11 heterologous protein production and purification

B. elliptica effector candidate 11 (BeE11) was amplified from *B. elliptica* isolate 9612 gDNA (BELL_012g00260.1) with the addition of an 18-nucleotide extension that adds a tag of 6 histidine residues to the C-terminus of the coding sequence, using the following two primers.

pPic9k-BeE11 FW: GAGAGGCTGAAGCTTACGTAACCCTCGACCCCGCTACCTC

pPic9k-BeE11 RV: GCGAATTAATTCGCGGCCGCATGATGATGATGATGATGAACACAGTTCTTTC-CACC

The amplicon was cloned into the linearized plasmid pPIC9k (Invitrogen) under transcriptional regulation of a MeOH sensitive promoter. The recombined plasmid was used to electroporate *Pichia pastoris* isolate GS115 following the manufacturer instructions (Invitrogen). Yeast fermentation for protein production was performed as follows. Fresh *Pichia*

cells were first inoculated in 5 mL YPG (yeast extract 10%; peptone 20%; glycerol 20%) and shake-incubated 6 hours at 28°C (200 rpm). Then, 1 mL preculture was used to inoculate 100 mL BMGY medium (1% yeast extract, 2% peptone, 1.34% Yeast Nitrogen Bases without amino acids, 1% glycerol, 100 mM KPO_4 pH = 6, 2% 500x biotin) and incubated overnight at 28°C (200 rpm). The following day, 0.5 mL MeOH was added to the flasks to initiate BeE11 expression and the cultures were kept growing at 28°C (200 rpm). Two days later, the yeast was pelleted and resuspended in new flasks containing 300 mL of BMMY medium (1% yeast extract, 2% peptone, 1.34% Yeast Nitrogen Bases without amino acids, 0,5% MeOH, 100 mM KPO_4 pH = 6, 2% 500x biotin), and shake-incubated overnight at 28°C (200rpm). The next day, 1.5 mL MeOH was added and the culture grown for an additional day at 28°C (200rpm). After 4 days of fermentation the cultures were harvested, pelleted and the derived supernatant was stored at 0°C until purification. Affinity-based purification was done with HisPur Ni-NTA resin (Thermo Scientific). 1 mL resin was equilibrated in a glass Econo-column (Bio-Rad) with 15 mL wash buffer (150 mM $NaPO_4$, pH = 8.5; 300 mM NaCl and 10 mM imidazole). Next, the supernatant harvested from *Pichia* cultures was gradually poured into the column to allow protein binding to the resin. The resin was washed with 2 mL buffer and the protein was eluted in two steps with 2 mL elution buffer at increasing imidazole concentration, collected in 2 mL protein low binding tubes and dialyzed overnight in 2 L 10 mM KPO_4 (pH = 6) using a dialysis membrane (Spectra/Por 3 Dialysis Membrane 3.5 kD MWCO, Repligen). The dialyzed protein was concentrated in Amicon Ultra-0.5 Centrifugal Filter Units (Merk), quantified via Bradford assay (BioRad), adjusted to a concentration of 100 µg/mLwith 10 mM KPO_4 (pH = 6) and stored at 0 °C until use.

RESULTS

Host specificity of *Botrytis* species

To assess host specificity under laboratory conditions, we tested the virulence of *B. elliptica* and *B. squamosa* in their hosts and non-host plants and compared them to the broad host range pathogen *B. cinerea* (**Figure 1**). All three species were inoculated in onion, lily and *N. benthamiana* leaves and lesion development was monitored. The generalist *B. cinerea* developed expanding lesions exclusively when inoculated on *N. benthamiana* leaves (**Figure 1A**), whereas the lesions in lily and onion leaves remained limited to the size of the inoculation droplet. Lesion expansion and disease progression were observed when *B. squamosa* was inoculated in onion leaves (**Figure 1B**) and when *B. elliptica* was inoculated in lily leaves (**Figure 1C**). In contrast, when *B. squamosa* and *B. elliptica* were cross-inoculated in lily and onion, respectively, the primary necrotic lesions did not expand over time and except for a few cases, they remained limited to the size of the inoculation droplet. In addition, inoculation of *B. squamosa* and *B. elliptica* on *N. benthamiana* leaves did not cause formation of expanding lesions. In conclusion, *B. squamosa* and *B. elliptica* caused expanding lesions on their reported natural host but not on the other tested plants.

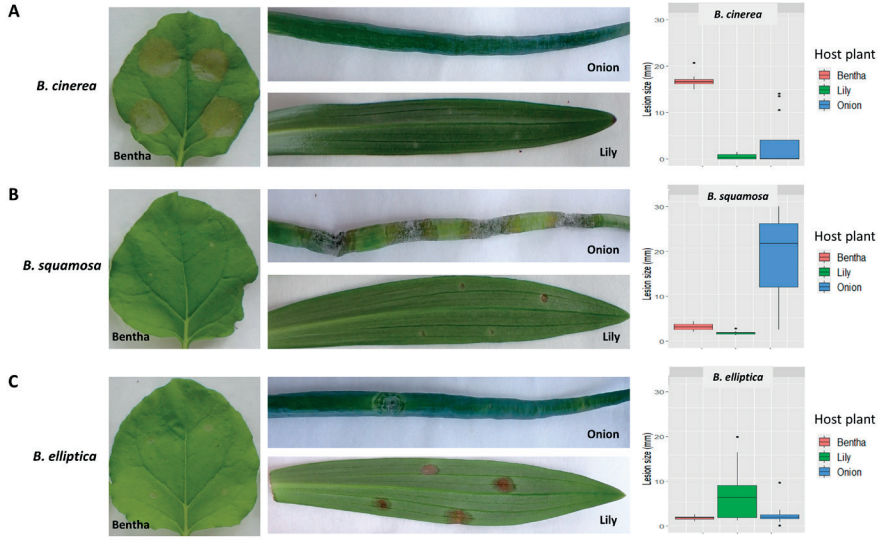

Figure 1. Inoculation of *B. cinerea* (A), *B. squamosa* (B) and *B. elliptica* (C) on *N. benthamiana*, onion and lily leaves confirms host-specificity. Disease symptoms were scored at 4 dpi and box plot diagrams represent the lesion diameters of the different Botrytis species on the respective plants. Each box represents all compiled lesion diameters (in mm) for a given host plant.

Liquid cultures of *Botrytis* species contain cell death inducing proteins

The analysis of the cell death inducing capacity of proteins secreted by the different *Botrytis* species was initiated by collecting culture filtrate (CF) samples from *B. squamosa* and *B. elliptica* grown in liquid cultures. The CFs were infiltrated into *N. benthamiana*, onion and lily to assess plant cell death responses. Plant responses were recorded at 3 dpi (**Figure 2**) and red light imaging (Landeo-Villanueva et al., 2021) was used to visualize plant cell death responses (Supplementary Figure S1). *B. elliptica* grown in presence of lily leaf extract, caused the most severe response in all tested plant species. Upon infiltration of this sample (CF number 1 in **Figure 2**, left panel), we observed collapse of the tissue, drying and intense yellowing/browning at the infiltrated area. By contrast, leaf infiltration with compounds collected from *B. elliptica* grown in presence of onion leaf extract (CF number 2 in **Figure 2** left panel) caused a milder response and only in lily leaves, where the infiltrated tissue showed a slight translucence. On the other hand, compounds collected from *B. squamosa* grown in presence of lily leaf extract (CF number 3 in **Figure 2**, left panel) caused a more severe response when compared to the compounds collected from *B. squamosa* grown in presence of onion leaf extract (CF number 4 in **Figure 3**, left panel). Both *B. squamosa* CF samples did not cause any clear response upon infiltration in lily and *N. benthamiana* leaves, although in the red light imaging system some cell death response could be observed (Supplementary Figure S1). When CF samples from *B. squamosa* grown in the presence of lily leaf extract were infiltrated in onion leaves, tissue collapse, drying and intense yellowing was observed. Infiltration of the medium used for the fungal liquid culture caused no detectable response in any of the tested plants (Supplementary Figure S1). CF samples contain proteins and secondary metabolites secreted by the fungus, both of which potentially possess cell death inducing capacity. To distinguish proteins mediated cell death inducing capacity from activity of other compounds, protein precipitation was performed to concentrate the proteins contained in the CF samples. After dialysis of the protein pellet, the samples were infiltrated in *N. benthamiana*, onion and lily leaves. Precipitation of the proteins did not notably affect the cell death inducing capacity of *B. elliptica* proteins, since the precipitated proteins derived from *B. elliptica* liquid culture grown in presence of lily leaf extract showed again the strongest cell death inducing capacity in all tested plants (sample A in **Figure 2**, right panel; Supplementary Figure S2). The symptoms appeared similar to those observed upon infiltration of the crude CF. In contrast, precipitation of the proteins contained in *B. squamosa* CF sample grown in presence of lily leaf extract resulted in substantial loss of cell death inducing capacity in onion leaves (**Figure 2**, right panel sample C; Supplementary Figure S2). Infiltration of the dialysis buffer caused no visible response in any of the plants tested (Supplementary Figure S2).

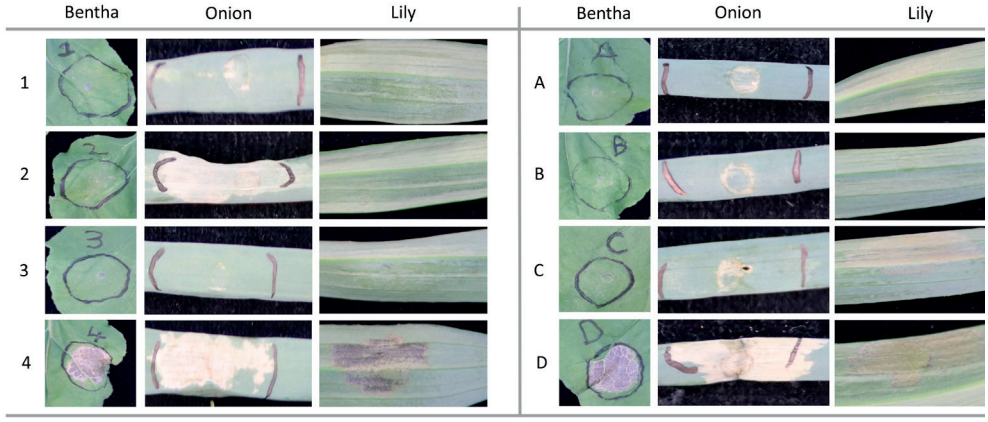

Figure 2. Leaf responses observed at 3 dpi caused by infiltration of crude CF samples (left panel) and AS precipitated compounds (right panel) obtained from liquid cultures of *B. elliptica* and *B. squamosa,* grown in two different media, on leaves of *N. benthamiana*, onion and lily. 1 = *B. elliptica grown* in GB5_lily; 2 = *B. elliptica* grown in GB5_onion; 3 = *B. squamosa* grown in GB5_lily; 4 = *B. squamosa* grown in GB5_onion. (A) = AS precipitation of *B. elliptica* CF grown in GB5_lily; (B) = AS precipitation of *B. elliptica* CF grown in GB5_onion; (C) = AS precipitation of *B. squamosa* CF grown in GB5_lily; (D) = AS precipitation of *B. squamosa* CF grown in GB5_onion.

Protein composition of the cell death inducing CF samples

The identity of the proteins contained in the CF samples that showed cell death inducing capacity was analyzed by mass spectrometry. The *B. elliptica* CF sample contained significant matches for a total of 166 proteins in the predicted secretome (Supplementary Table 1 and 2). More specifically, we detected 67 Carbohydrate-Active Enzymes (CAZymes, 40% of total number), 15 putative effectors (9%), 34 oxidoreductases (19%) and 22 proteases (13,5%). The remaining proteins represented enzymes related to lipid metabolism, different phosphatases, sugar and ion transporters, or proteins without a described domain. In the *B. squamosa* CF sample, 114 proteins with a predicted signal peptide could be detected. Compared to the CF of *B. elliptica*, the *B. squamosa* CF sample contains a considerably higher proportion of CAZymes (69, corresponding to 60% of the total number) but a lower proportion of proteases (7%) and only three putative effectors. Orthology analysis identified 85 protein orthogroups, all containing one single member from *B. elliptica* and one from *B. squamosa* (**Figure 3**, Supplementary table 2). Only two orthogroups consisted of proteins predicted to be putative effectors: G17 (ortholog to *B. cinerea* Spl1, Frías et al., 2011) and G58, a small (16 KDa) cysteine-rich protein of unknown function. Both CFs also contained a protein with a chorismate mutase domain that carries a predicted chloroplast targeting peptide (G63). To investigate the potential contribution to virulence of the 85 shared proteins detected in the CF samples, we analyzed the transcript levels of their corresponding genes at different timepoints during host infection (Supplementary Data 1). **Figure 3** shows a heatmap of the gene expression profile of orthologous genes of

B. squamosa and *B. elliptica* during infection. When examining the transcript levels in the two *Botrytis* species, three orthogroups displayed relatively high expression at 40-48 hpi: G17, G49 and G50. In contrast, other orthogroups had the highest relative expression at 16 hpi (G24, G29, G46, 58, 62 and 84) in both *B. squamosa* and *B. elliptica*. G24 encodes a putative endoglucanase (GH12) and G58 is predicted as a putative effector. Some orthologs showed different expression patterns between the two fungi, such as G09, G11, G18, G21, G23, G35 and G38. For instance, the orthogroup G21, which encodes a polygalacturonase also found in *B. cinerea*, was relatively highly expressed throughout infection in *B. elliptica*, but not in *B. squamosa*.

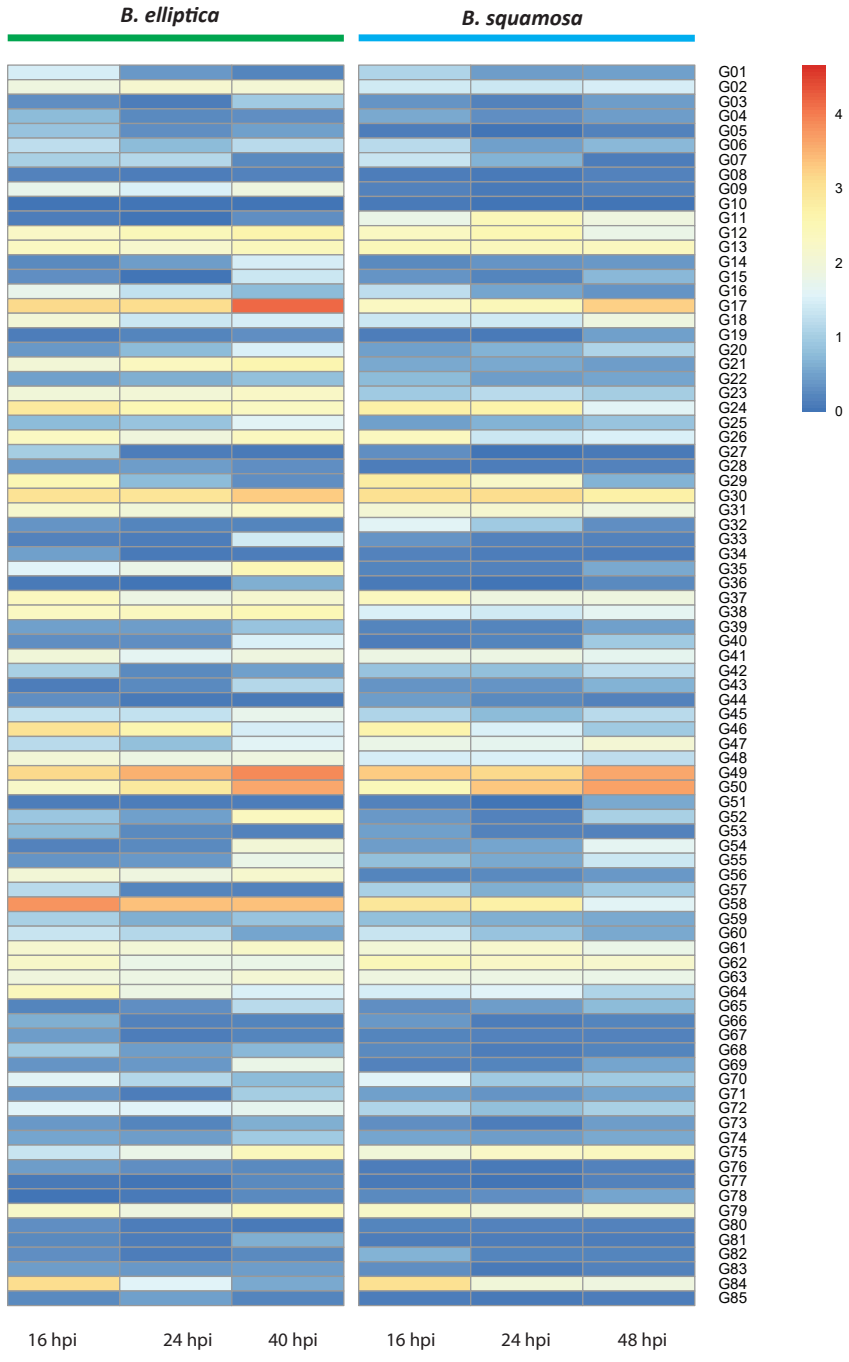

Figure 3. Heatmap showing expression profiles of genes of which the proteins were identified in the CF samples of both *B. elliptica* and *B. squamosa*. Genes from both species that belong to the same orthogroups are aligned horizontally. Expression is based on the average of three replicate RNAseq samples during different timepoints of infection of *B. elliptica* and *B. squamosa* on their respective host plants.

Cell death inducing capacity of protein fractions and heterologously expressed BeE11

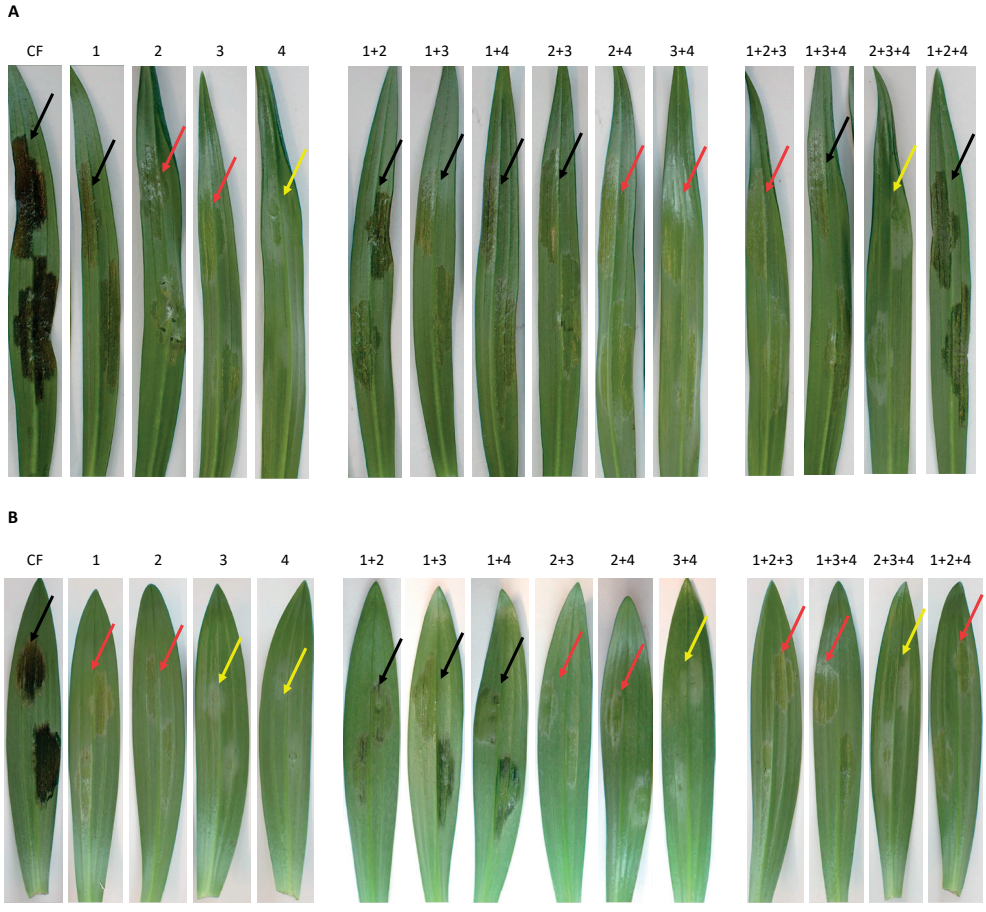

Figure 4. Leaf responses observed at 3 dpi on lily genotype LA (**A**) and L (**B**) upon infiltration of crude CF samples and protein fractions alone or in combination. Numbering of protein fractions 1, 2, 3 and 4 refers to the list in Table 1. Leaf tissue responding only with superficial maceration and translucence is indicated by yellow arrows. Leaf tissue responding with collapsing of epidermal and mesophyll layer is indicated by red arrows. Leaf tissue responding with melanization is indicated by black arrow.

Since the CF sample derived from *B. elliptica* liquid culture contained the highest number of effector candidates and caused the most pronounced necrotic response in all tested plants (**Figure 2**), the proteins contained in this sample were purified and fractionated via IEX and subsequently infiltrated in lily leaves (**Figure 4**). First of all, the leaf response in two lily genotypes shows that fraction 1 displayed the strongest necrotizing effect among the four fractions tested. In addition, an incremental necrotizing effect could be observed

when some of the fractions were infiltrated in combination compared to single fraction infiltration as in case of fractions 2+3 compared to fraction 2 and 3 alone. However, when fraction 2, 3 and 4 were combined, the leaf response showed only translucence as in case of fraction 4 infiltration alone. Moreover, when taking a closer look at the infiltrated tissue, three different types of responses could be distinguished. The most severe response was visible as brown, dry, melanized necrotic tissue (**Figure 4**, black arrows). This response was observed in all cases when fraction 1 was infiltrated alone or in combination with fraction 2 or 3 but not when fractions 1, 2 and 3 were all combined. Collapsed leaf epidermis and mesophyll (**Figure 4**, red arrows) were observed upon infiltration of fraction 2 or 3 alone, and in combination with fraction 4. The weakest response, visible as translucent tissue with only superficial maceration, was observed upon infiltration of Fraction 4 alone and in combination with fractions 2 and 3 together (**Figure 4**, yellow arrows). Protein composition of the different fractions was analyzed by mass spectrometry (Supplementary Table 2). One particular effector candidate (BeE11) was among the most abundant proteins in the fractions displaying the strongest necrotizing activity (fractions 1 and 2). This protein corresponds to the orthogroup G58 (**Figure 3** and Supplementary Table 1) which showed high transcript level in early stage of infection of both *B. elliptica* in lily and *B. squamosa* in onion. Therefore, BeE11 was selected for heterologous expression in *Pichia pastoris* to test the cell death inducing capacity when infiltrated as single purified protein. After yeast fermentation and His-tag affinity purification, a protein band was detected via immunoblotting at the expected size of 15-20 kDa (Supplementary Figure S3). The purified BeE11 protein was infiltrated in different lily genotypes and in *N. benthamiana* leaves at a concentration of 100 µg/mL. At 3 dpi only the lily genotype OT and *N. benthamiana* showed signs of tissue damage, which became visible as collapsed and darkened epidermal tissue in lily OT (**Figure 5A**), whereas *N. benthamiana* showed a more pronounced yellowing and drying at the infiltration spot (**Figure 5B**). On the other hand, infiltrated leaves of lily genotypes LA and L did not show any visible tissue damage. When the leaves were analyzed by light imaging, red light emission was detected from all infiltrated plants (**Figure 5A** and **B**, right panels), whereby the signal intensity appeared higher in the lily OT and in *N. benthamiana*.

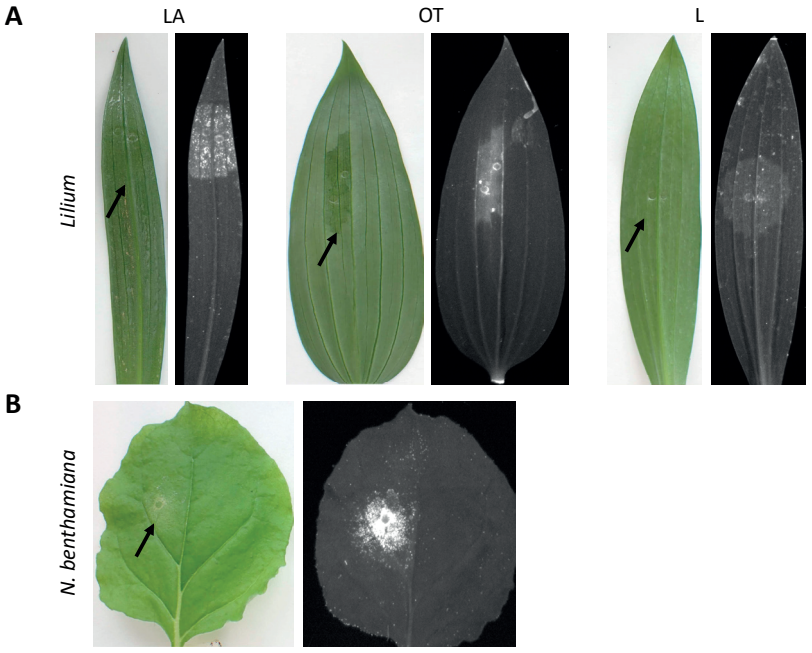

Figure 5. Leaf responses observed at 3 dpi in leaves of different lily genotypes (**A**) and *N. benthamiana* (**B**) upon infiltration of purified BeE11 visualized with normal light (left) and by red light emission. Black arrows indicated infiltrated leaf area.

DISCUSSION

Previously, the genomes of 16 *Botrytis* species were analyzed to identify unique genes that encode virulence factors associated to host specificity (Valero-Jiménez et al., 2020). However, no specific elements were found, suggesting that host specificity may be determined by a combination of different (quantitative) traits rather than by presence or absence of unique virulence factors. The aim of this study was to analyze shared features in the secretome of *B. elliptica* and *B. squamosa* that contribute to cell death induction and virulence on their host and non-host plants. This was done by comparing their genomes and by testing the cell death inducing capacity of their secreted proteins. Genome sequences were available for both species (Valero-Jiménez et al., 2020). However, since *B. elliptica* isolate 9401 was more virulent than the isolate *B. elliptica* 9612 previously sequenced by Valero-Jiménez et al. (2020) (**Chapter 2**), we newly sequenced *B. elliptica* isolate 9401 and further improved the assembly of the *B. squamosa* reference genome. The new genome assemblies of *B. elliptica* 9401 and *B. squamosa* MUCL31421 provided more accurate secretome (Malvestiti et al., 2022). The predicted secretomes of *B. squamosa* and *B. elliptica* were more similar to each other than either of the two species resembled the *B. cinerea* secretome, in concordance with their recent divergence and larger evolutionary distance to *B. cinerea*. When the composition of the proteins secreted by *B. elliptica* and *B. squamosa* in liquid cultures was analyzed, the *B. elliptica* CF sample contained a larger diversity of proteins than the *B. squamosa* CF sample. Upon leaf infiltration, the *B. elliptica* CF sample caused cell death not only in lily, but also in onion and *N. benthamiana* (**Figure 3**). On the other hand, the *B. squamosa* CF samples only caused severe necrotic responses in onion leaves. In addition, an incremental necrotizing activity was observed when some of the purified protein fractions were simultaneously infiltrated in lily (**Figure 4**). These observations suggest that the larger diversity and combined activity of *B. elliptica* secreted proteins might cause cell death not only in lily (Liliaceae), its natural host, but also in phylogenetically distant plant species such as *N. benthamiana* (Solanaceae) and onion (Amaryllidaceae). This hypothesis is supported by the fact that cell death induction and plant susceptibility in plant-necrotroph interactions often correlate in a quantitative manner. In the wheat-*P. nodorum* interaction, the quantitative level of plant susceptibility is correlated to the number of cell death inducing effectors that are produced by the fungus and the number of effector target loci present in the host (Tan et al., 2012; Haugrud et al., 2019). In addition, during fungal infection cell death inducing proteins are gradually expressed and secreted by the fungus and their levels must be sufficiently high to induce cell death responses that facilitate fungal colonization. Tests with CF samples and purified protein fractions can only partly mimic the events occurring during fungal infection. However, the response severity observed upon crude CF sample infiltration could not be reconstituted by any of the combinations of protein fractions that we tested. Moreover, in some cases infiltration of combined fractions caused a reduction in the severity of the leaf response compared to infiltration of a single fraction. This observation suggests that

some proteins may interfere with the necrotizing activity of other proteins when they are infiltrated in a mixed solution. The milder response may rely on disturbed biochemical interactions between putative necrotrophic effectors and their targets in the plant cell whereby the effector cannot be recognized and trigger cell death induction. CF samples that could induce host cell death in onion or lily contained subsets of (predicted) effectors as well as CAZymes and several proteases. The samples of *B. elliptica* and *B. squamosa* contained proteins that could be grouped into 85 orthogroups shared between the species. Not all genes in these orthogroups were expressed during host infection, suggesting that they may have different roles in the biology of these pathogens. RNAseq data of *B. elliptica*-infected lily and *B. squamosa*-infected onion revealed that 15-20 genes in each of the species display significant expression, including a subset of genes that displayed a transient expression peak in early phases of infection. Orthogroup G58, encoding a putative effector (BeE11), was particularly interesting since it was the most abundant effector candidate in the protein fractions displaying the strongest necrotizing activity. Therefore, BeE11 was selected for heterologous expression, to test its cell death inducing capacity when infiltrated as single protein. Upon BeE11 infiltration in three lily genotypes, differences in response severity were observed among the tested lilies, and these responses correlated with the susceptibility of the genotypes to *B. elliptica* isolate 9401 (**Chapter 2**). This observation indicates that differences in BeE11 sensitivity might be present in the lily germplasm and therefore, BeE11 can be implemented as biological tool to screen for insensitive lily genotypes with the prediction that those will display reduced susceptibility to *B. elliptica*. Moreover, a cell death response was observed also upon BeE11 infiltration in *N. benthamiana* leaves. This suggests that BeE11 cell death inducing capacity might not be restricted to lily since the orthologous gene is found also in *B. squamosa* and *B. cinerea*. The plant cellular target required for BeE11 recognition and PCD induction could be identified by searching for plant proteins which bind to the effector via proximity labelling (Qin et al., 2021). Finally, the contribution to fungal virulence of BeE11 remains to be assessed by generating CRISPR/Cas9-mediated deletion mutants (Leisen et al., 2020; Leisen et al., 2022).

SUPPLEMENTARY MATERIAL

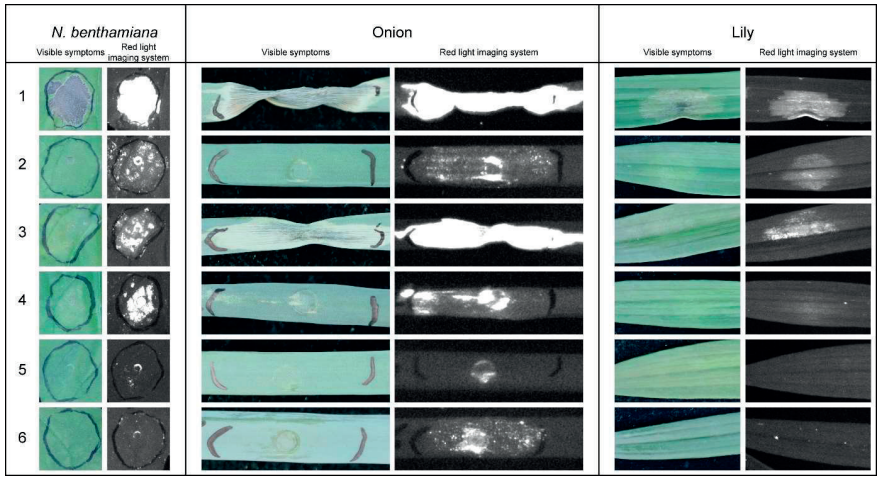

Supplementary Figure S1: Leaf responses observed at 3dpi caused by infiltration of CF samples obtained from liquid cultures of B. squamosa and B. elliptica on leaves of *N. benthamiana* (**A**), lily (**B**) and onion (**C**) visualized with normal light and with the red-light imaging system. 1 = *B. squamosa* grown in GB5_onion; 2 = *B. squamosa* grown in GB5_lily; 3 = *B. elliptica* grown in GB5_onion; 4 = *B. elliptica* grown in GB5_lily; 5 = GB5_onion mock; 6 = GB5_lily mock.

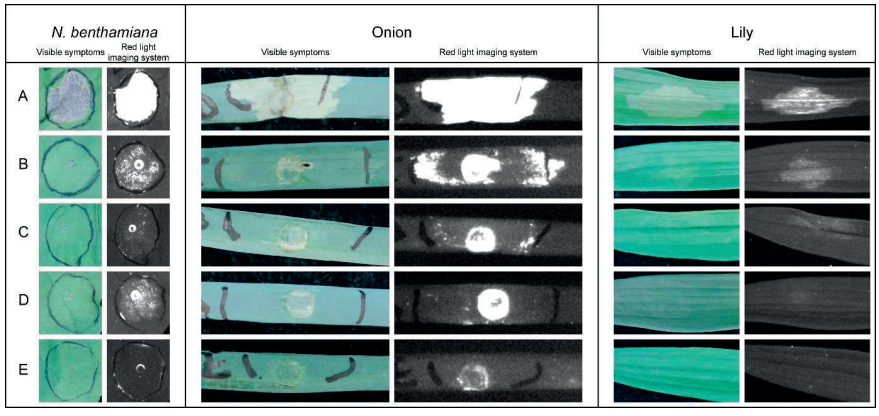

Supplementary Figure S2: Leaf responses observed at 3dpi caused by infiltration of ammonium sulphate precipitated compounds contained in the CF samples in *N. benthamiana* (**A**), lily (**B**) and onion (**C**) visualized with normal light and with the red-light imaging system. A = precipitate of *B. squamosa* CF grown in GB5_onion; B = precipitate of *B. squamosa* CF grown in GB5_lily; C= precipitate of *B. elliptica* CF grown in GB5_onion; D = precipitate of *B. elliptica* CF grown in GB5_lily; E = dialysis buffer.

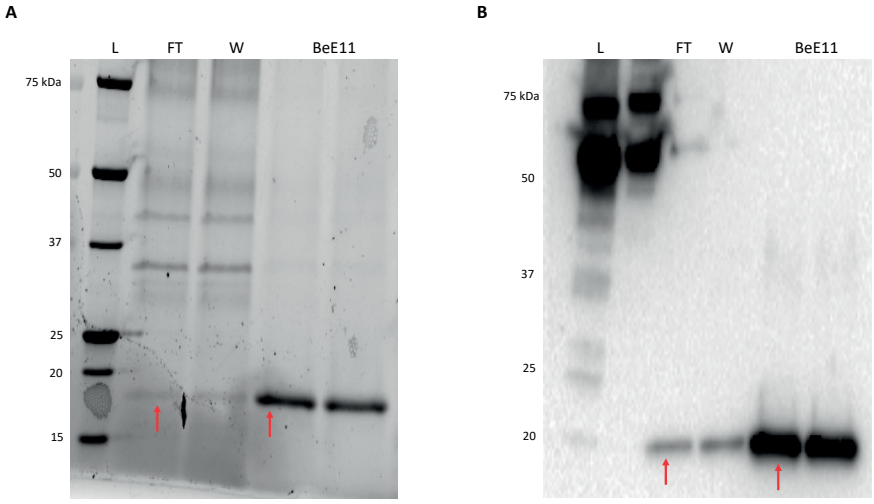

Supplementary Figure S3. Purification and immunodetection of BeE11, heterogously expressed in *Pichia pastoris*. BeE11 after purification with His-tag affinity resin next to Flow Through of yeast culture (FT) and washed resin (W) (**A**). Immunodetection with α-His primary and α-HRP secondary antibodies (**B**). BeE11 band at a size between 15 and 20 kDa is indicated by a red arrow. L = Ladder of size markers (BioRad).

Supplementary Table 1. Gene ID and functional annotation of the 85 orthogroups of proteins shared between the CF samples of *B. squamosa* and *B. elliptica*. GH = Glycosyl Hydrolase.

Orthogroup	Gene ID *B. elliptica*	Gene ID *B. squamosa*	Functional Annotation
G01	BELL_018g00720.1	BSQU_001g00680.1	Multicopper oxidase
G02	BELL_076g00320.1	BSQU_001g02190.1	Lysophospholipase
G03	BELL_024g00580.1	BSQU_001g05030.1	Carboxylesterase family
G04	BELL_024g00170.1	BSQU_001g05420.1	GH47 mannosidase
G05	BELL_004g01570.1	BSQU_001g07010.1	α-galactosidase
G06	BELL_004g02190.1	BSQU_001g07580.1	GH125 mannosidase
G07	BELL_026g00260.1	BSQU_001g09380.1	GH92 mannosidase
G08	BELL_026g00300.1	BSQU_001g09420.1	GH28 polygalacturonase
G09	BELL_061g00020.1	BSQU_002g00170.1	Esterase PHB depolymerase
G10	BELL_061g00210.1	BSQU_002g00340.1	GH71 glucanase
G11	BELL_008g01650.1	BSQU_002g01310.1	GH5 cellulase amylase
G12	BELL_008g02170.1	BSQU_002g01790.1	GH45 fungal cellulose binding domain
G13	BELL_008g00130.1	BSQU_002g06800.1	X8 domain, glucanosyltransferase
G14	BELL_008g00910.1	BSQU_002g07520.1	GH43 arabinofuranosidase or xylanase
G15	BELL_028g00300.1	BSQU_002g08230.1	neuraminidase
G16	BELL_037g00230.1	BSQU_003g00240.1	Calcineurin-like phosphoesterase
G17	BELL_037g00460.1	BSQU_003g00420.1	Cerato-platanin
G18	BELL_046g00520.1	BSQU_003g01170.1	unknown
G19	BELL_046g00310.1	BSQU_003g01380.1	GH5 cellulase
G20	BELL_046g00150.1	BSQU_003g01530.1	Carboxylesterase family
G21	BELL_046g00040.1	BSQU_003g01630.1	GH28 polygalacturonase
G22	BELL_002g01080.1	BSQU_003g02680.1	Pectate lyase
G23	BELL_002g01340.1	BSQU_003g02940.1	Pectinesterase
G24	BELL_002g01540.1	BSQU_003g03140.1	GH12 endoglucanase
G25	BELL_002g03270.1	BSQU_003g04800.1	Pectinesterase
G26	BELL_002g05670.1	BSQU_003g07060.1	Ribonuclease T2 family
G27	BELL_001g00710.1	BSQU_004g04000.1	unknown
G28	BELL_001g00640.1	BSQU_004g04070.1	GH5 cellulase
G29	BELL_017g00050.1	BSQU_004g07780.1	Pectate lyase
G30	BELL_020g00100.1	BSQU_005g00770.1	GH28 polygalacturonase
G31	BELL_020g00110.1	BSQU_005g00780.1	Pectinesterase
G32	BELL_032g00080.1	BSQU_005g05250.1	α-L-rhamnosidase
G33	BELL_019g01360.1	BSQU_005g07020.1	α-L-arabinofuranosidase
G34	BELL_091g00120.1	BSQU_006g00100.1	GH18 chitinase II
G35	BELL_060g00090.1	BSQU_006g01060.1	GH53 galactanase
G36	BELL_060g00390.1	BSQU_006g01360.1	GH65
G37	BELL_006g02500.1	BSQU_006g04260.1	Serine carboxyendopeptidase
G38	BELL_006g01900.1	BSQU_006g04840.1	Serine carboxyendopeptidase
G39	BELL_006g01650.1	BSQU_006g05070.1	GH5 cellulase
G40	BELL_006g00460.1	BSQU_006g06200.1	GDSL-like lipase/acylhydrolase
G41	BELL_006g00420.1	BSQU_006g06240.1	GH17 glucosidase
G42	BELL_062g00300.1	BSQU_006g06810.1	unknown
G43	BELL_021g00590.1	BSQU_007g01060.1	GH35 galactosidase
G44	BELL_075g00140.1	BSQU_008g00140.1	Carboxylesterase family
G45	BELL_088g00440.1	BSQU_008g00940.1	Serine carboxyendopeptidase

Supplementary Table 1. continue

Orthogroup	Gene ID *B. elliptica*	Gene ID *B. squamosa*	Functional Annotation
G46	BELL_005g01060.1	BSQU_008g02230.1	Phosphoesterase family
G47	BELL_005g01260.1	BSQU_008g02440.1	Serine carboxyendopeptidase
G48	BELL_047g00230.1	BSQU_008g05520.1	Cutinase
G49	BELL_022g00010.1	BSQU_008g05540.1	Unknown
G50	BELL_079g00240.1	BSQU_009g00250.1	Unknown
G51	BELL_023g00990.1	BSQU_009g02220.1	GH7, fungal cellulose binding domain
G52	BELL_025g01140.1	BSQU_009g04220.1	α-L-arabinofuranosidase
G53	BELL_003g01040.1	BSQU_010g01320.1	GH25 lysozyme protein
G54	BELL_003g01320.1	BSQU_010g01590.1	GH5 cellulase
G55	BELL_042g00530.1	BSQU_011g00290.1	GH35 galactosidase
G56	BELL_085g00380.1	BSQU_011g01130.1	GH28 polygalacturonase
G57	BELL_012g01180.1	BSQU_012g03080.1	Tuberculosis necrotizing toxin
G58	BELL_012g00260.1	BSQU_012g04030.1	unknown
G59	BELL_030g00180.1	BSQU_013g03720.1	GH20 hexoaminidase
G60	BELL_098g00050.1	BSQU_014g02730.1	Histidine phosphatase
G61	BELL_050g00660.1	BSQU_014g03460.1	GH17 glucosidase
G62	BELL_017g00540.1	BSQU_015g00480.1	Glucanosyltransferase
G63	BELL_017g02070.1	BSQU_015g01900.1	Chorismate mutase
G64	BELL_017g02270.1	BSQU_015g02090.1	GH62 arabinofuranosidase
G65	BELL_027g00720.1	BSQU_016g02200.1	GH28 polygalacturonase
G66	BELL_022g01430.1	BSQU_016g03320.1	GH15 glucoamylase
G67	BELL_010g02120.1	BSQU_017g00720.1	Pectate lyase
G68	BELL_010g02060.1	BSQU_017g00780.1	GH53 galactanase
G69	BELL_042g00530.1	BSQU_017g01530.1	GH35 galactosidase
G70	BELL_100g00120.1	BSQU_018g02600.1	Glyoxal oxidase
G71	BELL_039g00340.1	BSQU_018g02970.1	GH79 glucoronidase
G72	BELL_059g00400.1	BSQU_018g04350.1	Serine carboxyendopeptidase
G73	BELL_019g00980.1	BSQU_019g01480.1	GH39
G74	BELL_116g00070.1	BSQU_021g00030.1	α-L-rhamnosidase
G75	BELL_035g01190.1	BSQU_022g00070.1	GDSL-like lipase/acylhydrolase family
G76	BELL_035g01090.1	BSQU_022g00160.1	GH28 polygalacturonase
G77	BELL_035g00970.1	BSQU_022g00260.1	GH115 glucoronidase
G78	BELL_078g00050.1	BSQU_023g00390.1	GH28 polygalacturonase
G79	BELL_069g00320.1	BSQU_023g00470.1	GH17 glucosidase
G80	BELL_069g00280.1	BSQU_023g00510.1	GH76 mannanase
G81	BELL_089g00120.1	BSQU_024g00460.1	Carboxylesterase family
G82	BELL_089g00250.1	BSQU_024g00590.1	Glutamyltranspeptidase
G83	BELL_077g00070.1	BSQU_025g00710.1	GH28 polygalacturonase
G84	BELL_095g00220.1	BSQU_026g00140.1	unknown
G85	BELL_023g00250.1	BSQU_026g00910.1	FAD binding domain

Supplementary Table 2. Proteins detected after mass spectrometry analysis of *B. elliptica* CF samples and purified protein fractions. Proteins are grouped into CWDEs (green), proteases (grey), oxidoreductases (blue), putative effectors (red) and other secreted proteins (yellow). Gene ID, described protein domains and overall peptide intensity (IBAQ) are indicated. GH = Glycosyl Hydrolase.

GeneID	Functional annotation	IBAQ crude CF	IBAQ Fraction 1	IBAQ Fraction 2	IBAQ Fraction 3	IBAQ Fraction 4
BELL_027g00720.1	GH28 polygalacturonase	0	80483	7494200	0	0
BELL_085g00380.1	GH28 polygalacturonase	0	4858500	7410700	77082	0
BELL_085g00220.1	GH5	274700	0	22412000	0	46854
BELL_042g00530.1	GH35 lactosidase	3440200	84969	1059200	182320	938540
BELL_010g02060.1	GH53 galactanase	612070	53886	12993000	155010	169100
BELL_010g02120.1	Pectate lyase	4.1E+07	13123000	10775000	1953400	1034000
BELL_047g00230.1	Cutinase	832080	9100300	12186000	109180	101350
BELL_005g01340.1	GH16	1733700	1046300	1362700	66269	113840
BELL_050g00660.1	GH17 glucosidase	1.9E+07	17172000	6591900	10302000	25917000
BELL_023g00990.1	GH7	3.9E+07	54212000	67130000	469460	1410200
BELL_025g01140.1	α-L-arabinofuranosidase	3.6E+07	44140000	14972000	373930	2124800
BELL_017g00050.1	Pectate lyase	8.2E+07	87255	878380	3020900	9592700
BELL_017g02270.1	α-L-arabinofuranosidase	643730	74692	263500	0	64768
BELL_044g00620.1	ß-glucosidase	947900	12313000	15734000	131630	0
BELL_008g00130.1	Glucanosyltransferase	1.9E+07	13667000	28362000	7607700	12411000
BELL_008g00910.1	GH43 α-arabinosidase	838680	1578800	446360	0	0
BELL_016g00090.1	GH1 glucosidase	1040700	3198600	11258000	6408.4	0
BELL_008g01650.1	α-amylase	245390	0	0	0	62282
BELL_061g00210.1	α-1-3 glucanase	312030	0	0	0	0
BELL_077g00070.1	GH28 polygalacturonase	0	1900600	3422200	53223	152490
BELL_069g00280.1	GH76 α-mannanase	2449400	13457000	6635400	2210100	2281800
BELL_069g00320.1	GH17 glucosidase	1E+07	99646	407950	0	486700
BELL_078g00050.1	GH28 polygalacturonase	0	1286400	693970	19617	0
BELL_078g00170.1	α-L-rhamnosidase	2526700	1220100	14637000	278760	1018000
BELL_026g00300.1	GH28 polygalacturonase	33666	1278100	908800	0	9457
BELL_026g00260.1	GH92 mannosidase	8605000	178650	548590	2273000	10230000
BELL_004g02190.1	GH125 α-mannosidase	8316000	3740300	17153000	0	1167400
BELL_004g01570.1	α-galactosidase A, Ricin-type lectin domain	3.1E+07	9811400	60905000	48725	1592900
BELL_004g00190.1	GH16 concanavalin A	4912100	362990	0	0	0
BELL_024g00170.1	GH47 mannosidase	1E+07	10892000	68939000	0	450130

Supplementary Table 2. continue

GeneID	Functional annotation	IBAQ crude CF	IBAQ Fraction 1	IBAQ Fraction 2	IBAQ Fraction 3	IBAQ Fraction 4
BELL_089g00230.1	GH3 fibronectin type III-like domain	3073800	262890	1870800	33361	1446800
BELL_019g00980.1	GH39	5729500	9301000	14177000	12380	332830
BELL_019g01360.1	α-L-arabinofuranosidase	8475700	28114000	16481000	580180	1913200
BELL_019g01780.1	GDSL-like lipase/acylhydrolase	0	711510	3472500	0	0
BELL_032g00080.1	α-L-rhamnosidase	443680	31921	459460	24370	474090
BELL_020g00110.1	pectinesterase	4422600	2949900	266660000	4687200	224130
BELL_020g00100.1	GH28 polygalacturonase	2E+07	25264000	767750000	10700000	2415900
BELL_030g00180.1	GH20	5E+07	224070000	136150000	5770100	43661000
BELL_003g01320.1	GH5	1.2E+07	26629000	99131000	134920	939620
BELL_035g01190.1	GDSL-like lipase/acylhydrolase family	166440	28754000	22926000	1236800	163410
BELL_035g01090.1	GH28 polygalacturonase	0	0	734440	0	0
BELL_035g00970.1	GH115	218680	0	0	0	27062
BELL_001g03310.1	GH10 cellulose binding domain	4058200	610620	475730	289970	613640
BELL_001g00640.1	GH5	5211600	67566	0	646820	171820
BELL_007g00310.1	GH28 polygalacturonase	8133200	16468000	20096000	0	642670
BELL_006g00400.1	α-L-arabinofuranosidase	2374500	352710	720870	0	229780
BELL_006g00420.1	GH17 glucosidase	2794100	0	0	0	0
BELL_006g00460.1	GDSL-like lipase	2282300	10014000	6845400	295220	377840
BELL_006g01650.1	GH5	2177400	1112900	1127900	391520	260870
BELL_006g02480.1	Pectinesterase	6.6E+07	452800000	287520000	10984000	9412100
BELL_060g00390.1	GH65	907530	72051	4750600	33551	588480
BELL_060g00090.1	GH53 galactanase	2.4E+07	13360000	7553400	2802300	3139400
BELL_091g00120.1	GH18 class V chitinase ChiB1	4812200	0	0	0	1127700
BELL_002g05720.1	Pectate lyase	6036100	0	0	0	0
BELL_002g03270.1	Pectinesterase	673290	1491300	17124000	137950	25844
BELL_002g01540.1	GH12 glucanase	6.2E+07	255610000	341210000	805810	3575000
BELL_002g01340.1	Pectinesterase	3811000	30492000	27320000	2351600	154550
BELL_002g01080.1	Pectate lyase	100690	101200	71732000	32291	0
BELL_046g00040.1	GH28 polygalacturonase	5.2E+07	68536000	1539900000	22689000	38495000
BELL_046g00310.1	GH5	7903700	0	284150	73400	496930

Supplementary Table 2. continue

GeneID	Functional annotation	IBAQ crude CF	IBAQ Fraction 1	IBAQ Fraction 2	IBAQ Fraction 3	IBAQ Fraction 4
BELL_037g00430.1	xylanase	4877700	5732300	108510000	88973	354010
BELL_021g00790.1	GH76 α-mannanase	224140	593060	5480600	0	0
BELL_021g00590.1	GH 35 ß-galactosidase	136490	1001200	5280800	0	0
BELL_043g00440.1	Lytic polysaccharide mono-oxygenase	6721500	490870	173060	13604	415420
BELL_043g00230.1	GH3 lysosomal glucosidase	197420	25633	198290	0	0
BELL_099g00110.1	GH35 galactosidase	120300	456400	814680	9106.4	28586
BELL_039g00340.1	GH79 glucuronidase	453640	7996000	7432400	0	34015
BELL_022g00010.1	Aspartic protease AP1	88900000	18250000	15030000	27524	8705300
BELL_005g01260.1	Serine carboxyendopeptidase	921620	22125000	33719000	798650	0
BELL_088g00440.1	Serine carboxyendopeptidase	5728400	16829000	1E+08	298340	347870
BELL_056g00380.1	M35 metalloprotease	6102600	0	10256000	79826	467610
BELL_012g01270.1	Serine carboxyendopeptidase	1499900	7417700	1.26E+08	678580	0
BELL_011g01360.1	Serine carboxypeptidase	5433300	196420	858010	0	289820
BELL_034g00090.1	M14 zink carboxymetalloprotease	2806200	0	0	0	205870
BELL_077g00240.1	Subtilisin peptidase	10126000	71317	7781900	149680	688650
BELL_004g00400.1	Serine carboxyendopeptidase	1187100	385680	185370	0	0
BELL_064g00290.1	Serine carboxyendopeptidase	7225	1380000	3424500	0	0
BELL_013g01190.1	Serine carboxyendopeptidase	4395000	5141800	2.67E+08	2453300	2903500
BELL_009g02440.1	Serine carboxyendopeptidase	179530	557270	29680000	68055	21042
BELL_009g02470.1	Lysine-specific metallo-endopeptidase	27455000	1.01E+08	7E+08	429680	1899800
BELL_040g00580.1	Prolyl serine oligopeptidase S9	3163500	0	0	0	119840
BELL_062g00230.1	Serine carboxyendopeptidase	24497000	47754000	77739000	72344	2545700
BELL_006g00170.1	Eukaryotic aspartyl protease	4442600	0	0	0	255800
BELL_006g00510.1	Serine carboxyendopeptidase	834890	12114000	15525000	0	54696
BELL_006g01900.1	Serine carboxyendopeptidase	19105000	10203000	7.34E+08	2490300	7362300
BELL_006g02500.1	Serine carboxyendopeptidase	2419400	0	0	146870	1129600
BELL_038g00890.2	Eukaryotic aspartyl protease	1442900	0	0	0	0
BELL_059g00760.1	Serine carboxyendopeptidase	0	2306500	12056000	0	0
BELL_059g00400.1	Serine carboxyendopeptidase	2624600	15479000	4.18E+08	3282900	926670
BELL_027g00610.1	FAD binding domain	565090	9207500	9698400	69348	0

Supplementary Table 2. continue

GeneID	Functional annotation	IBAQ crude CF	IBAQ Fraction 1	IBAQ Fraction 2	IBAQ Fraction 3	IBAQ Fraction 4
BELL_022g01430.1	Tol-B like domain, phosphotriesterease	1.06E+08	81132000	9.97E+08	10470000	52280000
BELL_022g00910.1	GMC oxidoreductase	767970	37028	0	0	91807
BELL_113g00060.1	Catalase	5833000	11892000	39135000	1105.4	1450700
BELL_041g00320.1	FAD binding domain	157500	0	259420	0	82713
BELL_010g01590.1	GMC oxidoreductase	0	133630	201510	0	0
BELL_005g02530.1	Putative Cupper Redoxin domain	70375	622610	0	0	0
BELL_005g01060.1	Phosphoesterase	16269000	74266	2754500	5337.4	203110
BELL_075g00140.1	Carboxylesterase	5051500	21357000	1.52E+08	263230	293100
BELL_023g00250.1	FAD binding domain	121230	757280	1254000	0	0
BELL_031g00770.1	Carboxylesterase	6373300	15279000	68436000	1672200	3539500
BELL_008g00820.1	Multicopper oxidase	83137	175260	1302200	0	0
BELL_016g00950.1	Carboxylesterase	1080900	1000300	57452000	230520	1116300
BELL_061g00020.1	Esterase, PHB depolymerase	512230	3262400	3903500	105290	0
BELL_053g00390.1	Carboxylesterase	126790	1002300	12844000	0	0
BELL_004g03370.1	GDSL lipase/esterase	8521900	14417000	5.98E+08	1981600	2849500
BELL_024g00580.1	Carboxylesterase	104050	4421000	10554000	134520	0
BELL_076g00320.1	Lysophospholipase	5939000	21840000	41202000	26613	602280
BELL_018g01200.1	Tyrosinase melanin production	30087000	287560	3048300	8401000	31928000
BELL_018g00720.1	Multicopper oxidase	12419000	95656	1032600	517490	13158000
BELL_089g00120.1	Carboxylesterase	362960	17482000	12412000	346850	0
BELL_020g01940.1	Multicopper oxidase	1430500	0	0	0	0
BELL_030g00670.1	Crotonase	2059000	2203900	4685000	26863	159150
absent in Be9612	Phosphatidylinositol phosphoesterase	843920	1175200	4975300	0	91708
BELL_002g03820.1	Phosphoesterase	374350	50969	3903200	0	0
BELL_046g00150.1	Carboxylesterase	979340	925950	1098000	45477	330630
BELL_037g00330.1	FAD binding domain	0	3413400	3119400	15979	8951.6
BELL_037g00230.1	Calcineurin-like phosphoesterase	146460	1236500	1738200	0	0
BELL_003g04300.1	Calcium-dependent phosphotriesterase	0	0	459480	0	0
BELL_067g00340.1	FAD binding domain	0	182120	464610	0	0
BELL_067g00350.1	Enoyl-CoA hydratase/isomerase	0	189560	978370	0	0

Supplementary Table 2. continue

GeneID	Functional annotation	IBAQ crude CF	IBAQ Fraction 1	IBAQ Fraction 2	IBAQ Fraction 3	IBAQ Fraction 4
BELL_043g00600.1	Histidine phosphatase	9346700	45609000	1.78E+08	545430	668210
BELL_100g00120.1	Chitin recognition protein, Glyoxal oxidase	6975900	306110	2555200	4257800	8019200
BELL_027g00610.1	FAD binding domain	565090	9207500	9698400	69348	0
BELL_041g00030.1	unknown	176430	65989000	105640000	1121200	717340
BELL_047g00200.1	unknown	302820000	368670000	1.20E+08	17202000	112650000
BELL_012g00260.1	unknown (effector Candidate Be11)	120860000	997330000	7253200	2155700	1950300
BELL_008g02170.1	GH45 endoglucanase	39486000	1523100	2367800	402450	2846500
BELL_008g01470.1	unknown	5760300	68804000	67073000	792790	4103200
BELL_004g00250.1	unknown	510010	0	0	0	1475200
BELL_018g00060.1	unknown	0	0	7152200	0	0
BELL_013g01250.1	GH7 Concavalin A	8556900	0	186640	0	418370
BELL_057g00050.1	GH28 polygalacturonase	15164000	24944000	43833000	188380	1573700
BELL_057g00300.1	unknown	70145	0	2261700	0	0
BELL_003g01040.1	Llysozyme like protein	2472600	9428700	119880000	388550	89579
BELL_062g00300.1	unknown	98193000	4957700	7259600	2816600	7016200
BELL_002g01500.1	unknown	1140700	0	0	138000	0
BELL_046g00520.1	unknown	11348000	4627900	2271600	39355000	3122100
BELL_037g00460.1	Cerato-platanin	3515300000	1715400000	700510000	2191200000	287450000
BELL_017g02070.1	Chorismate mutase 2	9582000	5921300	0	7922900	33216000
BELL_022g01570.1	unknown	2661800	6071100	18314000	73278	173110
BELL_005g03550.1	Esterase, PHB depolymerase	6133800	2249600	23444000	48859	247410
BELL_095g00220.1	unknown	7659700	551450	377170	231340	633210
BELL_014g01270.1	unknown	6902400	73140	352500	0	808170
BELL_098g00190.1	Nucleoside hydrolase	0	0	1267400	0	0
BELL_098g00050.1	Histidine phosphatase	639840	0	8404600	0	40555
BELL_079g00240.1	unknown	15419000	2.42E+08	1.35E+08	21590000	1498000
BELL_023g00180.1	NPC1-like lysosomal membrane	78631	20344	5621700	39795	31477
BELL_017g00540.1	Glucanosyltransferase	20285000	372670	76787	2933900	27803000
BELL_044g00690.1	unknown	649130	72786	602280	0	0
BELL_031g01210.1	unknown	24210000	1.65E+08	1.59E+08	0	961140

Supplementary Table 2. continue

GeneID	Functional annotation	IBAQ crude CF	IBAQ Fraction 1	IBAQ Fraction 2	IBAQ Fraction 3	IBAQ Fraction 4
BELL_028g00300.1	unknown	4114300	6539600	23942000	946700	5018300
BELL_116g00070.1	unknown	733890	2612100	23320000	0	0
BELL_012g01180.1	tuberculosis necrotizing protein	2114000	8929500	32651000	401840	314910
BELL_045g00060.1	unknown	5868600	314710	4156200	0	201980
BELL_016g01840.1	unknown	225680	0	0	0	58418
BELL_089g00250.1	γ-glutamyltranspeptidase	613590	677430	2993500	72339	337860
BELL_001g01240.1	SnoaL-like domain of polyketide cyclase	4655100	30044000	49253000	0	396340
BELL_001g00710.1	unknown	26133000	0	206230	1670800	6604000
BELL_002g05670.1	Ribonuclease T2 family	3598300	4145500	4078800	654390	412630
BELL_002g03930.1	unknown	58616000	1.13E+08	2.96E+09	26198000	21919000
BELL_003g02660.1	Ribonuclease T2 family	448310	3191200	31853000	0	0
BELL_003g02550.1	unknown	4377500	4585000	6326300	0	354000
BELL_067g00120.1	GPI-anchored cell wall organization protein	10192000	1956900	1816800	4158100	14468000

Chapter 4

Functional characterization and cellular localization of the *Botrytis elliptica* Chorismate Mutase effector

Michele C. Malvestiti, Emma Groen, Henriek G. Beenen, Christiaan Schol and Jan A. L. van Kan

Wageningen University, Laboratory of Phytopathology, Wageningen, Netherlands

ABSTRACT

Fire blight is the most destructive disease on lilies which is caused by the Ascomycota *Botrytis elliptica*. This necrotrophic fungus causes disease by secreting effectors that induce host cell death. Previous research has identified effectors, including the *B. elliptica* Chorismate Mutase 2 (BeCMU2), that contribute to cause cell death in lily. In this study we aimed to determine the enzymatic activity as well as the *in planta* subcellular localization of BeCMU2. Amino acid sequence analysis predicted the presence of a chorismate mutase (CMU) enzyme domain. CMUs are enzymes that catalyze the conversion of chorismate to prephenate, the precursor of tyrosine and phenylalanine in plants and most microorganisms, as well as for salicylic acid biosynthesis in plants. Earlier studies identified chorismate mutase effectors from (hemi)biotrophs which can reduce salicylic acid biosynthesis in the host plant to promote virulence. CMU activity of BeCMU2 was confirmed by complementing a *Saccharomyces cerevisiae aro7* mutant that was deficient in the synthesis of phenylalanine and tyrosine. Further the conversion of chorismate to prephenate was spectrophotometrically determined with pure BeCMU2 protein. The plant response to BeCMU2 was assessed by infiltrating lily leaves with purified BeCMU2 protein and its contribution to fungal virulence was assessed by generating CRISPR-Cas9 *B. elliptica CMU2* deletion mutants. Remarkably, BeCMU2 contains a predicted chloroplast transit peptide. In order to test the functionality of this domain, BeCMU2 carrying or lacking the chloroplast transit peptide was fused to GFP and transiently expressed in *Nicotiana benthamiana* leaves. Confocal imaging showed that with both constructs, green fluorescence was located in the cytoplasm. Finally, BeCMU2 effector delivery and localization *in planta* was studied in *N. benthamiana* inoculated with *B. cinerea* expressing a BeCMU2::GFP fusion protein. This study provides indications that BeCMU2 may be involved in the biotrophic phase during fungal colonization of the host, however, the subcellular localization of BeCMU2 remains to be studied in further detail.

INTRODUCTION

Lily (*Lilium* spp., Liliaceae) is one of the most economically important flower bulbs worldwide and in the Netherlands 5300 hectares of land are dedicated to lily production (CBS, 2020). The assortment of lily genotypes comprises thousands of hybrids which have been generated via crosses between different *Lilium* species to combine different ornamental traits (van Tuyl et al., 1991; Lim et al., 2008; van Tuyl and Arens, 2011). Nevertheless the lily industry suffers huge losses because of several pests and diseases. The most serious threat is fire blight, a fungal disease caused by the filamentous Ascomycota *Botrytis cinerea* and *Botrytis elliptica* (Sclerotiniaceae). At the beginning, both fungi form small brownish necrotic spots on leaves and flowers. Under favorable conditions rapid outgrowth of necrotic lesions leads to death of the entire plant. However, while the generalist *B. cinerea* is known to occur only on senescing and damaged plant tissue and especially on cut lilies, the lily specific *B. elliptica* can infect healthy, vigorous plants thereby inflicting significant economic losses to the lily industry (Hou and Chen, 2003; Chastagner and Grafinkel, 2020). Fungi of the genus *Botrytis* are phytopathogenic Ascomycota with a necrotrophic lifestyle (Veloso and van Kan 2018). After an initial biotrophic interaction with the plant, *Botrytis* fungi kill host cells to acquire nutrients from the dead plant tissue. Host cell death is achieved by mean of secreted necrotrophic effectors which can trigger apoptosis-like programmed cell death (PCD) upon interaction with a host cellular target (van Baarlen et al., 2004; Zhang et al., 2014; Veloso and van Kan 2018, Steentjes et al., 2022; Leisen et al., 2022). In **Chapter 3**, the protein composition was analyzed of a sample obtained from *B. elliptica* liquid culture which caused a cell death response upon infiltration in lily, onion and tobacco leaves. Mass spectrometry identified 166 different proteins with a predicted signal peptide for secretion, including 15 predicted effectors. Besides the predicted effector candidates, one protein of 166 amino acids appeared particularly interesting because of the following reasons. Functional domain prediction revealed that the protein carries a chorismate mutase (CMU) enzyme domain (Paysan-Lafosse et al., 2022) and thus it was not predicted as effector (Sperschneider and Dodds, 2021). Nevertheless, the corresponding gene, named *B. elliptica Chorismate Mutase 2* (*BeCMU2*) possessed a highly unusual feature, namely a predicted chloroplast Transit Peptide (chlTP) (Sperschneider et al., 2017), which would suggest that this fungal protein might function inside plant chloroplasts.

CMUs catalyze the pericyclic Claisen rearrangement of chorismate to prephenate and are found in the bacterial, fungal, animal and plant kingdom. There are CMUs of different classes, based on protein structure and biochemical properties (Xue et al., 1994; Lee et al., 1995; Romero et al., 1995; Sträter et al., 1997; Helmstaedt et al., 2004). CMUs present in bacteria belong to the AroH class which is organized in a pseudo-α/β barrel, whereas eukaryotic CMUs belong to the AroQ class, which typically consists of α-helical proteins

(Lee et al., 1995; Sträter et al., 1997; Krappmann et al., 1999; Helmstädt et al., 2001 and 2004; Sasso et al., 2005). Plants, however, possess multiple CMUs of the AroQ class that are either active in chloroplasts or in the cytoplasm (Westfall et al., 2014). Besides being required in the aromatic amino acid biosynthesis, CMU activity is involved in the biosynthesis of salicylic acid (SA), a well-known plant defense hormone (Vlot et al., 2009; Rekhter et al., 2019; Lefevere et al., 2020).

Remarkably, different (hemi)biotrophic plant pathogenic fungi, as well as two plant pathogenic nematode taxa possess two CMU genes: the first encodes a typical cytoplasmic CMU putatively involved in the biosynthesis of aromatic amino acids, while the second encodes a secreted CMU protein which is involved in the interaction with the host plant (Doyle and Lambert, 2003; Vanholme et al., 2009; Djamei et al., 2011; Bauters et al., 2020; Assis et al., 2021; He et al., 2021). It was postulated that secreted CMU proteins act as effectors that contribute to virulence by interfering with SA biosynthesis in the host plant, thereby lowering SA-induced plant defense responses during pathogen invasion (Ding and Ding, 2020). Moreover, an ortholog of *BeCMU2* is present in the broad host range necrotrophic Ascomycota *Sclerotinia sclerotiorum* (*SsCMU2*; Liang and Rollins, 2018). We hypothesize that BeCMU2 represents an effector protein that contributes to fungal virulence in the *B. elliptica* – lily interaction. Therefore, this study aimed to characterize the predicted CMU enzyme and assess its contribution to fungal virulence as an effector. We tested BeCMU2 activity *in vitro* and *in planta* and generated *B. elliptica CMU2* deletion mutants via CRISPR-Cas9 mediated targeted gene replacement. Finally we verified whether BeCMU2 is translocated into plant cells and localizes in plant chloroplasts.

MATERIALS AND METHODS

Plant material and growth conditions

Bulbs of *Lilium* genotype "Asiatic" (A), "Longiflorum" (L), "Longiflorum-Asiatic" (LA) and "Oriental-Asiatic" (OA) were grown as described in **Chapter 2.** Mature leaves were harvested and used for disease assays and leaf infiltration. *Nicotiana benthamiana* plants were grown as described in **Chapter 2**.

Fungal material, inoculations and leaf infiltration

All fungal isolates used in this study are listed in Table 1. *B. elliptica* and *B. cinerea* isolates were stored as described in **Chapter 2**. *S. sclerotiorum* was stored as sclerotia at 0°C. Mycelium and spores of all *Botrytis* isolates were prepared as described in **Chapter 2**. Disease assays in lily OA and LA were carried out with *B. elliptica* isolate 9612 WT and *ΔBecmu2* deletion mutants and scored as described in **Chapter 2**. 100 µL BeCMU2 solution (100 µM) were infiltrated in leaves lily genotypes A and L and scored at 3 dpi by photographing with normal light and under the RFP channel of the ChemiDoc MP imaging system (Bio-Rad) (Landeo Villanueva et al., 2021). *N. benthamiana* inoculation with *B. cinerea* WT and mutants was carried out as described in **Chapter 2**.

Table 1. Fungi used in this study

Fungal species	Isolate	Source
B. elliptica	WT 9612	Chapter 2
B. elliptica	ΔBecmu2#3	generated in this study
B. elliptica	ΔBecmu2#5	generated in this study
B. cinerea	WT B05.10	van Kan et al., 2017
B. cinerea	BeCMU2::GFP#1	generated in this study
B. cinerea	BeCMU2::GFP#4	generated in this study
B. cinerea	BeCMU2::GFP#5	generated in this study
Sclerotinia sclerotiorum	1980 UF-70	Amselem et al., 2011
Saccharomyces cerevisiae	YO5479	Djamei et al., 2011
S. cerevisiae	Δaro7	Djamei et al., 2011
S. cerevisiae	Δaro7-pYES260::BeCMU2$^{24\text{-}166}$	generated in this study
S. cerevisiae	Δaro7-pYES260::SsCMU2$^{21\text{-}160}$	generated in this study
S. cerevisiae	Δaro7-pYES260::BeCMU2$^{24\text{-}166}{}_{\text{K105A, R116A}}$	generated in this study
S. cerevisiae	Δaro7-pYES260::SsCMU22U$^{21\text{-}160}{}_{\text{K102A, R113A}}$	generated in this study
Pichia pastoris	GS115	Invitrogen
P. pastoris	pPIC9K::BeCMU2$^{24\text{-}165}$6xHis	generated in this study

Bioinformatic analysis

BeCMU2 coding sequence was retrieved from the *B. elliptica* isolate 9612 genome (BELL_017g02070.1, Valero-Jiménez et al., 2020). *SsCMU2* coding sequence was retrieved from *S. sclerotiorum* genome 1980 UF-70 (XM_001584657.1; Amselem et al., 2011). Signal

peptide prediction was performed using SignalP 6.0 (Teufel et al., 2022). Domain prediction was performed with InterProScan (Paysan-Lafosse et al., 2022). Effector prediction was performed with EffectorP 3.0 (Sperschneider and Dodds, 2021). Presence of transit peptides for subcellular compartments was predicted with LOCALIZER (Sperschneider et al., 2017). Protein structure prediction was performed using AlphaFold2 (Jumper, 2021; Varadi et al., 2022). Amino acid sequences were aligned with Clustal Omega and displayed by using ESPript 3.0 (Robert and Gouet, 2014). All plasmids and oligonucleotides used in this study are listed in Supplementary Table 2 and 3, respectively.

Yeast complementation assay with *BeCMU2* and *SsCMU2*

CMU activity of BeCMU2 and SsCMU2 was tested via yeast complementation. *Saccharomyces cerevisiae* isolate YO5479 *Δaro7* lacking the CMU encoding gene (*ScAro7*) was used (Djamei et al., 2011) as recipient strain to be complemented with *BeCMU2* and *SsCMU2*, which were amplified from gDNA of *B. elliptica* isolate 9612 and *S. sclerotiorum* 1980 UF-70, respectively. Four expression constructs were cloned into the plasmid pYES260 under *Gal4* promoter regulation (Djamei et al., 2011). The four constructs included the two original *BeCMU2* and *SsCMU2* gDNA sequences lacking the signal peptide sequence ($BeCMU2^{24\text{-}166}$ and $SsCMU2^{21\text{-}160}$), and *BeCMU2* and *SsCMU2* gDNA sequences carrying two point mutations in the predicted catalytic site of the enzyme domain ($BeCMU2^{24\text{-}166}{}_{K105A,\ R116A}$ and $SsCMU2^{21\text{-}160}{}_{K102A,\ R113A}$) (Schnappauf et al., 1997 and 1998). All inserts were amplified with Phusion High-Fidelity DNA Polymerase (ThermoFisher Scientific) with primers containing at their 5'-end a 20 bp complementary sequence to the destination plasmid for homologous recombination. Homologous recombination of the inserts with the linearized pYES260 was conducted as described in **Chapter 3** and the reaction mix was used to electroporate *Escherichia coli* DH5α. After electroporation, the recombined plasmids were purified from *E. coli* liquid culture and sequenced before being used for yeast transformation, as described in Thompson et al. (1998). Transformed yeast colonies were selected by plating 100 µL of cell suspension on SD-URA containing agar plates and incubated 48 h at 30°C. Emerging colonies were screened via PCR. Positive transformants were grown as single colony overnight in 15 mL YPD with 100 µg/mL ampicillin. A dilution series (OD600 = 0.5; 0.1; 0.05; 0.01) was made and 15 µL yeast suspension was plate inoculated on SD-Phe-Tyr+Gal/Raf and YPD. Plates were incubated 48 h at 30°C and photographed with white light in the Chemidoc Imaging System (Bio-Rad).

Heterologous BeCMU2 production and purification

The DNA sequence encoding the mature BeCMU2 protein (lacking the signal peptide) was amplified from *B. elliptica* isolate 9612 genomic DNA using primers with an 18 bp extension that would insert a 6x His-tag at the C-terminus of the protein. The amplicon was cloned into the linearized plasmid pPIC9k (Invitrogen) via homologous recombination as described in **Chapter 3**. After confirming the insertion by PCR and sequencing, the plasmid

was used for electroporation of *P. pastoris* isolate GS115 following the manufacturer's instructions (Invitrogen). Yeast fermentation for protein production was performed as described in **Chapter 3**. Histidine affinity-based BeCMU2 purification was done with HisPur Ni-NTA resin (Thermo Scientific) as described in **Chapter 3**. After dialysis, the protein suspension was concentrated in Amicon Ultra-0.5 Centrifugal Filter Units (Merk), quantified via Bradford assay (BioRad), adjusted to a concentration of 100 µg/mL with 10 mM KPO_4 (pH = 6) and stored at 0 °C until use.

Chorismate mutase activity *in vitro* enzyme assay

CMU2 activity was tested as described in Gilchrist and Connelly (1987). A reaction mix containing 640 µL 1 M Tris-HCl (pH = 7.9), 100 µL H_2O, and 60 µL of BeCMU2 (corresponding to ca 5 µg of purified protein dissolved in 10 mM KPO_4 pH = 6) was prepared in a 1.5 mL protein low binding tube (Eppendorf). The reaction was started by adding 200 µL of chorismate (5 mM) (Sigma-Aldrich) and incubated at 25°C. Each minute, 100 µL of the reaction mix was removed and terminated in 100 µL of 6 N HCl in a 96 wells microtiter plate. This solution was left to incubate for 10 minutes (30°C) for the acidic conversion of prephenate into phenylpyruvate. Afterward, 400 µL of 4 N NaOH was added and the amount of phenylpyruvate was measured against a 1 N NaOH blank. Purified BeE11 (see **Chapter 3**), heat-denatured BeCMU2 protein (20 min, 99°C), and 10 mM KPO_4 (pH = 6) were used as controls. Absorption at 320 nm was quantified in a microplate fluorescence reader (CLARIOstar; BMG Labtech). The experiment was performed three times.

Generation of *ΔBecmu2* mutants by CRISPR-Cas9 mediated *B. elliptica* transformation

Donor DNA containing the hygromycin resistance cassette (hph) as selection marker was amplified from telomeric vector pTEL-Hyg (Leisen et al., 2020). To achieve double strand break (DSB) directed recombination, the hph cassette was amplified via overhang PCR with 60 bp flanks which were homologous to the 60 bp at the 5' and 3' end of BeCMU2, respectively. For targeted Cas9-mediated DSB, sgRNAs were designed and generated as described in Leisen et al. (2020) and purified using the RNA isolation Kit (Zymo Research Orange, CA, USA). Cas9-Stux2 protein used for fungal transformation was obtained from *E. coli* carrying pET24a_Cas9-Stux2-NLS-His as described in Leisen et al. (2020). *B. elliptica* transformation was carried out as described in Leisen et al. (2020) with some modifications. Fungal cultures were grown for 36 h at 20°C in a shaking incubator (150 rpm). No ice chilling was performed after protoplasting and all incubation steps were conducted at room temperature. Ribonucleotide-Protein (RNP) complex assembly was performed as described in Leisen et al. (2020) adding 2 µg of each sgRNAs to 6 µg of Cas9-Stux2 protein in cleavage buffer (20 mM HEPES, pH = 7.5, 100 mM KCl, 5% glycerol, 1 mM DTT, 0.5 mM EDTA, pH = 8.0, 2 mM $MgCl_2$). After RNP treatment, protoplasts were plated in SH medium containing 17,5 µg/mL hygromycin B and incubated in darkness at 20°C.

Four days after incubation, appearing fungal colonies were transferred onto MEA plates containing 80 µg/mL hygromycin B and screened via PCR. Homokaryotic *ΔBecmu2* were characterized with Phire Plant Direct PCR Kit (ThermoFisher Scientific, Bremen, Germany) using primers within the *BeCMU2* gene and outside the 60 bp flanks used for homologous recombination (Supplementary Figure S2). *ΔBecmu2* mutants were subsequently checked via growth assay for developmental phenotype by comparing colony growth to *B. elliptica* WT (Supplementary Figure S2).

Generation of *B. cinerea CMU2::GFP* mutants and *BeCMU2*::GFP *in planta* localization

B. cinerea isolate B05.10 was transformed with a construct containing the *BeCMU2* fused to *GFP*. The construct was cloned into the pNDH-OGG vector (Schumacher, 2012) via homologous recombination as described in **Chapter 3** and electroporated in *E. coli* DH5α. The recombined plasmid was purified from *E. coli* and sequenced before being used as template for amplifying donor DNA. Donor DNA (~3.5 kbp) containing the fusion construct BeCMU2::GFP and hph as selection marker was amplified from pNDH-OGG-BeCMU2::GFP plasmid using Phusion polymerase in an overhang PCR reaction with 60 bp long flanks which were homologous to the 60 bp at the 5' and 3' end of *BcniaD* (Schumacher, 2012). All steps of the transformation were performed as described in Leisen et al. (2020). Homokaryotic *ΔBcniaD* mutants were characterized with Phire Plant Direct PCR Kit (ThermoFisher Scientific, Bremen, Germany) using one primer within the *BeCMU2* gene and one primer within the 60 bp flanks used for homologous recombination (Supplementary Figure S3). *B. cinerea* mutants carrying the *BeCMU2::GFP* construct were subsequently checked for developmental phenotype (Supplementary Figure S3). Three distinct *B. cinerea* BeCMU2::GFP overexpressing mutants were inoculated in *N. benthamiana* leaves as described above. At 2 dpi leaf tissue samples were collected and analysed under the microscope.

BeCMU2 localization via *Agrobacterium tumefaciens* mediated transformation (ATTA)

One construct consisted in the mature *BeCMU2* coding sequence (BeCMU2$^{24\text{-}164}$), whereas in the second construct (BeCMU2$^{56\text{-}164}$) the chlTP was deleted. Both *BeCMU2* inserts were amplified from pYES260::BeCMU2 plasmid and cloned into pENTR/D-TOPO plasmid using the GateWay cloning kit (Thermofisher) following the manufacturer's instruction with some slight modifications. The codons of the last two amino acids (L, V) of *BeCMU2* were excluded from the reverse primer to avoid inversion of the gene sequence during plasmid recombination. After *E. coli* DH5α electroporation emerging colonies were PCR screened, grown overnight at 37°C and plasmid DNA was isolated and sequenced. Subsequently, pENTR/D-TOPO::BeCMU2$^{24\text{-}164}$ and pENTR/D-TOPO::BeCMU2$^{56\text{-}164}$ were used to set up the LR recombination reaction in the expression plasmid pBINKS-GWY-eGFP. The LR reaction

was performed following the manufacturer's protocol (Thermofisher). *E. coli* DH5α cells were electroporated with the reaction mix and plated on LBA plates (100 µg/mL kanamycin and 50 µg/mL spectinomycin). Emerging colonies were PCR screened, grown overnight at 37°C and plasmid DNA was isolated and sequenced. The pBINKS-GWY-eGFP plasmid carrying BeCMU2$^{24\text{-}164}$ or BeCMU2$^{56\text{-}164}$ were used to transform *A. tumefaciens* as described in van der Hoorn et al. (2000). pBinKS-GW-fl-PepMV-Cp-nostop-eGFP was used as a positive control for GFP signal detection in the cytoplasm, whereas pBINKS-GWY-eGFP was used as a negative control for no GFP detection. *A. tumefaciens* liquid cultures were infiltrated in *N. benthamiana* leaves at OD = 0.3. At 2 and 3 dpi the leaves were collected for GFP immunodetection and microscopical analysis. Proteins extraction from agroinfiltrated leaf tissue and GFP immunodetection with αGFP-HRP antibodies (MACS antibodies, Bergisch Gladbach, Germany) were carried out as described in Liebrand et al. (2012).

Confocal microscopy

Agroinfiltrated and *B. cinerea-BeCMU2::GFP* inoculated *N. benthamiana* leaves were cut into 1 cm^2 squares and placed on an objective slide with the abaxial side facing upwards. A few droplets of perfluorodecalin were applied to the plant tissue to remove air in the samples. Samples were analyzed with a Leica TCS SP2 AOBS laser scanning confocal microscope with 40x magnification (Leica Microsystem). The excitation wavelengths were set at 450 nm both for GFP and chlorophyll. The fluorescence signals for GFP and chlorophyll were detected at 505 – 525 nm and 580-620 nm emission wavelength, respectively.

RESULTS

BeCMU2 possesses chorismate mutase activity

The genome of *B. elliptica* contains two *CMU* genes, both encoding proteins belonging to the AroQ class: one is orthologous to *S. cerevisiae ARO7* and the second is orthologous to *S. sclerotiorum SsCMU2*. Furthermore, BeCMU2 was predicted to contain a chloroplast Transit Peptide (chlTP). **Figure 1A** shows an alignment between the protein sequences of *B. elliptica* CMU2 and its counterpart in *S. sclerotiorum*, *B. elliptica* ARO7 and its counterpart in *S. cerevisiae*, as well as two plant CMU proteins with a predicted chlTP. The alignment shows that BeCMU2 and SsCMU2 are totally unrelated to the described AroQ-type CMUs present in the plants *N. benthamiana* and *A. thaliana* (Westfall et al., 2014), as well as to the non-secreted AroQ-type CMU in *S. cerevisiae* (Lee et al., 1995) and in *B. elliptica*. Enzyme activity of BeCMU2 was tested in two different ways. In an *in vivo* assay the yeast *S. cerevisiae Δaro7* was complemented with the mature protein sequence of BeCMU2 and the its ortholog SsCMU2, and with a BeCMU2 and SsCMU2 constructs which carried a double point mutation in the predicted catalytic site of the CMU enzyme domain (**Figure 1B**). When the different yeast cultures were plated on selective media lacking tyrosine (Tyr) and phenylalanine (Phe), only the WT yeast and the *Δaro7* mutants complemented with the original BeCMU2 or SsCMU2 protein sequence grew, while yeast *Δaro7* mutants complemented with BeCMU2 or SsCMU2 constructs mutated in the predicted catalytic site did not grow (**Figure 1B**). Next, an *in vitro* assay was performed to assess the enzymatic activity of BeCMU2, produced in *Pichia pastoris*, using chorismate as substrate (**Figure 1C**). The curve shows the spectrophotometric absorbance over a time course of 10 min of phenylpyruvate, which derives from the acidic conversion of prephenate because of CMU activity. We observed an increase in the absorbance at 320 nm when purified BeCMU2 was incubated with chorismate (**Figure 1C**, red curve). Following a pattern which resembles the Michaelis-Menten kinetics (Michaelis and Menten, 1913) the curve levels off seven min after start of the reaction. CMU enzymes are capable of (partially) renaturing upon cooling down after heat-treatment (Görisch and Lingens, 1973; Ökvist et al., 2006), and a similar pattern was observed for the heat-denatured BeCMU2 (**Figure 1C**, blue curve), even though both the peak values of phenylpyruvate absorbance as well as the slope of the curve were lower. By contrast, incubation of a different effector protein, BeE11 (**Chapter 3**; **Figure 1C**, green curve) or KPO_4 buffer (**Figure 1C**, purple curve) with chorismate did not show any increase in spectrophotometric absorption of phenylpyruvate. Structure prediction showed that BeCMU2 is composed of three α-helices (**Figure 1D**, purple) and loops wherein the catalytic active residues of the CMU enzyme domain are located (**Figure 1D**, blue). Presence of only α-helices without β-sheets indicates that BeCMU2 and SsCMU2 indeed belong to the AroQ class of CMUs proteins (Lee et al., 1995). In addition, the predicted chlTP in BeCMU2 is located at positions 15 to 35 of the mature protein (**Figure 1D**, green).

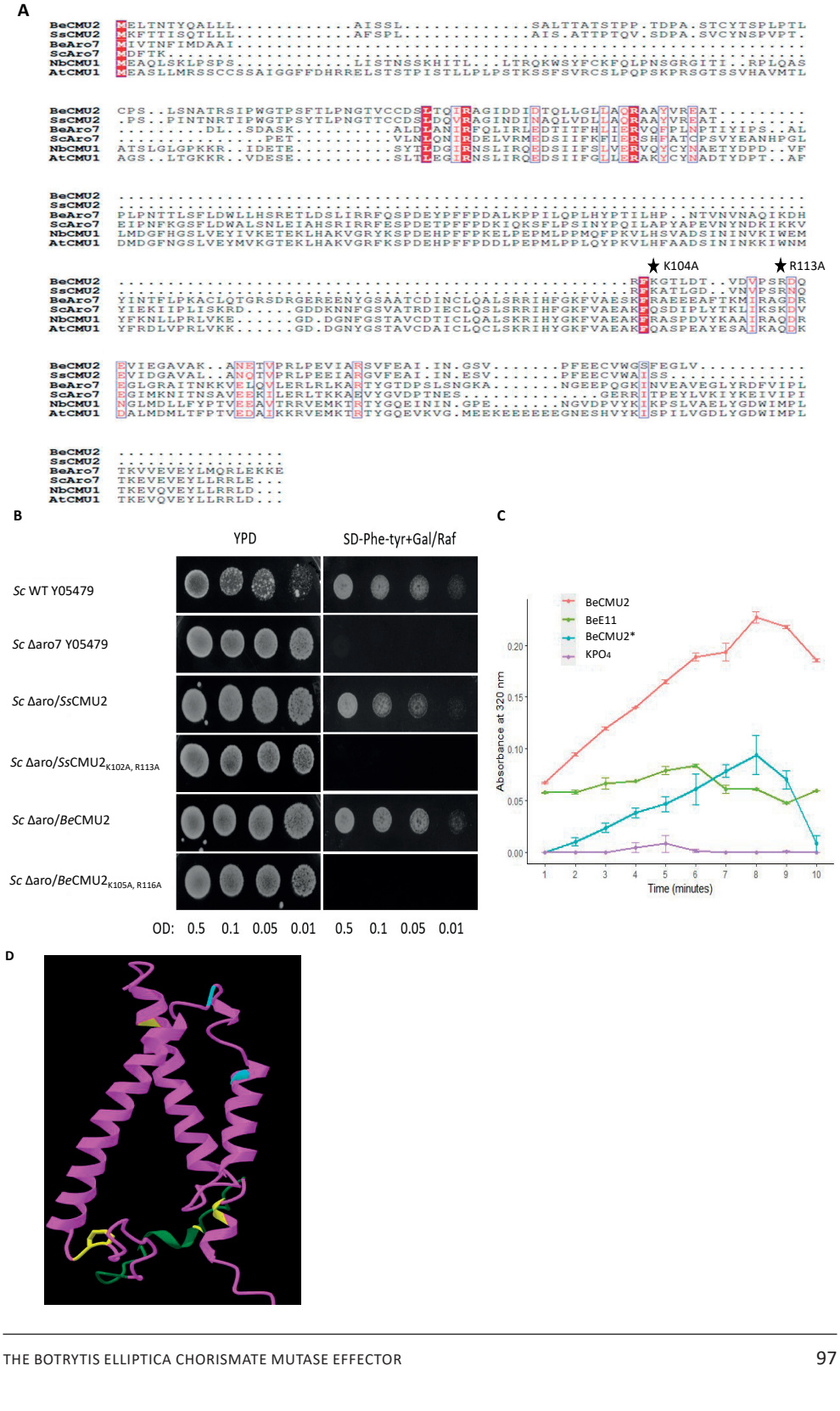
A
BeCMU2
SsCMU2
BeAro7
ScAro7
NbCMU1
AtCMU1
K104A
R113A
B
YPD
SD-Phe-tyr+Gal/Raf
Sc WT Y05479
Sc Δaro7 Y05479
Sc Δaro/SsCMU2
Sc Δaro/SsCMU2K102A, R113A
Sc Δaro/BeCMU2
Sc Δaro/BeCMU2K105A, R116A
OD: 0.5 0.1 0.05 0.01 0.5 0.1 0.05 0.01
C
BeCMU2
BeE11
BeCMU2*
KPO4
Absorbance at 320 nm
Time (minutes)
D

Figure 1. (**A**) Protein alignment of secreted *B. elliptica* chorismate mutase 2 (BeCMU2), secreted *S. sclerotiorum* chorismate mutase 2 (SsCMU2), intracellular *B. elliptica* chorismate mutase Aro7 (BeAro7), intracellular *S. cerevisiae* chorismate mutase (ScAro7), chloroplastic chorismate mutase 1 of *N. benthamiana* (NbCMU1) and *A. thaliana* (AtCMU1). Red boxes indicate conserved residues and blue outlined boxes contain amino acids belonging to the same group. The catalytic residues mutated in this study are indicated with black stars. (**B**) Yeast complementation assay with *BeCMU2* and *SsCMU2* and with $BeCMU2_{K105A,\ R116A}$ and $SsCMU2_{K102A,\ R113A}$ in *S. cerevisiae Δaro7* background. WT *S. cerevisiae* and complemented *ScΔaro7* mutants inoculated on YPD-agar and on selective medium lacking Tyr and Phe. (SD-Phe-Tyr+Gal/Raf). (**C**) BeCMU2 in vitro enzyme assay. Spectrophotometric absorption at 320 nm of phenylpyruvate upon BeCMU2 incubation with chorismate, measured over a time span of 10 minutes. KPO_4 buffer and BeE11 were used as negative controls along with heat denatured *BeCMU2*. All data were shown as mean ± S.E.M. (**D**) BeCMU2 protein structure prediction showing the three α-helices (purple), the predicted chlTP (green), cysteine residues (yellow), and the mutated catalytic sites (blue).

BeCMU2 causes a cell death response in the plant

The capacity of BeCMU2 to cause cell death was tested by infiltrating purified protein in lily and *N. benthamiana* leaves (**Figure 2**). BeCMU2 was produced in *Pichia pastoris* and purified by His-tag affinity purification. The protein band migrated at a size of ca. 50 kDa on SDS-PAGE gels and was detected via immunoblotting using anti-His antibodies (Supplementary Figure S1). The migration in the gel does not correspond to the predicted molecular weight of ca 17 kDa. The mature BeCMU2 protein contains four asparagine residues which could have caused protein glycosylation during heterologous expression in *P. pastoris* (Supplementary Figure S1). This hypothesis was confirmed by observing that deglycosylation of purified BeCMU2 resulted in migration at a size of around 20 kDa (Supplementary Figure S1). Pure BeCMU2 infiltration (at a concentration of 100 µg/mL) caused a visible necrotic response at 3dpi only in lily genotype A, in which the infiltrated area showed a brownish, heterogeneous discoloration (**Figure 2**, upper panel). In addition, the infiltrated tissue in this genotype appeared dry and collapsed. By contrast, both *N. benthamiana* and lily genotype L did not show any visible damage (**Figure 2**, upper panel). However, when the leaves were visualized with a light imaging system (**Figure 2** bottom panel), red light emission was detected in the infiltrated area of all plants (Landeo Villanueva et al., 2021).

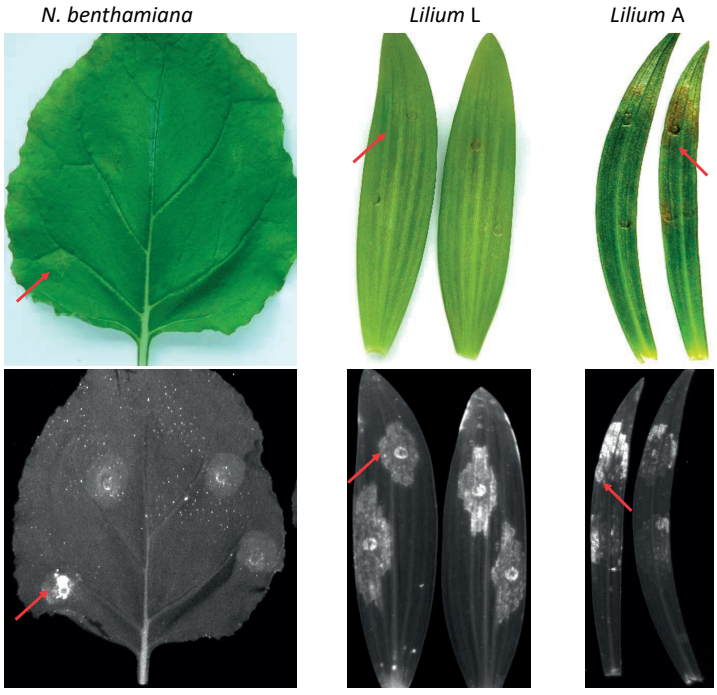

Figure 2. BeCMU2 protein infiltration in leaves of *N. benthamiana* and lily genotypes L and A. Leaf response was visualized at 3 dpi with normal light (upper panel) and by red light imaging (bottom panel). Infiltrated areas are indicated with red arrows.

BeCMU2 contributes to *B. elliptica* virulence in lily

The contribution of BeCMU2 to *B. elliptica* virulence was evaluated by comparing lesion development upon lily leaf inoculation with *B. elliptica* WT and *ΔBecmu2* mutants (**Figure 3**). At 4 dpi the lesions caused by the mutants were smaller than those caused by the WT fungus in both lilies tested (**Figure 3A** and **B**). More specifically, the lesion diameter caused by the *B. elliptica* WT ranged between 5 and 7 mm in lily LA, and between 3 and 5 mm in lily OA, respectively (**Figure 3B**). By contrast, lesion diameters upon inoculation of both *ΔBecmu2* mutants ranged between 2 and 5 mm in lily LA and between 1 and 3 mm in lily OA. Besides the difference in lesion sizes, we noticed a translucent area around the necrotic lesions in leaves of both lilies inoculated with *B. elliptica* WT that was not visible when the leaves were inoculated with both *ΔBecmu2* mutants (**Figure 3C**, yellow arrow).

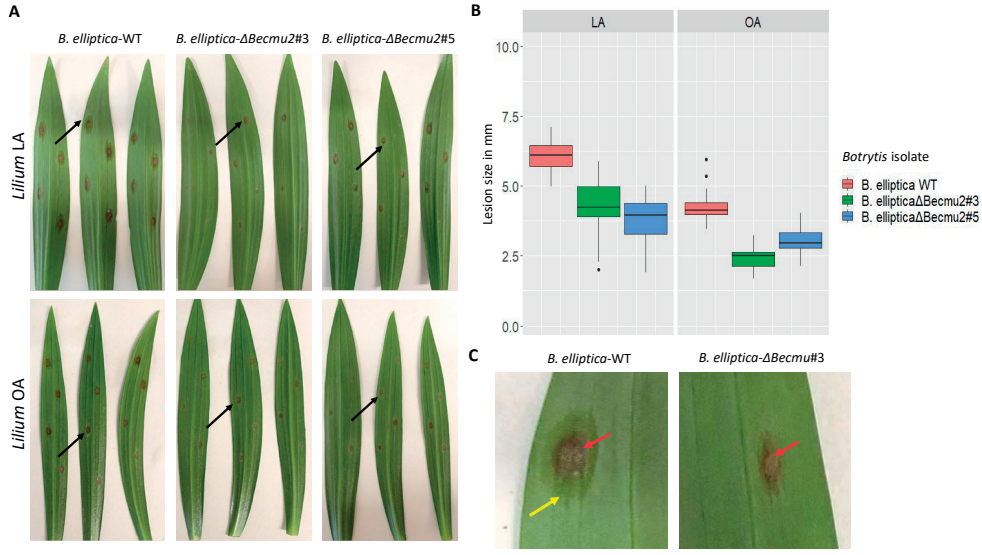

Figure 3. (**A**) Necrotic lesions at 4 dpi in lily genotypes LA and OA inoculated with *B. elliptica* WT and *B. elliptica ΔBecmu2* mutants indicated by black arrows. (**B**) Lesion diameters measured at 4 dpi in lily genotypes LA and OA inoculated with of *B. elliptica* WT and *ΔBecmu2* mutants. Lesion diameters are plotted for each genotype in separate panels. Each coloured box contains all lesion diameters measured for a given lily genotype in the two repetitions of the disease assays. (**C**) Close-up of symptoms caused *B. elliptica* WT and *B. elliptica ΔBecmu2* #3 in lily LA. Red arrow indicates necrotic area, yellow arrow indicates translucence.

BeCMU2 subcellular localization *in planta*

BeCMU2 was predicted to contain a chlTP which may be required to translocate the effector protein to the plant chloroplast after fungal secretion into the apoplast. This hypothesis was tested by agro-infiltrating *N. benthamiana* with BeCMU2$^{24\text{-}164}$::GFP and BeCMU2$^{56\text{-}164}$::GFP fusion constructs to assess the subcellular localization of BeCMU2 in presence and absence of the chlTP. A cytoplasmic reporter (PepMV-CP::GFP) was included and an empty pBINKS-GWY-eGFP was used as a negative control. At 2 dpi, the agro-infiltrated leaves were visualized with confocal microscopy for detection of GFP signal and chlorophyl autofluorescence (**Figure 4A**). Under the tested conditions, BeCMU2$^{24\text{-}164}$::GFP signal did not appear to overlap with the chloroplast autofluorescence signal as it was relatively homogeneously distributed in the cytoplasm of turgescent leaf cells and around the nuclei, analogously to BeCMU2$^{56\text{-}164}$::GFP and for PepMV-CP::GFP (**Figure 4A**). Given these observations, we hypothesize that the GFP reporter may have been cleaved from the fusion protein during *in planta* transient expression, as consequence of post-translational modification. In such a situation, the signal derived from the GFP reporter would be detected at random location within the plant cell. To test this hypothesis we performed GFP immunodetection after protein extraction from leaves samples agro-infiltrated with the different constructs (**Figure 4B**). In all cases, a band of ca. 27 kDa was detected which

corresponds to the cleaved GFP reporter. This band showed in all cases similar or higher intensity than the bands corresponding to the fusion proteins BeCMU2$^{24\text{-}164}$::GFP (42 kDa), BeCMU2$^{56\text{-}164}$::GFP (38 kDa) and PepMV-CP::GFP (55 kDa), respectively (**Figure 4B**, black arrows).

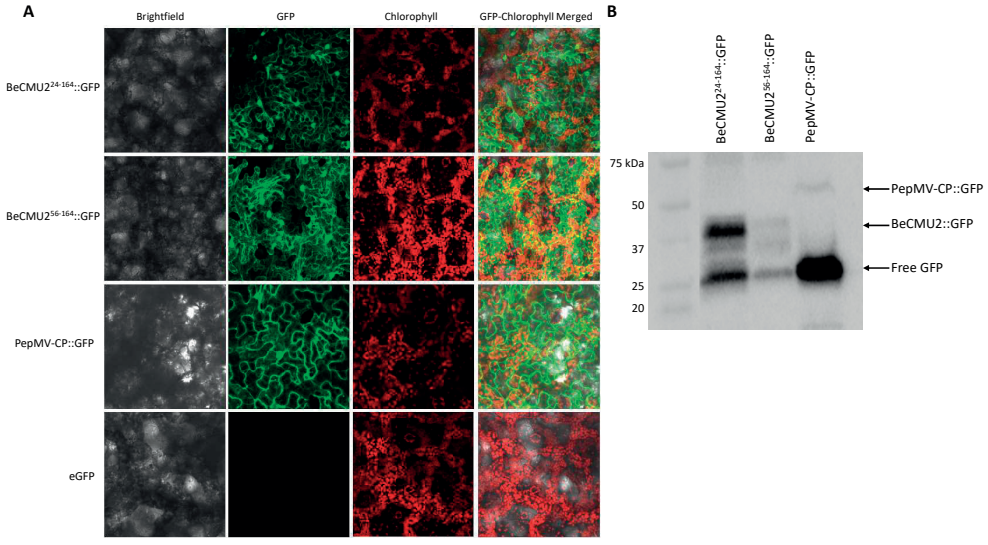

Figure 4. (**A**) Confocal imaging of *N. benthamiana* leaves transiently expressing BeCMU2::GFP (with or without chlTP) and the cytoplasmic reporter PepMV-CP::GFP. Samples were analysed at 2dpi with brightfield, GFP and chlorophyll filters, separately, and with both GFP and chlorophyll filters merged. (**B**) Immunodetection of GFP fusion proteins after protein extraction from agro-infiltrated *N. benthamiana* leaves. Bands of PepMV-CP::GFP, BeCMU2::GFP and free GFP are marked in the right margin.

During host tissue colonization, *Botrytis* fungi secretes effector proteins into the apoplast to promote infection. Therefore, we generated *B. cinerea* mutants expressing BeCMU2 fused to GFP to study effector delivery *in planta*. Because of the lily leaf thickness and since *B. cinerea* is mostly unable to form developing necrotic lesions in lily we decided to study BeCMU2 delivery and subcellular localisation *in planta* by inoculating *N. benthamiana* leaves with *B. cinerea* mutants expressing BeCMU2::GFP (**Figure 5**). It was observed that the GFP signal mostly accumulated in the young hyphae of growing mycelium, whereas GFP signal intensity was lower in septate fully developed hyphae (**Figure 5A**). When zooming in on plant tissue at the edge of the necrotic lesions, we observed that chloroplasts were surrounded by small vesicle-like structures (**Figure 5B**). Moreover, the strong GFP signal was detected in such vesicle-like structures appeared to diffuse to the chloroplasts thereby conferring them a green colour and making them visible when the tissue was visualized with the GFP filters. These vesicle-like structures could not be observed when the tissue was visualized with filters for detection of chlorophyll autofluorescence. From the acquired images, it remains unclear whether the vesicle-like structures were of plant

or fungal origin. Nevertheless, the more vesicle-like structures were located at the chloroplasts (**Figure 5B**), the stronger was the yellow colouration of the chloroplasts when the images for GFP and chlorophyl autofluorescence detection were merged. Similar observations were made when *N. benthamiana* leaves were inoculated with a two other independent *B. cinerea* BeCMU2::GFP mutant (Supplementary Figure S4).

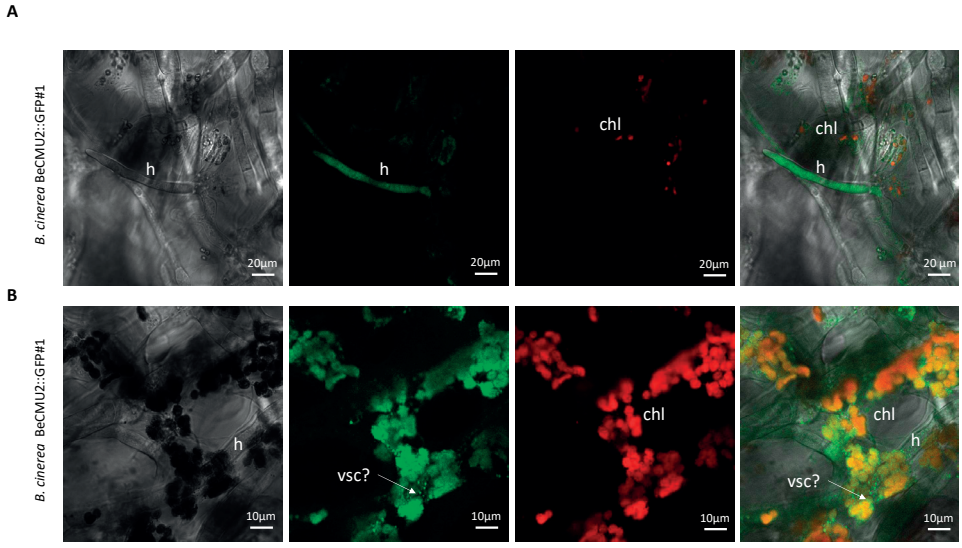

Figure 5. Confocal imaging of *N. benthamiana* leaves inoculated with a *B. cinerea* mutant carrying BeCMU2::GFP fusion reporter. Images were acquired at 2dpi with brightfield, GFP and chlorophyll filters, separately, and with GFP and chlorophyll filters merged. Leaf samples for microscopic analysis were excised from an area just outside the necrotic lesions caused by the fungal infection. (**A**) BeCMU2::GFP signal accumulation in young hyphae of *B. cinerea* BeCMU2::GFP isolate #1 growing mycelium. BeCMU2::GFP signal detection at 2dpi after N. benthamiana leaf inoculation with *B. cinerea* BeCMU2::GFP isolate #1 (**B**). h = fungal hyphae; chl = chloroplast; vsc = vesicle-like structures.

DISCUSSION

Pathogen effectors targeting plant subcellular compartments gained increasing attention in the past decade and evidence is emerging that chloroplasts play a pivotal role in regulating plant immune responses. Several plant pathogens including bacteria, fungi, nematodes and viruses use effectors which target the chloroplast to manipulate host defense responses such as generation of ROS (Reactive Oxygen Species), metabolic intermediates that function in retrograde signaling and the defense related signaling mediated by the phytohormones salicylic acid (SA) and jasmonic acid (Ishiga et al., 2017; Sowden et al., 2017; Lu and Yao 2018; Kretschmer et al., 2019). Among these effectors, enzymes with CMU activity have been discovered in several hemi-biotrophic plant pathogens. Their contribution to virulence was proposed to rely on the interference with the biosynthesis

of the defense-related hormone SA (Doyle and Lambert, 2003; Vanholme et al., 2009; Djamei et al., 2011; Bauters et al., 2020; Assis et al., 2021; He et al., 2021). During plant-microbe interaction, chorismate serves as substrate for the biosynthesis of SA which can be synthesized through two distinct pathways (**Figure 6**; Vlot et al., 2009; Dempsey et al., 2017; Klessig et al., 2018). In *Arabidopsis thaliana*, most pathogen-induced SA biosynthesis (~90%) derives from iso-chorismate, which is generated from chorismate by the activity of isochorismate synthases (ICS) (Torrens-Spence et al., 2019; Serrano et al. 2013; Lefevere et al., 2020; Dempsey et al., 2011; Garcion et al., 2008; Strawn et al., 2007; Wildermuth et al., 2001). On the other hand, a smaller proportion (~10%) derives from the Phenylalanine-Ammonia Lyase (PAL) pathway in the cytoplasm which requires CMU activity to convert chorismate into prephenate as precursor of Phe biosynthesis (**Figure 6**; Serrano et al. 2013; Lefevere et al., 2020; Dempsey et al., 2011; Garcion et al., 2008; Strawn et al., 2007). In other plant species such as rice (*Oryza sativa*, Poaceae) and tobacco (*Nicotiana tabacum*, Solanaceae) SA biosynthesis upon pathogen challenge mostly relies on the PAL pathway (Duan et al., 2014). To which extent the ICS and PAL pathways contribute to SA biosynthesis in lily is unknown.

The chloroplast membrane transporter EDS5 (ENHANCED DISEASE SUSCEPTIBILITY5) is required to export iso-chorismate from the chloroplast to the cytoplasm, and the cytoplasmic amidotransferase avrPphB SUSCEPTIBLE3 (PBS3) catalyzes the conjugation of glutamate to iso-chorismate to produce iso-chorismate-9-glutamate, which spontaneously decomposes into SA and 2-hydroxy-acryloyl-N-glutamate or it is converted into SA by the acyltransferase activity of EPS1 (Torrens-Spence et al., 2019; Rekhter et al., 2019). These three compartmentalized proteins (ICS1, EDS5 and PBS3) seem to guide SA flux from the chloroplast to the cytoplasm thereby protecting the pathway from pathogen perturbations (Rekhter et al., 2019). At this moment, all identified pathogen effectors with a CMU domain localize in the cytoplasm of the host cell (Kretschmer et al., 2019, Sowden et al., 2017). However, the mechanism by which the CMU effectors interfere with SA biosynthesis is not fully understood. The “competition model” proposed by Doyle and Lambert (2003) postulates that CMUs secreted by pathogens can channel chorismate outside the chloroplast to flow into the PAL pathway thereby diminishing SA biosynthesis in the chloroplast via ICS activity (Djamei et al., 2011, Qian et al., 2019 and Lefevere et al., 2020; Assis et al., 2021). In contrast to CMU effectors of hemi-biotrophic pathogens, little is known about CMU effectors in necrotrophic fungi. Only recently a CMU protein has been identified in the secretome of the necrotrophic Ascomycota *S. sclerotiorum* (Liang and Rollins, 2018) but no functional or localisation study has been published so far. In this study we investigated the enzyme activity, the contribution to virulence and the effector localization in host plant cells of the *B. elliptica* CMU2 effector.

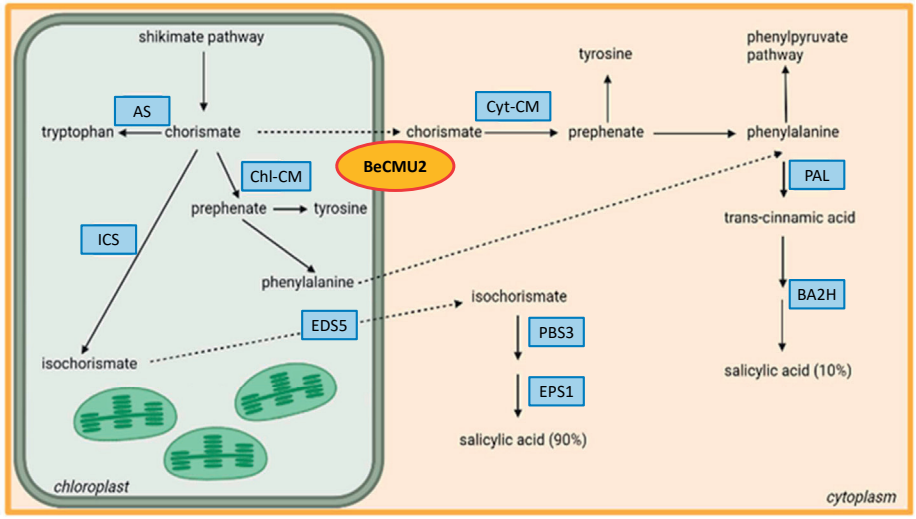

Figure 6. Biosynthesis routes of salicylic acid. The production of salicylic acid is mediated through two pathways both starting with chorismate as precursor. The Isochorismate synthase (ICS) pathway takes place in the chloroplast whereas the Phenylalanine Ammonia-Lyase (PAL) pathway is responsible for salicylic acid biosynthesis in the cytoplasm. Enzymes are depicted in blue boxes, black lines are conversion steps, dotted lines are transport routes from the chloroplast to the cytoplasm. EDS5, ENHANCED DISEASE SUSCEPTIBILITY5; AS, anthranilate synthase; Chl-CM, chloroplastic chorismate mutase; Cyt-CM, cytoplasmic chorismate mutase; ICS, isochorismate synthase; PAL, phenylalanine ammonia-lyase, PBS3, amidotransferase avrPphB SUSCEPTIBLE3; EPS1, BAHD Acyltransferase; BA2H, benzoic-acid-2-hydroxylase. Adapted from Rekhter et al. (2019); Torrens-Spence et al. (2019) and Lefevere et al. (2020).

BeCMU2 possesses CMU activity and contributes to *B. elliptica* virulence in lily

First, BeCMU2 enzymatic activity was assessed via yeast complementation and with an *in vitro* enzyme reaction. These experiments provided evidence that BeCMU2 indeed possess CMU activity (**Figure 1**). Despite a lack of sequence homology to other described plant- and pathogen-derived CMU proteins (with the exception of the *S. sclerotiorum* CMU2 effector reported by Liang and Rollins, 2018), structure prediction of BeCMU2 revealed the canonical α-helical secondary structure as reported for other eukaryotic AroQ-type CMU proteins (Sasso et al., 2005; Westfall et al., 2014). Based on sequence information and crystal structure determination, CMUs are classified into two groups. The bacterial CMUs fall under the AroH class and are known to be monofunctional enzymes (Lee et al., 1995; Sträter et al., 1997; Krappmann et al., 1999; Helmstädt et al., 2001 and 2004). By contrast, eukaryotic AroQ-type CMUs are capable to dimerize (Helmstädt et al., 2001; Sasso et al., 2005; Djamei et al. 2011; Westfall et al., 2014). The *Ustilago maydis* CMU1 was capable to form dimers with both the maize (*Zea mays*, Poaceae) chloroplastic (ZmCMU1) and the cytoplasmic (ZmCMU2) CMUs (Djamei et al. 2011). Whether BeCMU2

is also capable to dimerize with plant CMUs is unknown but can be studied *in vitro* via yeast two hybrid (Brückner et al., 2009) or *in vivo* via the split luciferase system (Cassonnet et al., 2011). This would allow to postulate that BeCMU2 dimerization with plant CMUs may disturb the chloroplast metabolism during fungal infection. Furthermore, allosteric regulation is a characteristic feature of chloroplastic plant AroQ-type CMUs as well as of fungal cytoplasmic CMUs, since they contain an additional domain which participates in allosteric regulation of the enzyme. By contrast, cytoplasmic plant AroQ-type and bacterial AroH-type CMUs are not allosterically regulated (Xue et al., 1994; Eberhard et al., 1996; Sträter et al., 1997; Krappmann et al., 1999; Helmstaedt et al., 2001 and 2004; Westfall et al., 2014). Studies of CMUs in *Arabidopsis* showed that the chloroplastic AtCMU1 and AtCMU3 are allosterically regulated by the three aromatic amino acids, whereas the cytoplasmic AtCMU2 is not (Westfall et al., 2014; Kroll et al., 2017). Tryptophan (Trp) enhances the activity of chloroplastic CMUs via feed-back loop inhibition of anthranilate synthase (AS) which competes with chloroplastic CMU for chorismate as substrate for Trp biosynthesis (Romero et al., 1995; Westfall et al., 2014; Kroll et al., 2017). By contrast, Tyr and Phe inhibit chloroplastic CMUs since they interfere with the binding of chorismate at the active catalytic site of the enzyme (Romero et al., 1995; Eberhard et al., 1996; Westfall et al., 2014; Kroll et al., 2017). It would be interesting to test whether the enzyme activity of BeCMU2 is allosterically regulated. This can be assessed by performing an *in vitro* enzyme assay in which purified BeCMU2 protein and chorismate are incubated together with Phe or Trp, respectively. Reduction in phenylpyruvate absorbance in presence of Phe and increase in phenylpyruvate absorbance in presence of Trp would confirm allosteric regulation of BeCMU2 activity. If allosteric inhibition of BeCMU2 can be demonstrated, it is as yet unclear what the advantage for the infection in lily would be.

Lily and *N. benthamiana* leaves infiltrated with purified BeCMU2 showed a response in the infiltrated tissue, visible as dry brownish tissue in lily genotype A but not in lily genotype L and in *N. benthamiana*, in which only red light emission could be detected (**Figure 2**). The red light signal derives from chlorophyl autofluorescence as a result of the abortion of photochemical activity in dying photosynthesizing plant tissue and is therefore considered as a sign of the occurrence of PCD (Landeo Villanueva et al., 2021). Most likely, the observed leaf response was caused by the infiltration of BeCMU2 at this concentration (100 µg/mL) that affected cell and chloroplast metabolism in a such a severe way that it caused PCD induction. Nevertheless, it cannot be excluded BeCMU2 may also induce cell death by acting as necrotrophic effector and thus upon BeCMU2 recognition by an (as yet unknown) receptor in the host cytoplasm or chloroplast. This can be tested by producing enzymatically non-functional BeCMU2. If the cell death response would still be observed upon infiltration of the enzymatic non-functional protein, this would indicate that the cell death inducing capacity of BeCMU2 relies on protein recognition rather than the enzymatic activity. Parallel, the contribution of BeCMU2 to fungal virulence was assessed by

comparing symptoms development upon inoculation of *B. elliptica* WT and two Δ*Becmu2* deletion mutants in lily (**Figure 2**). It is important to mention that these two mutants were two separate homokaryotic derivatives of the same primary heterokaryotic transformant. Therefore, additional, independent mutants need to be generated and tested as well as *BeCMU2* complementation needs to be conducted to check whether the virulence is restored. Reduction in lesion size was observed in both tested lily genotypes when they were inoculated with the *ΔBecmu2* deletion mutants compared to the WT isolate (**Figure 2C**). Most notably, the translucent area surrounding the necrotic spots, that was visible when the lilies were infected by *B. elliptica* WT, could not be observed in lilies infected with both *ΔBecmu2* mutants (**Figure 2D**, yellow arrow). As a result, also the size of the necrotic lesions was smaller in the leaves inoculated with *ΔBecmu2* mutants because the transition to the necrotrophic phase would be retarded since this transition requires an initial biotrophic interaction with the host to allow the fungus to accumulate sufficient biomass and suppress autophagy-like PCD (Veloso and van Kan 2018). This suggests that BeCMU2 may be delivered ahead of the invading hyphae before the primary necrotic lesions have been formed. In fact, BeCMU2 uptake in the plant cells and the capacity of interfering with SA biosynthesis would require living, metabolically active host cells with functional chloroplasts. In such a scenario, BeCMU2 might represent an important factor for the early biotrophic phase of the interaction with the host which is associated to the suppression of the initial defense responses. To validate this hypothesis, several experiments can be conducted. Hyphal staining with calcofluor white would allow to detect hyphae in the translucent area surrounding the necrotic lesions during lily infection with the WT fungus, whereas *B. elliptica ΔBecmu2* mutants would not be detected outside the necrotic spot. In addition, *BeCMU2* transcript level might be significantly higher in tissue collected from the translucent area than in the dry necrotic lesions, indicating that once the necrotic lesions are formed, CMU activity would no longer be required for disease development.

BeCMU2 effector delivery and subcellular localization *in planta*

With the aid of a prediction tool for effector subcellular localization (Sperschneider et al., 2017) it was found that BeCMU2 carries a 18 amino acid long predicted chlTP (SPLPTLCPSLSNATRSIP). Therefore, effector localization within the plant cell was assessed with two different approaches. First, the mature BeCMU2 with and without chlTP, was fused to GFP and agro-infiltrated in *N. benthamiana*. Confocal images however, showed GFP signal throughout the cytoplasm and around the nucleus, no matter whether the reporter construct carried the chlTP or not (**Figure 4A**). This observation can have different explanations. *A. tumefaciens* mediated T-DNA insertion into the plant nucleus leads to mRNA translation by plant ribosomes. Proteins carrying a signal peptide for secretion are recognized by a protein complex called signal-recognition particles (SRP). Upon recognition, the SRP complex brings the ribosome to the endoplasmic reticulum (ER)

where translation is completed and the signal peptide is cleaved off. In the ER, proteins are folded into their correct shapes and are then transported to the Golgi apparatus. In the Golgi, proteins undergo post-translational modifications required for proper protein folding before being transported to their final destination such as subcellular organelles and the plasma membrane, or before being secreted into the apoplast. In absence of a signal peptide for secretion, the newly synthesized protein will reside in the plant cytoplasm or it will be transported back to the nucleus. Moreover, GFP immunodetection from agro-infiltrated tissues showed that the samples contained a high amount of free GFP in addition to the BeCMU2::GFP fusion protein (**Figure 4C**). The high amount of free GFP detected probably derives from proteolytic cleavage of GFP from the fusion protein. Based on these observations, it is impossible to determine whether BeCMU2 localized at the chloroplast or not because the strong GFP fluorescence in the cytoplasm could have masked the detection of BeCMU2::GFP in the chloroplast. In a second approach *B. cinerea* mutants carrying BeCMU2::GFP were generated, whereby the signal peptide for secretion was maintained in the *BeCMU2* coding sequence. These fungal mutants were inoculated in *N. benthamiana* leaves and the infected tissue was observed under the confocal microscope. Strong GFP fluorescence was observed in the tips of young hyphae (**Figure 5A**), where the effector probably accumulated before being secreted into the apoplast. When zooming in on *N. benthamiana* cells we observed that in some places the GFP signal overlapped with the red light signal derived from chlorophyll autofluorescence in the chloroplast, and it was not homogeneously distributed in the cytoplasm as observed in agro-infiltrated leaves. GFP fluorescence was especially strong in small (< 1 µm) vesicle-like structures which surrounded the chloroplasts but were not part of the chloroplast itself since they were not detected when the images were acquired with the chlorophyl fluorescence filters (**Figure 5B** and Supplementary Figure S4). These results provide preliminary indications that BeCMU2 might localise at the chloroplast after secretion into the apoplast. However, it remains to be answered how the effector can enter the plant cell before subsequently being translocated to the chloroplast. Given the absence of any known endocytotic uptake motif, such as the tripeptide Asn-Gly-Asp which is required for internalisation of the *P. nodorum* effector SnToxA (Manning et al., 2008), there may be a role of the vesicle-like structures. Recent studies have highlighted the importance of clathrin vesicles in several fungal species including *B. cinerea* for protein translocation through the fungal cytoplasm, for protein uptake from the environment and for effector delivery (Schultzhaus et al., 2017; Bairwa et al., 2019; Wytinck et al., 2020; Souibgui et al., 2021). *B. cinerea* carrying mutated clathrin heavy chain was negatively affected in pathogenicity (Souibgui et al., 2021). Whether the vesicle-like structures observed in our microscopic images are of plant or fungal origin remains unknown. Brefeldin A might be used to block fungal effector secretion into the apoplast as shown for the rice blast fungus *Magnaporthe oryzae* (Giraldo et al., 2013) and for the Oomycota *Phytophthora infestans* (Wang et al., 2017). If BeCMU2 delivery into the apoplast and uptake into the plant cell

occurs via fungal vesicles, brefeldin A treatment would prevent the formation of vesicle-like structures and the GFP signal would not overlap with chlorophyl autofluorescence at the chloroplast. Even though additional experiments are needed to confirm that BeCMU2 may localize at the chloroplast, this studied identified a secreted and enzymatically active CMU effector in the necrotrophic Ascomycota *B. elliptica*. Our observations suggest the BeCMU2 may contribute to virulence in the early phases of *B. elliptica* infection in lily thereby supporting the hypothesis that necrotrophic fungi of the genus *Botrytis* and *Sclerotinia* require an initial biotrophic interaction with the host for successful disease development (Liang and Rollins 2018, Veloso and van Kan 2018).

SUPPLEMENTARY MATERIAL

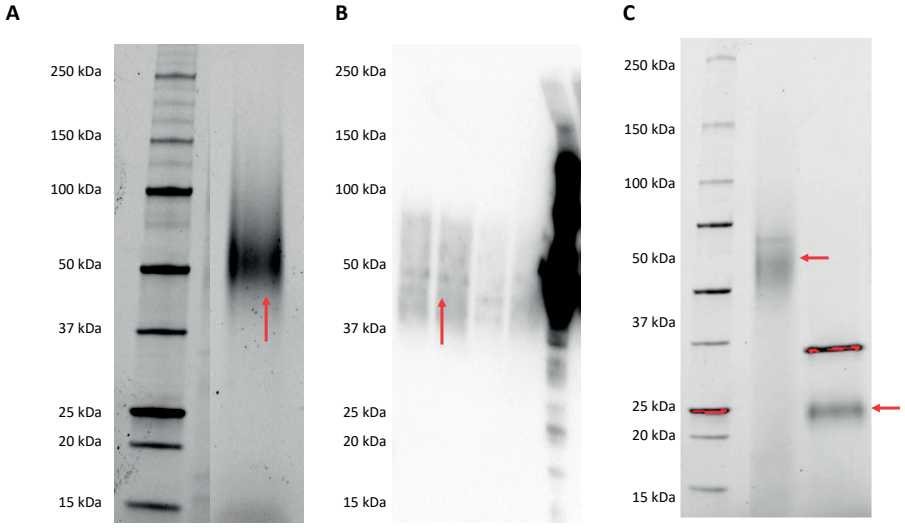

Supplementary Figure S1. Purification, immunodetection and deglycosylation of the heterogously expressed BeCMU2 protein. BeCMU2 after purification with His-tag affinity resin (**A**). BeCMU2 band at ca. 50 kDa is indicated by a red arrow. BeCMU2-6xHis immunodetection with α-His primary and α-HRP secondary antibodies. BeCMU2 band at ca. 50 kDa is indicated by a red arrow (**B**). BeCMU2 deglycosylation. BeCMU2 bands before and after deglycosylation at ca. 50 kDa and ca. 25 kDa, respectively, are indicated by a red arrow (**C**).

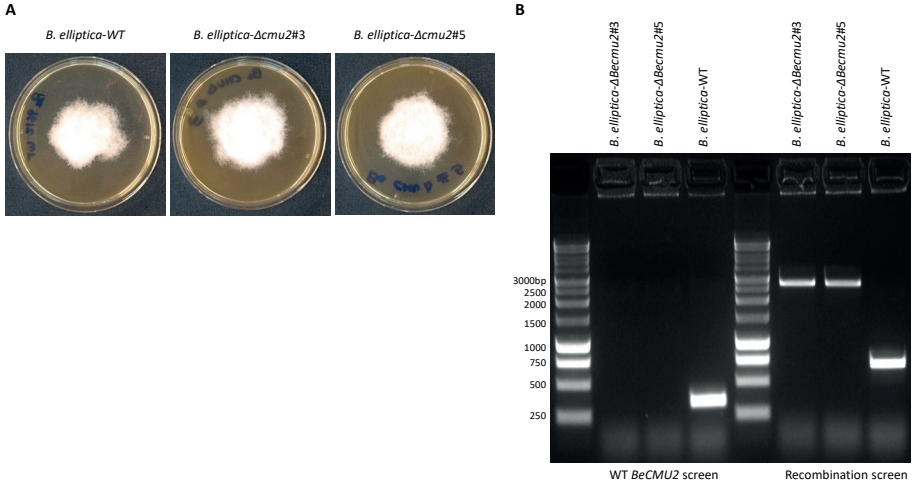

Supplementary Figure S2. Phenotypic and molecular characterisation of *B. elliptica* 9612 *ΔBecmu2* mutants #3 and #5 used in this study. Fungal radial growth on MAE at 4dpi (**A**). Gel electrophoresis showing *BeCMU2* deletion in *B. elliptica* mutants using primers within *BeCMU2* (WT *BeCMU2* screen) and outside the 60bp flanks selected for homologous recombination during CRISPR-Cas9 mediated transformation (recombination screen) (**B**).

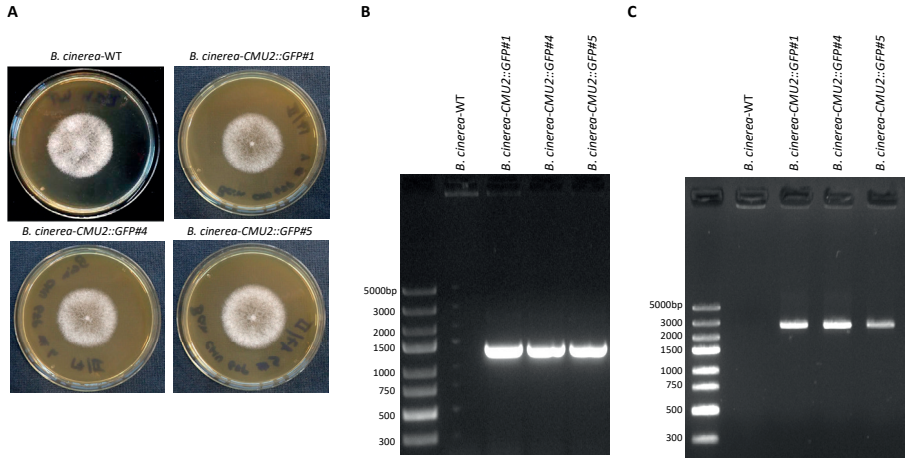

Supplementary Figure S3. Phenotypic and molecular characterisation of *B. cinerea 05.10* mutants #1, #4 and #5 carrying the fusion reporter gene *BeCMU2::GFP* at the BcniaD locus used in this study. Fungal radial growth on MAE at 4dpi (**A**). Gel electrophoresis showing *BeCMU2::GFP* insertion at the *BcniaD* locus in *B. cinerea* mutants using primers aligning to the GFP sequence and to the 5' BcNiaD 60bp flanks (**B**) and using primers aligning to the BeCMU2 sequence and to the 3' BcNiaD 60bp flanks selected for homologous recombination during CRISPR-Cas9 mediated transformation (**C**).

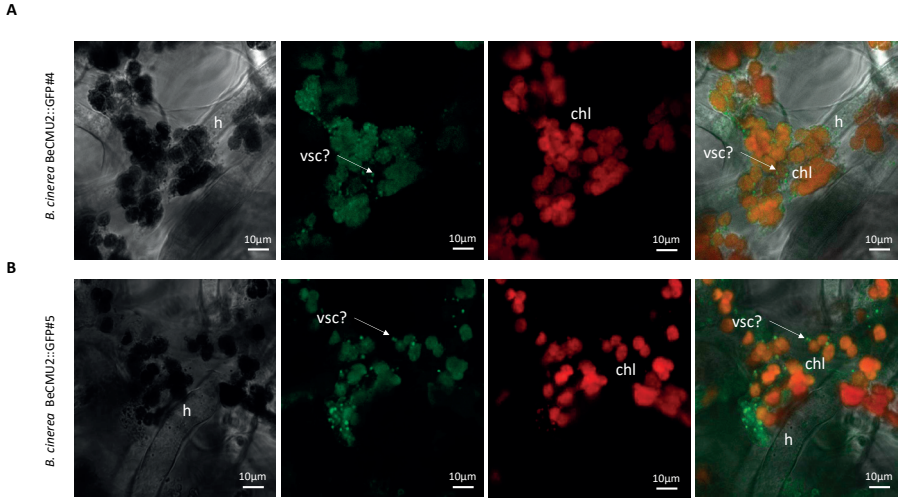

Supplementary Figure S4. Confocal imaging of *N. benthamiana* leaves inoculated with two other independent *B. cinerea* mutant isolates carrying *BeCMU2::GFP*. Images were acquired at 2dpi with brightfield, GFP and chlorophyll filters and with both GFP and chlorophyll filters merged. Leaf samples for microscopical analysis were excised from the area just outside the necrotic lesions caused by the fungal infection. GFP detection and co-localization at the chloroplasts during infection of *B. cinerea* BeCMU2::GFP isolates #4 (**A**) and #5 (**B**). h = fungal hyphae; chl = chloroplast; vsc = putative vesicle-like structures.

Supplementary Table 1. Plasmids used in this study

Plasmid	Cloning strategy	Source
pYES260	-	Djamei et al., 2011
pYES260::BeCMU2$^{24\text{-}166}$	MultiS one step cloning	generated in this study
pYES260::BeCMU2$^{24\text{-}166}_{\text{K105A, R116A}}$	MultiS one step cloning	generated in this study
pYES260::SsCMU2$^{21\text{-}160}$	MultiS one step cloning	generated in this study
pYES260::SsCMU2$^{21\text{-}160}_{\text{K102A, R113A}}$	MultiS one step cloning	generated in this study
pPIC9K-6xHis	-	Invitrogen
pPIC9K::BeCMU2$^{24\text{-}165}$6xHis	MultiS one step cloning	generated in this study
pENTR/D-TOPO::BeCMU2$^{24\text{-}164}$	Gateway Cloning	generated in this study
pENTR/D-TOPO::BeCMU2$^{56\text{-}164}$	Gateway Cloning	generated in this study
pBINKS-GWY-eGFP	-	Liebrand et al., 2012
pBINKS-GWY::BeCMU2$^{24\text{-}164}$-eGFP	Gateway cloning	generated in this study
pBINKS-GWY::BeCMU2$^{56\text{-}164}$-eGFP	Gateway Cloning	generated in this study
pBINKS-GWY-fl-PepMV-Cp-nostop-eGFP	-	Liebrand et al., 2012
pNDH-OGG	-	Schumacher, 2012
pNDH-OGG::BeCMU2-GFP	MultiS one step cloning	generated in this study
pTEL-HYG	-	Leisen et al., 2020

Supplementary Table 2. Oligonucleotides used in this study

Primer	5'-3' sequence	Application
FW-pYES linearization	CAGTGTGCTGGAATTCTGCA	pYES backbone amplification for plasmid linearization
RV-pYES linearization	TTACAGCTGCTAGTAGTCCG	
FW-BeCMU2$^{24\text{-}166}$ pYES flank	CGGACTACTAGCAGCTGTAAATGACATCCACACCCCCTACCGA	Recombination of BeCMU2$^{24\text{-}166}$ with linearized pYES
RV-BeCMU2$^{24\text{-}166}$ pYES flank	TGCAGAATTCCAGCACACTGCTACACCAGCCCTTCAAAACTCC	
FW-BeCMU2$^{24\text{-}166}{}_{\text{K105A, R116A}}$	GACGAGATTCGCAGGGACATTGGATACGGTGGATGTACCGAGTGCAGATCAAGAGG	Mutagenesis primer for construct BeCMU2$^{24\text{-}166}{}_{\text{K105A, R116A}}$
RV-BeCMU2$^{24\text{-}166}{}_{\text{K105A, R116A}}$	CCTCTTGATCTGCACTCGGTACATCCACCGTATCCAATGTCCCTGCGAATCTCGTC	
FW-SsCMU2$^{21\text{-}160}$ pYES flank	CGGACTACTAGCAGCTGTAAATGGCCACAACCCCTACACAAGT	Recombination of SsCMU2$^{21\text{-}160}$ with linearized pYES
RV-SsCMU2$^{21\text{-}160}$ pYES flank	TGCAGAATTCCAGCACACTGTTAAGAAGAAATCGCCCAAACACAC	
FW-SsCMU2$^{21\text{-}160}{}_{\text{K102A, R113A}}$	GACGAGATTCGCGGCAACGTTGGGTGATGTGAATGTGCCGAGTGCAAATCAGGAGG	Mutagenesis primer for construct SsCMU2$^{21\text{-}160}{}_{\text{K102A, R113A}}$
RV-SsCMU2$^{21\text{-}160}{}_{\text{K102A, R113A}}$	CCTCCTGATTTGCACTCGGCACATTCACATCACCCAACGTTGCCGCGAATCTCGTC	
FW-BeCMU2$^{24\text{-}164}$-pENTRY	CACCATGACATCCACACCCCCTAC	GFP fusion constructs ATTA
FW-BeCMU2$^{56\text{-}164}$-pENTRY	CACCATGTGGGGAACCCCTTCATTC	
RV-BeCMU2$^{24\text{-}164}$-pENTRY	CCCTTCAAAACTCCCC	
FW-BeCMU2-pPIC9K	GAGAGGCTGAAGCTTACGTAACATCCACACCCCCTACCG	Recombination of *BeCMU2* in pPIC9K
FW-BeCMU2-pPIC9K	GCGAATTAATTCGCGGCCGCATGATGATGATGATGATGCACCAGCCCTTCAAAACTCC	
FW-BeCMU2-GFP-pNDH	CCATCACATCACAATCGATCCAACCATGGAACTCACTAATACATAC	Recombination of *BeCMU2* in pNDH-OGG
RV-BeCMU2-GFP-pNDH	CTTATCTACATACGCTAAGCGGCCGCCTACACCAGCCCTTCAAAAC	
BcniaD sgRNA1	AAGCTAATACGACTCACTATAGGATGGATGGCCATGAATTCGTGTTTTAGAGCTAGAAATAGCAAG	sgRNA for *BcniaD* deletion
FW BcniaD-pTEL-HYG-donor	ATGGCTAGTGCTCAATTCATGAATGAACACTCTTCCGAGGCTGATGCGGAGATGTCGAAATGCTGGCCTTTTGCTCACATGCATG	Donor DNA generation for *BcniaD* deletion
RV BcniaD-pTEL-HYG-donor	TCAAAAGAAAAGTATATCTTGATCCTTCCATCCCAAATCCGACAATATCCCATGCACACTATCGCCGGAAAGGACCCGCAAATG	
FW BcniaD deletion inside	GTTGTAAGATTTTGTCAGCTTTTATATC	*BcniaD* deletion check
RV BcniaD deletion inside	ATCTACATCTCTGCTCGTTCC	
RV BcniaD deletion outside	GATACTATATTCAAACATCCTCTCTCCC	
BeCMU2 sgRNA1	AAGCTAATACGACTCACTATAGGCGTGTAGCATTAGAAAGCGAGTTTTAGAGCTAGAAATAGCAAG	sgRNAs for *BeCMU2* deletion

Supplementary Table 2. Continue

Primer	5'-3' sequence	Application
BeCMU2sgRNA2	AAGCTAATACGACTCACTATAGGATGCCGCTCTTTGAGCTAGGGTTTTAGAGCTAGAAATAGCAAG	
FW BeCMU2-pTEL-HYG-donor	CTCAACTTCAAACAATTAACCTTGATCGCCTTGAAAAAACTTCATAATCTTAAAGTTTATTGCTGGCCTTTTGCTCACATGCATG	Donor DNA generation for *BeCMU2* deletion
RV BeCMU2-pTEL-HYG-donor	ATTTCCGTTCAATTTGGCATTCACACCTACACTCACTGCCGCAGACATACCAAAATCACTATCGCCGGAAAGGACCCGCAAATG	
FW BeCMU2 deletion inside	CTAATACATACCAAGCTCTCTTGCTCGC	*BeCMU2* deletion check
RV BeCMU2 deletion inside	CCTCTTGATCTCTACTCGGTACATCCAC	
FW BeCMU2 deletion outside	CGGACGCACTCTACTCGAGTACCTAC	
RV BeCMU2 deletion outside	CGTCTCCCTGCTAATTTCCGTTCAATTTG	

Chapter 5

The phytotoxic fungal secondary metabolite botrydial causes cell death and contributes to *Botrytis elliptica* virulence in *Lilium*

Michele C. Malvestiti, Si Qin, Henriek G. Beenen and Jan A. L. van Kan

Wageningen University, Laboratory of Phytopathology, Wageningen, Netherlands

ABSTRACT

Botrydial is a phytotoxic secondary metabolite of the fungal genus *Botrytis*. The compound can cause cell death in dicot plants and is considered a virulence factor in *Botrytis cinerea*. However, the phytotoxicity of botrydial has not been investigated in monocots. Chemically, botrydial represents a bicyclic sesquiterpene which is synthetized by a cluster of six biosynthetic genes. The functional botrydial biosynthetic gene cluster is present in the generalist *B. cinerea* and in the lily specialist *B. elliptica*. In this study we tested the cell death inducing capacity of botrydial in lily by applying pure botrydial on leaves and tepals. Variation in cell death responses was observed between the different tissues and among the different lily genotypes tested. We detected botrydial production in *B. elliptica in vitro* cultures and *in planta* transcriptional activity of *Bebot2,* the key botrydial biosynthetic gene, during infection in lily. Finally *B. elliptica Bebot2* deletion mutants were generated via CRISPR-Cas9 mediated transformation to assess the contribution of botrydial to fungal virulence in lily. In all lily genotypes tested a statistically significant reduction in lesion size was observed upon inoculation with the *B. elliptica Bebot2* deletion mutants as compared to the wild type fungus. Taken together, these results provide evidence that under the tested conditions, botrydial contributes to fungal virulence in the *B. elliptica*-lily interaction.

INTRODUCTION

Lily (*Lilium* spp., Liliaceae) is one of the most important ornamental plants worldwide and its production is threatened by several pests and diseases. Among them, the most destructive is fire blight, a fungal disease caused by the Ascomycota *Botrytis elliptica* and *B. cinerea* (Sclerotiniaceae). Both fungi initially form small brownish necrotic spots on leaves and flowers of the infected lily. Under favourable environmental conditions rapid outgrowth of necrotic spots leads to death of the entire plant. While the generalist *B. cinerea* occurs mainly at post-harvest stage on damaged and senescing plant tissue, *B. elliptica* is host-specific in lily and can inflict serious economic losses since it is able to cause disease also on healthy, vigorous plants (**Chapter 2**). *Botrytis* fungi are filamentous Ascomycota with a necrotrophic life style. After an initial biotrophic interaction with the host plant, *Botrytis* fungi kill the host cells to acquire nutrients for growth and reproduction from the dead plant tissue (Veloso and van Kan, 2018). Host cell death is achieved by means of fungal secreted compounds which can force the plant cell to commit suicide by triggering apoptotic-like Programmed Cell Death (PCD) (van Baarlen et al., 2004; Veloso and van Kan, 2018). These compounds are referred to as necrotrophic effectors, which comprise PCD inducing proteins (Leisen et al., 2022; Steentjes et al., 2022) and phytotoxic secondary metabolites (Collado et al., 2000 and 2007). In *Botrytis*, the best studied phytotoxic secondary metabolite is the bicyclic sesquiterpene botrydial (BOT) (Colmenares et al., 2002; Deighton et al., 2001; Pinedo et al., 2008). This compound is produced by *B. cinerea* during plant infection where it induces host immune responses such as accumulation of reactive oxygen species and the upregulation of expression of genes encoding pathogenesis related proteins (Deighton et al., 2001; Rossi et al., 2011). In addition, BOT was shown to be capable of causing cell death when exogenously applied on leaf and fruit tissue of phylogenetically unrelated dicot species such as *Nicotiana tabacum* and *Capsicum annuum* (Solanaceae), *Phaseolus vulgaris* (Fabaceae) and *Arabidopsis thaliana* (Brassicaceae) (Rebordinos et al., 1996; Deighton et al., 2001; Rossi et al., 2011). Since absence of BOT production in certain *B. cinerea* isolates was shown to correlate to reduced fungal virulence in different host plants, BOT is considered to be a virulence factor in the *B. cinerea*-host interaction (Pinedo et al., 2008; Siewers et al., 2005). Within the *B. cinerea* genome, the genes involved in the biosynthesis of BOT are clustered in a specific locus. The BOT gene cluster consists of six genes encoding biosynthetic enzymes and one gene encoding a transcription factor (Porquier et al., 2016). *Bcbot2* encodes a sesquiterpene cyclase which represents the key-enzyme for the biosynthesis of the sesquiterpene backbone of the toxin, since it converts farnesyl pyrophosphate (FPP) into presilphiperfolan-8-beta-ol (Pinedo et al., 2008). *Bcbot1*, *Bcbot3* and *Bcbot4* encode cytochrome P450 proteins, while *Bcbot5* and *Bcbot7* respectively encode an acetyl transferase and a dehydrogenase that are involved in the biosynthesis of the final form of the secondary metabolite (Porquier et al., 2016). The transcriptional activation of the gene cluster is regulated by a $Zn(II)_2Cys_6$

transcription factor, encoded by *Bcbot6* (Porquier et al., 2016). Although all studies on BOT biosynthesis and phytotoxicity have been conducted in *B. cinerea* and dicot plant species, functional BOT biosynthetic gene clusters are also present in other members of the genus *Botrytis* that are host-specific in monocot plant taxa such as *B. elliptica* in lily (Valero-Jiménez et al., 2020). The BOT clusters in *B. cinerea* and *B. elliptica* are located in different genomic regions, are both flanked by a gypsy/copia repeat on one side, and the *B. cinerea* BOT cluster contains an additional internal transposon (Valero-Jiménez et al., 2020). This study focusses on the role of BOT in the *B. elliptica*-lily pathosystem. This was investigated first by assessing the BOT production in *B. elliptica* during fungal solid and liquid cultures. Secondly we tested whether BOT displays phytotoxic activity in lily by exogenously applying purified BOT onto lily leaves and tepals. Finally we determined the contribution of BOT to *B. elliptica* virulence during lily infection by generating *Bebot2* deletion mutants and by comparing in disease assays the lesion size development of the mutants to the wild type fungus.

MATERIALS AND METHODS

Plant material and growth conditions

Bulbs of *Lilium* spp. genotype "Asiatic" (A), "Longiflorum" (L) and "Longiflorum-Asiatic" (LA 1 and LA 2) were grown as described in **Chapter 2**. Mature leaves as described by Bar and Ori (2014) were harvested and used for disease assays. Lilies carrying flower buds at initiation of bud colour were harvested as cut flowers and transported to the laboratory to be inoculated or treated with BOT. Conidia inoculations and exogenous BOT application in lily flowers were conducted within 2 days after bud opening.

Fungal isolates and growth conditions

B. elliptica and *B. cinerea* isolates used in this research (Table 1) were stored as conidia suspensions in 20% glycerol at -80 °C. Fungi were grown let sporulate as described in **Chapter 2**. After harvesting, conidia were counted and stored as **Chapter 2**.

Table 1. Fungal isolates used in this study

Fungal species	Isolate name	Source/Reference
B. elliptica	WT 254-8	Chapter 2
B. elliptica	ΔBebot2#2	this study
B. elliptica	ΔBebot2#3	this study
B. cinerea	WT B05.10	Van Kan et al., 2017
B. cinerea	ΔBcbot2#1	Leisen et al., 2020
B. cinerea	ΔBcboa6	Dalmais et al., 2011

BOT detection in fungal cultures

B. elliptica and *B. cinerea* isolates were grown on modified Czapek-Dox agar plates (50 g glucose, 1g yeast extract, 5 g KH_2PO_4, 2 g $NaNO_3$, 0.5 g $MgSO_4 \cdot 7H_2O$, 0.01 g $FeSO_4 \cdot 7H_2O$ and 15 g technical agar for 1 L medium, pH adjusted to 6.5 ~ 7.0) were incubated at 20°C under constant light for seven days. The agar containing fungal mycelia and conidia were excised into small pieces (~0.8 cm x 0.8 cm) and transferred into Erlenmeyer flasks. Pure ethylacetate (EtOAc) was poured into the flasks until the agar pieces were covered, followed by extraction via ultra-sonication for 15 min. The EtOAc extract was collected through a filter paper, and the extraction was repeated once using the same agar pieces. The EtOAc extract was dried by nitrogen flow and subsequently re-dissolved in 300 µL pure acetone. The presence of BOT was analyzed on thin-layer chromatography (TLC). Samples were spotted on a Silica gel 60 F_{254} (Aluminium TLC plate, silica gel coated with fluorescent indicator F254), and a mobile phase of 40% EtOAc : 60% hexane (v/v) was used.

BOT production and purification

The production and purification of BOT and analysis of its purity was performed as described by Pinedo et al. (2008) with minor modifications. Liquid cultures of *B. cinerea Δboa6* mutant (Dalmais et al., 2011) in modified Czapek-Dox medium were incubated one week at 25°C under constant light. Metabolites including BOT were extracted with pure EtOAc from the culture filtrate with 1:1 ratio EtOAc/extract (v/v) for three times. The EtOAc extract was condensed using a rotary evaporator. BOT was purified via column chromatography (CC) by loading the condensed extract on the column (Aluminium TLC Silicagel 60 F_{254}) with the first mobile phase 40% EtOAc : 60% hexane (v/v) and the second of 80% EtOAc : 20% hexane (v/v). The fractions collected by the eluent of CC were run on a TLC plate using a Silica gel 60 F_{254} (Aluminium TLC plate, silica gel coated with fluorescent indicator F254) using as a mobile phase of 4 EtOAc : 6 hexane (v/v). All fractions containing BOT were combined and the solvent was evaporated to determine the dry weight of the sample. The purity of BOT in the sample was analysed by ^{1}H NMR on an Agilent 400 MHz spectrometer, and $CDCl_3$ was used as the solvent and reference for the NMR.

Quantification of cell death intensity upon BOT application on leaves and tepals

Droplets of 5 µL BOT (500 µM) dissolved in 40% acetone were applied on the right side of the abaxial surface of lily leaves or adaxial surface of lily tepals, whereas 5 µL droplets of 40% acetone were applied as negative control on the left side. Four droplets of BOT were applied to each leaf and two to three droplets were applied to each tepal. The response was evaluated by exposing treated lilies under the RFP channel of the ChemiDoc MP imaging system (Bio-Rad) (Landeo Villanueva et al., 2021). Response evaluation in tepals and leaves was done respectively at 2 and 3 days after BOT treatment. The mean red light

emission intensity in the BOT-treated area was quantified by the circle volume tool in the ImageLab software (Bio-Rad), and the signal in the area treated by 40% acetone (no symptom) was quantified in the same way to be used as a background. The intensity of cell death response triggered by BOT was shown as the ratio of the mean intensity (BOT-treated area) to the mean intensity (negative control area).

Generation of *ΔBebot2* mutants by CRISPR-Cas9 mediated *B. elliptica* transformation

All oligonucleotides used in this study are listed in Supplementary Table 1. Donor DNA containing the hygromycin resistance cassette (hph) as selection marker was amplified from purified telomeric vector pTEL-Hyg (Leisen et al., 2020) isolated from *E. coli* liquid culture grown with 50 µg/mL kanamycin overnight in the shaker incubator (28 °C; 200 rpm). To achieve homologous recombination, the hph cassette was amplified via overhang PCR with 60 bp long flanks which were homologous to the 60 nucleotides at the 5' and 3' end of *Bebot2* (BELL_060g00490; Valero-Jimenéz et al., 2020). SgRNAs for targeted Cas9-mediated double strand break in exon 1 and exon 2 of *Bebot2* were designed and generated as described in Leisen et al. (2020) and purified as described in **Chapter 4**. Cas9-Stu^{x2} protein used for fungal transformation was obtained as described in **Chapter 4**. *B. elliptica* isolate 254-8 transformation was carried out as described in **Chapter 4**. Four days after protoplast regeneration, appearing fungal colonies were transferred into MEA plates containing 80 µg/mL hygromycin B and screened via PCR. Homokaryotic *BeΔbot2* mutants were characterized with Phire Plant Direct PCR Kit (ThermoFisher Scientific, Bremen, Germany) using primers within the *Bebot2* gene and outside the 60 bp flanks used for homologous recombination (Supplementary Figure S1C). The development of *BeΔbot2* mutants was checked by comparing colony growth and sclerotia formation to *B. elliptica* isolate 254-8 WT (Supplementary Figure S1A and B).

Infection assays of *B. elliptica* and *B. cinerea* in lily leaves and flowers

From each lily genotype, 20 mature leaves were detached from 6 different plants and transported to the laboratory for inoculation. Per genotype, three random detached leaves were placed in plastic boxes on petri-dish lids lying on wet filter paper. The leaves were inoculated with each *B. elliptica* and *B. cinerea* isolate as described in **Chapter 2**. After 4 days of incubation at constant temperature (19-21 °C) and under ambient day/night light regime, inoculated leaves were photographed and lesion diameter measurements were taken with a caliper as described in **Chapter 2**. Disease assays on flowers were carried out with two just opened flowers that were harvested from the inflorescence of lilies and fixed into wet floral foam, which were placed into plastic boxes containing tap water. Tepal inoculation with each *B. elliptica* and *B. cinerea* isolate was conducted as described in **Chapter 2**. Three separate rounds of inoculation for leaves and tepals were conducted for each fungal isolate-lily genotype combination.

Gene expression analysis

Leaves of lily genotype A and LA 2 were inoculated with each *B. elliptica* as described in **Chapter 2**. Each area inoculated with *B. elliptica* was excised by a scalpel into ~5 mm x 5 mm squares from the infected leaf at either 16, 24 or 40 hours post inoculation (hpi). Three biological replicates were acquired. Harvested leaf samples were freeze-dried and used for RNA extraction with the Maxwell® 16 LEV Plant RNA Kit (Promega). Synthesis of cDNA was performed using 1 µg RNA as input and the M-MLV reverse transcriptase (Promega). Reverse transcription quantitative real-time PCR (RT-qPCR) was performed using the SensiMix SYBR Hi-ROX Kit (Bioline).

RESULTS

B. elliptica can produce BOT and deletion of *Bebot2* gene abolishes the production of BOT

B. cinerea WT B05.10 is known to be capable of producing BOT, and deletion of the *Bcbot2* gene in B05.10 abolished BOT biosynthesis (Pinedo et al., 2008). To verify whether the ortholog of *Bcbot2* in *B. elliptica* (*Bebot2*) functions as the sesquiterpene cyclase for BOT synthesis in *B. elliptica*, CRISPR-Cas9 mediated transformation was performed to knock out *Bebot2* in the *B. elliptica* isolate 254-8. Two independent deletion mutants were obtained. PCR analyses identified *ΔBebot2#2* and *ΔBebot2#3* as homokaryotic deletion mutants (Supplementary Figure S1A). Both *Bebot2* deletion mutants were genotyped to be homokaryotic knockout transformants free of the wild type *Bebot2* gene, and displayed sclerotia formation as the recipient isolate 254-8 (Supplementary Figure S1A and B). However, *ΔBebot2#2* and *ΔBebot2#3* showed slightly slower radial growth rate than the WT 254-8 on the Malt-extract agar (Supplementary Figure S1C).

BOT production in *B. elliptica* WT 254-8, *ΔBebot2#2* and *ΔBebot2#3*, was investigated by running EtOAc extracts of solid *in vitro* fungal cultures on TLC. Pure BOT sample, as well as extracts from *in vitro* cultures of the *B. cinerea* WT B05.10 and the *ΔBcbot2#1* mutant were run on the same TLC as controls. A pink band migrating at the position of pure BOT was observed in *B. cinerea* WT B05.10 extract but not in *ΔBcbot2#1* extract (**Figure 1A**). For *B. elliptica* isolates, WT 254-8 was able to produce BOT, while *ΔBebot2#2* and *ΔBebot2#3* mutants were not (**Figure 1A**).

We observed that all genes of the BOT cluster were highly expressed in *B. elliptica* 9401 and 9612 during infection in lily, according to the RNA sequencing dataset described in **Chapter 3**. Since the expression profile of BOT genes in *B. elliptica* isolate 254-8 was unknown, reverse RT-qPCR was performed to examine the *Bebot2* transcript levels in *B. elliptica* WT isolate 254-8, *ΔBebot2#2* and *ΔBebot2#3* during infection in leaves of two

lily genotypes, Asiatic (A) and Longiflorum-Asiatic 2 (LA 2). The mRNAs of *Bebot2* in *B. elliptica* 254-8 WT on both genotype A and genotype LA 2 was detected at 16 hours post inoculation (hpi), increased at 24 hpi, and then it slightly decreased at 40 hpi (**Figure 1B**). No significant difference in the *Bebot2* expression level was found in WT 254-8 between its infection on genotype A and genotype LA2 at each timepoint (**Figure 1B**). *Bebot2* transcript was not detected in *ΔBebot2#2* and *ΔBebot2#3* mutants during infection on lily leaves (**Figure 1B**).

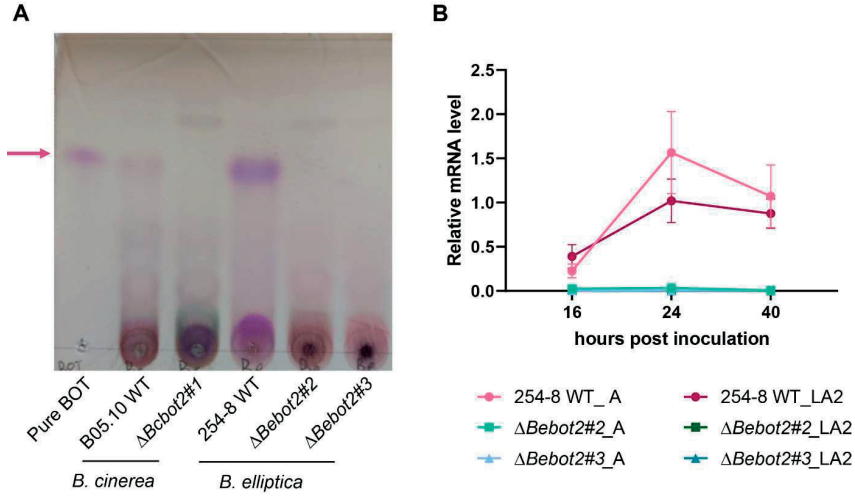

Figure 1. TLC analysis of EtOAc extracts from in vitro solid cultures of *B. cinerea* wild type (WT) isolate B05.10, *ΔBcbot2*#1 mutant, *B. elliptica* WT isolate 254-8 , *ΔBebot2*#2 and *ΔBebot2*#3 mutants using a mobile phase of 40% EtOAc – 60 % hexane **(A)**. The pink band on the TLC shows the presence and migration of BOT in the sample (Rf = 0.7), indicated by a pink arrow on the left. The transcript level of *Bebot2* in *B. elliptica* WT 254-8, *ΔBebot2*#2 and *ΔBebot2*#3 during infection on lilies (genotypes A and LA2) **(B)**.

BOT induces cell death in lily leaves and tepals, with variation between genotypes

After confirming that *B. elliptica* WT 254-8 could produce BOT during lily infection, we tested whether BOT can cause cell death in lily by applying pure BOT on leaves and tepals of four lily genotypes (genotypes A, LA1, LA2 and L). BOT sensitivity was quantified as the signal intensity of red light emission (Landeo Villanueva et al., 2021) at 3 days and 2 days after BOT treatment, respectively.

We observed that both leaves and tepals of all four tested lily genotypes were sensitive to BOT (**Figure 2** and **3**). Moreover, the signal intensity varied among the different lilies. In BOT-treated leaves, genotype LA 1 and LA 2 were the most sensitive, while genotype

A was the least sensitive (**Figure 2B**). Leaves of genotype L showed significantly lower sensitivity than genotype LA 1, slightly lower sensitivity than genotype LA 2 but with no statistically significant difference, and significantly higher sensitivity than genotype A (**Figure 2B**). Analogously, tepals of lily genotype A showed the lowest sensitivity to BOT, whereas tepals of genotype LA 2 and L were the most sensitive, and genotype LA 1 was intermediate (**Figure 3B**). A control treatment with 40% acetone (on the left side of the treated leaves or tepals) triggered no response at all.

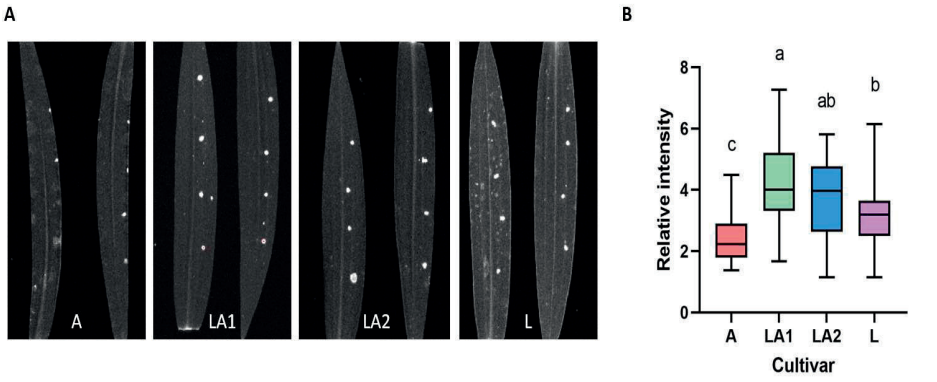

Figure 2. BOT sensitivity in leaves of lily genotypes A, LA 1, LA 2 and L visualized by red light emission (**A**). Boxplot showing signal intensities detected at 3 days after BOT treatment (**B**). Red light signal intensity detected upon BOT treatment in lily leaves is shown in the boxplot with the mean value (horizontal line) and the data from min to max (error bar) for each box. Each box contains 40 datapoints from two independent experiments, statistical analysis was performed by one-way ANOVA with Tukey's honestly significant difference (HSD) test.

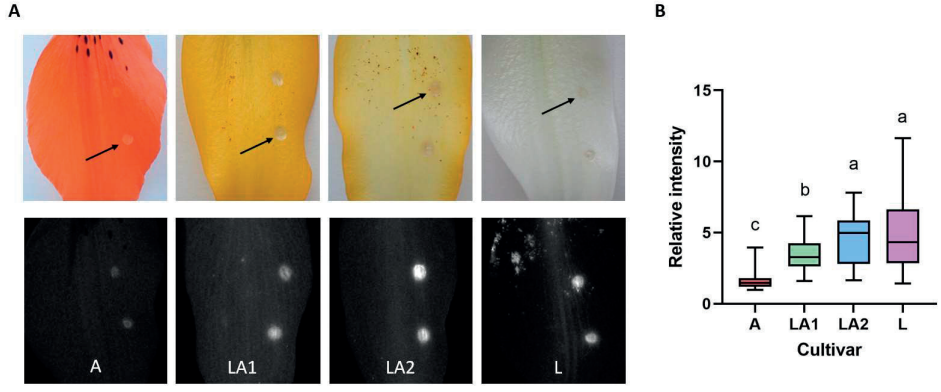

Figure 3. BOT sensitivity in tepals of lily genotypes A, LA 1, LA 2 and L, visualized with normal light (upper panel) or by red light emission (bottom panel) (**A**). Necrotic spots observed upon BOT treatment are indicated with a black arrow. Boxplot showing signal intensities detected at 2 days after BOT treatment (**B**). Red light signal intensity detected upon BOT treatment lily tepals is shown in the boxplot with the mean value (horizontal line) and the data from min to max (error bar) for each box. Each box contains 40 datapoints from two independent experiments, statistical analysis was performed by one-way ANOVA with Tukey's honestly significant difference (HSD) test.

BOT contributes to *B. elliptica* virulence in lily leaves and tepals

The contribution of BOT to virulence of *B. elliptica* in lily was evaluated by comparing lesion development in lily leaves and tepals upon inoculation of the *ΔBebot2#2* and *ΔBebot2#3* mutants and the *B. elliptica* WT 254-8. The four tested lily genotypes displayed differences in lesion sizes upon inoculation of *B. elliptica* WT isolate 254-8, on both leaves and tepals (**Figure 4A** and **B** and **5A** and **B**). Among the four tested lilies, genotype A developed the largest lesions on leaves ranging between 12 and 22 mm whereas leaves of genotype L showed the smallest lesions on leaves, which ranged between 5 and 12 mm (**Figure 4A** and **B**). Leaves of the genotypes LA 1 and LA 2 developed lesions of similar size whereby the majority ranged between 10 and 15 mm (**Figure 4A** and **B**). Analogously to leaves, the largest lesions were found on tepals of genotypes A and LA 2 (ranging between 6 and 16 mm) whereas the smallest lesions were observed on genotype L (ranging between 4 and 8 mm) (**Figure 5A** and **B**). When the lilies were inoculated with the mutants *ΔBebot2#2* and *ΔBebot2#3* a reduction in lesion size was observed both on leaves and tepals of all the tested lilies, except from tepals of genotype L (**Figure 4A** and **C**, and **Figure 5A** and **C**). When comparing the sizes of lesions developing upon inoculation with *B. elliptica* WT to those of the two *ΔBebot2* mutants, the most pronounced reduction in lesion size was found on leaves of genotypes A and LA 1 (**Figure 4C**). Upon leaf inoculation with the two *ΔBebot2* mutants the lesion size observed on genotype A ranged between 2 and 22 mm (for *B. elliptica* WT lesions ranged between 12 and 22 mm) while the lesion sizes observed on genotype LA 1 ranged between 1 and 9 mm (for *B. elliptica* WT lesions ranged between 3 and 17 mm). By contrast, when comparing tepal inoculation with the two *ΔBebot2* mutants to tepal inoculation with *B. elliptica* WT, differences in lesions size were less pronounced than in leaves. Except from genotype L, the lesion sizes of the *ΔBebot2* mutants on tepals were significantly smaller than those of the recipient (**Figure 5C**).

In parallel, the contribution of BOT to virulence of *B. cinerea* in lily leaves and tepals was assessed by comparing lesion size development upon inoculation of *B. cinerea* WT B05.10 and *ΔBcbot2#1* of the same four genotypes. No expanding lesion was observed when leaves were inoculated with any of the *B. cinerea* isolates (Supplementary Figure S2). Small expanding lesions were observed on tepals inoculated with *B. cinerea* WT and *ΔBcbot2#1*, and a slight reduction in lesion size was observed for the *ΔBcbot2#1* mutant only on genotype A (Supplementary Figure S3).

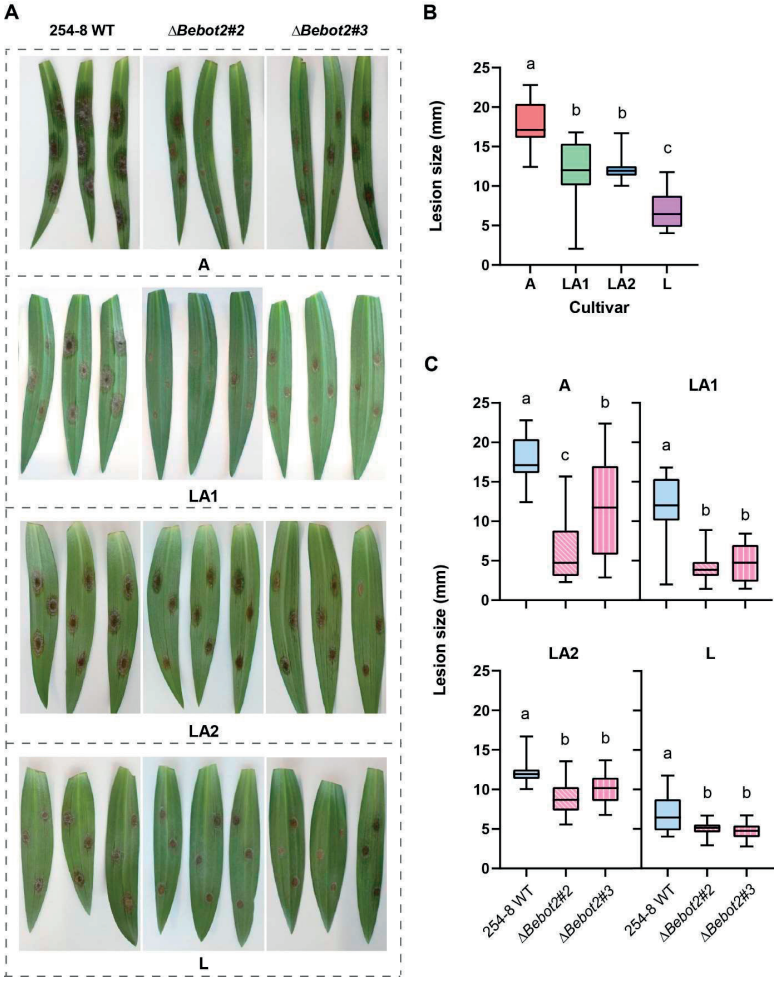

Figure 4. Lesions observed at 4 dpi upon inoculation with *B. elliptica* WT 254-8, *ΔBebot2*#2 and Δ*Bebot2*#3 on leaves of lily genotype A, LA 1, LA 2 and L, shown by (**A**) photos with normal light, (**B**) a boxplot showing only lesion sizes measured upon inoculation with *B. elliptica* WT 254-8 on all tested genotypes, and (**C**) boxplots showing lesion sizes measured upon inoculation with both *ΔBebot2* mutants compared to *B. elliptica* WT on each genotype. Each box in plot (**B**) and (**C**) contains 24 datapoints from two independent experiments, the statistical test was performed by one-way ANOVA with Tukey's HSD.

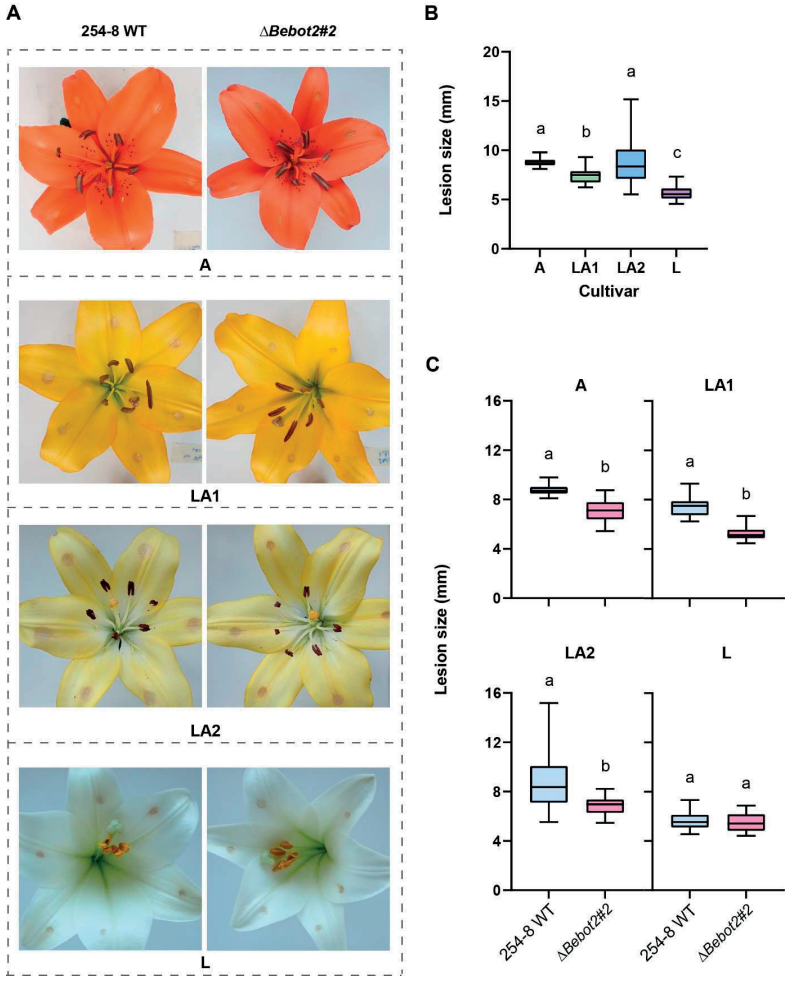

Figure 5. Lesions observed at 2 dpi upon inoculation with *B. elliptica* WT 254-8, *ΔBebot2*#2 and *ΔBebot2*#3 on tepals of lily genotypes A, LA 1, LA 2 and L, shown by (**A**) photos with normal light, (**B**) a boxplot showing only lesion sizes measured upon inoculation with *B. elliptica* WT 254-8 on all tested genotypes, and (**C**) boxplots showing lesion sizes measured upon inoculation with *ΔBebot2*#2 compared to *B. elliptica* WT on each genotype. Each box contains 24 datapoints from two independent experiments, the statistical test was performed by one-way ANOVA with Tukey's HSD (**B**) and t-test (**C**).

DISCUSSION

In this study we investigated the role of BOT in the *B. elliptica* – lily interaction. Given the presence of the complete BOT biosynthetic gene cluster in *B. elliptica* (Valero-Jiménez et al., 2020) BOT production was assessed during *in vitro* grown fungal culture and during lily infection. In agreement with RNAseq analysis of *B. elliptica* isolates 9401 and 9612 (Malvestiti et al., 2022), the gene encoding the key enzyme for BOT biosynthesis (*Bebot2*) showed increasing transcript levels in the course of the first 24 h after lily leaves inoculation with the *B. elliptica* isolate used in this study (*B. elliptica* 254-8). In addition, BOT could be extracted and detected from *in vitro* grown *B. elliptica* cultures. These findings confirm the functionality of the BOT biosynthetic gene cluster present in the *B. elliptica* genome and provide strong indications that BOT belongs to the arsenal of the cell death inducing compounds used by *B. elliptica* to infect lily. This hypothesis is further supported by the observation that exogenous BOT application on leaves and tepals of different lily genotypes caused a cell death response. Even if no necrotic spots (recognizable as brownish, dry and collapsed tissue) were visible with naked eye on leaves upon BOT treatment, emission of red light was detected. This light signal derives from chlorophyl autofluorescence as a result of the abortion of photochemical activity in dying photosynthesizing plant tissue and is therefore considered as a sign of the occurrence of PCD (Landeo Villanueva et al., 2021). Necrotic symptoms were observed on BOT-treated tepals, both by the naked eye and by the red-light imaging. After measuring the red light signal intensity upon BOT application, differences in intensities were observed among the different lily tissues and genotypes tested. By correlating the red light signal intensity to plant tissue sensitivity to BOT, it was noticed that the lily genotypes differed in sensitivity to BOT (**Figures 2** and **3**). The variation in red light signal intensity detected on BOT-treated leaves was in some cases influenced by the difference in the size of areas showing red light signal (**Figure 2A**) despite that the same volume of BOT solution was applied to all genotypes. This could be affected by differences in leaf surface architecture, composition and thickness of the epicuticular layers between the tested lilies. These factors collectively may have influenced the diffusion of the droplet and the penetration of BOT, and thus may have had an impact on the response of the plant to the compound. Differently from leaves, the areas on tepals treated with BOT were not noticeably different among the tested genotypes (**Figure 3A**). This indicates that the red light signal intensities detected on tepals may reflect more accurately the plant sensitivity to BOT.

Next to the differences in BOT sensitivity among the tested genotypes, we observed that the lesions caused by *ΔBebot2* mutants were significantly smaller than the lesions caused by *B. elliptica* WT (**Figure 4** and **5**) except for lesions on tepals of genotype L. One would expect that if a given lily genotype shows lower sensitivity to BOT than another, the absence of BOT during infection (as in case of the *ΔBebot2*) would affect the fungal

virulence to a lower extent, in comparison to a more BOT-sensitive lily. However, the tested lily genotypes in this study did not show such correlation. For instance, genotype A had the lowest red light signal intensity in response to BOT treatment (both in leaves and tepals, **Figure 2** and **3**) but showed the greatest reduction in lesion size when comparing symptoms caused by the *ΔBebot2* mutants to symptoms caused by *B. elliptica* WT (**Figure 4** and **5**). It is possible that the BOT treatment alone does not provide the complete biological context for the role of BOT produced by *B. elliptica* during infection on lilies. Other virulence factors might require BOT to function in a synergistic manner during the fungal colonization in genotype A but not in the other tested genotypes. Therefore, when BOT is not produced in the *ΔBebot2* mutants, the activity of such additional virulence factors might also be reduced, leading to a more pronounced reduction in lesion size on genotype A than on other tested lilies. The observed reduction in lesion size upon *ΔBebot2* mutants inoculation might be specific for this particular Asiatic genotype. Asiatic lily hybrids are derived from crosses of *Lilium* species which belong to the phylogenetic section *Sinomartagon.* This section is characterized by large genetic diversity because of its polyphyletic origin (Huang et al., 2018; H. T. Kim et al., 2019; J. S. Kim and Kim, 2018; Li et al., 2022) and significant variation in *B. elliptica* susceptibility was found among Asiatic genotypes obtained from crosses of different *Lilium* spp. belonging to the section *Sinomartagon* (**Chapter 2**). It would be interesting to examine additional genotypes from the Asiatic group and check whether they also display low sensitivity to BOT and a remarkable reduction in lesion size upon inoculation with *ΔBebot2* mutants in comparison to the *B. elliptica* WT. Opposite to genotype A, no reduced virulence of *ΔBebot2#2* as compared to the WT *B. elliptica* 254-8 was observed on tepals of the genotype L (**Figure 5**), which is one of the genotypes most sensitive to BOT (**Figure 3**). This could be explained by considering the fact that tepals of genotype L might be highly sensitive to many cell death-inducing molecules other than BOT that are produced by the *B. elliptica* isolate. Accordingly, the secretion of these molecules by *ΔBebot2#2* could compensate the absence of BOT and still trigger strong cell death in the plant tissue, resulting in similar aggressiveness of *ΔBebot2#2* to the WT fungus.

It was surprising to observe that the colony diameters of *ΔBebot2* mutants were slightly smaller than the *B. elliptica* WT when the fungi were grown in solid cultures (Supplementary Figure S1), since the *ΔBcbot2#1* mutant was reported to show a similar growth rate as *B. cinerea* WT (Leisen et al., 2020). The reduced *in vitro* colony diameter of *ΔBebot2* mutants might be the consequence of the toxicity of the precursor farnesyl diphosphate (FPP) to *B. elliptica.* Alternatively it can be an impact of the different downstream products of FPP converted by different secondary metabolite biosynthetic enzymes of *B. elliptica* from *B. cinerea*. It is known that the cyclization of FPP catalyzed by a sesquiterpene cyclase (STC) is a universal and key step for the biosynthesis of different sesquiterpenes. There are six *STC* genes in *B. cinerea* WT strain B05.10 (*Bcstc1-5* and *7*)

(Izquierdo-Bueno et al., 2018; Suárez et al., 2023; van Kan et al., 2017), whereas five *STC* genes can be found in the genome of *B. elliptica* (*Bestc1, 3-5* and *7*) according to the genome assembly published before (Valero-Jiménez et al., 2020). Among the six *Bcstc* genes in *B. cinerea*, the metabolic products of *Bcstc1* (*Bcbot2*), *Bcstc5* (*Bcaba5*) and *Bcstc7* have been identified as botrydial, abscisic acid, and (+)-4-epi-eremophilenol, respectively (Pinedo et al., 2008; Izquierdo-Bueno et al., 2018; Suárez et al., 2020). Thus, the effect of *Bebot2* deletion on the physiology of *B. elliptica* might be different than in *B. cinerea*. Besides, the magnitude of reduced lesion size of *ΔBebot2* mutants *in planta* was generally larger than the reduced colony diameter *in vitro*. Thus, BOT is still considered to play a role in the virulence of *B. elliptica* on these lily genotypes.

This study revealed two major findings. First, we presented that BOT can induce cell death responses in lilies. This is the first report of BOT phytotoxicity in a monocot, and it is worth investigating whether BOT can cause cell death also in other monocot taxa unrelated to lily. This might be a reasonable assumption since also onion (*Allium cepa*, Amaryllidaceae) leaf-specific pathogen *B. squamosa* harbours a functional BOT biosynthetic gene cluster (Valero-Jiménez et al., 2020) which is expressed during early stages of onion leaf infection (Malvestiti et al., 2022). Whether the molecular mechanisms required for plant cell death induction upon BOT perception are conserved between monocot and dicot taxa awaits further investigation. Secondly, we showed that BOT can be considered as a virulence factor in the *B. elliptica*-lily pathosystem. Furthermore, the next step would be to quantify how much BOT contributes to fungal virulence in combination with other factors. We have successfully generated *ΔBebot2* mutants using the CRISPR-Cas9 mediated transformation in this study, and it is promising to study the role of multiple virulence factors using this technique (Leisen et al., 2020).

SUPPLEMENTARY MATERIAL

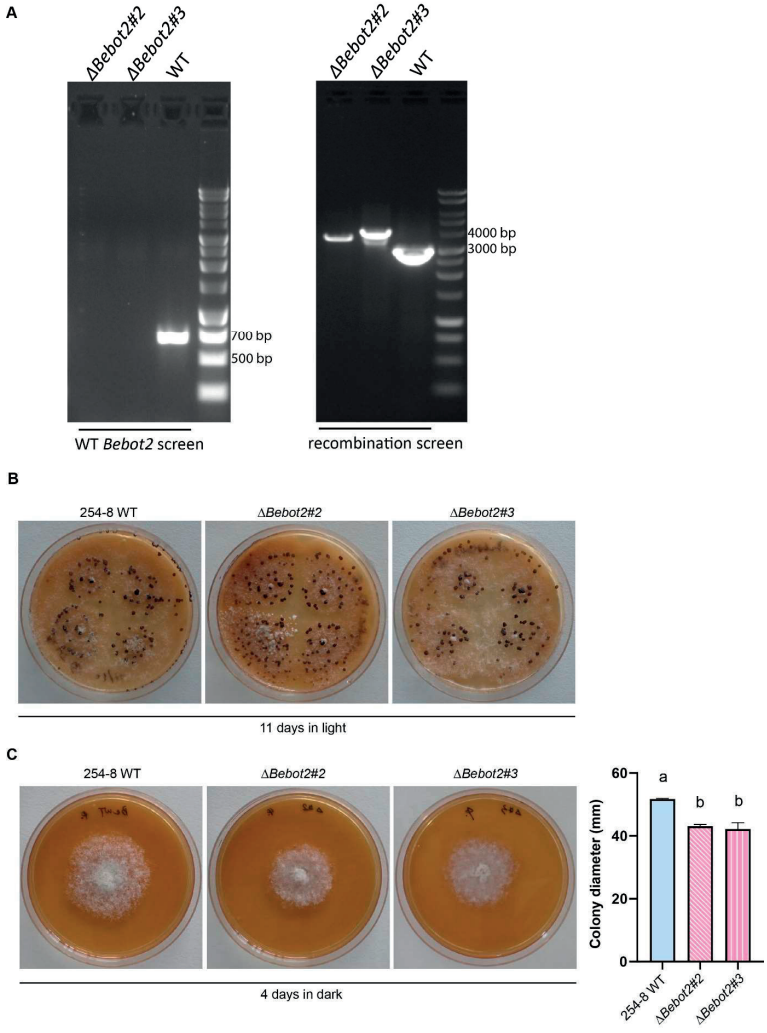

Supplementary Figure S1. Molecular characterization of *ΔBebot2*#2 and *ΔBebot2*#3 (**A**), sclerotia formation on 11-day-old MEA plates under constant light (**B**), and radial growth rate of *ΔBebot2*#2 and *ΔBebot2*#3 compared to WT 254-8 on 4-day-old MEA plates in dark (**C**). The radial growth rate was represented by the colony diameter (mm) measured from two dimensions of each colony, which is shown in the bar chart with the mean and standard error resulted from four separate plates (**C**). The statistical test was performed by one-way ANOVA with Tukey's HSD.

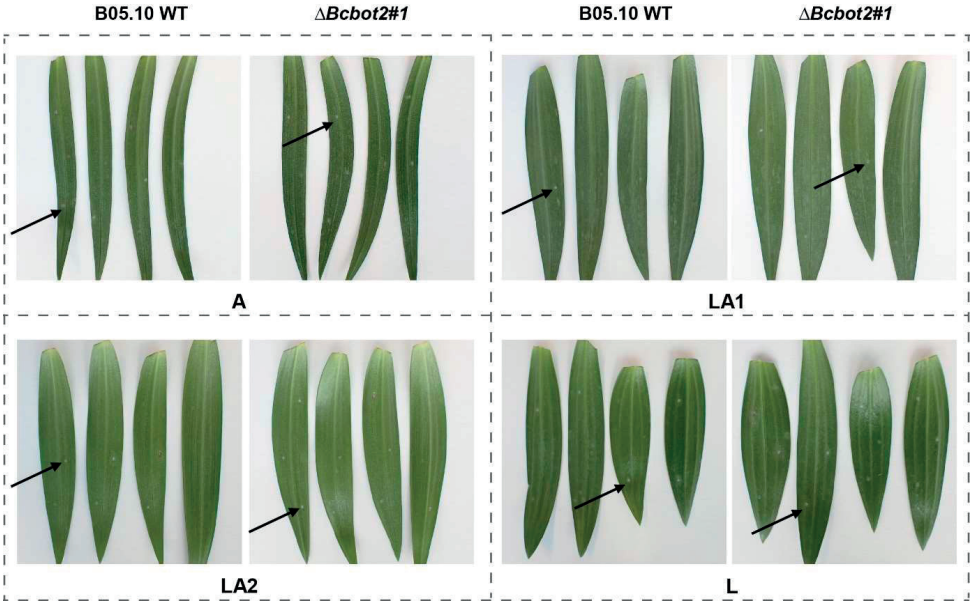

Supplementary Figure S2. Non-expanding lesions (indicated by black arrows) were observed at 4 dpi upon inoculation with *B. cinerea* WT B05.10 and *ΔBcbot2*#1 on leaves of lily genotypes A, LA1, LA2 and L.

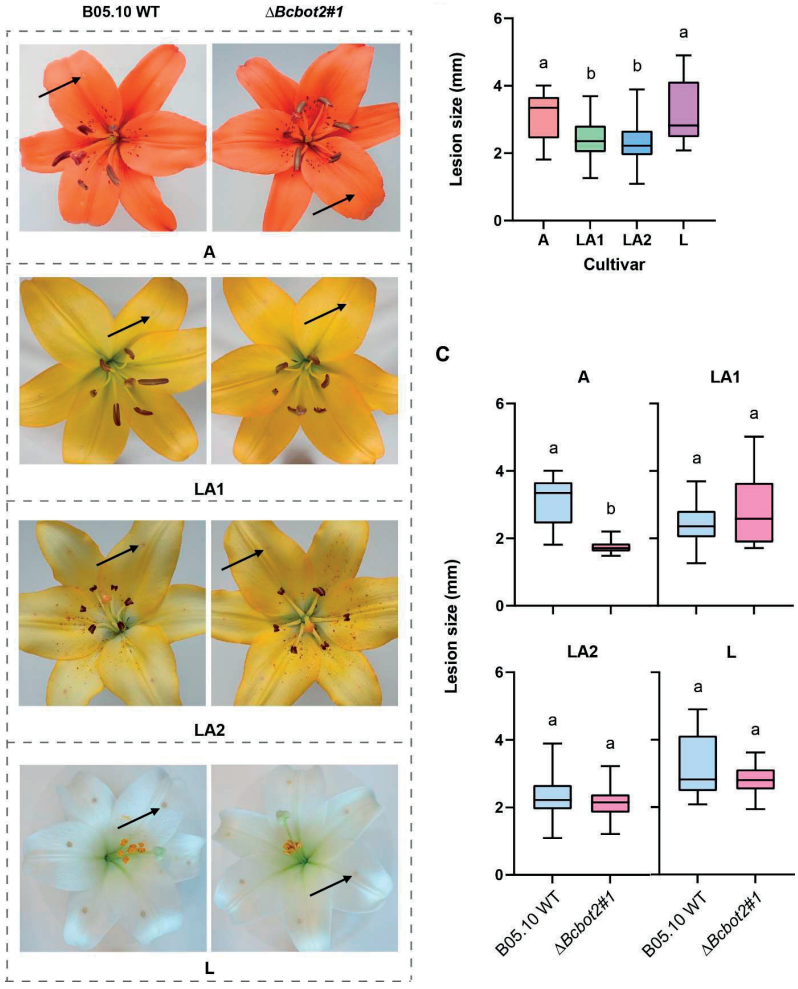

Supplementary Figure S3. Differences in lesion size observed at 2dpi upon inoculation with *B. cinerea* WT B05.10 and *ΔBcbot2*#1 on tepals of lily genotypes A, LA1, LA2 and L. (**A**) Photos taken under normal light condition, in which lesions are indicated by black arrows. (**B**) A boxplot showing only lesion sizes measured upon inoculation with *B. cinerea* WT B05.10 on all tested genotypes. (**C**) Boxplots showing lesion sizes measured upon inoculation with *ΔBcbot2*#1 compared to *B. cinerea* WT on each genotype. The mean value (horizontal line) and the data from min to max (error bar) are displayed for each box in the boxplots. Each box contains 24 datapoints from two independent experiments, and the statistical test was performed by one-way ANOVA with Tukey's HSD (**B**) and t-test (**C**).

Supplementary Table 1. Oligonucleotides used in this study

Oligonucleotide	Sequence	Application
Bebot2 sgRNA1	AAGCTAATACGACTCACTATAGGATGATAGAACCAAAGAGGTCGTTTTAGAGCTAGAAATAGCAAG	sgRNAs for *BeBot2* deletion
Bebot2 sgRNA2	AAGCTAATACGACTCACTATAGCGATGAATTTCAACAAGGCCGGTTTTAGAGCTAGAAATAGCAAG	
Bebot2 donor DNA generation F	ATGGCGATACCAGCACTTGAATCTCAGCTACACGACGCCGACACGGCCTCCAGCGATATGTGCTGGCCTTTTGCTCACATGCATG	Donor DNA for *Botrytis* transformation
Bebot2 donor DNA generation R	TCATGCCACGAGCACGTCTTTAGCGGGCGGCAGGTACATGATACCTGTTTCATGGACATATCGCCGGAAAGGACCCGCAAATG	
Bebot2 check outside 5'	GCACTTGCACTAGATTTCGACGTC	*Bebot2* transformation check outside recombination flanks
Bebot2 check outside 3'	GGAAGACGCAGCAGGAGAGTAATG	
Bebot2 check inside 5'	CAGCGATATGAGCAGCAACAGCAC	*Bebot2* transformation check inside gene sequence
Bebot2 check inside 3'	CGTTGTCACCCATGATGGCAATGGTC	
Bebot2 RT-qPCR 5'	ACGAATGCTATAGGCGGTGG	*BeBot2* and *BeActA* gene expression quantification
Bebot2 RT-qPCR 3'	CTCAGGACCCAGGTAACGAC	
BeactA RT-qPCR 5'	GAGCGGTGGTATCCACGTTACT	
BeactA RT-qPCR 3'	CAATGATCTTGACCTTCATCGAT	

Chapter 6
General Discussion

INTRODUCTION

The lily represents one of the most cultivated ornamental flowering plants worldwide but the lily production has to deal with several pests and diseases. Lily pests and pathogens include insects such as beetles (*Lilioceris lilii*) (Salisbury, 2003), thrips (*Liothrips vaneeckii*) (Mound and Tree 2008) and aphids (*Neomyzus circumflexus*) (Asjes and Blom-Barnhoorn, 2000), nematodes which cause damage both in roots (*Pratylenchus* spp.) and leaves (*Aphelenchoides* spp.) (Vieira et al., 2017), viruses such as lily symptomless virus (LSV), cucumber mosaic virus (CMV) and lily mottle virus (LMoV), which are often transmitted via aphids (Zhang et al., 2017), and fungi such as *Fusarium oxysporum* f. sp. *lilii* which infects lily bulbs causing losses during storage (Shahin et al., 2009; Arens et al., 2012). However, the most serious threat for lily cultivation is represented by the foliar necrotrophic Ascomycota *Botrytis elliptica* and *B. cinerea*, causal agents of the lily fire blight disease (Reddy, 2016). While the generalist *B. cinerea* is mostly found on cut lily flowers in the post-harvest stage, the lily specific *B. elliptica* can infect young and vigorous plant during the entire growth season. Early signs of *Botrytis* infection are small brownish necrotic spots on leaves. Under warm, cloudy and moist weather conditions the necrotic spots can expand and coalesce, and the whole leaf collapses. From the necrotic tissue, *Botrytis* can infect the neighboring plants by producing conidia which are transported by wind and rain, causing a very rapid spread of the disease. To combat all these pathogens and especially *Botrytis*, lily breeders and growers still mostly rely on chemical protection. A Dutch newspaper in 2019 reported that the lily is by far the crop receiving the most chemical treatments in the Netherlands, almost 130 kg of active compounds in a year per hectare of cultivated land (Volkskrant 2019). Compared to lily, food crops (such as potato) or other ornamental flower bulbs (such as tulip, *Tulipa* spp., Liliaceae) are treated with around 20 kg of chemical agents in a year per hectare (Volkskrant 2019). For obvious reasons, this strategy is not eco-sustainable anymore. Therefore, disease management practices which exploit natural sources of plant resistance are urgently needed to reduce and eventually replace chemical protection. Given that *Botrytis* fire blight is the most widespread and destructive disease in lily, this study was dedicated to gain deeper understanding of the interaction between *Botrytis elliptica* and lily. Several aspects of the pathosystem were investigated, focusing on the variation in susceptibility to fire blight in the lily germplasm and on the role of cell death inducing necrotrophic effectors (NEs) of the fungus. Overall, the aim of this thesis was to set the stage for the development of an alternative strategy to protect lilies. I attempted to provide the lily breeders with the fundamental biological knowledge that empowers them to select for lily genotypes which harbour natural sources of fire blight resistance.

Disease assays are not efficient to identify sources of fire blight resistance

The genus *Lilium* comprises approximately 120 described species which are phylogenetically divided in seven taxonomic sections (Angiosperm Phylogeny Group, 2020; Pelkonen and Pirttilä, 2012; Li et al., 2022). During its long and prosperous breeding history, thousands of lily hybrids have been generated via intrasectional crosses between different *Lilium* species which are distributed among four hybrid groups: Asiatic (A), Longiflorum (L), Trumpet (T), and Oriental (O). Artificial pollination, embryo rescue and polyploidization techniques allowed to generate a variety of intersectional hybrids in which diverse ornamental traits were combined (van Tuyl et al., 1991; Lim et al., 2008; van Tuyl and Arens, 2011), leading to the development of the intersectional hybrid groups LA (Longiflorum-Asiatic), LO (Longiflorum-Oriental), OA (Oriental-Asiatic) and OT (Oriental-Trumpet). Among lily growers and breeders it is known that certain lilies are less susceptible to *B. elliptica* than others and several studies have tried to identify natural sources of host resistance in the lily germplasm (Doss et al., 1986 and 1988; Beers et al., 2005; Balode, 2009; Daughtrey and Bridgen, 2013; Hu et al., 2017; Gao et al., 2018; Jang et al., 2018; Chastagner and Grafinkel, 2020). Since the level of susceptibility was assessed via disease assays, these studies reported a large variation in disease susceptibility among genotypes from the four hybrid groups. The lack of consistency both in the methodology used to assess the level of plant susceptibility and fungal virulence, as well as in the plant and fungal material used to perform the disease assays, prevented the researchers from obtaining a clear overview of the variation in susceptibility in the lily germplasm and in the variation in virulence in the *B. elliptica* population. Despite my effort to increase the consistency in the methodology and biological material, I also encountered several issues in the evaluation of the plant susceptibility and fungal virulence after having conducted the disease assays (**Chapter 2**). It was observed that the outcome of the interaction can be influenced by the season and by the developmental stage of the plant. In both repetitions of the disease assays, lilies planted in late spring and tested in the summer showed significantly larger lesions than lilies planted at the end of the winter and tested in spring, when they were inoculated with *B. elliptica* conidia. This difference could be attributed to the faster transition to the flowering stage when the lilies were grown during the late spring/early summer season under influence of the day length. The development of a lily plant after bulb outgrowth may substantially vary depending not only on the genotype but also on weather conditions. Consequently the immune system may react differently to pathogen attack depending on the physiological state of the plant. In such an unpredictable scenario, it is difficult to quantify the contribution of abiotic factors such as light, temperature and humidity on the outcome of the interaction with the pathogen, even if the disease assays were conducted under laboratory conditions. Although Asiatic, Longiflorum and LA hybrids were in my experiments generally more susceptible than LO, OT and Oriental hybrids, significant variation in lesion size was observed among individual genotypes belonging to the same hybrid group (**Chapter 2**). This indicates that the general classification (by the breeders

and the lily research community) of the Asiatic as "highly susceptible" and the Oriental as "highly resistant" hybrid group is an oversimplification. Recent molecular phylogenetic studies of nuclear ribosomal internal transcribed spacer (ITS) and plastid genome of 95 different *Lilium* species revealed that the Asiatic group (section *Sinomartagon*) represents a polyphyletic clade (Kim and Kim, 2018; Li et al., 2022). Some Asiatic species such as *L. matangense*, *L. fargesii* and *L. nanum* cluster in a subclade which is closely related to the species of the Oriental group (section *Archelirion*). By contrast other species of the section *Sinomartagon* such as *L. lancifolium*, *L. bulbiferum* and *L. amabile* cluster together on a different subclade which includes also *L. longiflorum* (Kim and Kim, 2018; Li et al., 2022). Consequently, depending on the original *Lilium* species used in intrasectional crosses and on the parent line to which the F1 hybrids were backcrossed to combine the desired ornamental traits in new Asiatic hybrid genotypes, traits conferring resistance to *Botrytis* fire blight may have been retained to different extents in the genomes of the new hybrid genotypes. Thus, given the genetic complexity in the lily germplasm and the large assortment of lily hybrid genotypes, it remains technically complicated and laborious to reliably rank a set of lily genotypes based on their level of susceptibility. Therefore, even though the disease assays conducted in this study (**Chapter 2**) provided robust indications that certain lily hybrids are more susceptible than others, the methods to explore the genetic potential of the germplasm to display its resistance in controlled conditions would not be technically and logistically feasible on the scale that is required for the lily breeding industry. My experiments showed an interesting correlation between disease susceptibility and the severity of cell death responses observed upon infiltration of the fungal culture filtrate (CF) in a given lily genotype (**Chapter 2**). Moreover, the leaf response observed upon infiltration of the *B. elliptica* CF sample was consistent among replicates on multiple leaves and infiltration spots. On the other hand, depending on which lily genotype was tested, leaf infiltration with the crude CF sample yielded a spectrum of different responses which included necrosis, visible as brown tissue coloration, yellowing and chlorosis, translucence or maceration of the leaf epidermal layer and tissue collapse (**Chapter 2** and **3**). Considering the complex protein composition of the CF samples, the diversity of responses observed in the infiltrated leaves does not allow to straightforwardly quantify the level of effector sensitivity and to compare it among different lily genotypes, and to correlate a certain phenotype observed in infiltrated leaves to the cell death inducing activity of specific effectors. Nevertheless, proteinaceous effectors contained in the CF sample are essential for cell death induction and thus for pathogenicity of *B. elliptica* in lily (van Baarlen et al., 2004), and therefore, this finding provided the first evidence that *B. elliptica* secreted effectors capable of inducing cell death can be used to screen the lily germplasm in a more efficient way to identify effector-insensitive lily with the prediction that they will display reduced fire blight susceptibility. These observations set the stage for the development of an effector-assisted screening to identify lily genotypes displaying increased resistance to fire blight.

The impact of effector-assisted screening

Effector-assisted breeding relies on the selection of plant genotypes which show insensitivity to purified effector proteins, with the prediction that such plants will show increased resistance to the disease caused by the pathogen producing that effector. This strategy has been successfully implemented in Australia, North-America and Europe to develop wheat (*Triticum aestivum*, Poaceae) genotypes displaying increased resistance to the fungus *Parastagonospora nodorum*, causal agent of the Septoria Nodorum Blotch (SNB) disease in wheat (Ficke et al., 2018; Tommasini et al., 2007). This fungus requires NEs to induce host cell death and cause disease in wheat (Oliver et al., 2012). NEs are "recognized" by the corresponding Host Susceptibility Gene (HSG) which triggers host programmed cell death (PCD) upon interaction with NEs. At present, nine pairs of NE-HSGs have been identified (**Chapter 1**; Friesen and Faris, 2021; Haugrud et al., 2022). NEs contribute to fungal virulence and plant susceptibility in a quantitative manner. The more NEs are produced by a given fungal isolate, and the more matching HSGs are present as functional alleles in the plant, the more virulent is the pathogen and the more susceptible is the host (Haugrud et al., 2019; Faris and Friesen 2020). In the case of SNB, breeders have used single purified NEs to screen the wheat germplasm for NE insensitivity. This allowed them to combine insensitivity traits from diverse wheat lines to obtain increased SNB resistance in the new wheat genotypes (Cowger et al., 2020; Downie et al., 2018; Ruud et al. 2017; Tan et al., 2015). SnToxA was the first *P. nodorum* NE delivered to Australian wheat breeders in 2009. SnToxA was produced in *E. coli* and then distributed to the breeders allowing them to test 30,000 wheat plants annually. Subsequently around 6,000 doses of two other *P. nodorum* NE SnTox1 and SnTox3 were provided to the wheat breeders. The impact of the implementation of SnToxA can be estimated by looking at the crop acreage of SnToxA-sensitive wheat. In Western Australia, the area planted with SnToxA-sensitive wheat genotypes decreased from 30% in 2009–2010 to 17% in 2012–2013. Susceptible wheat amounted in total 200,000 tons yield losses. On average, wheat prices amounted at that time to approximately $250 per ton. Therefore, cultivation of SnToxA-insensitive wheat allowed to increase the revenues for the growers by $50 million. Analogous reduction in yield losses can be predicted in other regions of Australia. A large part of this reduction can be addressed to the attention that growers have paid to the losses caused by SNB (Vleeshouwers and Oliver 2014).

Compared to disease assays with fungal spores under laboratory, greenhouse and field conditions, screening for effector sensitivity via protein infiltration represents an efficient strategy and shows the following advantages. Leaf infiltration with purified NE proteins yields a cell death response upon NE recognition. Alternatively, no cell death response is observed when the plant genotype does not contain or express the HSG responsible for NE recognition and PCD initiation in the host. This simple read-out enables the breeders to use effector sensitivity as a prediction for plant susceptibility, depending on the

number of NEs that are capable of causing cell death upon infiltration in a given wheat genotype, thereby avoiding large scale disease assays and complex statistics. Screening segregating populations of young offspring plants simply by protein infiltration represents a non-destructive assay since breeders can immediately discard plants showing effector sensitivity and keep only the individuals which do not show cell death responses upon effector infiltration. Effector infiltration can be carried out by one person in the laboratory, in the greenhouse or in the field, thereby saving time and resources. As the assay does not involve treatments with living fungi, even the effector-sensitive plants will not be diseased and can be utilized for other breeding purposes breeding purposes. Because *Botrytis* species also require NEs to induce PCD and establish disease in the host (van Baarlen et al., 2004; Mbengue et al., 2016; Veloso and van Kan 2018), an analogous effector-assisted strategy as used for SNB in wheat, can be implemented to identify resistance sources in the assortment of lily genotypes. Thereby, *B. elliptica* NE proteins may represent valuable tools to screen the lily germplasm and to identify lily genotypes which display insensitivity to the NEs produced by *B. elliptica*. In this research, three different NE candidates were identified in *B. elliptica* and produced to assess their cell death inducing capacity in lily. Two of them were of proteinaceous nature, namely BeE11 (**Chapter 3**) and BeCMU2 (**Chapter 4**), and one was the phytotoxic sesquiterpene botrydial (**Chapter 5**). The small cysteine-rich protein BeE11 can be considered a typical NE candidate for effector-assisted screening since BeE11 protein infiltration in lily leaf caused a response that was clearly visible in BeE11 sensitive genotypes. Because BeE11 lacks described enzyme domains, this secreted protein is unlikely involved in manipulation of the host metabolism. Thus, the cell death inducing capacity of BeE11 may rely on a one-to-one interaction with a (still unidentified) plant receptor protein that triggers PCD induction upon recognition of BeE11. On the other hand, both botrydial and BeCMU2 do not represent ideal tools for effector-assisted screening for the following reasons. For botrydial, the costly and laborious techniques required for production and purification of the sesquiterpene represent the major limiting factor (**Chapter 5**). In addition, assays with botrydial require that the compound is applied in an acetone solution which cannot be infiltrated into leaves because of the detrimental effect of acetone on plant cell integrity. Application on the leaf surface may lead to rapid evaporation, thereby diminishing the permeation of botrydial into the cuticle. Moreover, the cell death response detected in leaf tissue upon botrydial application could be visualized only with the aid of the red light imaging system (Landeo Villanueva et al., 2021), because we did not observe any brownish, dry, collapsed necrotic tissue in the spots treated with botrydial (**Chapter 5**). By contrast, in case of the BeCMU2 protein we are dealing with a different type of effector. Even though experiments are required unravel the exact mode of action of BeCMU2, it is most likely that the observed cell death response to BeCMU2 occurs as a result of the physiological disruption of chloroplast function rather than being a consequence of receptor-mediated PCD induction upon BeCMU2 perception in an “inverse gene-for-gene” interaction. Accordingly, we noticed

that the cell death response was heterogeneous in the leaf area infiltrated with BeCMU2 (**Chapter 4**). This might hamper to obtain a clear black-and-white read out when scoring different lily genotypes for BeCMU2 sensitivity rendering BeCMU2 unsuitable for an effective germplasm screening. The major impact of BeCMU2 on plant susceptibility may rely on its capacity to interfere with salicylic (SA) biosynthesis and thus with the early defense-related responses upon fungal infection. Based on the preliminary results shown in **Chapter 4**, it remains unclear how the BeCMU2 protein enters the plant cytoplasm. Furthermore it remains to be confirmed whether translocation from the host cytoplasm into the plant chloroplast occurs and is required for the contribution of BeCMU2 to fungal virulence. Protein translocation mechanism from the cytoplasm to the chloroplast consists of cargo proteins and the molecular machinery. Cargo proteins contain a specific N-terminal cleavable signal sequence, the chlTP (Bruce, 2000; Lee et al., 2006). Prolines in chlTP are crucial for efficient protein translocation into chloroplasts (Lee et al., 2018) and 4 prolines are present in the 18 amino acid long predicted chlTP of BeCMU2 (**Chapter 4**). The molecular machinery contains several components that recognize this targeting peptide and execute the import process (Lee and Hwang, 2018). The chloroplast import process initiates with a specific sorting of chloroplast-destined proteins in the cytoplasm which contains a protein quality control mechanism to remove unfolded or misfolded proteins, to avoid formation of cytotoxic non-specific protein aggregates in the cell (Lee et al., 2009, 2013 and 2016). These precursor proteins then bind to the outer chloroplast membrane, where the chlTP is cleaved by a stromal peptidase. The released chlTP interacts with different members of the Tic-Toc import complex which mediates the import of the protein into the chloroplast through the import channel (Lee et al., 2013 and 2018). To validate BeCMU2 translocation to the chloroplast during fungal infection, several experiments can be conducted. For example, chimeric BeCMU2::GFP fusion reporters can be constructed which lack the chlTP or in which the effector chlTP is either replaced by a plant chlTP or by a plant nuclear localization signal (NLS) (Liu et al., 2015). These reporter constructs can be used to transform *B. cinerea* and such a transformant can be inoculated on *N. benthamiana* to obtain more information about BeCMU2 localization in infected tissue. Upon deletion of the chlTP from the BeCMU2 protein sequence, no GFP signal would be detected at the chloroplast. The GFP signal observed in **Chapter 4** (**Figure 5B**) would be restored upon replacement of the effector chlTP with a plant chlTP. Finally, by replacing the effector chlTP by a NLS, GFP signal would be expected to end up in the plant nucleus.

Finally, it is important to mention that effector-assisted screening would only be effective if the NEs used to screen the lily germplasm would significantly contribute to fungal virulence as shown for the *P. nodorum* effectors SnToxA and SnTox1 (Liu et al., 2012 and 2016; Tan et al., 2015). The NE repertoire can display extensive functional redundancy as shown in *B. cinerea* (Leisen et al., 2021) and *P. nodorum* (Tan et al., 2015; Bertazzoni et al., 2021), meaning that the fungus can compensate the absence of a single NE by the activity

of other NEs without affecting virulence (Haugrud et al., 2019). This hypothetical redundancy in NE activity can be tested by generating NE deletion mutants in the fungus and by comparing fungal virulence of the mutant to the recipient isolate (Leisen et al., 2021). In case *B. elliptica* would also show redundancy in NE activity, lilies displaying increased resistance to *B. elliptica* can be identified only by testing them for insensitivity to multiple effectors. Taking this into account, next to the three NEs discussed above, this research enabled the identification of at least 10 additional candidate NEs in the protein fraction displaying cell death inducing capacity in lily and which showed high transcript level in early stages of infection in lily (**Chapter 3**). These additional 10 candidate NEs might be required to obtain more information regarding the quantitative differences in susceptibility among different lily genotypes and therefore, they await investigation at molecular level (**Chapter 1**, **Figure 2**). Besides the practical advantages of effector-assisted screening discussed above, knowledge derived from NE activity would be of scientific importance. Functional characterization of NEs would enable to study the NE target in the plant and thereby shed light on the (sub-)cellular components that are co-opted by the fungus for PCD induction in the host plant and which are essential for disease development. This would allow to make a step further in the breeding programs for the development of resistant genotypes, because it will give insights in the distribution and in the variation of specific NE targets within the *Lilium* germplasm. Plant cell components conferring effector sensitivity in a given genotype can be exploited to develop DNA-markers to enable the selection of effector insensitive genotypes with the prediction that they will display increased resistance to *Botrytis* fire blight.

RiPPs, beyond the canonical fungal effector proteins

In plant pathogenic fungi, effector candidates are usually identified as small secreted cysteine-rich proteins which lack transmembrane and described enzyme domains. After translation by the ribosomes and cleavage of the signal peptide for secretion, effectors are released by the fungus at the interface with plant cells as mature proteins where they subsequently (presumably) interact with a specific component of the plant cell to promote virulence. However, in the last twenty years, evidence emerged that fungi produce and secrete a wide array of bioactive peptides which undergo post-translational modification (PTM) before being delivered to the host or the environment. Such peptides have been defined as ribosomally synthetized and post-translationally modified peptides (RiPPs). Fungal RiPPs do not only occur in plant pathogenic fungi as they can also be involved in sexual reproduction (Martin et al., 2011), internal signaling and regulation of the metabolism (Homer et al., 2016) and may possess antimicrobial, nematocidal and insecticidal activity (Hallen et al., 2007; Umemura 2020; Kessler et al., 2022a; Vogt and Künzler, 2019; Montalban-López et al., 2021). Given their versatile functions in fungal biology and their widespread presence in the different fungal taxa, RiPPs have gained increasing attention. For readers interested in learning more comprehensively about the chemical

classes of RiPPs, I recommend several reviews (Arnison et al., 2013; Montalban-López et al., 2021; Umemura 2020; Kessler et al., 2022a). Based on their amino acid sequence composition and biosynthetic pathway fungal RiPPs can be divided into two major groups (Ma et al., 2018a; Outram et al., 2021a; Kessler et al., 2022a; Umemura 2020). The first group encompasses peptides which contain tandem amino acid repeats (Ma et al., 2018a; Montalban-López et al., 2021; Outram et al., 2021a; Kessler et al., 2022a; Umemura 2020). This type of RiPPs is synthetized by a biosynthetic gene cluster (BGC) that includes the gene encoding the precursor peptide, which contains tandem repeats of amino acid sequences, and associated enzymes required for different types of PTMs (Arnison et al., 2013; Vogt and Künzler, 2019; Umemura 2020; Montalban-López et al., 2021). A recent large scale fungal secretome mining (La Marquer et al., 2019) showed that the length of amino acid tandem repeats may vary from three to 352 amino acids and the number of repeats ranged from three to 129. After removal of the signal peptide for secretion, the core peptides are first excised from the precursor peptide. This excision is mediated by endopeptidase cleavage by means of either prolyl oligopeptidases or by kexin-type serine endocarboxypeptidases (KEX) present in the Golgi apparatus. Importantly, each repetitive peptide in the precursor protein contains a KEX specific cleavage site (KR, KK RR) (Ma et al., 2018a; Montalban-López et al., 2021; Outram et al., 2021; Kessler et al., 2022a; Umemura 2020). Subsequently, the core peptide is modified by enzymes encoded in the same gene cluster which are required to form the final product. One prominent example of cyclic RiPPs that contribute to fungal virulence is victorin, a phytotoxic compound found in the oat (*Avena sativa*, Poaceae) necrotrophic Ascomycota *Cochliobolus victoriae* which is required for PCD induction and pathogenicity in oat genotypes carrying the dominant *Vb* HSG (Gilbert and Wolpert, 2013). Victorin consists of a mixture of closely related heterodetic hexapeptides which are ether bond-cyclized. Analysis of the *C. victoriae* genome identified three copies of precursor peptide genes (*vicA1–3*) with variable numbers of "GLKLAF" core peptide repeats corresponding to the victorin core peptide backbone (Kessler et al., 2022b). Interestingly, the precursor peptide encoding genes *vicA1–3* are located in repeat-rich, gene-sparse regions of the genome and cluster together with the enzymes required for the corresponding PTMs (Kessler et al., 2022b). In addition, the fescue (*Festuca* spp., Poaceae) endophytic fungus *Epychloë festucae* is known to produce the bioactive cyclic peptide epichloëcyclin (Johnson et al., 2015). Even if the exact biological function of epichloëcyclin during endophytic interaction with the host plant remains elusive, this compound consists of five highly homologous cyclic peptides, which are encoded from their precursor peptide gene *gigA* (Johnson et al., 2015). The epichloëcyclin BGC was identified based on co-expression of *gigA* with three other genes and contained a KEX cleavage motif, a DUF3328 domain-containing protein encoding gene which is essential for cyclisation of the core peptide, and a gene of unknown function (Johnson et al., 2015). Next, the CgEP1 effector from the hemi-biotrophic Ascomycota *Colletotrichum graminicola* is required for anthracnose development in maize (Vargas et al., 2016). The

CgEP1 gene is present in three allelic variants containing four to six near-identical tandem peptide repeats, whereby each repeat contains a motif for translocation into the plant nucleus (Vargas et al., 2016). Nevertheless, the biological function as well as the role of the tandem repeats remain unknown. Finally, the maize hemi-biotrophic Basidiomycota *Ustilago maydis* secretes at least two cyclic RiPPs namely Rep1 and Rsp3 to promote host infection. The Rep1 precursor protein is cleaved into multiple short peptides by KEX before secretion from the fungus. The peptides form tightly bound amyloid-like hydrophobic filaments on the hyphal membrane thereby facilitating proper formation of aerial hyphae and hyphal attachment to the host cell (Wösten et al., 1996; Müller et al., 2008). On the other hand, the repetitive secreted protein Rsp3 is involved in the inhibition of the antifungal activity of mannose-binding maize proteins (Ma et al., 2018b). The second group of fungal RiPPs includes peptides which undergo KEX cleavage of a N-terminal pro-domain before secretion. The best described example is the SnTox3 protein which represents a cell death inducing effector secreted by the necrotrophic fungus *P. nodorum* during infection in wheat (Outram et al., 2021b). SnTox3 is first synthetized as a pro-domain containing protein which subsequently undergoes KEX cleavage before being delivered into the wheat apoplast as mature effector. The pro-domain is not required for the PCD inducing capacity of SnTox3 when the effector is infiltrated as purified protein into *Snn3* harboring wheat genotypes (Outram et al., 2021b).

Filamentous plant pathogenic Ascomycota harbor a significantly higher number of predicted RiPPs encoding genes than other fungi (La Marquer et al., 2019) and the identification of their genomic location begins with an *in silico* analysis of fungal DNA. Fungal RiPPs discovery has so far been conducted in a top-down approach starting with the identification of their corresponding BGC and by performing backward analysis from the chemical structure in combination with transcriptomic analysis. Recent development of high throughput genome sequencing methods allowed to perform more extensive bottom-up genome mining enabling the identification of the genomic location of additional RiPPs based on homologous sequences in the genes encoding the precursor peptide and the post-translationally modifying enzymes (La Marquer et al., 2019; Umemura 2020; Kessler et al., 2022a). More specifically, gene clusters involved in RiPP biosynthesis were identified by the occurrence of amino acids repeats containing KEX cleavage sites in the precursor peptide, in combination with a predicted DUF3328 domain-containing protein encoded in close genomic proximity (Umemura 2020; Kessler et al., 2022a). For this purpose, new search tools named RiPPMiner and fRIPPA have been developed and implemented in the discovery of novel fungal RiPPs (Vignolle et al., 2020; Kessler et al., 2022a). However, the actual bioinformatic tools lack both the specificity and the sensitivity to identify completely novel RiPPs because these search engines rely on previous structural and functional knowledge of RiPPs encoding genes and BGCs, which is at this point in time still sparse. Furthermore, evidence of the functionality of the BCG mostly relies on transcriptomic

data. The difficulties in the functional expression of RiPPs are not only related to their chemical diversity, but also on the high reactiveness of the post-translationally modifying enzymes and on the instability of the mature RiPP itself (Glassey et al., 2021). More efficient protocols for RiPPs expression in heterologous systems are being developed whereby expression, modification and purification of diverse RiPPs can be conducted under uniform conditions (Glassey et al., 2021). In an alternative approach Green and co-workers compared the metabolic profile of the apoplastic fluid in *Lolium perenne* (Poaceae) upon infection with the endophytic fungus *Epichloë festucae* and in non-inoculated *L. perenne*. Genome information in combination with tandem mass spectrometry and metabolite mining tools allowed to identify the endophyte-specific RiPPs, peramine and epichloëcyclins, as well as a large number of unknown fungal metabolites that were only detected in the infected tissue (Green et al., 2020). Candidate genes encoding RiPPs were listed in a genome-wide survey conducted by Umemura et al. (2020) among 1461 isolates belonging to 8 different phyla in the fungal kingdom. In *B. elliptica* this study identified 15 genes containing a signal peptide for secretion followed by multiple repetitive stretches of amino acids that terminated with KEX cleavage sites. Among these 15 putative RiPPs, one was predicted to encode a *B. elliptica* pheromone, 12 are predicted effectors, four of which are found only in *Botrytis* species, and 7 of which were located in the proximity of a DUF3328 domain-containing protein (Umemura 2020). Both their biosynthetic pathway and biological function await molecular investigation, but at the same time their discovery may open new perspectives in the context of effector-assisted screening in lily. If short bioactive peptides are sufficient for PCD induction in RiPP-sensitive lily genotypes, such peptides could be chemically synthesized and tested in the plant. This would allow to bypass the more laborious heterologous expression and purification of effectors that is usually performed to obtain proteins that can be implemented to identify and eliminate effector-sensitive plant genotypes.

Conclusion

The research performed in this study set the stage for the development of an effector-assisted screening in the lily germplasm. The collected genomic, transcriptomic and proteomic data have identified the first *B. elliptica* effectors displaying PCD-inducing capacity that can be exploited as biological tool in the selection of effector-insensitive lilies with the prediction that these will display increased resistance to *Botrytis* fire blight. On the other hand, this study also highlighted the biological complexity of the *B. elliptica*-lily interaction. Unique virulence factors that allowed *B. elliptica* to evolve as lily-specific pathogen remain elusive, as well as the molecular mechanisms underlying the increased fire-blight resistance of certain lily genotypes. Continued efforts to understand the pathogenicity mechanisms at cellular, molecular and biochemical level are needed to support resistance breeding as a long-term solution for the control of lily fire blight.

LIST OF REFERENCES

Abeysekara, N. S., Friesen, T. L., Keller, B., and Faris, J. D. (2009). Identification and characterization of a novel host–toxin interaction in the wheat–*Stagonospora nodorum* pathosystem. Theorethical and Applied Genetics, 120 (1), 117–126.

Abeysekara, N. S., Faris, J. D., Chao, S., McClean, P. E., and Friesen, T. L. (2012). Whole genome QTL analysis of *Stagonospora nodorum* blotch resistance and validation of the SnTox4-Snn4 interaction in hexaploid wheat. Phytopathology, 102, 94–104.

Albert, I., Böhm, H., Albert, M., Feiler, C. E., Imkampe, J., Wallmeroth, N., and Nürnberger, T. (2015). An RLP23–SOBIR1–BAK1 complex mediates NLP-triggered immunity. Nature plants, 1 (10), 1-9.

Amselem, J., Cuomo, C. A., van Kan, J. A., Viaud, M., Benito, E. P., Couloux, A., and Dickman, M. (2011). Genomic analysis of the necrotrophic fungal pathogens *Sclerotinia sclerotiorum* and *Botrytis cinerea*. PLoS Genetics, 7 (8), e1002230.

Andersen, L. (2021). The Road Towards a More Sustainable Flower Bulb Sector in the Duin-en Bollenstreek. https://www.centre-for-sustainability.nl/the-greenport-hub

Angiosperm Phylogeny Group (APG) (2020). http://www.mobot.org/MOBOT/research/APweb/orders/lilialesweb.htm#Liliaceae (accessed September 19, 2020).

Arenas, Y. C., Kalkman, E. R., Schouten, A., Dieho, M., Vredenbregt, P., Uwumukiza, B., and van Kan J. A. L. (2010). Functional analysis and mode of action of phytotoxic Nep1-like proteins of *Botrytis cinerea*. Physiological and Molecular Plant Pathology, 74 (5-6), 376–386.

Arens, P., Bijman, P., Tang, N., Shahin, A., and van Tuyl, J. M. (2012). Mapping of disease resistance in ornamentals: A long haul. Acta Horticulturae, 953, 231–237.

Arens, P., Shahin, A., and van Tuyl, J. M. (2014). (Molecular) Breeding of *Lilium*. Acta Horticulturae, 1027, 113–127.

Arnison, P. G., Bibb, M. J., Bierbaum, G., Bowers, A. A., Bugni, T. S., Bulaj, G., and Van Der Donk, W. A. (2013). Ribosomally synthesized and post-translationally modified peptide natural products: overview and recommendations for a universal nomenclature. Natural product reports, 30 (1), 108-160.

Arzate-Fernández, A. M., Miwa, M., Shimada, T., Yonekura, T., and Ogawa, K. (2005). Genetic diversity of Miyamasukashi-yuri (*Lilium maculatum* Thunb. var. *bukosanense*), an endemic and endangered species at Mount Buko, Saitama, Japan. Plant Species Biology, 20, 57–65.

Asjes C. J., Blom-Barnhoorn,and G. J. (2002). Control of aphid vector spread of lily symptomless virus and lily mottle virus by mineral oil/insecticide sprays in *Lilium*. Acta Horticulturae, 570, 277–281.

Assis, R. de A. B., Sagawa, C. H. D., Zaini, P. A., Saxe, H. J., Wilmarth, P. A., Phinney, B. S., Salemi, M., Moreira, L. M., and Dandekar, A. M. (2021). A secreted chorismate mutase from *Xanthomonas arboricola* pv. *juglandis* attenuates virulence and walnut blight symptoms. International Journal of Molecular Sciences, 22 (19), 10374.

Azole-resistance selection in *Aspergillus fumigatus*. Rijks Instituut voor Volksgezondheid en Milieuhygiëne, December 2017.

Bailey, K. , Çevik, V., Holton, N., Byrne-Richardson, J., Sohn, M., Coates, K. H., Woods-Tör, A., Aksoy, H. M., Hughes, L., Baxter, L., Jones, J. D. G., Beynon, J., Holub, E. B., and Tör, M. (2011). Molecular cloning of ATR5Emoy2 from *Hyaloperonospora arabidopsidis*, an avirulence determinant that triggers RPP5-mediated defense in *Arabidopsis*. Molecular Plant-Microbe Interaction, 24, 827-838.

Bairwa, G., Caza, M., Horianopoulos, L., Hu, G., and Kronstad, J. (2019). Role of clathrin-mediated endocytosis in the use of heme and hemoglobin by the fungal pathogen *Cryptococcus neoformans*. Cellular Microbiology, 21 (3), e12961.

Balint-Kurti, P. (2019). The plant hypersensitive response: concepts, control and consequences. Molecular Plant Pathology. 20(8), 1163-1178.

Balode, A. (2009). Breeding for resistance against *Botrytis* in lily. Acta Horticulturae, 836, 143–148.

Bar, M., and Ori, N. (2014). Leaf development and morphogenesis. Development, 141, 4219–4230.

Bates, D., Kliegl, R., Vasishth, S., and Baayen, H. (2015). Parsimonious mixed models. arXiv:1506.04967

Battelli, R., Lombardi, L., Rogers, H. J., Picciarelli, P., Lorenzi, R., and Ceccarelli, N. (2011). Changes in ultrastructure, protease and caspase-like activities during flower senescence in *Lilium longiflorum*. Plant Science, 180, 716–725.

Bauters, L., Kyndt, T., De Meyer, T., Morreel, K., Boerjan, W., Lefevere, H., and Gheysen, G. (2020). Chorismate mutase and isochorismatase, two potential effectors of the migratory nematode *Hirschmanniella oryzae*, increase host susceptibility by manipulating secondary metabolite content of rice. Molecular Plant Pathology, 21 (12), 1634-1646.

Beers, C. M., Barba-Gonzalez, R., van Silfhout, A. A., Ramanna, M. S., and van Tuyl, J. M. (2005). Mitotic and meiotic polyploidization in lily hybrids for transferring *Botrytis* resistance. Acta Horticulturae, 673, 449–452.

Berkmen, M. (2012). Production of disulfide-bonded proteins in *Escherichia coli*. Protein expression and purification, 82 (1), 240-251.

Bertazzoni, S., Jones, D. A., Phan, H. T., Tan, K. C., and Hane, J. K. (2021). Chromosome-level genome assembly and manually-curated proteome of model necrotroph *Parastagonospora nodorum* Sn15 reveals a genome-wide trove of candidate effector homologs, and redundancy of virulence-related functions within an accessory chromosome. BMC Genomics, 22 (1), 382.

Bi, K., Liang, Y., Mengiste, T., and Sharon, A. (2022). Killing softly: a roadmap of *Botrytis cinerea* pathogenicity. Trends in Plant Science, 28 (2), 211-222.

Bi, K., Scalschi, L., Jaiswal, N., Mengiste, T., Fried, R., Sanz, A. B., and Sharon, A. (2021). The *Botrytis cinerea* Crh1 transglycosylase is a cytoplasmic effector triggering plant cell death and defense response. Nature Communication, 12(1), 1-15

Boeckx, T., Winters, A. L., Webb, K. J., and Kingston-Smith, A. H. (2015). Polyphenol oxidase in leaves: is there any significance to the chloroplastic localization? Journal of Experimental Botany, 66, 3571–3579.

Böhm, H., Albert, I., Oome, S., Raaymakers, T. M., Van den Ackerveken, G., and Nürnberger, T. (2014). A conserved peptide pattern from a widespread microbial virulence factor triggers pattern-induced immunity in *Arabidopsis*. PLoS Pathogens, 10(11), e1004491.

Bray, N. L., Pimentel, H., Melsted, P., and Pachter, L. (2016). Near-optimal probabilistic RNA-seq quantification. Nature Biotechnology, 34 (5), 525–527.

Bruce, B.D. (2000). Chloroplast transit peptides: structure, function and evolution. Trends in Cell Biology, 10, 440-447.

Brückner, A., Polge, C., Lentze, N., Auerbach, D., and Schlattner, U. (2009). Yeast two-hybrid, a powerful tool for systems biology. International Journal of Molecular Sciences, 10 (6), 2763-2788.

Carreón-Anguiano, K.G., Islas-Flores, I., Vega-Arreguín, J., Sáenz-Carbonell, L., and Canto-Canché, B. (2020) EffHunter: A Tool for Prediction of Effector Protein Candidates in Fungal Proteomic Databases. Biomolecules, 10, 712.

Cassonnet, P., Rolloy, C., Neveu, G., Vidalain, P. O., Chantier, T., Pellet, J., and Jacob, Y. (2011). Benchmarking a luciferase complementation assay for detecting protein complexes. Nature Methods, 8 (12), 990-992.

Centraal Bureau voor de Statistiek (2020). Which flower bulbs are most common? https://longreads.cbs.nl/the-netherlands-in-numbers-2020/which-flower-bulbs-are-most-common/

Chastagner, G. A., and Garfinkel, A. R. (2020). Diseases affecting ornamental geophytes and their control. In: Achieving sustainable cultivation of ornamental plants. 1st Edition, (11), 367-414. Burleigh Dodds Science Publishing.

Chilvers, M. I., and du Toit, L. J. (2006). Detection and identification of *Botrytis* species associated with neck rot, scape blight, and umbel blight of onion. Plant Health Programs, 7, 38.

Choquer, M., Rascle, C., Gonçalves, I. R., de Vallée, A., Ribot, C., Loisel, E. and Poussereau, N. (2021). The infection cushion of *Botrytis cinerea*: a fungal 'weapon' of plant-biomass destruction. Environmental Microbiology, 23 (4), 2293-2314.

Collado, I. G., Sánchez, A. J. M., and Hanson, J. R. (2007). Fungal terpene metabolites: Biosynthetic relationships and the control of the phytopathogenic fungus *Botrytis cinerea*. Natural Product Reports, 24 (4), 674–686.

Collado, I., Aleu, J., Hernandez-Galan, R., and Duran-Patron, R. (2000). *Botrytis* Species: An Intriguing Source of Metabolites with a Wide Range of Biological Activities. Structure, Chemistry and Bioactivity of Metabolites Isolated from Botrytis Species. Current Organic Chemistry, 4 (12), 1261–1286.

Colmenares, A. J., Aleu, J., Durán-Patrón, R., Collado, I. G., and Hernández-Galán, R. (2002). The putative role of botrydial and related metabolites in the infection mechanism of *Botrytis cinerea*. Journal of Chemical Ecology, 28 (5), 997–1005.

Cowger, C., Ward, B., Brown-Guedira, G., and Brown, J. (2020). Role of effector sensitivity gene interactions and durability of quantitative resistance to *Septoria nodorum* blotch in Eastern US wheat. Frontiers in Plant Science, 11, 155.

Cowger, C., Ward, B., Brown-Guedira, G., and Brown, J. K. (2020). Role of effector-sensitivity gene interactions and durability of quantitative resistance to Septoria nodorum blotch in Eastern US wheat. Frontiers in Plant Science, 11, 155.

Dagvadorj, B., Outram, M. A., Williams, S. J., and Solomon, P. S. (2022). The necrotrophic effector ToxA from *Parastagonospora nodorum* interacts with wheat NHL proteins to facilitate Tsn1-mediated necrosis. The Plant Journal, 110(2), 407-418.

Dalmais, B., Schumacher, J., Moraga, J., le Pêcheur, P., Tudzynski, B., Collado, I. G., and Viaud, M. (2011). The *Botrytis cinerea* phytotoxin botcinic acid requires two polyketide synthases for production and has a redundant role in virulence with botrydial. Molecular Plant Pathology, 12 (6), 564–579.

Daughtrey, M. L., and Bridgen, M. P. (2013). Evaluating resistance responses to *Botrytis elliptica* in field grown lilies. Acta Horticulturae, 1002, 313–318.

De Jong, P. C. (1974). Some notes on the evolution of lilies. Yearbook of North American Lily Society, 27, 23–28.

Deighton, N., Muckenschnabel, I., Colmenares, A. J., Collado, I. G., and Williamson, B. (2001). Botrydial is produced in plant tissues infected by *Botrytis cinerea*. Phytochemistry, 57 (5), 689–692.

Deising, H.B., Werner, S., and Wernitz, M. (2000). The role of fungal appressoria in plant infection. Microbes Infections, 2, 1631–1641.

Dempsey, D. A., Vlot, A. C., Wildermuth, M. C., and Klessig, D. F. (2011). Salicylic Acid Biosynthesis and Metabolism. The Arabidopsis Book, 9, e0156.

Dempsey, D. M. A., and Klessig, D. F. (2017). How does the multifaceted plant hormone salicylic acid combat disease in plants and are similar mechanisms utilized in humans? BMC Biology, 15, 23.

Dickman, M., Park, Y., Oltersdorf, T., Li, W., Clemente, T., and French, R. (2001). Abrogation of disease development in plants expressing animal antiapoptotic genes. Proceedings of the National Academy of Sciences, 98 (12), 6957–6962.

Dickman, M., Williams, B., Li, Y., de Figueiredo, P., and Wolpert, T. (2017). Reassessing apoptosis in plants. Nature Plants, 3(10), 773-779.

Ding, P., and Ding, Y. (2020). Stories of salicylic acid: a plant defense hormone. Trends in Plant Science, 25 (6), 549-565.

Djamei, A., Schipper, K., Rabe, F., Ghosh, A., Vincon, V., Kahnt, J., Osorio, S., Tohge, T., Fernie, A. R., Feussner, I., Feussner, K., Meinicke, P., Stierhof, Y. D., Schwarz, H., MacEk, B., Mann, M., and Kahmann, R. (2011). Metabolic priming by a secreted fungal effector. Nature, 478 (7369), 395–398.

Domazakis, E., Lin, X., Aguilera-Galvez, C., Wouters, D., Bijsterbosch, G., Wolters, P. J., and Vleeshouwers, V. G. A. A. (2017). Effectoromics-based identification of cell surface receptors in potato. In: Shan, L., He, P. (eds) Plant Pattern Recognition Receptors. Methods in Molecular Biology, vol 1578, 337-353. Humana Press, New York, NY.

Doss, R. P., Chastagner, G. A., and Riley, K. L. (1986). Screening ornamental lilies for resistance to *Botrytis elliptica*. Scientia horticulturae, (30), 237–246.

Doss, R. P., Christian, J. K., and Chastagner, G. A. (1988). Infection of Easter lily leaves from conidia of *Botrytis elliptica*. Canadian Journal of Botany, 66, 1204–1208.

Downie, R. C., Bouvet, L., Furuki, E., Gosman, N., Gardner, K. A., Mackay, J., and Cockram, J. (2018). Assessing European wheat sensitivities to *Parastagonospora nodorum* necrotrophic effectors and fine-mapping the Snn3-B1 locus conferring sensitivity to the effector SnTox3. Frontiers in Plant Science, 9, 881.

Downie, R. C., Bouvet, L., Furuki, E., Gosman, N., Gardner, K. A., Mackay, I. J., Mantello, C. C., Mellers, G., Phan, H., Rose, G. A., Tan, K.-C., Oliver, R., and Cockram, J. (2018). Assessing European wheat sensitivities to *Parastagonospora nodorum* necrotrophic effectors and fine-mapping of the *Snn3-B1* locus conferring sensitivity to the effector SnTox3. Frontiers in Plant Science, 9, 881.

Downie, R. C., Lin, M., Corsi, B., Ficke, A., Lillemo, M., Oliver, R. P., and Cockram J. (2021). *Septoria* nodorum blotch of wheat: disease management and resistance breeding in the face of shifting disease dynamics and a changing environment. Phytopathology, 111(6), 906-920.

Doyle, E. A., and Lambert, K. N. (2003). *Meloidogyne javanica* chorismate mutase 1 alters plant cell development. Molecular Plant-Microbe Interactions, 16 (2), 123–131.

Du, J. and Vleeshouwers, V. G. A. A. (2017). New strategies towards durable late blight resistance in potato, in The Potato Genome. Compendium of Plant Genomes, Kumar, C.S., Xie, C., and Kumar, T.J., Eds., Cham: Springer-Verlag, 161.

Du, J., Rietman, H., and Vleeshouwers, V. G. A. A. (2014). Agroinfiltration and PVX agroinfection in potato and *Nicotiana benthamiana*. Journal of visualized experiments: JoVE, (83).

Du, Y. P., Bi, Y., Yang, F. P., Zhang, M. F., Chen, X. Q., Xue, J., Zhang, X. H. (2017). Complete chloroplast genome sequences of *Lilium*: insights into evolutionary dynamics and phylogenetic analyses. Scientific Reports, 7, 1–10.

Duan, L., Liu, H., Li, X., Xiao, J., and Wang, S. (2014). Multiple phytohormones and phytoalexins are involved in disease resistance to Magnaporthe oryzae invaded from roots in rice. Physiologia Plantarum. 152, 486–500.

Duba, A., Goriewa-Duba, K., and Wachowska, U. (2018). A review of the interactions between wheat and wheat pathogens: *Zymoseptoria tritici*, *Fusarium* spp. and *Parastagonospora nodorum*. International Journal of Molecular Science, 19 (4), 1138.

Eberhard, J., T. Ehrler, T., Epple, P., Felix, G., Raesecke, H.-R., Amrhein, N., and Schmid, J. (1996). Cytosolic and plastidic chorismate mutase isozymes from *Arabidopsis thaliana*: molecular characterization and enzymatic properties. The Plant Journal, 10 (5), 815–851.

European Commission (2020). Farm to Fork Strategy. For a fair, healthy and environmentally-friendly food system.

Fang Hsieh, T., Wen Huang, J., and Hsiang, T. (2001). Light and scanning electron microscopy studies on the infection of oriental lily leaves by Botrytis elliptica. European Journal of Plant Pathology, 107, 571–581.

Faris, J. D., and Friesen, T. L. (2020). Plant genes hijacked by necrotrophic fungal pathogens. Current Opinion in Plant Biology, 56, 74-80.

Faris, J. D., Overlander, M. E., Kariyawasam, G. K., Carter, A., Xu, S. S., and Liu, Z. (2020). Identification of a major dominant gene for race-nonspecific tan spot resistance in wild emmer wheat. Theoretical and Applied Genetics, 133, 829–841.

Faris, J. D., Zhang, Z., Lu, H., Lu, S., Reddy, L., Cloutier, S., and Friesen, T. L. (2010). A unique wheat disease resistance-like gene governs effector-triggered susceptibility to necrotrophic pathogens. Proceedings of the National Academy of Sciences, 107 (30), 13544–13549.

Ficke A., Cowger C., Bergstrom G., and Brodal G. (2018). Understanding yield loss and pathogen biology to improve disease management: Septoria nodorum blotch-a case study in wheat. Plant Diseases, 102, 696–707.

Fillinger, S., and Elad Y., (2016). *Botrytis* – the Fungus, the Pathogen and Its Management in Agricultural Systems. Springer, 413-486.

Frías, M., González, C., and Brito, N. (2011). BcSpl1, a cerato-platanin family protein, contributes to *Botrytis cinerea* virulence and elicits the hypersensitive response in the host. New Phytologist, 192 (2), 483–495.

Frías, M., González, M., González, C., and Brito, N. (2016). BcIEB1, a *Botrytis cinerea* secreted protein, elicits a defense response in plants. Plant Science, 250, 115–124.

Friesen T. L., Faris J. D., Solomon P. S., and Oliver, R. P. (2008). Host-specific toxins: effectors of necrotrophic pathogenicity. Cell Microbiology, 10 1421–1428,

Friesen T. L., Meinhardt S.W., and Faris J. D. (2007). The *Stagonospora nodorum*-wheat pathosystem involves multiple proteinaceous host-selective toxins and corresponding host sensitivity genes that interact in an inverse gene-for-gene manner. Plant Journal, 51, 681–692.

Friesen, T. L. and Faris J. D. (2012). Characterization of plant-fungal interactions involving necrotrophic effector-producing plant pathogens. In: Bolton M. D., and Thomma B. P. H. J. (eds) Plant fungal pathogens: methods and protocols, Methods in Molecular Biology, vol 835.

Friesen, T. L., and Faris, J. D. (2010). Characterization of the wheat-*Stagonospora nodorum* disease system: what is the molecular basis of this quantitative necrotrophic disease interaction? Canadian Journal of Plant Pathology, 32, 20–28.

Friesen, T. L., and Faris, J. D. (2021). Characterization of effector–target interactions in necrotrophic pathosystems reveals trends and variation in host manipulation. Annual Review of Phytopathology, 59, 77-98.

Friesen, T. L., Chu, C., Xu, S. S., and Faris, J. D. (2012). SnTox5–Snn5: a novel *Stagonospora nodorum* effector–wheat gene interaction and its relationship with the SnToxA–Tsn1 and SnTox3–Snn3–B1 interactions. Molecular Plant Pathology, 13 (9), 1101-1109.

Friesen, T. L., Zhang, Z., Solomon, P. S., Oliver, R. P., and Faris, J. D. (2008). Characterization of the interaction of a novel *Stagonospora nodorum* host-selective toxin with a wheat susceptibility gene. Plant Physiology, 146 (2), 682.

Furukawa, T., Ushiyama K., and Kishi, K. (2005). *Botrytis* blight of Taiwanese toad lily caused by *Botrytis elliptica* (Berkeley) Cooke. Journal of General Plant Pathology, 71, 95–97.

Furukawa, T., Ushiyama, K., and Kishi, K. (2005). *Botrytis* blight of Taiwanese toad lily caused by *Botrytis elliptica* (placeCityBerkeley) Cooke. J. Gen. Plant Pathol. 71, 95–97.

Gao, X., Cui, Q., Cao, Q. Z., Zhao, Y. Q., Liu, Q., He, H. B., and Zhang, D. (2018). Evaluation of resistance to *Botrytis elliptica* in *Lilium* hybrid cultivars. Plant Physiology and Biochemistry, 123, 392–399.

Gao, Y., Faris, J. D., Liu, Z., Kim, Y. M., Syme, R. A., Oliver, R. P., and Friesen T. L. (2015). Identification and characterization of the SnTox6-*Snn6* interaction in the *Parastagonospora nodorum*-wheat pathosystem. Molecular Plant-Microbe Interaction, 28, 615–625.

Garcion, C., Lohmann, A., Lamodière, E., Catinot, J., Buchala, A., Doermann, P., and Métraux, J. P. (2008). Characterization and biological function of the ISOCHORISMATE SYNTHASE2 gene of Arabidopsis. Plant physiology, 147 (3), 1279-1287.

Garfinkel, A. R., Lorenzini, M., Zapparoli, G., and Chastagner, G. A. (2017). *Botrytis euroamericana*, a new species from peony and grape in North America and Europe. Mycologia, 109 (3), 495–507.

Gilchrist, D.G., and Connelly, J.A. (1987). Chorismate mutase from mung bean and sorghum. Methods in Enzymology, 142, 450-463.

Giraldo, M.C., Dagdas, Y.F., Gupta, Y.K., Mentlak, T.A., Yi, M., Martinez-Rocha, A.L., Saitoh, H., Terauchi, R., Talbot, N.J., and Valent, B. (2013). Two distinct secretion systems facilitate tissue invasion by the rice blast fungus *Magnaporthe oryzae*. Nature Communications, 4, 1996.

Glassey, E., King, A. M., Anderson, D. A., Zhang, Z., and Voigt, C. A. (2022). Functional expression of diverse post-translational peptide-modifying enzymes in *Escherichia coli* under uniform expression and purification conditions. PlosOne, 17 (9), e0266488.

Görisch, H., and Lingens, F. (1973). Chorismate mutase from *Streptomyces aureofaciens*: a heat-stable enzyme. Journal of Bacteriology, 114 (2), 645-651.

Green, K. A., Berry, D., Feussner, K., Eaton, C. J., Ram, A., Mesarich, C. H., Solomon P., Feussner I., and Scott, B. (2020). *Lolium perenne* apoplast metabolomics for identification of novel metabolites produced by the symbiotic fungus *Epichloë festucae*. New Phytologist, 227 (2), 559-571.

Hallen, H. E., Luo, H., Scott-Craig, J. S., and Walton, J. D. (2007). Gene family encoding the major toxins of lethal *Amanita* mushrooms. Proceedings of the National Academy of Sciences, 104 (48), 19097-19101.

Hammond-Kosack, K. E., and Rudd, J. J. (2008). Plant resistance signaling hijacked by a necrotrophic fungal pathogen. Plant signaling and behavior, 3, 993–995.

Haugrud, A. R. P., Zhang, Z., Richards, J. K., Friesen, T. L., and Faris, J. D. (2019). Genetics of variable disease expression conferred by inverse gene-for-gene interactions in the wheat-*Parastagonospora nodorum* pathosystem. Plant Physiology, 180 (1), 420–434.

Haugrud, A. R., Zhang, Z., Friesen, T. L., and Faris, J. D. (2022). Genetics of resistance to *Septoria nodorum* blotch in wheat. Theoretical and Applied Genetics, 1-23.

Haugrud, A. R., Zhang, Z., Richards, J. K., Friesen, T. L., and Faris, J. D. (2019). Genetics of variable disease expression conferred by inverse gene-for-gene interactions in the wheat-*Parastagonospora nodorum* pathosystem. Plant physiology, 180 (1), 420-434.

He, Q., Liu, Y., Liang, P., Liao, X., Li, X., Li, X., Shi, D., Liu, W., Lin, C., Zheng, F., and Miao, W. (2021). A novel chorismate mutase from *Erysiphe quercicola* performs dual functions of synthesizing amino acids and inhibiting plant salicylic acid synthesis. Microbiological Research, 242, 126599.

Helmstaedt, K., Heinrich, G., Merkl, R., and Braus, G. H. (2004). Chorismate mutase of *Thermus thermophilus* is a monofunctional AroH class enzyme inhibited by tyrosine. Archives of Microbiology, 181, 195-203.

Helmstaedt, K., Krappmann, S., and Braus, G. H. (2001). Allosteric regulation of catalytic activity: *Escherichia coli* aspartate transcarbamoylase versus yeast chorismate mutase. Microbiology and Molecular Biology Reviews, 65 (3), 404-421.

Homer, C. M., Summers, D. K., Goranov, A. I., Clarke, S. C., Wiesner, D. L., Diedrich, J. K., and Madhani, H. D. (2016). Intracellular action of a secreted peptide required for fungal virulence. Cell Host and Microbe, 19 (6), 849-864.

Hortipoint (2017). https://www.hortipoint.nl/vakbladvoordebloemisterij/bollensector-schriktierse-vondst-resistente-schimmel. (Accessed on 29 May 2019).

Hou, P. F., and Chen, C. Y. (2003). Early stages of infection of lily leaves by *Botrytis elliptica* and *B. cinerea*. Plant Pathology, 12, 103–108.

Hu, F., Liu, G., Hu, Y., Guo, R., Zhu, L., Luo, F., and Wang F. (2017). Authenticity identification and leaf blight resistance evaluation of the F1 hybrids from two *Lilium* genotypes 'Sorbonne'and 'Francia'. Physiological and Molecular Plant Pathology, 100, 194–200.

Huang, J., Hsieh, T. F., Chastagner, G. A., and Hsiang, T. (2001). Clonal and sexual propagation in *Botrytis elliptica*. Mycological Research, 105(7), 833-842.

Huang, J., Yang, L. Q., Yu, Y., Liu, Y. M., Xie, D. F., Li, J., and Zhou, S.D. (2018). Molecular phylogenetics and historical biogeography of the tribe *Lilieae* (Liliaceae): bidirectional dispersal between biodiversity hotspots in place Eurasia. Annals of Botany, 122, 1245–1262.

Huang, J., Yang, L.-Q., Yu, Y., Liu, Y.-M., Xie, D.-F., Li, J., He, X.-J., and Zhou, S.-D. (2018). Molecular phylogenetics and historical biogeography of the tribe *Lilieae* (Liliaceae): bi-directional dispersal between biodiversity hotspots in Eurasia. Annals of Botany, 122, 1245–1262.

Hunziker, L., Tarallo, M., Gough, K., Guo, M., Hargreaves, C., Loo, T. S., and Bradshaw, R. E. (2021). Apoplastic effector candidates of a foliar forest pathogen trigger cell death in host and non-host plants. Scientific Reports, 11 (1), 19958.

Hyde, K. D., Nilsson, R. H., Alias, S. A., Ariyawansa, H. A., Blair, J. E., Cai, L., and Zhou, N. (2014). One stop shop: Backbones trees for important phytopathogenic genera. Fungal Diversity 67, (1), 21–125.

Ishiga, Y., Watanabe, M., Ishiga, T., Tohge, T., Matsuura, T., Ikeda, Y., and Mysore, K. S. (2017). The SAL-PAP chloroplast retrograde pathway contributes to plant immunity by regulating glucosinolate pathway and phytohormone signaling. Molecular Plant-Microbe Interactions, 30 (10), 829-841.

Izquierdo-Bueno, I., González-Rodríguez, V. E., Simon, A., Dalmais, B., Pradier, J. M., le Pêcheur, P., Mercier, A., Walker, A. S., Garrido, C., Collado, I. G., and Viaud, M. (2018). Biosynthesis of abscisic acid in fungi: identification of a sesquiterpene cyclase as the key enzyme in *Botrytis cinerea*. Environmental Microbiology, 20 (7), 2469–2482.

Jang, J. Y., Subburaj, S., Lee, G. J., and Kim, H. S. (2018). In vitro screening for *Botrytis* leaf blight resistance in *Lilium* species. Scientia Horticulturae. 239, 133–140.

Jeblick, T., Leisen, T., Steidele, C.E., Albert, I., Müller, J., Kaiser, S., Mahler, F., Sommer, F., Keller, S., Hückelhoven, R. and Hahn, M., (2023). *Botrytis* hypersensitive response inducing protein 1 triggers noncanonical PTI to induce plant cell death. Plant Physiology, 191(1), pp.125-141.

Johnson, R. D., Lane, G. A., Koulman, A., Cao, M., Fraser, K., Fleetwood, D. J., and Johnson, L. J. (2015). A novel family of cyclic oligopeptides derived from ribosomal peptide synthesis of an in planta-induced gene, *gigA*, in *Epichloë* endophytes of grasses. Fungal Genetics and Biology, 85, 14-24.

Jones, D. A. B., Rozano, L., Debler, J. W., Mancera, R. L., Moolhuijzen, P. M., and Hane, J. K. (2021). An automated and combinative method for the predictive ranking of candidate effector proteins of fungal plant pathogens. Scientific Reports, 11, 19731.

Jumper, J. (2021). Highly accurate protein structure prediction with AlphaFold. Nature, 596, 583–589.

Juturu, V., and Wu, J. C. (2018). Heterologous protein expression in *Pichia pastoris*: latest research progress and applications. ChemBioChem, 19 (1), 7-21.

Kabbage, M., Kessens, R., Bartholomay, L., and Williams, B. (2017). The life and death of a plant cell. Annual Review of Plant Biology, 68, 375–404.

Kamenetsky, R. (2014). Flower biology in *Lilium*: achievements and research challenges. Acta Horticulturae, 1027, 65–74.

Kanneganti, T. D., Huitema, E. and Kamoun, S. (2007). In planta expression of oomycete and fungal genes. Plant-Pathogen Interactions: Methods and Protocols, 35-43.

Kariyawasam, G. K., Carter, A. H., Rasmussen, J. B., Faris, J. D., Xu, S. S., Mergoum, M., and Liu, Z. (2016). Genetic relationships between race-nonspecific and racespecific interactions in the wheat–*Pyrenophora tritici-repentis* pathosystem. Theoretical and Applied Genetics, 129, 897–908.

Kariyawasam, G. K., Richards, J. K., Wyatt, N. A., Running, K. L., Xu, S. S., Liu, Z., and Friesen, T. L. (2022). The *Parastagonospora nodorum* necrotrophic effector SnTox5 targets the wheat gene *Snn5* and facilitates entry into the leaf mesophyll. New Phytologist, 233 (1), 409-426.

Kessler, S. C., and Chooi, Y. H. (2022). Out for a RiPP: challenges and advances in genome mining of ribosomal peptides from fungi. Natural Product Reports, 39 (2), 222-230.

Kessler, S. C., Zhang, X., McDonald, M. C., Gilchrist, C. L., Lin, Z., Rightmyer, A., and Chooi, Y. H. (2020). Victorin, the host-selective cyclic peptide toxin from the oat pathogen *Cochliobolus victoriae*, is ribosomally encoded. Proceedings of the National Academy of Sciences, 117 (39), 24243-24250.

Kim, H. T., Lim, K. B., and Kim, J. S. (2019). New Insights on Lilium Phylogeny Based on a Comparative Phylogenomic Study Using Complete Plastome Sequences. Plants 2019, Vol. 8, Page 547, 8 (12), 547.

Kim, J. S., and Kim, J. H. (2018). Updated molecular phylogenetic analysis, dating and biogeographical history of the lily family (Liliaceae: Liliales). Botanical Journal of the Linnean Society, 187 (4), 579–593.

Klessig, D. F., Choi, H. W., and Dempsey, D. M. A. (2018). Systemic acquired resistance and salicylic acid: past, present, and future. Molecular Plant-Microbe Interaction. 31, 871–888.

Koladia, V. M., Faris, J. D., Richards, J. K., Brueggeman, R. S., Chao, S., and Friesen, T. L. (2017). Genetic analysis of net form net blotch resistance in barley lines CIho 5791 and Tifang against a global collection of *P. teres f. teres* isolates. Theoretical and Applied Genetics, 130, 163–173.

Kombrink, A. (2012). Heterologous production of fungal effectors in *Pichia pastoris*. In: Bolton, M. D., Thomma, B. P. H. J. (eds) Plant Fungal Pathogens. Methods in Molecular Biology, vol 835. Humana Press.

Krappmann, S., Helmstaedt, K., Gerstberger, T., Eckert, S., Hoffmann, B., Hoppert, M., and Braus, G. H. (1999). The *aroC* gene of *Aspergillus nidulans* encodes a monofunctional, allosterically regulated chorismate mutase. Journal of Biological Chemistry, 274 (32), 22275-22282.

Kretschmer, M., Damoo, D., Djamei, A., and Kronstad, J. (2019). Chloroplasts and plant immunity: where are the fungal effectors? Pathogens, 9 (1), 19.

Krogh, A., Larsson, B., Von Heijne, G., and Sonnhammer, E. L. (2001). Predicting transmembrane protein topology with a hidden Markov model: application to complete genomes. Journal of molecular biology, 305 (3), 567-580.

Kroll, K., Holland, C. K., Starks, C. M., and Jez, J. M. (2017). Evolution of allosteric regulation in chorismate mutases from early plants. Biochemical Journal, 474 (22), 3705–3717.

Kurtz, S., Phillippy, A., Delcher, A. L., Smoot, M., Shumway, M., Antonescu, C., and Salzberg, S.L. (2004). Versatile and open software for comparing large genomes. Genome Biology, 5 (2), 1–9.

Landeo Villanueva, S., Malvestiti, M. C., van Ieperen, W., Joosten, M. H. A. J., and van Kan, J. A. L. (2021). Red light imaging for programmed cell death visualization and quantification in plant–pathogen interactions. Molecular Plant Pathology, 22 (3), 361–372.

Le Marquer, M., San Clemente, H., Roux, C., Savelli, B., and Frei dit Frey, N. (2019). Identification of new signalling peptides through a genome-wide survey of 250 fungal secretomes. BMC Genomics, 20 (1), 1-15.

Lee, A.Y., Karplus, P.A., Ganem, B. and Clardy, J. (1995). Atomic structure of the buried catalytic pocket of *Escherichia coli* chorismate mutase. Journal of the American Chemical Society, 117, 3627–3628.

Lee, D. W., and Hwang, I. (2018). Evolution and design principles of the diverse chloroplast transit peptides. Molecules and Cells, 41 (3), 161.

Lee, D.W., Jung, C., and Hwang, I. (2013). Cytosolic events involved in chloroplast protein targeting. Biochimica et Biophysica Acta (BBA)-Molecular Cell Research, 1833 (2), 245-252.

Lee, D.W., Kim, S.J., Oh, Y.J., Choi, B., Lee, J., and Hwang, I. (2016). *Arabidopsis* BAG1 functions as a cofactor in Hsc70-mediated proteasomal degradation of unimported plastid proteins. Molecular Plant 9 (10), 1428-1431.

Lee, D.W., Lee, S., Lee, G.J., Lee, K.H., Kim, S., Cheong, G.W., and Hwang, I. (2006). Functional characterization of sequence motifs in the transit peptide of *Arabidopsis* small subunit of rubisco. Plant Physiology, 140, 466-483.

Lee, D.W., Yoo, Y.J., Razzak, M.A., and Hwang, I. (2018). Prolines in transit peptides are crucial for efficient preprotein translocation into chloroplasts. Plant Physiology, 176, 663-677.

Lee, S., Lee, D.W., Lee, Y., Mayer, U., Stierhof, Y.D., Lee, S., Jurgens, G., and Hwang, I. (2009). Heat shock protein cognate 70-4 and an E3 ubiquitin ligase, CHIP, mediate plastid-destined precursor degradation through the ubiquitin-26S proteasome system in *Arabidopsis*. Plant Cell, 21, 3984-4001.

Lefevere, H., Bauters, L., and Gheysen, G. (2020). Salicylic acid biosynthesis in plants. Frontiers in Plant Science, 11, 1–7.

Leisen, T., Bietz, F., Werner, J., Wegner, A., Schaffrath, U., Scheuring, D., and Hahn, M. (2020). CRISPR/Cas with ribonucleoprotein complexes and transiently selected telomere vectors allows highly efficient marker-free and multiple genome editing in *Botrytis cinerea*. PloS Pathogwns, 16 (8), e1008326.

Leisen, T., Werner, J., Pattar, P., Safari, N., Ymeri, E., Sommer, F., Schroda, M., Suárez, I., Collado, I. G., Scheuring, D., and Hahn, M. (2022). Multiple knockout mutants reveal a high redundancy of phytotoxic compounds contributing to necrotrophic pathogenesis of *Botrytis cinerea*. PLoS Pathogens, 18 (3) e1010367.

Lenarčič T., Albert I., Böhm H., Hodnik V., Pirc K., Zavec A.B., Podobnik M., Pahovnik D., Žagar E., Pruitt R., and Nürnberger, T. (2017). Eudicot plant-specific sphingolipids determine host selectivity of microbial NLP cytolysins. Science, 358, 1431-1434.

Li, J., Cai, J., Qin, H. H., Price, M., Zhang, Z., Yu, Y., and Gao, X. F. (2022). Phylogeny, age, and evolution of tribe *Lilieae* (Liliaceae) based on whole plastid genomes. Frontiers in Plant Science, 12, 3158.

Liang, X., and Rollins, J. A. (2018). Mechanisms of broad host range necrotrophic pathogenesis in *Sclerotinia sclerotiorum*. Phytopathology, 108 (10), 1128-1140.

Liebrand, T. W., Smit, P., Abd-El-Haliem, A., de Jonge, R., Cordewener, J. H., America, A. H., Sklenar, J., Jones, A. M., Robatzek, S., Thomma, B. P., Tameling, W. I. and Joosten, M. H. A. J. (2012). Endoplasmic reticulum-quality control chaperones facilitate the biogenesis of Cf receptor-like proteins involved in pathogen resistance of tomato. Plant Physiology, 159, 1819–1833.

Lim, K. B., Barba-Gonzalez, R., Zhou, S., Ramanna, M. S., and Van Tuyl, J. M. (2008). "Interspecific hybridization in lily (*Lilium*): taxonomic and commercial aspects of using species hybrids in breeding," in 1st Floriculture, ornamental and plant biotechnology: advances and topical issues, eds. Teixeira de Silva, J. A., 5, 146–151. Isleworth: Global Science Books.

Lin, X., Olave-Achury, A., Heal, R., Pais, M., Witek, K., Ahn, H. K., and Jones, J. D. (2022). A potato late blight resistance gene protects against multiple *Phytophthora* species by recognizing a broadly conserved RXLR-WY effector. Molecular Plant, 15 (9), 1457-1469.

Liu J., Gaj T., Wallen M.C., and Barbas, C.F. (2015). Improved cell-penetrating zinc-finger nuclease proteins for precision genome engineering. Molecular Therapy-Nucleic Acids, 4:e232. pmid:25756962.

Liu, Z., Faris, J. D., Meinhardt, S., Ali, S., Rasmussen, J., and Friesen, T. L. (2004). Genetic and physical mapping of a gene conditioning sensitivity in wheat to a partially purified host-selective toxin produced by *Stagonospora nodorum*. Phytopathology, 94 (10), 1056–1060.

Liu, Z., Gao, Y., Kim, Y. M., Faris, J. D., Shelver, W. L., de Wit, P. J., and Friesen, T. L. (2016). SnTox1, a *Parastagonospora nodorum* necrotrophic effector, is a dual-function protein that facilitates infection while protecting from wheat-produced chitinases. New Phytologist, 211 (3), 1052-1064.

Liu, Z., Zhang, Z., Faris, J. D., Oliver, R. P., Syme, R., McDonald, M. C., and Friesen, T. L. (2012). The cysteine rich necrotrophic effector SnTox1 produced by *Stagonospora nodorum* triggers susceptibility of wheat lines harboring *Snn1*. PLoS Pathogens, 8 (1), e1002467.

Liu, Z., Zurn, J. D., Kariyawasam, G., Faris, J., Shi, G., Jansen, J., and Acevedo, M. (2017). Inverse gene-for-gene interactions contribute additively to tan spot susceptibility in wheat. Theoretical and Applied Genetics, 130, 1267–1276.

Lo Presti, L., Lanver, D., Schweizer, G., Tanaka, S., Liang, L., Tollot, M., Zuccaro, A., Reissmann, S., and Kahmann, R. (2015). Fungal effectors and plant susceptibility. Annual Reviews of Plant Biology, 66, 513–545.

Lobstein, J., Emrich, C.A., Jeans, C., Faulkner, M., Riggs, P. and Berkmen, M. (2012). SHuffle, a novel *Escherichia coli* protein expression strain capable of correctly folding disulphide bonded proteins in its cytoplasm. Microbial Cell Factories, 11, 56.

Lorang J. M., Carkaci-Salli N., and Wolpert T. J. (2004). Identification and characterization of victorin sensitivity in *Arabidopsis thaliana*. Molecular Plant Microbe Interaction, 17, 577–582.

Lorang, J. M., Sweat, T. A., and Wolpert, T. J. (2007). Plant disease susceptibility conferred by a "resistance" gene. Proceedings of the National Academy of Sciences, 104 (37), 14861–14866.

Lorrain, C., Gonçalves dos Santos, K. C., Germain, H., Hecker, A., and Duplessis, S. (2019). Advances in understanding obligate biotrophy in rust fungi. New Phytologist, 222 (3), 1190-1206.

Ma, L. S., Pellegrin, C., and Kahmann, R. (2018a). Repeat-containing effectors of filamentous pathogens and symbionts. Current Opinion in Microbiology, 46, 123-130.

Ma, L. S., Wang, L., Trippel, C., Mendoza-mendoza, A., Ullmann, S., Moretti, M., and Kahmann, R. (2018b). The *Ustilago maydis* repetitive effector Rsp3 blocks the antifungal activity of mannose-binding maize proteins. Nature Communication, 9 (1), 1711.

Malvestiti, M. C., Steentjes, M. B., Beenen, H. G., Boeren, S., van Kan, J. A. L., and Shi-Kunne, X. (2022). Analysis of plant cell death-inducing proteins of the necrotrophic fungal pathogens *Botrytis squamosa* and *Botrytis elliptica*. Frontiers in Plant Science, 13.

Manning, V.A., Hamilton, S.M., Karplus, P.A., and Ciuffetti, L.M. (2008). The Arg-Gly-Asp containing, solvent-exposed loop of Ptr ToxA is required for internalization. Molecular Plant Microbe Interactions, 21, 315–325.

Marasek-Ciolakowska, A., Nishikawa, T., Shea, D. J., and Okazaki, K. (2018). Breeding of lilies and tulips—interspecific hybridization and genetic background. Breeding Science, 68 (1), 35–52.

Markham, J. E., and Hille, J. (2001). Host-selective toxins as agents of cell death in plant-fungus interactions, Molecular Plant Pathology, 2, (4) 229–239.

Martin, S.H., Wingfield, B.D., Wingfield, M.J., and Steenkamp, E.T. (2011). Causes and consequences of variability in peptide mating pheromones of ascomycete Fungi. Molecular Biology and Evolution, 28 (7), 1987-2003.

Mbengue, M., Navaud, O., Peyraud, R., Barascud, M., Badet, T., Vincent, R., and Raffaele, S. (2016). Emerging trends in molecular interactions between plants and the broad host range fungal pathogens *Botrytis cinerea* and *Sclerotinia sclerotiorum*. Frontiers in Plant Science, 7, 422.

McDonald, M. C., Oliver, R. P., Friesen, T. L., Brunner, P. C., and McDonald, B. A. (2013). Global diversity and distribution of three necrotrophic effectors in *Phaeosphaeria nodorum* and related species. New Phytologist, 199 (1), 241-251.

Mercier, A., Carpentier, F., Duplaix, C., Auger, A., Pradier, J. M., Viaud, M., and Walker, A.S. (2019). The polyphagous plant pathogenic fungus *Botrytis cinerea* encompasses host-specialized and generalist populations. Environmental Microbiology, 21 (12), 4808–21.

Mesarich, C. H., Ökmen, B., Rovenich, H., Griffiths, S. A., Wang, C., Karimi Jashni, M., and De Wit, P. J. (2018). Specific hypersensitive response–associated recognition of new apoplastic effectors from *Cladosporium fulvum* in wild tomato. Molecular Plant-Microbe Interactions, 31 (1), 145-162.

Michaelis, L. and Menten, M.L. (1913). „Die Kinetik der Invertinwirkung". Biochemische Zeitung, 49, 333–369.

Minina, E. A., Bozhkov, P. V., and Hofius, D. (2014). Autophagy as initiator or executioner of cell death. Trends Plant Science, 19 (11), 692-697.

Montalbán-López, M., Scott, T. A., Ramesh, S., Rahman, I. R., Van Heel, A. J., Viel, J. H., and van der Donk, W. A. (2021). New developments in RiPP discovery, enzymology and engineering. Natural Product Reports, 38 (1), 130-239.

Mound, L. A., and Tree, D. J. (2008). The oriental lily-flower thrips '*Taeniothrips eucharii*' (Whetzel) (Thysanoptera: *Thripidae*) new to Australia. The Australian Entomologist, 35 (4), 159-160.

Müller, O., Schreier, P.H., and Uhrig, J.F. (2008). Identifcation and characterization of secreted and pathogenesis-related proteins in *Ustilago maydis*. Molecular Genetics and Genomics, 279, 27-39.

Munafo, J. P. Jr., and Gianfagna, T. J. (2011). Antifungal activity and fungal metabolism of steroidal glycosides of Easter lily (*Lilium longiflorum* Thunb.) by the plant pathogenic fungus, *Botrytis cinerea*. Journal of agricultural and food chemistry, 59 (11) 5945-5954.

Nejat, N., Rookes, J., Mantri N. L., and Cahill, D.M. (2017). Plant–pathogen interactions: toward development of next-generation disease-resistant plants. Critical Reviews in Biotechnology, 37 (2), 229-237.

Nielsen, K. and Yohalem, D. S. (2001). Origin of a polyploid *Botrytis* pathogen through interspecific hybridization between *Botrytis aclada* and *B. byssoidea*. Mycologia, 93, 1064–1071.

Nishikawa, T. (2007). Molecular phylogeny of the genus *Lilium* and its methodical application to other taxon. Ph.D. Thesis. University of Agriculture and Technology. Tokyo, Japan.

Nishikawa, T., CityplaceOkazaki, K., Uchino, T., Arakawa, K., and Nagamine, T. (1999). A molecular phylogeny of Lilium in the internal transcribed spacer region of nuclear ribosomal DNA. Journal of Molecular Evolution, 49, 238-249.

Noar, R. D., and Daub M. E., (2016). Transcriptome sequencing of *Mycosphaerella fijiensis* during association with *Musa acuminata* reveals candidate pathogenicity genes. BMC Genomics ,17, 690.

Noda, J., Brito, N., and González, C. (2010). The *Botrytis cinerea* xylanase Xyn11A contributes to virulence with its necrotizing activity, not with its catalytic activity. BMC Plant Biology, 10 (1), 1–15.

Oh, S. K., Young, C., Lee, M., Oliva, R., Bozkurt, T. O., Cano, L. M., and Kamoun, S. (2009). In planta expression screens of *Phytophthora infestans* RXLR effectors reveal diverse phenotypes, including activation of the *Solanum bulbocastanum* disease resistance protein Rpi-blb2. The Plant Cell, 21 (9), 2928-2947.

Ökvist, M., Dey, R., Sasso, S., Grahn, E., Kast, P., and Krengel, U. (2006). 1.6 Å crystal structure of the secreted chorismate mutase from *Mycobacterium tuberculosis*: novel fold topology revealed. Journal of Molecular Biology, 357 (5), 1483-1499.

Oliver, R. P., and Solomon, P. S. (2010). New developments in pathogenicity and virulence of necrotrophs. Current Opinion in Plant Biology, 13 (4), 415-419.

Oliver, R. P., Friesen, T. L., Faris, J. D., and Solomon, P. S. (2012). *Stagonospora nodorum*: From pathology to genomics and host resistance. Annual Reviews of Phytopathology, 50, 23–43.

Oliver, R. P., Lichtenzveig, J., Tan, K.-C., Waters, O., Rybak, K., Lawrence, J., Friesen, T. L., and Burgess, P. (2014). Absence of detectable yield penalty associated with insensitivity to Pleosporales necrotrophic effectors in wheat grown in the West Australian wheat belt. Plant Pathology, 63, 1027-1032.

Outram, M. A., Solomon, P. S., and Williams, S. J. (2021a). Pro-domain processing of fungal effector proteins from plant pathogens. PLoS Pathogens, 17 (10), e1010000.

Outram, M. A., Sung, Y. C., Yu, D., Dagvadorj, B., Rima, S. A., Jones, D. A., and Williams, S. J. (2021b). The crystal structure of SnTox3 from the necrotrophic fungus *Parastagonospora nodorum* reveals a unique effector fold and provides insight into *Snn3* recognition and pro-domain protease processing of fungal effectors. New Phytologist, 231 (6), 2282-2296.

Paysan-Lafosse, T., Blum, M., Chuguransky, S., Grego, T., Pinto, B. L., Salazar, G.A., Bileschi, M. L., Bork, P., Bridge, A., Colwell, L., Gough, J., ..., and Bateman, A. (2022). InterPro in 2022. Nucleic Acids Research, 51 (D1), D418-D427.

Pedro, H., Yates, A. D., Kersey, P. J., and De Silva, N. H. (2019). Collaborative annotation redefines gene sets for crucial phytopathogens. Frontiers in Microbiology, 10, 2477.

Pelkonen, V.-P., and Pirttilä, A.-M. (2012). Taxonomy and Phylogeny of the Genus *Lilium*. Floriculture and Ornamental Biotechnology. 6(2), 1-8.

Phan, H. T., Rybak, K., Furuki, E., Breen, S., Solomon, P. S., Oliver, R. P., and Tan, K. R. (2016). Differential effector gene expression underpins epistasis in a plant fungal disease. Plant Journal, 87 (4), 343–354.

Pinedo, C., Wang, C., Pradier, J., Dalmais, B., Choquer, M., Pascal, L., Morgant, G., Collado, I. G., Cane, D. E., and Viaud, M. (2008). The Sesquiterpene Synthase from the Botrydial Biosynthetic Gene Cluster of the Phytopathogen *Botrytis cinerea*. ACS chemical biology, 3 (12), 791-801.

Pirc K., Clifton L.A., Yilmaz N., Saltalamacchia A., Mally M., Snoj T., Žnidaršič N., Srnko M., Borišek J., Parkkila P., and Anderluh, G. (2022). An oomycete NLP cytolysin forms transient small pores in lipid membranes. Science Advances, 8 (10), eabj9406.

Porquier, A., Morgant, G., Moraga, J., Dalmais, B., Luyten, I., Simon, A., Pradier, J. M., Amselem, J., Collado, I. G., and Viaud, M. (2016). The botrydial biosynthetic gene cluster of *Botrytis cinerea* displays a bipartite genomic structure and is positively regulated by the putative Zn(II)2Cys6 transcription factor BcBot6. Fungal Genetics and Biology, 96, 33–46.

Qin, W., Cho, K. F., Cavanagh, P. E., and Ting, A. Y. (2021). Deciphering molecular interactions by proximity labeling. Nature Methods, 18 (2), 133-143.

Qian, Y., Lynch, J.H., Guo, L., Rhodes, D., Morgan, J.A., and Dudareva, N. (2019). Completion of the Cytosolic Post-Chorismate Phenylalanine Biosynthetic Pathway in Plants. Nature Communication, 10, 15.

Radoman, B., Grünwald-Gruber, C., Schmelzer, B., Zavec, D., Gasser, B., Altmann, F., and Mattanovich, D. (2021). The degree and length of O-Glycosylation of recombinant proteins produced in *Pichia pastoris* depends on the nature of the protein and the process type. Biotechnology Journal, 16 (3), 2000266.

Raffaele, S., and Kamoun, S. (2012). Genome Evolution in Filamentous Plant Pathogens: Why Bigger Can Be Better. Nature Reviews Microbiology, 10 (6), 417–430.

Rebordinos, L., Cantoral, J. M., Prieto, M. V., Hanson, J. R., and Collado, I. G. (1996). The phytotoxic activity of some metabolites of *Botrytis cinerea*. Phytochemistry, 42 (2), 383–387.

Reddy, P. P. (2016). Lilies. Sustainable Crop Protection under Protected Cultivation, 381-391.

Rekhter, D., Lüdke, D., Ding, Y., Feussner, K., Zienkiewicz, K., Lipka, V., and Feussner, I. (2019). Isochorismate-derived biosynthesis of the plant stress hormone salicylic acid. Science, 365 (6452), 498-502.

Richards, J. K., Kariyawasam, G. K., Seneviratne, S., Wyatt, N. A., Xu, S. S., Liu, Z., and Friesen, T. L. (2022). A triple threat: the *Parastagonospora nodorum* SnTox267 effector exploits three distinct host genetic factors to cause disease in wheat. New Phytologist, 233 (1), 427-442.

Rietman, H., Bijsterbosch, G., Cano, L. M., Lee, H. R., Vossen, J. H., Jacobsen, E., Visser, R. G. F., Kamoun, S., and Vleeshouwers, V. G. A. A. (2012). Qualitative and quantitative late blight resistance in the potato cultivar Sarpo Mira is determined by the perception of five distinct RXLR effectors. Molecular Plant-Microbe Interaction, 25, 910-919.

Rocafort, M., Bowen, J. K., Hassing, B., Cox, M. P., McGreal, B., de la Rosa, S., and Mesarich, C. H. (2022). The *Venturia inaequalis* effector repertoire is dominated by expanded families with predicted structural similarity, but unrelated sequence, to avirulence proteins from other plant-pathogenic fungi. BMC Biology, 20 (1), 1-24.

Rogers, H. J. (2013). From models to ornamentals: how is flower senescence regulated? Plant Molecular Biology, 82, 563–574.

Romero, R. M., Roberts, M. F., and Phillipson, J. D. (1995). Anthranilate synthase in microorganisms and plants. Phytochemistry, 39, 263–276.

Rossi, F. R., Gárriz, A., Marina, M., Romero, F. M., Gonzalez, M. E., Collado, I. G., and Pieckenstain, F. L. (2011). The sesquiterpene botrydial produced by *Botrytis cinerea* induces the hypersensitive response on plant tissues and its action is modulated by salicylic acid and jasmonic acid signaling. Molecular Plant-Microbe Interactions, 24 (8), 888–896.

Royal Flora Holland (2020). Annual report RFH-Jaarverslag-2021.pdf (royalfloraholland.com)

Ruud, A. K., Dieseth, J. A., and Lillemo, M. (2018). Effects of three *Parastagonospora nodorum* necrotrophic effectors on spring wheat under Norwegian field conditions. Crop Science, 58 (1), 159-168.

Ruud, A. K., Windju, S., Belova, T., Friesen, T. L., and Lillemo, M. (2017). Mapping of SnTox3–*Snn3* as a major determinant of field susceptibility to *Septoria nodorum* leaf blotch in the SHA3/CBRD× naxos population. Theoretical and Applied Genetic, 130 (7), 1361–1374.

Salisbury, A. (2003). Two parasitoids of the Lily beetle, *Lilioceris lilii* (Scopoli) (Coleoptera: *Chrysomelidae*), in Britain, including the first record of *Lemophagus errabundus* Gravenhorst (Hymenoptera: *Ichneumonidae*). British Journal of Entomology and Natural History, 16 (2), 103-104.

Sasso, S., Ramakrishnan, C., Gamper, M., Hilvert, D. and Kast, P. (2005). Characterization of the secreted chorismate mutase from the pathogen *Mycobacterium tuberculosis*. The FEBS Journal, 272 (2), 375-389.

Saunders, D. G. O., Win, J., Cano, L. M., Szabo, L. J., Kamoun, S. and Raffaele, S. (2012). Using hierarchical clustering of secreted protein families to classify and rank candidate effectors of rust fungi. PLoS ONE, 7, e29847.

Schnappauf, G., Lipscomb, W. N., and Braus, G. H. (1998). Separation of inhibition and activation of the allosteric yeast chorismate mutase. Proceedings of the National Academy of Sciences, 95 (6), 2868-2873.

Schnappauf, G., Sträter, N., Lipscomb, W. N., and Braus, G. H. (1997). A glutamate residue in the catalytic center of the yeast chorismate mutase restricts enzyme activity to acidic conditions. Proceedings of the National Academy of Sciences, 94 (16), 8491-8496.

Schouten, A., Van Baarlen, P., and Van Kan, J. A. L. (2008). Phytotoxic Nep1-like proteins from the necrotrophic fungus *Botrytis cinerea* associate with membranes and the nucleus of plant cells. New Phytologist, 177 (2), 493-505.

Schouten, A., Wagemakers, L., Stefanato, F. L., Kaaij, R. M., and van Kan, J. A. L. (2002). Resveratrol acts as a natural profungicide and induces self-intoxication by a specific laccase. Molecular Microbiology, 43, 883–894.

Schultzhaus, Z., Johnson, T. B., and Shaw, B. D. (2017). Clathrin localization and dynamics in *Aspergillus nidulans*. Molecular Microbiology, 103, 299–318.

Schumacher, J. (2012). Tools for *Botrytis cinerea*: new expression vectors make the gray mold fungus more accessible to cell biology approaches. Fungal Genetics and Biology, 49 (6), 483-497.

Schürch, S., Linde, C. C., Knogge, W., Jackson, L. F., and McDonald, B. A. (2004). Molecular population genetic analysis differentiates two virulence mechanisms of the fungal avirulence gene *NIP1*. Molecular Plant-Microbe Interaction, 17 (10), 1114–1125.

Shackley, B., Zaicou-Kunesch, C., Curry, J., Nicol, D., Shankar, M., and Thomas, G. (2020). Western Australia Crop Sowing Guide. Grains Research and Development Corporation, Department of Primary Industries and Regional Development.

Shahin, A., Arens, P., Van Heusden, S., and van Tuyl, J. M. (2009). Conversion of molecular markers linked to *Fusarium* and virus resistance in Asiatic lily hybrids. Acta Horticulturae, 836, 131–136.

Shahin, A., Smulders, M. J., van Tuyl, J. M., Arens, P., and Bakker, F. T. (2014). Using multi-locus allelic sequence data to estimate genetic divergence among four *Lilium* (Liliaceae) genotypes. Frontiers in Plant Science, 5, 567.

Shen, X. X., Steenwyk, J. L., La Bella, A. L., Opulente, D. A., Zhou, X., Kominek, J., and Rokas, A. (2020). Genome-scale phylogeny and contrasting modes of genome evolution in the fungal phylum Ascomycota. Science Advance, 6 (45), eabd0079.

Shi, G., Friesen, T. L., Saini, J., Xu, S. S., Rasmussen, J. B., and Faris, J. D. (2015). The wheat *Snn7* gene confers susceptibility on recognition of the *Parastagonospora nodorum* necrotrophic effector SnTox7. The Plant Genome, 8 (2).

Shi, G., Zhang, Z., Friesen, T. L., Raats, D., Fahima, T., Brueggeman, R. S., and Faris, J. D. (2016). The hijacking of a receptor kinase–driven pathway by a wheat fungal pathogen leads to disease. Science Advances 2, e1600822.

Shibuya, K., Yamada, T., and Ichimura, K. (2016). Morphological changes in senescing petal cells and the regulatory mechanism of petal senescence. Journal of Experimental Botany, 67, 5909–5918.

Siewers, V., Viaud, M., Jimenez-Teja, D., Collado, I. G., Gronover, C. S., Pradier, J.-M., Tudzynski, B., and Tudzynski, P. (2005). Functional analysis of the cytochrome P450 monooxygenase gene bcbot1 of *Botrytis cinerea* indicates that botrydial is a strain-specific virulence factor. Molecular Plant-Microbe Interactions, 18 (6), 602–612.

Souibgui, E., Bruel, C., Choquer, M., de Vallée, A., Dieryckx, C., Dupuy, J. W., and Poussereau, N. (2021). Clathrin is important for virulence factors delivery in the necrotrophic fungus *Botrytis cinerea*. Frontiers in Plant Science, 12, 668937.

Sowden, R. G., Watson, S. J., and Jarvis, P. (2017). The role of chloroplasts in plant pathology. Essays in Biochemistry, 62 (1), 21-39.

Sperschneider J., and Dodds P. (2021). EffectorP 3.0: prediction of apoplastic and cytoplasmic effectors in fungi and oomycetes. Molecular Plant-Microbe Interaction, 35 (2), 146-156.

Sperschneider, J., Catanzariti, A. M., DeBoer, K., Petre, B., Gardiner, D. M., Singh, K. B., and Taylor, J. M. (2017). LOCALIZER: subcellular localization prediction of both plant and effector proteins in the plant cell. Scientific Reports, 7 (1), 1-14.

Staats, M., Van Baarlen, P., and van Kan, J. A. L. (2007). AFLP analysis of genetic diversity in populations of *Botrytis elliptica and Botrytis tulipae* from the Netherlands. European Journal of Plant Pathology, 117, 219–235.

Staats, M., van Baarlen, P., Schouten, A., and van Kan, J. A. L. (2007). Functional analysis of NLP genes from *Botrytis elliptica*. Molecular Plant Pathology, 8 (2), 209-214.

Stassen, J., den Boer, E., Vergeer, P. W. J., Andel, A., Ellendorff, U., Pelgrom, K., Pel, M., Schut, J., Zonneveld, O., Jeuken, M. J. W., and van den Ackerveken, G. (2013). Specific *in planta* recognition of two GKLR proteins of the downy mildew *Bremia lactucae* revealed in a large effector screen in lettuce. Molecular Plant-Microbe Interaction, 26, 1259.

Steentjes, M. B. F., Herrera Valderrama, A. L., Fouillen, L., Bahammou, D., Leisen, T., Albert, I., Nürnberger, T., Hahn, M., Mongrand, S., Scholten, O. E., and van Kan, J. A. L. (2022). Cytotoxic activity of Nep1-like proteins on monocots. New Phytologist, 235 (2), 690–700.

Steentjes, M. B. F., Tonn, S., Coolman, H., Langebeeke, S., Scholten, O. E., and van Kan, J. A. L. (2021). Visualization of three *Sclerotiniaceae* species pathogenic on onion reveals distinct biology and infection strategies. International Journal of Molecular Science, 22 (4), 1865.

Stergiopoulos, I., Collemare, J., Mehrabi, R., and De Wit, P. J. (2013). Phytotoxic secondary metabolites and peptides produced by plant pathogenic Dothideomycete fungi. FEMS Microbiology Reviews, 37 (1), 67-93.

Sträter, N., Schnappauf, G., Braus, G., and Lipscomb, W. N. (1997). Mechanisms of catalysis and allosteric regulation of yeast chorismate mutase from crystal structures. Structure, 5 (11), 1437–1452.

Strawn, M. A., Marr, S. K., Inoue, K., Inada, N., Zubieta, C., and Wildermuth, M. C. (2007). *Arabidopsis* isochorismate synthase functional in pathogen-induced salicylate biosynthesis

exhibits properties consistent with a role in diverse stress responses. Journal of Biological Chemistry, 282 (8), 5919–5933.

Suárez, I., Gonzaíez-Rodríguez, V. E., Viaud, M., Garrido, C., and Collado, I. G. (2023). Identification of the sesquiterpene cyclase Involved in the biosynthesis of (+)-4-Epi-eremophil-9-en-11-ol derivatives isolated from *Botrytis cinerea*. ACS Chemical Biology, 16, 50.

Tan, K. C., Ferguson-Hunt, M., Rybak, K., Waters, O. D. C., Stanley, A. W., Bond, S. C., and Oliver, R. P. (2012). Quantitative variation in effector activity of ToxA isoforms from *Stagonospora nodorum* and *Pyrenophora tritici-repentis*. Molecular Plant-Microbe Interaction. 25, 515–522.

Tan, K. C., Oliver, R. P., Solomon, P. S., and Moffat, C. S. (2010). Proteinaceous necrotrophic effectors in fungal virulence. Functional Plant Biology, 37 (10), 907-912.

Tan, K. C., Phan, H. T., Rybak, K., John, E., Chooi, Y. H., Solomon, P. S., and Oliver, R. P. (2015). Functional redundancy of necrotrophic effectors–consequences for exploitation for breeding. Frontiers in Plant Science, 6, 501.

Tan, K.-C., Ferguson-Hunt, M., Rybak, K., Waters, O. D., Stanley, W. A., Bond, C. S., and Oliver, R. P. (2012). Quantitative variation in effector activity of ToxA isoforms from *Stagonospora nodorum* and *Pyrenophora tritici-repentis*. Molecular Plant-Microbe Interaction, 25 (4), 515–522.

Tan, K.-C., Oliver, R. P., Solomon, P. S., and Moffat, C. S. (2010). Proteinaceous necrotrophic effectors in fungal virulence. Functional Plant Biology, 37 (10), 907–912.

Terhem, R. B., Staats, M., and van Kan, J. A. L. (2015). Mating type and sexual fruiting body of *Botrytis elliptica*, the causal agent of fire blight in lily. European Journal of Plant Pathology, 142 (3), 615-624.

Teufel, F., Almagro Armenteros, J. J., Johansen, A. R., Gíslason, M. H., Pihl, S. I., Tsirigos, K. D., Winther, O., Brunak, S., von Heijne, G., and Nielsen, H. (2022). SignalP 6.0 Predicts All Five Types of Signal Peptides Using Protein Language Models. Nature Biotechnology, 40, 1023–1025.

Thanthrige, N., Jain, S., Bhowmik, S. D., Ferguson, B. J., Kabbage, M., Mundree, S., and Williams, B. (2020). Centrality of BAGs in plant PCD, stress responses, and host defense. Trends in Plant Science, 25 (11), 1131-1140.

Thompson, J. R., Register, E., Curotto, J., Kurtz, M., and Kelly, R. (1998). An improved protocol for the preparation of yeast cells for transformation by electroporation. Yeast, 14 (6), 565-571.

Todd, J. N. A., Carreón-Anguiano, K. G., Islas-Flores, I., and Canto-Canché, B. (2022). Fungal Effectoromics: a world in constant evolution. International Journal of Molecular Science, 23, 13433.

Tommasini, L., Schnurbusch, T., Fossati, D., Mascher, F., and Keller, B. (2007). Association mapping of *Stagonospora nodorum* blotch resistance in modern European winter wheat varieties. Theoretical and Applied Genetics, 115, 697-708.

Torrens-Spence, M. P., Bobokalonova, A., Carballo, V., Glinkerman, C. M., Pluskal, T., Shen, A., and Weng, J. K. (2019). PBS3 and EPS1 complete salicylic acid biosynthesis from isochorismate in Arabidopsis. Molecular plant, 12 (12), 1577-1586.

Umemura, M. (2020). Peptides derived from Kex2-processed repeat proteins are widely distributed and highly diverse in the Fungi kingdom. Fungal Biology and Biotechnology, 7 (1), 1-23.

Valero-Jiménez, C. A., Steentjes, M. B. F., Slot, J. C., Shi-Kunne, X., Scholten, O. E., and van Kan, J. A. L. (2020). Dynamics in secondary metabolite gene clusters in otherwise highly syntenic and stable genomes in the fungal genus *Botrytis*. Genome Biology and Evolution, 12 (12), 2491–2507.

Valero-Jiménez, C. A., Steentjes, M. B., Slot, J. C., Shi-Kunne, X., Scholten, O. E., and van Kan, J. A. L. (2020). Dynamics in secondary metabolite gene clusters in otherwise highly syntenic

and stable genomes in the fungal genus *Botrytis*. Genome Biology and Evolution, 12 (12), 2491–2507.

Valero-Jiménez, C. A., Veloso, J., Staats, M., and van Kan, J. A. L. (2019). Comparative genomics of plant pathogenic *Botrytis* species with distinct host specificity. BMC Genomics, 20 (1), 1–12.

Van Baarlen, P., Staats, M. and van Kan, J. A. L. (2004). Induction of programmed cell death in lily by the fungal pathogen *Botrytis elliptica*. Molecular Plant Pathology, 5(6), 559–574.

Van den Ende J. E., and Pennock-Vos I. M. G. (1997). Primary sources of inoculum of *Botrytis elliptica* in lily. Acta Horticulturae No. 430: 591-595.

Van Der Burgh, A. M., Postma, J., Robatzek, S., and Joosten, M. H. A. J. (2019). Kinase activity of SOBIR1 and BAK1 is required for immune signaling. Molecular Plant Pathology, 20 (3), 410-422.

Van der Hoorn, R. A., Laurent, F., Roth, R. and de Wit, P. J. G. M. (2000). Agroinfiltration is a versatile tool that facilitates comparative analyses of Avr 9/Cf-9-induced and Avr 4/Cf-4-induced necrosis. Molecular Plant-Microbe Interactions, 13, 439–446.

Van Doorn, W. G., and Woltering, E. J. (2008). Physiology and molecular biology of petal senescence. Journal of Experimental Botany, 59, 453–480.

Van Doorn, W. G., Balk, P. A., van Houwelingen, A. M., Hoeberichts, F. A., Hall, R. D., CityplaceVorst, O., and van Wordragen, M. F. (2003). Gene expression during anthesis and senescence in *Iris* flowers. Plant Molecular Biology, 53, 845–863.

Van Kan J. A. L. (2006). Licensed to kill: the lifestyle of a necrotrophic plant pathogen. Trends Plant Science, 11 (5), 247-53.

Van Kan, J. A. L., Stassen, J. H. M., Mosbach, A., van der Lee, T. A. J., Faino, L., Farmer, A. D., Papasotiriou, D. G., Zhou, S., Seidl, M. F., Cottam, E., ..., and Scalliet, G. (2017). A gapless genome sequence of the fungus *Botrytis cinerea*. Molecular Plant Pathology, 18 (1), 75–89.

Van Tuyl J. M., and Arens P. (2011). *Lilium*: Breeding History of the Modern Cultivar Assortment. Acta Horticulturae, 900, 223–230.

Van Tuyl, J. M. (1985). Effect of temperature on bulb growth capacity and sensitivity to summer sprouting in *Lilium longiflorum* Thunb. Scientia Horticulturae, 25, 177–187.

Van Tuyl, J. M., van Diën, M. P., van Creij, M. G. M., van Kleinwee, T. C. M., Franken, J., and Bino, R. J. (1991). Application of in vitro pollination, ovaryculture, ovule culture and embryo rescue for overcoming incongruity barriers in interspecific *Lilium* crosses. Plant Science, 74, 115–126.

Vanholme, B., Kast, P., Haegeman, A., Jacob, J., Grunewald, W. I. M., and Gheysen, G. (2009). Structural and functional investigation of a secreted chorismate mutase from the plant-parasitic nematode *Heterodera schachtii* in the context of related enzymes from diverse origins. Molecular Plant Pathology, 10 (2), 189-200.

Varadi, M., Anyango, S., Deshpande, M., Nair, S., Natassia, C., Yordanova, G., Yuan, D., Stroe, O., Wood, G., Laydon, A., Zídek, A., Green, T., Tunyasuvunakool, ..., and Velankar, S. (2022). AlphaFold Protein Structure Database: Massively expanding the structural coverage of protein-sequence space with high-accuracy models. Nucleic Acids Research, 50 (D1), D439–D444.

Vargas, W. A., Sanz-Martín, J. M., Rech, G. E., Armijos-Jaramillo, V. D., Rivera, L. P., Echeverria, M. M., and Sukno, S. A. (2016). A fungal effector with host nuclear localization and DNA-binding properties is required for maize anthracnose development. Molecular Plant-Microbe Interactions, 29 (2), 83-95.

Veloso, J., and van Kan, J. A. L. (2018). Many shades of grey in *Botrytis*–host plant interactions. Trends in plant science, 23 (7), 613-622.

Vieira, P., Mowery, J., Kilcrease, J., Eisenback, J. D., and Kamo, K. (2017). Characterization of *Lilium longiflorum* cv.'Nellie White' infection with root-lesion nematode *Pratylenchus penetrans* by bright-field and transmission electron microscopy. Journal of Nematology, 49 (1), 2.

Vignolle, G. A., Mach, R. L., Mach-Aigner, A. R., and Derntl, C. (2020). Novel approach in whole genome mining and transcriptome analysis reveal conserved RiPPs in *Trichoderma* spp. BMC genomics, 21 (1), 1-12.

Vleeshouwers, V. G. A. A., and Oliver, R. P. (2014). Effectors as tools in disease resistance breeding against biotrophic, hemibiotrophic, and necrotrophic plant pathogens. Molecular Plant-Microbe Interactions, 27 (3), 196-206.

Vleeshouwers, V. G. A. A., Rietman, H., Krenek, P., Champouret, N., Young, C., Oh, S. K., and van der Vossen, E. A. (2008). Effector genomics accelerates discovery and functional profiling of potato disease resistance and *Phytophthora infestans* avirulence genes. PLoS one, 3 (8), e2875.

Vleeshouwers, V. G. G. A., and Rietman, H. (2009). *In planta* expression systems. In: Oomycete Genetics and Genomics: Diversity, Interactions, and Research Tools. eds Lamour, K. and Kamoun, S. 23, 455-475. John Wiley and Sons Publishing.

Vleeshouwers, V. G. G. A., Driesprong, J.-D., Kamphuis, L.G., Torto-Alalibo, T., van't Slot, K. A. E., Govers, F., Visser, R. G. F., Jacobsen, E., and Kamoun, S. (2006). Agroinfection-based high-throughput screening reveals specific recognition of INF elicitins in Solanum. Molecular Plant Pathology, 7, 499-510.

Vlot, A. C., Dempsey, D. M. A., and Klessig, D. F. (2009). Salicylic acid, a multifaceted hormone to combat disease. Annual Review of Phytopathology, 47, 177-206.

Vogt, E., and Künzler, M. (2019). Discovery of novel fungal RiPP biosynthetic pathways and their application for the development of peptide therapeutics. Applied Microbiology and Biotechnology, 103, 5567-5581.

Vogt, E., Sonderegger, L., Chen, Y. Y., Segessemann, T., and Künzler, M. (2022). Structural and functional analysis of peptides derived from KEX2-processed repeat proteins in agaricomycetes using reverse genetics and peptidomics. Microbiology Spectrum, 10 (6), e02021-22.

Walker, B. J., Abeel, T., Shea, T., Priest, M., Abouelliel, A., Sakthikumar, S., and Earl, A. M. (2014). Pilon: an integrated tool for comprehensive microbial variant detection and genome assembly improvement. PloS One 9 (11), e112963.

Wang, S., Boevink, P. C., Welsh, L., Zhang, R., Whisson, S. C., and Birch, P. R. (2017). Delivery of cytoplasmic and apoplastic effectors from *Phytophthora infestans* haustoria by distinct secretion pathways. New phytologist, 216 (1), 205-215.

Westfall, C. S., Xu, A., and Jez, J. M. (2014). Structural evolution of differential amino acid effector regulation in plant chorismate mutases. Journal of Biological Chemistry, 289 (41), 28619–28628.

Wildermuth, M. C., Dewdney, J., Wu, G., and Ausubel, F. M. (2001). Isochorismate synthase is required to synthesize salicylic acid for plant defence. Nature, 414 (6863), 562-565.

Wolpert T.J., Dunkle L.D. and Ciuffetti L.M. (2002). Host-selective toxins and avirulence determinants: what's in a name? Annual Reviews of Phytopathology, 40 251–285,

Wolpert, T. J., and Lorang, J. M. (2016). Victoria Blight, defense turned upside down. Physiological and Molecular Plant Pathology, 95, 8–13.

Wolpert, T. J., Dunkle, L. D., and Ciuffetti, L. M. (2002). Host-selective toxins and avirulence determinants: what's in a name? Annual Reviews of Phytopathology, 40,251–285.

Wösten, H.A.B., Bohimann, R., Eckerskorn, C., Lottspeich, F., Bolker, M., and Kahmann, R. (1996). A novel class of small amphipathic peptides affect aerial hyphal growth and surface hydrophobicity in *Ustilago maydis*. The EMBO Journal, 15 (16), 4274-428.

Wytinck, N., Sullivan, D. S., Biggar, K. T., Crisostomo, L., Pelka, P., Belmonte, M. F., and Whyard, S. (2020). Clathrin mediated endocytosis is involved in the uptake of exogenous double-stranded RNA in the white mold phytopathogen *Sclerotinia sclerotiorum*. Scientific reports, 10 (1), 12773.

Xiong, L., Boeren, S., Vervoort, J., and Hettinga, K. (2020). Dataset on proteomic changes of whey protein after different heat treatment. Data Brief, 29, 105227.

Xue, Y., Lipscomb, W. N., Graf, R., Schnappauf, G., and Braus, G. (1994). The crystal structure of allosteric chorismate mutase at 2.2-Å resolution. Proceedings of the National Academy of Sciences, 91, 10814–10818.

Yamada, T., Ichimura, K., and van Doorn, W. G. (2006). DNA degradation and nuclear degeneration during programmed cell death in petals of *Antirrhinum*, *Argyranthemum*, and *Petunia*. Journal of Experimental Botany, 57, 3543–3552.

Yang, Y., Yang, X., Dong, Y., and Qiu, D. (2018). The *Botrytis cinerea* xylanase BcXyl1 modulates plant immunity. Frontiers in Microbiology, 9, 2535.

Yoder O. C. (1980). Toxins in pathogenesis, Annual Review in Phytopathology, 18 103–129.

Zhang Y., Zhang Y., Qiu D., Zeng H., Guo L., and Yang X. (2015). BcGs1, a glycoprotein from *Botrytis cinerea*, elicits defense response and improves disease resistance in host plants. Biochemical and Biophysical Research Communications, 457, 627–34.

Zhang, L., Kars, I., Essenstam, B., Liebrand, T. W., Wagemakers, L., Elberse, J., and van Kan, J. A. L. (2014). Fungal endopolygalacturonases are recognized as microbe-associated molecular patterns by the *Arabidopsis* receptor-like protein RESPONSIVENESS TO BOTRYTIS POLYGALACTURONASES1. Plant Physiology, 164 (1), 352–364.

Zhang, X., Nguyen, N., Breen, S., Outram, M. A., Dodds, P. N., Kobe, B., and Williams, S. J. (2017a). Production of small cysteine-rich effector proteins in *Escherichia coli* for structural and functional studies. Molecular plant pathology, 18 (1), 141-151.

Zhang, Y., Wang, Y., Xie, Z., Yang, G., Guo, Z., and Wang, L. (2017b). Simultaneous detection of three lily viruses using Triplex IC-RT-PCR. Journal of Virological Methods, 249, 69-75.

Zhang, Z. C., Friesen, T. L., Simons, K. J., Xu, S. S., and Faris, J. D. (2009). Identification, development and validation of markers for marker-assisted selection against the *Stagonospora nodorum* toxin sensitivity genes *Tsn1* and *Snn2* in wheat. Molecular Breeding, 23, 35–49

Zhang, Z. C., Running, K. L. D., Seneviratne, S., Haugrud, A. R. P., Szabo-Hever, A., Shi, G. J., and Faris, J. D. (2021). A protein kinase-major sperm protein gene hijacked by a necrotrophic fungal pathogen triggers disease susceptibility in wheat. The Plant Journal, 106, 720–732.

Zhang, Z., Friesen, T. L., Xu, S. S., Shi, G., Liu, Z., Rasmussen, J. B., and Faris, J. D. (2011). Two putatively homoeologous wheat genes mediate recognition of SnTox3 to confer effector-triggered susceptibility to *Stagonospora nodorum*. The Plant Journal, 65, 27–38.

Zhu, W., Ronen, M., Gur, Y., Minz-Dub, A., Masrati, G., Ben-Tal, N., and Sharon, A. (2017). BcXYG1, a secreted xyloglucanase from *Botrytis cinerea*, triggers both cell death and plant immune responses. Plant Physiology, 175 (1), 438–456.

Zurbriggen, M. D., Carrillo, N., Tognetti, V. B., Melzer, M., Peisker, M., Hause, B., and Hajirezaei, M. R. (2009). Chloroplast-generated reactive oxygen species play a major role in localized cell death during the non-host interaction between tobacco and *Xanthomonas campestris* pv. vesicatoria. The Plant Journal, 60 (6), 962-973.

SUMMARY

The lily is one of the most appreciated ornamental worldwide but the lily industry is continuously threatened by pests and diseases. Among them, the most disastrous is fire blight, caused by the necrotrophic Ascomycota *Botrytis elliptica* and *B. cinerea*. Infected lilies initially show small brownish necrotic lesions on leaves and flowers. Outgrowth of necrotic lesions leads to rapid death of the entire plant. While *B. cinerea* usually occur on flowering and senescing lilies especially at post-harvest stage, *B. elliptica* infect lilies throughout the entire growth season. To protect lilies from fire blight, chemical control is still the most adopted approach. Because of resistance development in fungi and due to the damage caused to soil-water ecosystems, this approach is neither effective nor eco-sustainable. In this project we set the stage for an alternative strategy to protect lilies. By investigating the molecular mechanisms conferring pathogenicity of *B. elliptica* in lily, we aimed to identify and produce effector proteins that are required for cell death induction and disease establishment in lily. This will enable the development of a protein-based screening to identify lily genotypes which display increased fire blight resistance. In **Chapter 1** I described the life style of necrotrophic fungal pathogens such as *B. elliptica*, specifically referring to the importance of cell death induction and the role of cell death inducing effectors proteins identified in several plant-necrotroph interactions.

Given the complexity of the lily germplasm and the genetic variation found in the *B. elliptica* population, in **Chapter 2** differences in fire blight susceptibility between lily genotypes and differences in virulence between fungal isolates were quantified by conducting disease assays on leaves and flowers of a panel of lily genotypes with a set of different *B. elliptica* isolates. Significant variation in symptom severity was observed in different genotype-isolate combinations and a correlation was observed between the lesion diameters on leaves and flowers of the lily genotypes. At this point, we selected two aggressive and one mild *B. elliptica* isolates to compare the cell death inducing capacity of their secreted proteins in lily. Upon protein infiltration in lily leaves, it was observed that the severity of cell death responses among the diverse lilies correlated well to their disease susceptibility. These results indicate that susceptibility to fire blight in lily is mediated by the sensitivity to *B. elliptica* effectors in a quantitative manner. In **Chapter 3** the secretome and the transcriptome of *B. elliptica* during infection in lily were analyzed and compared to the secretome and transcriptome of the sister taxon *B. squamosa*, causal agent of onion leaf blight. Despite their occurrence on different hosts, genomic and transcriptomic data suggested that both species share effector genes which are highly expressed during infection in their respective hosts. A list of candidate effector genes was generated by combining genomic, transcriptomic and proteomic data. From the list, one effector candidate was selected for heterologous expression to test its cell death inducing capacity when infiltrated in lilies as single protein. The differences in response between lily geno-

types upon protein infiltration make this effector an interesting tool for effector-assisted selection in lily.

For successful host infection, fungi must overcome plant defense responses. A large variety of these responses are regulated by the phytohormone salicylic acid. Several plant pathogens can interfere with the biosynthesis of salicylic acid by mean of effector proteins encoding a chorismate mutase. *B. elliptica* possesses and produces such an effector during infection in lily. The *B. elliptica* chorismate mutase effector (BeCMU2) was studied in **Chapter 4**. First, the enzyme activity of BeCMU2 was tested in a complementation assay in yeast and with an enzyme assay. Next, the purified BeCMU2 protein was shown to be capable of cell death induction when infiltrated in lily and tobacco leaves. At this point, the contribution of BeCMU2 to fungal virulence was tested by generating CRISPR-Cas9 deletion mutant and by comparing symptoms upon lily inoculation with the mutants and the recipient *B. elliptica* isolate. Deletion of the *Becmu*2 gene resulted in a reduction in virulence though the molecular mechanism for host cell death induction remains to be studied. The presence of a chloroplast targeting peptide in BeCMU2 suggests that the effector operates in the lily chloroplast and could influence the levels of salicylic acid in the host. Preliminary experiments were performed to assess the subcellular localization of BeCMU2 by transient expression of a fusion reporter construct in tobacco.

Besides effector proteins, fungal phytotoxic secondary metabolites contribute to cell death induction and virulence in *Botrytis*-host plant interaction. The best studied phytotoxic secondary metabolite is botrydial, a sesquiterpene exclusively found in species of the fungal genus *Botrytis*. Analogously to *B. cinerea*, the functional botrydial biosynthetic gene cluster is found also in *B. elliptica*. **Chapter 5** focusses on the role of botrydial in the *B. elliptica*-lily pathosystem. First, botrydial production in *B. elliptica* solid cultures and transcriptional activity of the key gene required for botrydial biosynthesis during infection in lily were assessed. Then, the cell death inducing capacity of botrydial in lily was confirmed by monitoring the cell death response upon pure botrydial application on lily leaves and flowers. Finally the contribution of botrydial to *B. elliptica* virulence in lily was assessed by generating *B. elliptica Bebot2* deletion mutants. In all lilies tested a reduction in lesion size was observed upon inoculation with the *B. elliptica Bebot2* deletion mutants as compared to the wild type fungus. Taken together, these results provide evidence that botrydial represents a virulence factor in the *B. elliptica*-lily interaction. **Chapter 6** provides a general discussion of the thesis work and emphasizes the importance of investigating fungal pathogenicity mechanisms at genetic-molecular level to support the development of plant genotypes that harbor natural sources of disease resistance. The advantages of effector-assisted screening to set up breeding programs for the development of *Botrytis*-resistant lily genotypes in comparison to the infection assays-based screening methods are discussed. Finally, I presented recent developments regarding the study

of a new group of fungal bioactive peptides, the so-called Ribosomally Synthesized and Post-translationally Modified Peptides (RiPPs). These compounds are gaining increasing attention in the scientific community not only because of their contribution to virulence in plant-fungus interactions but more broadly for the potential implementation of novel synthetically engineered bioactive compounds in the prevention of human diseases.

ACKNOWLEDGMENTS

The author of this dissertation is grateful to the Dutch Organization for Scientific Research (NWO) for funding this research project.

The author is grateful to the lily breeders Arie Vletter, Arie Peterse and Bart Brugmans (Gebr. Vletter & Den Haan), Anita de Haan, Hans van den Biggelaar and Floris Slob (Hobaho by Dümmen Orange), Walter de Wit and Wijnand van der Kooij (De Jong Lelies Holland B. V.), Niels Mak (Mak Breeding B. V.), Gijs Roozendaal and Pieter Jan Kos (World Breeding B.V.), and William Quaedvlieg and Derek Stol (Koninklijke van Zanten B. V.) for supporting the research project by providing the plant material used to carry out the experiments.

The author is grateful to Rohan van Genderen, Wilfred Krijnen, Marcel Otten and Rinie Verwoert for their help in taking care of the lilies grown in the greenhouses of Nergena.

The author is grateful to his students Thomas and Emma, for providing essential help in conducting this research.

The author is grateful to all members of the Phytopathology Department for providing a collaborative environment where this research has been carried out. Special thanks are addressed to Andrea Lorena Herrera Valderrama, Chris School, Sergio Landeo-Villanueva, Si Qin, Xiaoqian Shi-Kunne and Victor Coca Ruiz for their cooperation in conducting this research.

The author is grateful to Dr Sjef Boeren and Dr Henk Franssen for providing valuable feedback on the execution and evaluation of the experiments.

The author is grateful to Toos, Arnold, Jan and Leo van Berkel and to Annie de Jong-Goes for their sustain and support in the difficult moments.

The author is grateful to his promoters Prof. Dr Richard Immink and Dr Paul Arens for their contribution in the preparation of the project, for the fruitful and scientific discussions and for their feedback on this dissertation.

Special thanks are addressed to Dr Jan van Kan for his guidance during the entirety of the research activity.

ABOUT THE AUTHOR

Michele Carlo Malvestiti was born on the 4th of September 1991 in Gallarate, a small town situated 15 km Est of the river Ticinus in the Province of Cisalpine Gaul. In the summer 2010 he moved to Vienna (Austria) to start his academic education at the Universität Wien. There he held the BSc degree in Biology with specialization in Botany after having conducted research activity on heavy metal stress tolerance in Bryophytes under the supervision of Frau Prof. Dr Irene Lichtscheidl and on the plant species association in a post-glacier moraine area under the supervision of Herr Prof. Dr Joseph Greimler and Frau Prof. Dr Luise Ehrendorfer-Schratt. In the summer 2016 he moved to Wageningen (Netherland) where he started a MSc in Plant Sciences at the University of Wageningen. Michele obtained the specialization in Plant Pathology after completing his MSc Thesis in which he conducted research activity on the role of onion bulb antifungal compounds in the *Botrytis*-onion interaction under the supervision of Dr Jan van Kan. In the spring 2018 Michele moved to Lisse (Netherland) where he performed his internship with the flower bulb breeders of the Hobaho (Dümmen Orange). In Lisse he conducted research activity on *Botrytis* and *Fusarium* diseases in tulips, roses and orchids. At the same time Michele kept his collaboration with Dr Jan van Kan, Prof. Dr Richard Immink and Dr Paul Arens to prepare a PhD project proposal about effector proteins of *Botrytis elliptica* as tools for resistance breeding in lily against fire blight disease. With this project proposal he applied for fundings at the PhD talented program Groen Top Sector of the NWO, the Dutch Organization for Scientific Research. After obtaining the funding, Michele started his PhD trajectory in February 2019 at the Laboratories of Phytopathology of the University of Wageningen under the supervision of Dr Jan van Kan.

LIST OF PUBLICATION

Landeo Villanueva, S., Malvestiti, M. C., van Ieperen, W., Joosten, M. H., and van Kan, J. A. L. (2021). Red light imaging for programmed cell death visualization and quantification in plant–pathogen interactions. Molecular Plant Pathology, 22 (3), 361-372.

Malvestiti, M. C., Immink, R. G., Arens, P., Quiroz Monnens, T., and van Kan, J. A. L. (2021). Fire blight susceptibility in *Lilium* spp. correlates to sensitivity to *Botrytis elliptica* secreted cell death inducing compounds. Frontiers in Plant Science, 12.

Malvestiti, M. C., Steentjes, M. B., Beenen, H. G., Boeren, S., van Kan, J. A. L., and Shi-Kunne, X. (2022). Analysis of plant cell death-inducing proteins of the necrotrophic fungal pathogens *Botrytis squamosa* and *Botrytis elliptica*. Frontiers in Plant Science, 13.

Education Statement of the Graduate School Experimental Plant Sciences

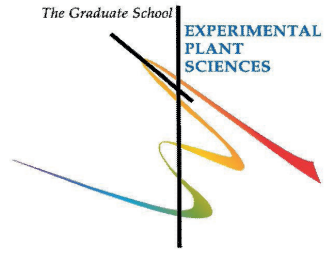

Issued to: Michele C. Malvestiti
Date: 19 June 2023
Group: Laboratory of Phytopathology
University: Wageningen University & Research

1) Start-Up Phase	**date**	**cp**
► First presentation of your project		
Effector proteins of Botrytis elliptica as tools for resistance breeding in lily against fire blight disease	28 June 2019	1,5
► Writing or rewriting a project proposal		
► MSc courses		
Subtotal Start-Up Phase		*1,5*
2) Scientific Exposure	**date**	**cp**
► EPS PhD days		
EPS PhD days 'Get2Gether', Soest (NL)	10 - 11 February 2020	0,6
EPS PhD days 'Get2Gether', Soest (NL)	3 - 4 May 2022	0,6
► EPS theme symposia		
EPS theme 2 symposium & Willie Commelin Scholten Day 'Interactions between plants and biotic agents', Wageningen (NL)	1 February 2019	0,3
EPS theme 2 symposium & Willie Commelin Scholten Day 'Interactions between plants and biotic agents', online	9 February 2021	0,2
EPS theme 3 symposium 'Metabolism and Adaptation', Nijmegen (NL)	21 October 2019	0,3
► Lunteren Days and other national platforms		
Annual Meeting 'Experimental Plant Sciences', Lunteren (NL)	8 - 9 April 2019	0,6
Annual Meeting 'Experimental Plant Sciences', online	12 - 13 April 2021	0,5
Annual Meeting 'Experimental Plant Sciences', Lunteren (NL)	11 - 12 April 2022	0,6
NWO Life Congress – Communication in Life, Bunnik (NL)	28 - 29 May 2019	0,6
NWO Life Congress – Networks in Life, online	26-28 May 2021	0,6
► Seminars (series), workshops and symposia		
Nick Talbot - 'Investigating the biology of plant infection by rice blast fungus'	2 April 2019	0,1
Eva Stukenbrock - 'Causes and consequences of chromosome stability in a fungal plant pathogen	13 December 2019	0,1
Thorsten Nürnberger - 'Microbial virulence and plant immunity stimulating activities of microbial cytolysin'	3 February 2020	0,1
Peter Solomon - 'How the study of necrotrophic effectors advanced our understanding of the enigmatic PR-1 protein'	20 April 2020	0,1

	Luigi Faino - 'Evolution of minichromosomes in Fusarium'	25 May 2020	0,1
	Phytopathology Symposium, Ede (NL)	15 December 2022	0,3
	Phytopathology Symposium, Ede (NL)	6 April 2023	0,3
►	Seminar plus		
	Nick Talbot - discussion with PhD candidates Laboratory of Phytopathology	2 April 2019	0,1
	Eva Stukenbrock - discussion with PhD candidates Laboratory of Phytopathology	13 December 2019	0,1
	Thorsten Nürnberger - discussion with PhD candidates Botrytis group	3 February 2020	0,1
►	International symposia and congresses		
	BotrySclero Symposium, online	8 - 11 June 2020	0,8
	Fungal Genetics Conference, Pacific Grove, CA (US)	15 - 20 March 2022	1,5
	BotrySclero Symposium, Avignon (FR)	13 - 17 June 2022	1,4
	European Conference on Fungal Genetics, Innsbruck (AT)	5 - 8 March 2023	1,2
►	Presentations		
	ORNATO 2019, Puebla (MX), oral presentation	14 October 2019	1,0
	BotrySclero Symposium (online), oral presentation	10 June 2020	1,0
	NWO Life Congress – Networks in Life (online), poster presentation	26 - 28 May 2021	1,0
	Fungal Genetics Conference, Pacific Grove, CA (US), poster presentation	15 - 20 March 2022	1,0
	BotrySclero Symposium, Avignon (FR), poster presentation	8 - 12 June 2022	0,0
	European Conference on Fungal Genetics, Innsbruck (AT), poster presentation	6 March 2023	1,0
►	Interviews		
►	Excursions		
	Subtotal Scientific Exposure		*16,2*
	3) In-Depth Studies	**date**	**cp**
►	Advanced scientific courses & workshops		
	SLU-WUR course 'Plant Breeding and Biotechnology', Wageningen (NL)	11 - 13 June 2019	1,6
	10th EPS Utrecht PhD Summer School 'Environmental Signaling in Plants', Utrecht (NL)	26 - 28 August 2019	0,9
	VLAG course 'Advanced Proteomics', Wageningen (NL)	7 - 10 February 2023	1,4
►	Journal club		
	Botrytis group literature discussion sessions	2019 - 2023	1,5
	Laboratory of Phytopathology expert meetings literature discussion	2020 - 2021	1,0
►	Individual research training		
	Subtotal In-Depth Studies		*6,4*

4) Personal Development	**date**	**cp**
► General skill training courses		
WGS PhD Competence Assessment, Wageningen (NL)	April 2019	0,3
WGS workshop 'Scientific Publishing', Wageningen (NL)	17 April 2019	0,3
WGS course 'Project and Time Management', Wageningen (NL)	September - October 2021	1,5
► Organisation of meetings, PhD courses or outreach activities		
Organizer PhD and PostDoc meetings at Laboratory of Phytopathology	September 2021 - June 2022	1,0
Member of selection commitee for new chair of Laboratory of Phytopathology	March - July 2020	1,0
Member of the Laboratory of Phytopathology Management Team	March - October 2022	1,0
► Membership of EPS PhD Council		
Subtotal Personal Development		5,1

5) Teaching & Supervision Duties	**date**	**cp**
► Courses		
Molecular Aspects of Biointeractions PHP30806	2020, 2021, 2022	3,0
Plant Microbe Interaction PHP30306	2020, 2021	
► Supervision of BSc/MSc students		
BSc Thesis Sikke van der Weg	May - August 2019	3,0
MSc Thesis Thomas Quirroz Monnens	November 2019 - September 2020	
MSc Thesis Xander Zuijdgeest	February - September 2021	
MSc Thesis Emma Groen	January - October 2022	
MSc Thesis Leonhard Pachinger	January - July 2023	
MSc Thesis Ruben McCarthy	January - July 2023	
Subtotal Teaching & Supervision Duties		6,0

TOTAL NUMBER OF CREDIT POINTS*		35,2

Herewith the Graduate School declares that the PhD candidate has complied with the educational requirements set by the Educational Committee of EPS with a minimum total of 30 ECTS credits.

* A credit represents a normative study load of 28 hours of study.